FINAL REPORT

New Tools for Estimating and Managing Local/Regional Air Quality Impacts of Prescribed Burns

SERDP Project RC-1648

FEBRUARY 2013

Wayne Miller
University of California, Riverside

SERDP
DOD ▪ EPA ▪ DOE

REPORT DOCUMENTATION PAGE

Form Approved
OMB No. 0704-0188

1. REPORT DATE *(DD-MM-YYYY)*	**2. REPORT TYPE**	**3. DATES COVERED** *(From - To)*
09 -12 -2013	Final	06/01/2008-2/28/2014

4. TITLE AND SUBTITLE

New Tools for Estimating and Managing Local/Regional Air Quality of Prescribed Burns

5a. CONTRACT NUMBER
WQ12HQ-08-C-0041

5b. GRANT NUMBER

5c. PROGRAM ELEMENT NUMBER

6. AUTHOR(S)

Miller, J Wayne

5d. PROJECT NUMBER
RC-1648

5e. TASK NUMBER

5f. WORK UNIT NUMBER

7. PERFORMING ORGANIZATION NAME(S) AND ADDRESS(ES)

Regents of the University of California
200 University Office Blvd
Riverside, CA 92521

8. PERFORMING ORGANIZATION REPORT NUMBER

9. SPONSORING / MONITORING AGENCY NAME(S) AND ADDRESS(ES)

USACE Humphreys Engr Ctr
SPT ACTIVITY
7701 Telegraph Road
Alexandria, VA 22315

10. SPONSOR/MONITOR'S ACRONYM(S)
ATTN: CECT-HC

11. SPONSOR/MONITOR'S REPORT NUMBER(S)

12. DISTRIBUTION / AVAILABILITY STATEMENT

13. SUPPLEMENTARY NOTES

14. ABSTRACT

Wildland fires are expected to increase as a consequence of climate change forces and more data were needed to help facility managers carry out prescribed burns, especially for the burning of southwestern and southeastern wild land fuels. As a consequence, RC-1648 and RC-1649 projects were funded to provide new information on the properties of the fuels in the field and models for the burning rates using both field and laboratory data. The combined projects collected and analyzed the most comprehensive data for gaseous and particulate matter emissions from these sources. Further the use of continuous instruments allowed the direct measurement of the emission factors for gases and particulate matter as the burns transitioned from flaming to smoldering regimes. Included in the final report and about 20 published journal articles are new and improved emission factors for criteria pollutants, selected hazardous air pollutants and elemental factors in EPA's AP-42 format for wildfire for DoD facilities with southeastern and southwestern fuels. A key finding in the RC -1648 project was the discovery that the percentage of graphic carbon is related to the fire intensity and the emissions rates of black and brown carbon. The complicated EPA CMAQ model was compared to the BlueSky framework. The later appears to be more useful to local land managers in developing estimated smoke emissions from prescribed burns.

15. SUBJECT TERMS

Continuous measurements of particle and gaseous emissions from wildland fires, rates of burning, southwestern and southeastern fuels.

16. SECURITY CLASSIFICATION OF:			**17. LIMITATION OF ABSTRACT**	**18. NUMBER OF PAGES**	**19a. NAME OF RESPONSIBLE PERSON**
a. REPORT	**b. ABSTRACT**	**c. THIS PAGE**			**19b. TELEPHONE NUMBER** *(include area code)*

Standard Form 298 (Rev. 8-98)
Prescribed by ANSI Std. Z39.18

Table of Contents

List of Figures

List of Tables

List of Acronyms and Definitions

AFB	Air Force Base
APM	Aerosol Particle Mass analyzer for determination of exact particle mass
AQ	Air quality
$C_2 - C_3$	Molecules with either 2 or 3 carbons atoms
CH_4	Methane
CMAQ	Community Multiscale Air Quality, an EPA air quality model
CO	Carbon monoxide
CO_2	Carbon dioxide
CONSUME	Models of fuel consumption using various input data
CPC	ultrafine Condensation Particle Counters for number concentration;
CRDS	Cavity RingDown Spectrometer for monitoring reactive chemicals
DMA	Differential Mobility Analyzer
DMM	Dekati® Mass Monitor to measure real time PM mass and size distribution
DoD	Department of Defense
EAD	Electrical Aerosol Detector to measure active particle surface area
FCCS	Fuel Characteristic Classification System
FEPS	Fire Emission Production Simulator
FOFEM	First Order Fire Effects Model
f-SMPS	Fast Scanning Mobility Particle Sizer for real time measurement of PM size distribution
FTIR	Fourier Transform Infrared spectrometer used for measuring gas-phase chemicals
GC-FIDs	Gas chromatographs with flame ionization detectors for hydrocarbon analyses
GC-MS	gas chromatograph-mass spectrometer for measuring molecules of high molecular weight and PAH compounds
GPS	Global Positioning System
HCN	Hydrogen cyanide
HR-ToF-AMS	High-Resolution Time-of-Flight Aerosol Mass Spectrometer to track evolution of the chemical composition of the aerosol
LC-ToF MS	Liquid Chromatograph Time of Flight Mass Spectrometer for determining trace amounts of hydrocarbons, especially SOA precursors
MFSL	Missoula Fire Sciences Lab, USDA Forest Service, Rocky Mountain Research Station, 5775 W U.S. Highway 10, Missoula, MT 59808-

	9361
MM5	NCAR/Penn State Mesoscale Model version 5 for meteorology
NH3	Ammonia
NOx	Nitrogen oxides (NO, NO_2),
O_3	Ozone
OVOC	Oxygenated volatile organic compounds
PAH	Polynuclear aromatic hydrocarbon
PAN	Peroxyacetyl nitrate
PAS	Photoelectric Aerosol Sensor for PAH on particles
PM	Particulate Matter
$PM_{2.5}$	Particulate Matter smaller than 2.5 micons
PTR-MS	Proton Transfer Reaction- Mass Spectrometer to track evolution of key reactive organic gases
RFL	Riverside Fire Lab, USDA Forest Service, Pacific Southwest Research Station, 4955 Canyon Crest Drive, Riverside, CA 92507
SASEM	Simple Approach Smoke Estimation Model
SEMS	Scanning Electrical Mobility Spectrometers for particle sizing, number counts, and instrument calibration;
SMOKE	Sparse Matrix Operator Kernel Emissions; used for inventory input to the air quality models
SOA	Secondary Organic Aerosol
SVOCs	Semi-Volatile Organic Compounds, usually C_{10+}
TDLAS	long path-length Tunable Diode Laser Absorption Spectrometer for formaldehyde and NO2 monitoring
TDMA	Tandem Differential Mobility Analyzer to measure organic and/or water uptake by particles
UCR	University of California at Riverside
UM	University of Montana
USDA	United States Department of Agriculture
USMC	United States Marine Corps
VOCs	Volatile Organic Compounds, usually C_3-C_{10}
WRAP	Western Regional Air Partnership

Keywords

Wildland fire, Chaparral, Emory oak savanna, criteria emissions, toxic emissions, PM mass emissions, PM particle size distribution, Organic and elemental carbon, Black carbon, Aerosol Mass Spectrometer

Acknowledgements

The Science Team associated with RC-1648 would like to acknowledge the very helpful participation of the US Forest Service in Montana for their help in setting up the experimental instruments and for providing access to accommodations that allowed much more data to be collected than originally planned. The Team also acknowledges the helpful analyses carried out by Ms. Kathy Cocker at UCR. The Team acknowledges the funding provided by SERDP without which this project and research could not have been carried out.

Abstract:

Objectives. SERDP's Statement of Need NUMBER: SISON-08-03 called for proposals "to evaluate the air quality aspects of prescribed burning in the different ecological systems managed by Department of Defense (DoD)." RC-1648 responded to the SON with measurements of fuel loading, fuel consumption and the emission factors for gases, metals, and particulate matter (PM) on DoD facilities in the West and Southwest. These measurements provide input for a detailed model-based assessment of the regional air quality impact of prescribed burning. The measurements and model results produced in this report will provide DoD land managers and regional air quality agencies with the data needed to more accurately predict the air quality impacts of prescribed burning.

Technical Approach: The complex science issues associated with fires and their impact on the local and regional air quality were handled by assembling a team of US Forest Service and academic experts for fire spread, emission measurements and emission modeling with personnel at DoD sites. The SERDP process added a scientific advisory committee to provide guidance on advancing the science and a focus on help needed by DoD resource managers. The technical approach involved both lab and field measurements. Key measurements were made at the US Forest Service lab in Montana where individual wildland fuels were burned during a total of seventy seven runs, including triplicate tests for many fuels. Forty nine of the runs were southwestern fuel types. Gas phase emissions were measured with traditional methods and a new infrared tool, specifically developed for this SERDP project, which allowed first time measurement of many oxygenated hydrocarbons and ozone initiators. Instruments from the University of California, Riverside (UCR) particle science labs were added and these enabled first-of-a-kind and continuous emission measurements of the chemical and physical properties of the particulate matter over the course of a fire: from the flaming to the smoldering phase.

Prescribed burns and emission measurements in the field followed to validate lab-measured emissions factors. The field equipment included an instrument-packed airplane that followed the airborne solid and liquid particulates and gases released from the fire for hours in order to learn what happens to aged smoke. Later a few exploratory trials in UCR's atmospheric reactors aged smoke for hours to learn if results would be similar to the aircraft findings.

In the final task, EPA air quality models were used to forecast the concentration and elevation history of gases and smoke released from a fire. These results were compared with SMARTFIRE and BlueSky, which are simpler models to run.

Results: Improved fuel characterization and consumption data. Data for southwestern fuels such as chaparral and the Emory oak (*Quercus emoryi*) woodlands were scarce. Wildland fuels at three military facilities in California and Arizona were sampled, characterized, and compared with other work. Data included measured field and chemical properties as well as the consumption rates during prescribed burns. Collectively, these data provide improved values for the fuel consumption rates during fire and are available for managers of military facilities and neighboring lands.

Improved emission factors and new test methods were the main emphasis for the project. Emissions data for gases, metals and particulate matter (PM) were generally lacking for the fuels burned in this project. Using EPA's AP-42, *Compilation of Air Pollutant Emission Factors,* as a guide, the project produced new emission factors for criteria pollutants (CPs) and selected hazardous air pollutants (HAPs). The CPs included CO, NOx, SOx, $PM_{2.5}$ mass and lead (Pb).

HAPs included: aldehydes, ketones, ammonia (NH_3), benzene/toluene/xylene (BTEX), and polycyclic aromatic compounds (PAHs). Formaldehyde was the main aldehyde measured in the fire. In addition to the CPs and HAPs, the measurements in RC-1649 led to the greatest improvement in emission factors for previously undocumented oxygenated gaseous compounds and HONO, an important ozone precursor.

The RC-1648 team used real time instruments to characterize the chemical and physical nature of the aerosols and particulate matter. These new methods followed the path of burning from flaming to smoldering and reported the instantaneous change in particle diameter distribution, number and aerosol composition. For example the Aerosol Mass Spectrometer monitored the elemental chemistry and levoglucosan, a known marker for biomass fires. In addition to PM mass, we determined the elemental and organic fractions of the mass and thirty-eight elements on the filter. Ions, including SO_4, NO_3, Cl, Br, Na, NH_4, K and Ca, were analyzed on the filter.

One limitation of lab fires is the combustion process is over in minutes and the products are quickly vented. In real fires, reactions take place over hours as the plume migrates downwind away from the source. In this project, an instrumented aircraft flew in the downwind plume to sample smoke that was hours old to learn about the transformations. However, aircraft monitoring is expensive, so RC-1648 carried out exploratory runs in an atmospheric reactor filled with combustion products and monitored the changes to the emissions over hours under various conditions. The exploratory trials showed results similar to aircraft data suggesting further atmospheric reactors studies.

A significant advancement in data analysis of emissions from wildland fires came during the data analysis task. Traditionally data are fitted to combustion efficiency. RC-1648 showed the percentage of total filterable carbon that is graphic in nature enables one to model the release of black carbon, brown carbon and lighter molecules, like levoglucosan. This parameter is a surrogate for fire intensity and provided a surprisingly good fit.

Air Quality Modeling. The work involved modeling the emissions with the Community Multi-scale Air Quality Model (CMAQ) model and forecasting the impact on air quality around Vandenberg. Winter sun intensity limits ozone formation so gaseous values were low; however, the comparison of model and field data looked promising. Trials with BlueSky were better than SMARTFIRE and may offer advantages over CMAQ for land managers.

Benefits:

- Developed improved models relating to fuel types, fuel loadings, and consumption estimates for Southwest chaparral and oak fuels
- Improved emission factors for criteria pollutants, selected HAPs and elemental factors in EPA's AP-42 format for wildfire for DoD facilities with southeastern and southwestern fuels.
- Field data showed DoD facilities should consider entrainment of dust into the plume before prescribed burns as significant amounts of lead and antimony were detected in the ground-based filter samples at Vandenberg AFB. Filters from laboratory burning of the fuels did not include these elements in any significant quantity suggesting a non-fuel source.
- A new mathematical model was developed to predict the release of black carbon, brown carbon and lighter molecules, like levoglucosan, from wildland fires.

- Air quality modeling suggest that the BlueSky framework might be more useful to local land managers that the complex US EPA CMAQ.

1 Objective:

This section describes the objectives of the research, specifically as it relates to the SERDP Statement of Need (SON) and provides direction into the working hypotheses that formed the basis of the research approach.

1.1 SERDP Statement of Need (SON)

SERDP's statement of Need NUMBER: SISON-08-03 called for proposals "to evaluate the air quality aspects of prescribed burning in the different ecological systems managed by Department of Defense (DoD)." DoD land managers use prescribed burning in fire-adapted ecosystems to benefit native vegetation and animal species, to maintain training areas and ranges, and to reduce wildfire risk on DoD and neighboring lands. However many bases are in non-attainment areas or close to population centers and require permits for prescribed burns. Such permits are declined if smoke management authorities estimate that the impact of such fires on the local and regional air quality will be unacceptable.

To meet the challenges presented in the SON, a proposal was submitted by a team of science experts from three US Forest Service labs, two universities and DoD personnel from five bases. The proposal observed that many DoD facilities in the West had fuel types, such as chaparral, that differed significantly from eastern fuels and for which fire consumption and emissions data were severely lacking. Team members were added after contracting; see Table 1-1.

Table 1-1 List of Project Team Members

Fuel Data and Burn Models

- Dr. David Weise, CoPI — USDA Forest Service
- Dr. Shankar Mahalingam — UCR –ME Department
- Dr. Marko Princevac — UCR –ME Department

Emissions: Gaseous/Aerosol/PM/Climate Change

- Dr. Robert Yokelson, — U of Montana,Chem
- Dr. Wei Min Hao — USDA Forest Service
- Dr. J Roberts — NOAA
- Dr. A. Miller — NIOSH
- Dr. John Seinfeld — Caltech
- Dr. David Cocker — UCR- Chem/Env Eng
- Dr. Heejung Jung — UCR –ME Department
- Dr. Wayne Miller, PI — UCR- Chem/Env Eng
- Dr. Asa Awuku — UCR- Chem/Env Eng

Air Quality Modeling

- Dr. Gail Tonnesen, CoPI — UCR- CE-CERT
- Dr. Shawn Urbanski — USDA Forest Service
- Dr. Francis Fujioka — USDA Forest Service

Military Personnel

- Vandenberg AFB; Forts Hunter-Liggett and Huachuca

The problems raised by SERDP's SON were complex and required multiple and distinct skills to develop a solution. Hence the team proposed attacking the SON problem in three separate science areas with experts in each area. Furthermore each thrust area was divided into a number of tasks. The three major thrust areas as proposed consisted of:

- Fuels data and burn models development
- Characterization (chemical and physical) of gaseous, particulate and aerosol emissions
- Air quality modeling

With access to advanced emissions measurement facilities, specialized instruments and the latest modeling techniques, the team laid a clear action plan with many steps using these tools, valued at millions of dollars, to move the boundary of knowledge forward as related to the science of biomass burning in the West. It was selected for award.

1.2 Merging Three Proposals for Greater Benefits

During the review process, two other proposals that focused on prescribed burning of eastern fuels were selected for award. One project, RC-1649, proposed a novel infrared instrument design that enabled the identification of the difficult to measure oxygenated hydrocarbon class of compounds. Oxygenated compounds make up a significant portion of the hydrocarbons released in biomass burning and data was almost non-existent. The other proposal, RC-1647, focused on a unique grid definition for air quality modeling during a prescribed burn. As the three teams had a common goal of finding a deeper knowledge associated with prescribed burns, the logical approach for enhanced advancement of the science was for all three teams to work together from the beginning. SERDP set up several conference calls and the teams enthusiastically endorsed the idea of collaborating. As a consequence of these discussions, the teams worked closely together during the project. Further this assured that all the biomass burning at the Forest Service labs in Montana would have the best instruments from both teams. Proposals were modified to reflect the collaborative approach.

In addition to the selected proposals, other labs, namely National Oceanic and Atmospheric Administration *(*NOAA) and National Institute for Occupational Safety and Health *(*NIOSH*)* recognized the unique opportunities offered in the SERDP program so they joined with their own research funding. This approach allowed the SERDP funding to be further leveraged by the addition of resources and specialized instruments from several government labs valued in millions of dollars.

1.3 Technical Objectives:

After merging the teams, the objectives of the research project remained basically the same. Namely provide new information characterizing the fuel consumption, pollutant emissions, and air quality impacts associated with prescribed burning in different ecological systems for DoD managed facilities in the West and Southwest. Specific objectives for this proposal became:

- Develop improved models relating fuel types, fuel loadings, and consumption estimates for southwest chaparral and oak woodlands/savannah.
- Develop improved emission factors under flaming and smoldering conditions for:
    - Criteria pollutants: CO, NO_x, SO_x and $PM_{2.5}$.
    - Toxics: aldehydes, ketones and BTEX

    - Others: CO_2, CH_4 and THC. , EC, OC, ions, elements (K, Cl…), secondary PM
- Provide insight on using air quality tools to enable DoD sites to calculate the impact of criteria pollutants and other emissions on local and regional air quality from prescribed burns under both flaming and smoldering regimes.

1.4 Deliverables

A number of deliverables are planned as the project moves towards completion of the various objectives. These deliverables are outlined below.

1.4.1 Improved fuel characterization & consumption data

- Fuel loading model for chaparral and oak woodland/savannah
- Improved prescribed fire consumption estimates for chaparral and oak woodland/savannah

1.4.2 Improved emissions factors & new test methods

- Emission factors for primary $PM_{2.5}$, heavy metals, volatile organic compounds, and reactive gases under flaming and smoldering conditions
- Characterization of secondary $PM_{2.5}$ and its emission factors.
- Creation of emission factor data in AP-42 format for inclusion in EPA's "look-up" tables
- New fire/smoke application data for real-time aerosol and PM instruments.

1.4.3 Prediction of AQ differences for prescribed burns & wildfires

- Sensitivity analysis of key parameters to measure to improve AQ modeling
- Predictive models of the impact of prescribed burns on local/regional AQ
- Prediction of the difference in impact on AQ for prescribed vs. wildfire

2 Background:

This section discusses the environmental issues and research goals in terms of DoD needs and regulatory requirements. A brief summary of the state of knowledge at the start of this research is provided in order to frame the specific technical objectives of the project.

2.1 Fuel Characterization and Combustion

Approximately 5.7 million hectares (17%) of the vegetation in California is classified as brush; 1.62 million hectares of southern and central California are covered by the shrub complex known as chaparral. The composition of this shrub complex varies from the coast to the interior and from north to south; however, there are several common species or genera that comprise the majority of plants. Some of the principal species in chaparral are chamise (*Adenostoma fasciculatum*), ceanothus (*Ceanothus spp.*), manzanita (*Arctostaphylos spp.*), and scrub oak (*Quercus berberidifolia*). Chaparral is a significant component of the vegetation at several military bases in California including Camp Pendleton (USMC), Vandenberg AFB, Fort Hunter-Liggett, and the former Fort Ord as shown in Figure 2-1.

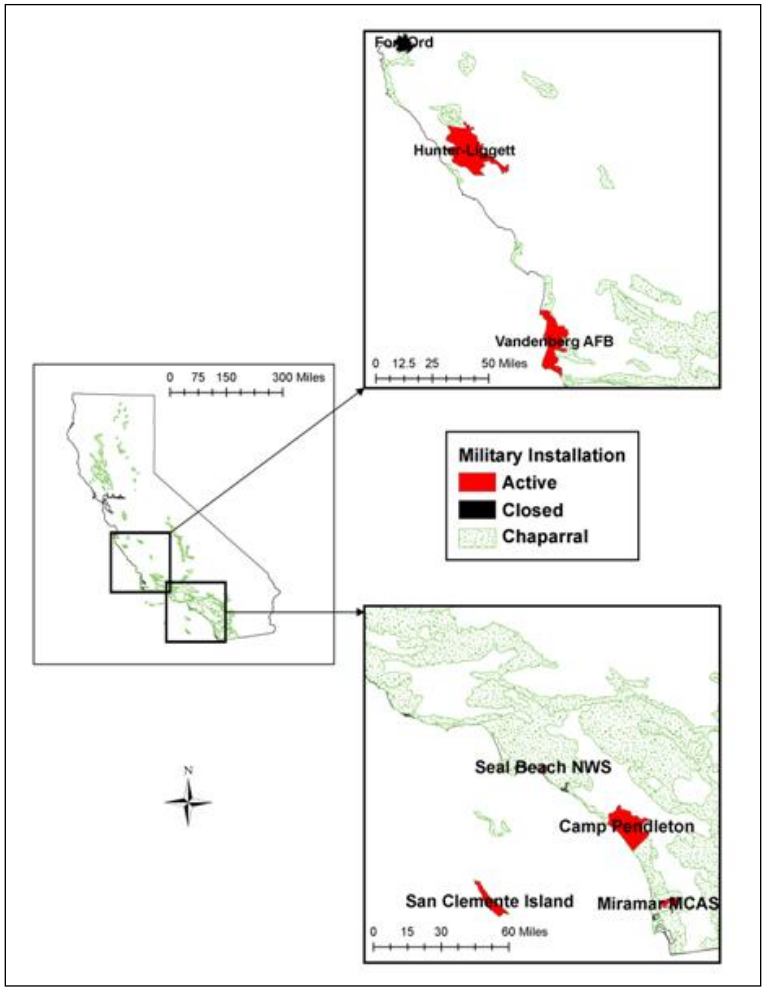

Figure 2-1 DoD Installations with Chaparral and Coastal Sage Vegetation Types

Some of the same plant genera (*Quercus*, *Arctostaphylos*) are also found in the Emory oak woodlands located at Fort Huachuca. The Emory oak savanna fuel type at Fort Huachuca has similar structure to the blue oak (*Quercus douglasii*)/valley oak (*Quercus lobata*)/California live oak (*Quercus agrifolia*) savanna at Fort Hunter-Liggett and adjoining Camp Roberts as well as much of the foothill region of the central valley of California.

For fire behavior prediction, three fuel models are typically used to describe the fuel loading of chaparral – fuel models 4, 5, and 6 (Albini, 1976) with little field verification that the parameters in these fuel models are accurate. While new fuel models have been proposed for chaparral (Weise et al., 1997; Scott and Burgan, 2004), these models have also not been verified with field data at these installations. Additionally, the information included in fire behavior fuel models is not sufficient to estimate fuel consumption or smoke emissions (Weise and Wright, 2013; Ottmar, 2014)

During this project we planned to improve fuel characterization and consumption data with five sub-tasks outlined in Table 2-1.

Table 2-1 Fuels Research Areas Advanced during Project

1	Identify Southwestern fuels of interest, existing data and consumption models.
2	Sample Southwestern fuels, measure field & chemical properties.
3	Collect fuel samples & develop beds for lab tests.
4	Field sampling: pre-burn and post burn.
5	Improve existing fuel consumption rates with mass of pollutants emitted during burning.

2.2 Emissions and Emission Factor Measurement

The most common method to estimate total emissions for a fire is to establish an arbitrary spatial/temporal entity and multiply the (burned area) × (mass of fuel consumed per unit burned area) × (mass of emissions per unit mass of dry fuel burned). The mass of emissions per unit mass of dry fuel burned for any emitted species is that species emission factor (EF). For both laboratory and airborne measurements the most accurate EF are determined using the carbon mass balance method (Ward and Radke 1993). The assumption is that all the carbon in the fuel is released as trace gases and particles and then detected. This is a good assumption when CO_2, CO, CH_4, non-methane organic compounds, and $PM_{2.5}$ are all measured. Then, for each gaseous or particulate species the carbon in that species is divided by the total carbon emitted and multiplied by the grams of carbon per kilogram of fuel and the ratio of the compounds molecular mass to the molecular mass of carbon (Yokelson et al., 1996).

While the chemical composition and emission factors for a few ecosystems are well characterized (e.g. Amazon tropical forests and South African savannas), fire emissions for some of the most important fire-adapted ecosystems managed by DoD in the Southwest and West are poorly understood and those were the focus of this project.

A precise estimate of the total mass emitted for each pollutant comprising initial fire emissions is necessary, but not sufficient for understanding and accurately predicting the air quality impacts of biomass burning. A key consideration for understanding fire emissions and emission factors is the dynamics of fire behavior and the science complexity associated with the multiple processes.

For example, rapid emissions from an intense flaming fire differ markedly in rates and composition from the emissions associated with a lazy burn that smolders for days. In addition parameters associated with the biomass, like moisture and packing, and atmospheric conditions can modify transport phenomena and fire behavior and the metrics associated with emissions. Thus with up to orders of magnitude differences in the associated emissions, it is important to recognize that emission rates are highly variable and closely correlated with the fire behavior, biomass state and atmospheric conditions. As indicated in Figure 2-2, multiple science areas are associated with fires making the understanding of emissions and emission factors more complex and difficult.

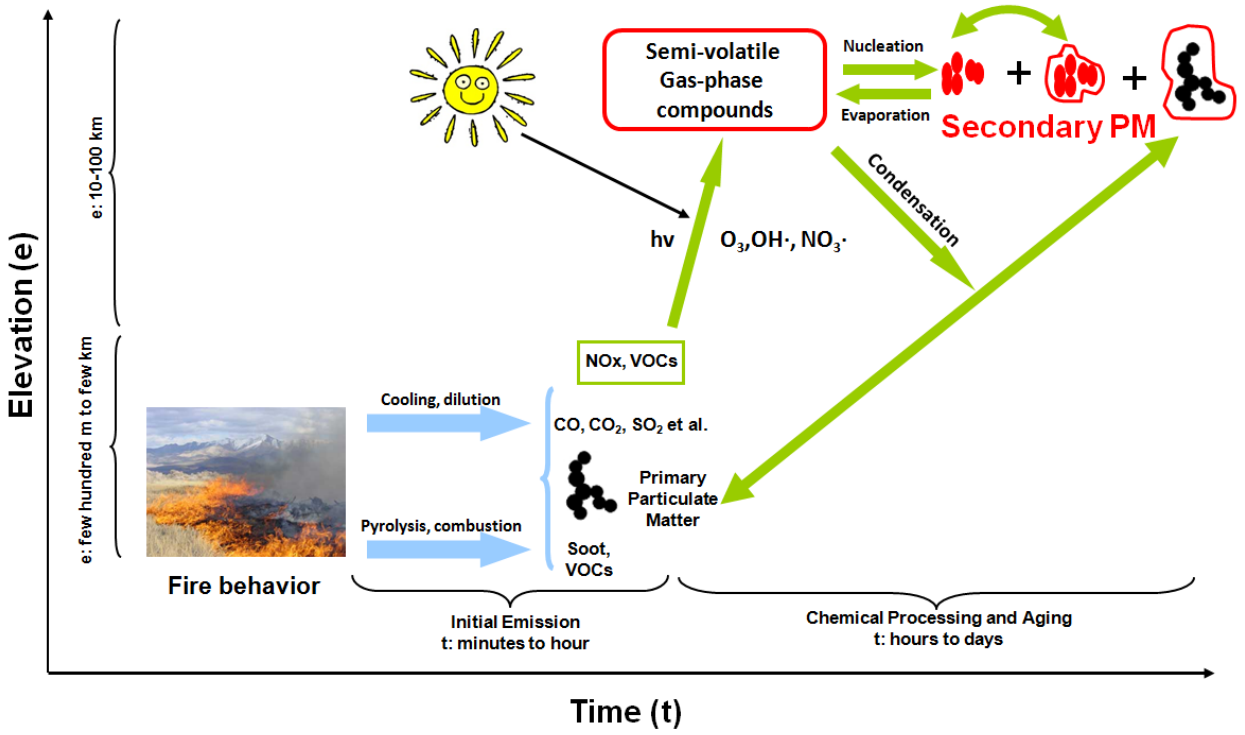

Figure 2-2 Multiple Science Areas Add Complexity to Understanding Fires & Emissions

As indicated in Figure 2-2, fresh smoke from burning biomass is a complex mixture of gases and aerosols. The amount and composition of fire emissions depends on wide range of variables related to fuel characteristics (type, structure, loading, chemistry, moisture) and fire behavior. Fuel characteristics are ecosystem specific and resultant properties are heavily influenced by land use history and environmental conditions (e.g. seasonal weather patterns that drive fuel moisture or anthropogenic nitrogen and sulfur deposition that impact fuel chemistry). It is fuel characteristics, along with meteorology and topography that control fire behavior.

While accurate estimates of the total mass emitted for each pollutant comprising initial fire emissions is necessary, knowing the total mass is not sufficient for understanding and predicting the air quality impacts of biomass burning. For example as the fire enters the smoldering regime, the emission will change. Furthermore, as the released smoke plume is aged and transported over long distances (10 – 100s km), the emissions are transformed by photochemistry, heterogeneous processes, and mixing with ambient air, leading to the formation of secondary pollutants. In particular, the oxidation of reactive organic gases in the presence of nitrogen oxides and sunlight leads to the formation of secondary aerosol, which contributes up to 60% of the particulate

matter in many urban and rural areas. Identifying the mechanisms controlling secondary pollutant formation requires a detailed synthesis of laboratory measurements, in-situ plume following measurements with instrumented aircraft, and sophisticated photochemical and aerosol models (e.g. CMAQ).

The background research provided a stepping off point to the research areas carried out in this work. These areas are indicated in Table 2-2. Italicized tasks were added during the project.

Table 2-2 Emissions Research Areas Advanced during Project

1	Test and calibrate new PM/aerosol instruments at Forest Service Riverside Fire Lab
2	Exploratory studies of primary and secondary PM in UCR chamber
3	Measure gas/PM emissions from burns of chaparral in FS fire science lab
4	Measure gas/PM emissions from burns of oak woodlands in FS fire science lab
5	Measure gas/PM emissions from burns of longleaf pine in FS fire science lab
6	Measure gas/PM emissions from prescribed burns of chaparral and oak savannah/woodlands
7	Create emission rate data in EPA AP-42 format for gaseous, PM, metals and reactive gases
8	Compare AMS biomass markers in lab with field & aircraft data.
9	Extend exploratory studies of secondary reactions in UCR atmospheric chamber. Measure black carbon.
10	Collect data during prescribed burn of chaparral at California site.

2.3 Model the Contributions of Burning Relative to Other Sources

Fires are large emission area sources that release gases and particles into the troposphere and are associated with elevated ozone (O_3) levels, particulate matter (PM) pollution, and visibility degradation throughout the world. Accurately estimating the magnitude, timing, location, and plume dynamics of fire emissions is both a challenging problem in emissions modeling and a key uncertainty for evaluating the impacts of these sources on ambient air quality. Wiedenmeyer et al. (2006) developed a method for estimating fire emissions in North and Central America using a combination of satellite and ground-based measurements. Different groups have developed fire emissions estimates on both regional (Air Sciences, Inc., 2004, 2005; Dennis, et al., 2005) and global scales (Hoelzemann et al., 2004; Ito and Penner, 2004) for specific fire events or fire seasons. Fire models also exist for estimating fire emissions from local fuel loading and moisture information (Anderson et al., 2004). In the most extensive fire emissions study in the U.S., the Western Regional Air Partnership (WRAP) prepared emissions inventories for wild fires, prescribed burning and agricultural burning for the western US for calendar year 2002 (Air Sciences, Inc., 2004, 2005). WRAP also completed modeling studies of the effects of each fire type on visibility and regional haze (Tonnesen et al., 2005, 2006). WRAP developed inventories of all fires during 2002, and developed estimates of mass emissions rates, diurnal profiles, plume rise height and chemical speciation for each fire type. For air quality modeling, the Sparse Matrix Operator Kernel Emissions (SMOKE) processing system (CEP, 2005) was used to prepare the fire emissions for input to the CMAQ or CAMx air quality modeling systems. Due to

the lack of adequate data on the composition of fire emissions, a simplified chemical speciation profile was used to estimate the chemical species used in the CMAQ model.

The air quality model also simulates the photochemical formation of secondary organic aerosols (SOA) from the fire gas VOC emissions. The WRAP diurnal profiles assume that the majority of emissions occur during the day with much lower smoldering emissions at other hours. Fire emissions can be lofted vertically several hundreds if not thousands of meters, depending on the fire size, fuel conditions, and meteorology. Two different approaches have been implemented in SMOKE for extending the emissions from fires into the aloft layers of air quality models. An early approach developed by the WRAP uses default assumptions for fire plume rise height based solely on fire size. A recently implemented approach (Adelman et al., 2007) uses fire heat flux and local meteorology data to calculate plume rise height for each individual fire. There have been limited comparisons of these two approaches (e.g., see Adelman et al., 2007), but without new data to evaluate the plume rise algorithms it is not yet possible to judge which approach is more correct. There are significant uncertainties in each of the emissions parameters summarized above, and the lab and field studies proposed in this project are designed to develop improved data for mass emissions rates, gas and PM chemical speciation, diurnal profiles, and plume rise heights. Research areas for this project are listed in Table 2-3.

During the project two goals were added. Goal 4 recognized the complexity of CMAQ and investigated alternatives widely used in modeling smoke, namely Bluesky and SMARTFIRE. One of the prescribed burns was used to compare the two methods. The added fifth goal of comparing CMAQ v4.7 and v5.0 did not occur as the EPA release of v5 was late.

Table 2-3 Air Quality Modeling Emissions Research Areas Advanced during Project

1	Explore model sensitivity to input of total emissions, emission speciation and plume rise.
2	Validate model performance with new data from controlled burns.
3	Model impact of marine air on emissions.
4	Compare AQ results using fire emissions from Bluesky framework and SMARTFIRE
5	Air quality modeling with CMAQ v4.7 & v5.0

3 Materials and Methods:

This section is intended to provide enough detail about experimental design and technique to enable another researcher to repeat the effort. However, details are not provided if the methods and results are covered in a peer reviewed article. As explained earlier, the project needed multiple experts to reach the final goal. Further the work was organized and carried out in a sequence of steps that permitted subsequent goals areas to build on the results of earlier steps. The approach for this project is outlined in Figure 3-1 and that order is used to present information in this section.

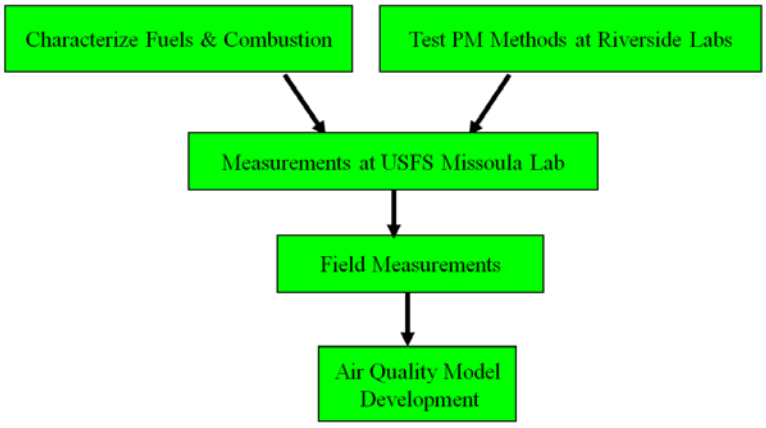

Figure 3-1 Technical Approach Followed a Series of Steps

3.1 Improve Characterization of Fuels and Combustion

The proposal received support from five DoD sites in the West ranging from near the border with Mexico in eastern Arizona to Monterey, California (Figure 3-2). Plant species varied at each site so it was important to meet with personnel at each site to discuss their participation.

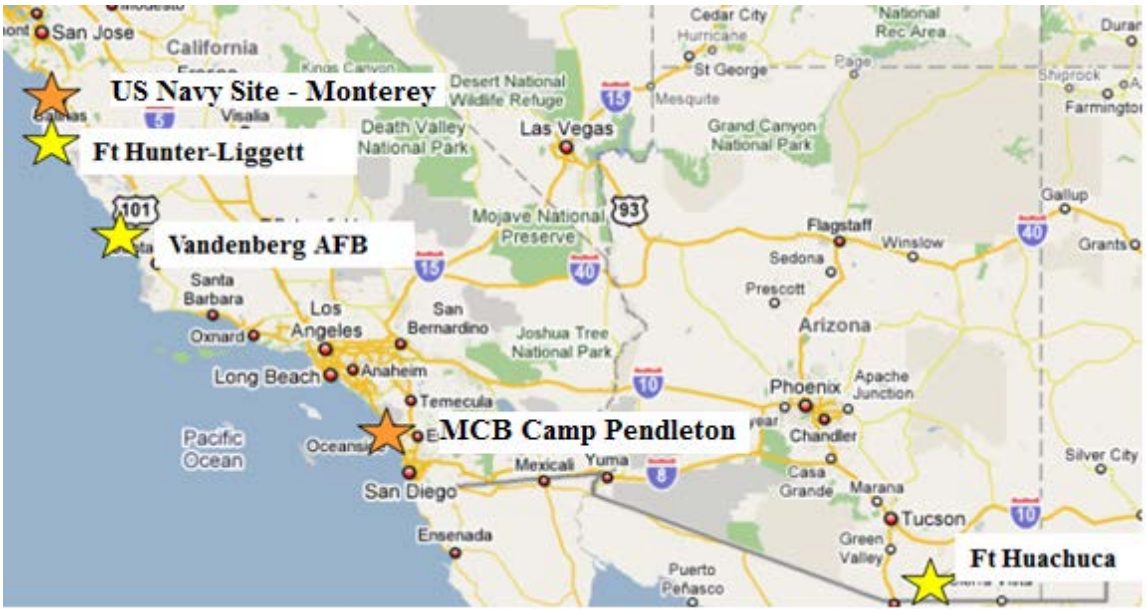

Figure 3-2 DoD Partner Sites in the West for SERDP Proposal

3.1.1 Identify the fuel types of interest to DOD facilities in California and Arizona.

While five sites supported the proposal, two sites were dropped during the project. Camp Pendleton had permitting problems and the Navy post graduate school in Monterey was too busy to provide the meteorological data. Thus we focused on three facilities –Vandenberg AFB and Forts Hunter-Liggett and Huachuca - where we could have burns of fuels in the laboratory and in the field that were representative of the Southwest.

Meetings were held with Fire Department personnel at Vandenberg AFB (AFV --Dan Ardoin, Mark Smith), Fort Hunter-Liggett (FHL --Jeff Minetti, Kevin Dougherty), and Fort Huachuca (HUA --Andrew Leiendecker, Wes Camp) in November 2008 and January 2009 to identify specific areas and fuel types where prescribed burns were planned for 2009 and 2010. A typical fire plan is shown in Figure 3-3. At the meetings, we explained a key element of the proposed SERDP project work was to learn more about which plant species were at their site and how we planned to get emissions factors from a series of lab burns under controlled conditions at the US Forest Service lab in Montana laboratory. After the lab burns, we would require field burns to validate the lab data so we talked about our participation in collection of field data during either the small-scale fires used for training or during prescribed burns. Each of their scheduled burns had a designated time so it was important to learn their 'burn' schedule matched the available time on the US Forest Service twin Otter plane. As a result of the discussions, Field tests were planned at Vandenberg AFB, Fort Huachuca and Fort Hunter-Liggett.

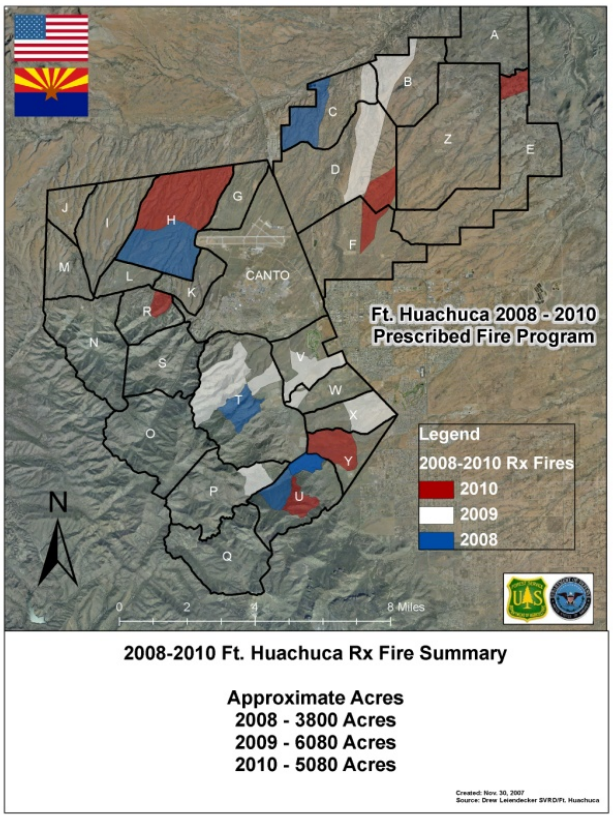

Figure 3-3 Burn Plan for Ft. Huachuca

The southwestern fuel types Identified by DoD personnel for prescribed burns during the meetings at the three facilities are listed in Table 3-1. Some information was available on the same plant species but not from the same sites. Older fuel loading data were found in the USFS Fuel Characteristic Classification System (Ottmar et al., 2007) and in existing photo series. Fuel bed descriptions from the original (Albini 1976) and the expanded fire behavior fuel models (Scott and Burgan 2005) were included in this project.

Table 3-1 Southwestern Fuel Types Identified by DoD Personnel for Prescribed Burns. Camp Lejeune and Fort Benning Fuel Types Studied by RC-1649 and RC-1647, respectively.

Location	Fuel type (fuel code)	Figure	Species
Fort Hunter-Liggett	Chamise, scrub oak (chs)	Figure 3-4	chamise (*Adenostoma fasciculatum),*scrub oak *(Quercus berberidifolia)*
	Ceanothus (cea)	Figure 3-5	chaparral whitethorn (*Ceanothus leucodermis*)
Vandenberg AFB	Maritime chaparral (mch)	Figure 3-6	Santa Barbara ceanothus (*Ceanothus impressus* var. *impressus),* sedgeleaf buckbrush (*Ceanothus cuneatus* var. *fascicularis),* black sage (*Salvia mellifera)*
	Coastal sage scrub (cos)	Figure 3-7	*Salvia mellifera*, California goldenbush (*Ericameria ericoides),* California sagebrush (*Artemisia californica)*
	California sagebrush (cas)	Figure 3-8	*Artemisia californica, Ericameria ericoides*
	Manzanita (man)	Figure 3-9	shagbark manzanita (*Arctostaphylos rudis),* La Purissima manzanita (*Arctostaphylos purissima)*
Fort Huachuca	Oak savanna (oas)	Figure 3-10	Emory oak (*Quercus emoryi),* Lehmann lovegrass (*Eragrostis lehmanniana)*
	Oak woodland (oaw)	Figure 3-11	*Quercus emoryi,* pointleaf manzanita (*Arctostaphylos pungens)*
	Masticated mesquite (mes)		velvet mesquite (*Prosopis velutina),* desertbroom (*Baccharis sarothroides)*
Camp Lejeune	1 year herbaceous (1yr)		Lyonia lucida, Ilex glabra
	2 year herbaceous (2yr)		Lyonia lucida, Ilex glabra
	Chipped understory hardwood (cuh)		Acer rubrum, Persea borbonia, Gordonia lasianthus
	Understory hardwood (uh)		Acer rubrum, Persea borbonia, Gordonia lasianthus
	Pocosin (poc)		Lyonia lucida, Ilex glabra
Fort Benning	Pine needles (lit)		Pinus taeda, Pinus echinata, Pinus elliottii, Pinus palustris

Subsequent to the on-site meetings, a series of photographs were taken by the US Forest Service experts to provide visual data of a representative stand of the particular plant species. Such photos are used to provide easy identification of the plant species and the fuel geometry in a natural setting. These photos were to serve as references for the geometry/arrangement of the field examples in the combustion laboratory so the lab burns would simulate natural fires. As explained later, lab samples with the same geometry as found in nature did not burn well so a special geometry was designed to provide more data from the laboratory burns.

Figure 3-4 Chamise and Scrub Oak Fuel Type – Fort Hunter-Liggett (1/13/2009)

Figure 3-5 Ceanothus Fuel Type – Fort Hunter-Liggett (1/13/2009)

Figure 3-6 Maritime Chaparral Fuel Type – Vandenberg AFB (1/14/2009)

Figure 3-7 Coastal Sage Scrub Fuel Type – Vandenberg AFB (1/14/2009)

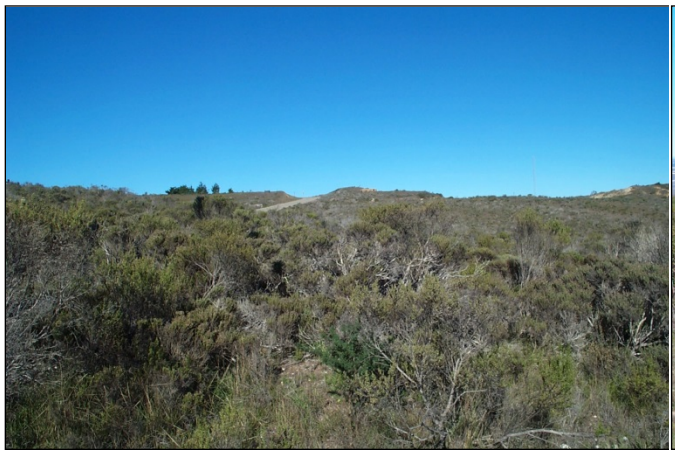

Figure 3-8 California Sagebrush Fuel Type – Vandenberg AFB (1/14/2009)

Figure 3-9 Manzanita Fuel Type – Vandenberg AFB (1/14/2009)

Figure 3-10 Emory Oak Savanna Fuel Type – Fort Huachuca (1/21/2009)

Figure 3-11 Emory Oak Woodland Fuel Type – Coronado National Forest (1/21/2009)

3.1.2 Conduct field sampling to describe fuel types in terms of loading by size class, fuel bed depths, and fuel bed structure.

Because the primary objective of this research was to develop emission factors for chaparral and grass fuels, field sampling focused on these fuels. Pre- and post-fire fuel sampling was used to estimate the amount and type of fuels consumed during the lab test burns associated with the prescribed burns in chaparral. Chaparral fuels data exist in the literature (Countryman and Philpot, 1970; Rothermel and Philpot, 1972; Regelbrugge and Conard, 1994; Riggan et al., 1994; Hardy et al., 1996; Ottmar et al., 2000). Most of the studies were conducted south of the DoD bases in this study.

In order to characterize the fuels, fuel bed height, canopy depth, species composition, and loading by size class were sampled in 1 m x 10 m rectangular plots within areas that were scheduled to be burned using prescribed fire at AFV, FHL, and HUA as shown in Figure 3-12. A minimum of 10 plots were located within each burn area. If necessary, the burn area was stratified by fuel type and sampling occurred in each fuel type. Each rectangular plot was permanently marked and subdivided into 10 1 m^2 subplots and oriented perpendicular to the slope. Fuel bed height and height to the shrub crown base were measured along the outer edges of the plot at 1 m intervals. Fuel bed depth is the difference in these two height measures. The shrub species was recorded at each point also. These measurements enabled us to calculate derived fuel bed properties such as bulk density and porosity.

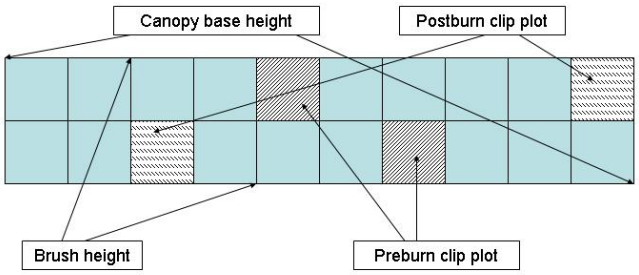

Figure 3-12 Plot Layout for Fuel Characterization

Past research has shown that fuels < 1.27 cm diameter constitute the bulk of the fuel consumed in chaparral fires; however, fire behavior fuels are described in size classes <0.63 cm, 0.63-2.54

cm, 2.54-7.62 cm. Double sampling was used to estimate the fuel loading by size class (Cox 1952, Freese 1962). The total loading of all foliage and branches < 2.54 cm were visually estimated for all 10 subplots. Within a plot, two (1 pre-burn, 1 post-burn) of the 10 subplots were randomly selected and all fuel < 2.54 cm were harvested and separated into 2 size classes (< 0.63 cm, 0.63-2.54 cm). Two samples of the material were collected for fuel moisture content determination in the lab by oven-drying. For each m^2 subplot, the moisture content samples were averaged and used to estimate the dry mass of the field-weighed samples. A regression between the estimated and clipped fuel loadings is being developed and used to estimate loading of the estimated subplots. Litter and duff were collected from these two subplots for lab processing. Fuel consumption will be estimated following the prescribed burn by performing the same ocular estimates of fuel loading for each subplot and harvesting all burned material < 2.54 cm in diameter. Litter and duff will also be collected as part of the post-burn sampling. The same procedures will be used for the lighter grass fuels (grass, herbaceous) except crown base height will not be measured.

3.1.3 Conduct lab analyses of dominant plant species by fuel type to provide elemental analysis information for emissions

Samples of each of the fuels in Table 3-1 were harvested in January 2009 and shipped to Missoula, MT to be burned in the laboratory phase of the project. Chamise and scrub oak were harvested along McKern Trail in Training Area 11 at Fort Hunter-Liggett (FL). Maritime chaparral and coastal sage scrub were harvested on a tableland north of San Antonio Creek while the Manzanita and California sagebrush fuel types were harvested on Lompoc Terrace at Vandenberg Air Force Base (AFV). The Emory oak savanna fuel type was collected at Fort Huachuca (HUA) and the Emory oak woodland type was collected on the Coronado National Forest south of HUA since access to the training area at HUA was restricted during our visit. Approximately 8-10 kg of each fuel type was shipped in large boxes to maintain as much plant structure as possible.

The harvested plants were divided into small samples, dried and ground for elemental analysis for carbon, hydrogen, nitrogen, oxygen and sulfur at both UC Riverside and Missoula Fire Labs. The harvested plants were analyzed for chemical composition by first grinding the plant tissues (wood and foliage) into a uniform coarse material using a Thomas Model 4 Wiley® Mill[1]. The samples were further ground to extremely fine particles using a mortar grinder. Approximately 5g of each fuel sample was analyzed for carbon, hydrogen, nitrogen, sulfur and oxygen (C, H, N, S, O) using a Thermo Fisher Scientific FlashEA 1112 Series Elemental Analyzer. The vegetation components comprising the fuel beds were also analyzed for selected elements by an outside laboratory (University of Idaho Analytical Sciences Laboratory) for chlorine, potassium and sodium (Cl, K, Na) content.

3.2 Multiple Platforms for Emissions Measurements

The measurement of emissions and the development of emission factors was the core deliverable of the project; a goal for which over 50% of the funding was allocated. Accordingly there were a number of approaches and research platforms or tools proposed in the original work plan since no single approach or tool could be expected to provide all the answers. Among the team

[1] The use of trade names is provided for informational purposes only and does not constitute endorsement by the U.S. Department of Agriculture or Department of Defense.

members, UCR was the partner primarily charged with measuring the chemical and physical nature of the particulate matter released from the fire. Toward that end, UCR had proposed several unique instruments which would be used for the first time in characterizing fires. One example was the aerosol mass spectrometer (AMS). The AMS was designed and sold as a lab unit for measuring the properties of aerosols in ambient air, not air laden with soot from a roaring fire. Accordingly the AMS needed to be tested and adjusted for heavy concentrations of particles in the US Forest Service lab in Riverside before shipping it off to Montana as explained below. The description and measurement capability of the research labs are listed in Table 3-2.

Table 3-2 Different Research Platforms used for Measuring Emissions

Platform	Measures			Description
	Gases	**PM**	**Other**	
UCR laboratory reactors	✓	✓	✓	Used for O_3 & secondary aerosol studies; has latest instruments.
US Forest Service -- Riverside Fire Lab (RFL)		✓		Small scale facility; useful for pilot burns & tests of UCR gaseous & PM instruments.
USFS -- Missoula Fire Sciences Lab (MFSL)	✓	✓	✓	Best fire simulation lab with 2 ton gas & PM instrument capability. Captures full emissions.
DoD field sites	✓	✓	✓	Location of prescribed burns & collection of field data for model validation.

3.3 Exploratory Equipment Testing

One of the key goals for the project was to apply new gaseous and PM/aerosol measurement methods in order to expand the knowledge about the properties of gaseous and aerosol emissions from biomass burning. The Battelle-University of Montana project team was focusing on new gaseous methods. UCR was responsible for providing aerosol instruments that were proven for measurement at the levels of pollutants found at atmospheric levels. However, UCR did not have experience with their instruments at the high levels associated with biomass burning, including elevated organic aerosol loadings and a heavily oxygenated aerosol. The plan was to carry out a series of exploratory trials with a goal of determining the best operating conditions for the UCR instruments.

With the demanding test schedule planned for the USFS Montana Fire Science Lab (MFSL) it was important to carry out exploratory tests in Riverside and learn how to tailor the atmospheric instruments to operate at the higher concentrations that were anticipated in Montana. The USFS Fire Lab (RFFL) at Riverside does not have the capabilities of MFSL so a temporary sampling system was constructed including: 1) adding a horizontal duct above the fire pit with large enough conical hood to capture most of the emissions; 2) installing a fan at the duct exit to develop a draft inside the duct to equal that of the natural fire and 3) adding a sampling system. A schematic of the experimental setup is shown in Figure 3-13 and actual photos of the experimental setup are provided in Figure 3-14. Note the aerosol sampling probe faced

downstream in order to avoid macro PM fragments from the combustion process that might have damaged the UCR instruments.

At the same time that we planned to test the specialized atmospheric instruments the USFS presented the team with a project to measure the impact of adding low-density polyethylene film to woodpiles. In California covering the woodpiles with polyethylene film defines the whole pile as trash and trash burning is not permitted. Thus the project to adapt the AMS and other instruments to fire conditions was enriched by the new project. The performed study focused on assessment of whether or not inclusion of LDPE in simulated silvicultural piled debris altered smoke emissions.

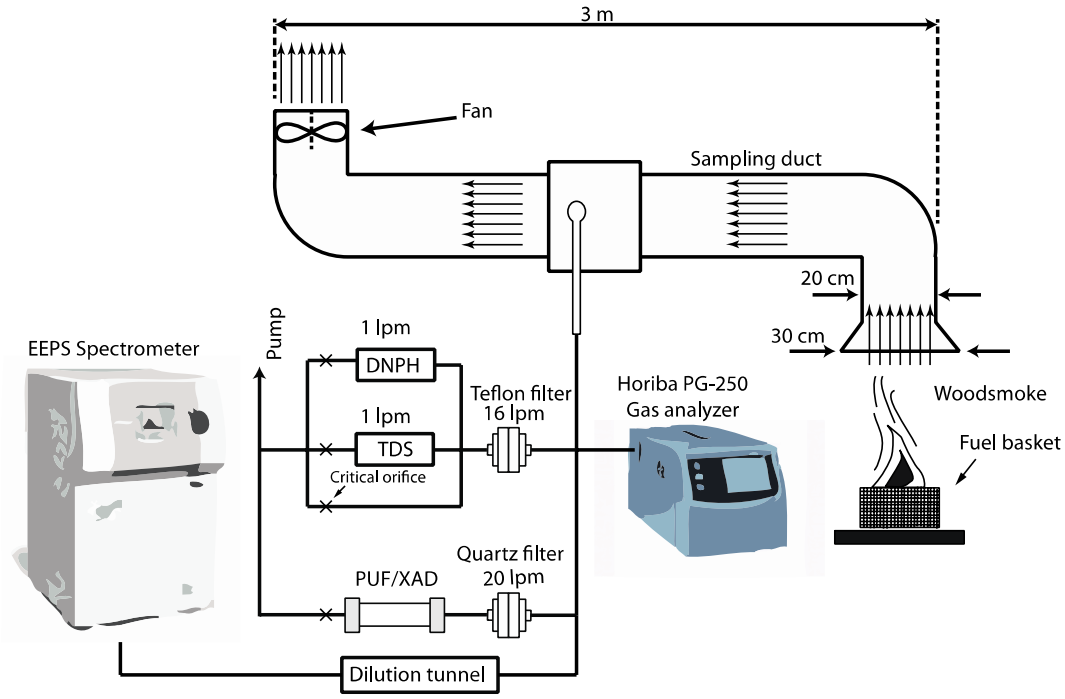

Figure 3-13 Schematic of Experimental Setup

Three replicates of manzanita (*Arctostaphylos sp*) branches (2 kg) up to 2.54 cm diameter with three levels of LDPE (0, 5, or 50 g) were burned in a coarse mesh basket so the air freely flowed inside the pile (n=9). The basket was placed on insulated bricks underneath the hood.

For all tests, we measured the gas concentrations for NO_x, CO, CO_2 and air toxics, including PAHs. PM mass was collected on Quartz and Teflon®[2] filters. For the particulate phase, a two-stage diluter with a dilution ratio of about 17 was made and used. Continuous measurements of PM were made with an EEPS for fast particle size distribution measurements and DustTrak™ for measuring mass concentration. In addition we tested the AMS, PTR-MS, and SMPS. Overall the exploratory experiments were successful and gave us confidence that the instruments designed for atmospheric levels could be adapted to the higher level expected at MFSL.

[2] The use of trade names is provided for informational purposes only and does not constitute endorsement by the U.S. Department of Agriculture.

Figure 3-14 Actual Photographs of the Experimental Setup at the Riverside Fire Lab

3.3.1 RFL Trials: Gaseous Emissions

The concentrations of criteria pollutants and CO_2 gases in the raw exhaust and the dilution tunnel were measured with a Horiba PG-250 portable multi-gas analyzer. The PG-250 simultaneously measures up to five separate gas components using the measurement methods recommended by the EPA. The signal output of the instrument was interfaced directly with a laptop computer through an RS-232C interface to record measured values continuously. Major features of the Horiba PG-250 include a built-in sample conditioning system with sample pump, filters, and a thermoelectric cooler. The performance of the Horiba PG-250 was tested and verified under the U.S. EPA ETV program. Details of the gases and the ranges for the Horiba instrument are shown in Table 3-3. Note that the Horiba instrument measured sulfur dioxide (SO_2); however, reference ISO 8178-1 reports that the direct measurement for SO_2 is usually less precise than calculating the concentration from fuel sulfur analysis and assuming that the fuel sulfur is converted to sulfur dioxide.

For quality control, UCR carried out analyzer checks with calibration gases both before and after each test to check for drift. The measured drift is used to correct measurements made during the monitoring period. Because the instrument measures the concentration of five gases, the EPA protocol gases were used for calibration and consisted of a blend of several gases (super-blend) made to within 1% specifications. Drift was determined to be within manufacturer specifications of ± 1% full scale per day, except for SO_2 set at ± 2% F.S./day.

Table 3-3 Operating Ranges for the Horiba PG-250 Instrument

Component	Detector	Ranges
Nitrogen Oxides (NOx)	Heated Chemiluminescence Detector (HCLD)	0-25, 50, 100, 250, 500, 1000, & 2500 ppmv
Carbon Monoxide (CO)	Non dispersive Infrared Absorption (NDIR)	0-200, 500, 1000, 2000, & 5000 ppmv
Carbon Dioxide (CO_2)	Non dispersive Infrared Absorption (NDIR)	0-5, 10, & 20 vol%
Sulfur Dioxide (SO_2)	Non dispersive Infrared Absorption (NDIR)	0-200, 500, 1000, & 3000 ppmv
Oxygen	Zirconium oxide sensor	0-5, 10, & 25 vol%

Carbonyls were collected on 2,4-dinitrophenylhydrazine (DNPH) coated silica cartridges (Waters Corp., Milford, MA) behind the Teflon® filter as shown in Figure 3-13. A critical flow orifice was used to control the 1.0 LPM flow through the cartridge. Sampled cartridges are extracted using 5 mL of acetonitrile and injected into Agilent 1100 series high performance liquid chromatograph (HPLC) equipped with a diode array detector. The column used was a 5 µm Deltabond AK resolution (200cm x 4.6mm ID) with upstream guard column. The HPLC sample injection and operating conditions were set up according to the specifications of the SAE 930142HP protocol.

Light Hydrocarbons (C_4 to C_{10}), with special emphasis on 1,3 butadiene; benzene; toluene; ethylbenzene and xylenes. Hundreds of molecules starting about C_4 (butadiene) through C_{10} were collected and concentrated on an adsorbent column composed with a multi-bed carbon bed including molecular sieve, activated charcoal, and carbotrap resin and analyzed by desorption into a gas chromatograph (GC). The most volatile compounds in the exhaust gas are adsorbed first and the remaining compounds will adsorb sequentially in relation to their volatility. Flow through the TDS tube was controlled by a critical flow orifice to about of 0.081 liters/minute. The GC sample injection, column, and operating condition are set up according to the specifications of SAE 930142HP Method-2 for C_4-C_{12} hydrocarbons.

Heavy Hydrocarbons (C_{10} to C_{30}), including naphthalene and poly aromatic hydrocarbons (PAHs). The diluted exhaust was collected through a quartz filter and into a column packed with polyurethane foam (PUF)/XAD-4 resin. A portion of the quartz filter was used to analyze for the elemental and organic carbon, as described in the previous section. Both the PUF/XAD-4 cartridge and the remainder of quartz filter was extracted with methylene chloride and analyzed using a modified method EPA TO13A protocol (GC-MS analysis) to determine total emission rates for PAHs and n-alkanes. Details on the analysis method are found in Shah et al., 2004.

3.3.2 RFL Trials: Real-Time Trace Gaseous Emissions

Proton Transfer Reaction - Mass Spectrometry (PTR-MS) is a very sensitive technique for online monitoring of volatile organic compounds (VOCs) in ambient air. The PTR-MS instrument consists of an ion source that is directly connected to a drift tube plus an analyzing system, like a quadrupole mass analyzer. Commercially available PTR-MS instruments have a response time of about 100ms and reach a detection limit in the single digit pptv region. The PTR-MS allows direct analysis of ambient samples and absolute concentrations to be determined without calibration. Its use is limited for molecules at high concentrations and for which the

proton affinity is low so a challenge of the RFL trials was to design a dilution system that adapted the PTRMS to the planned burns at MFSL.

3.3.3 RFL Trials: Particulate Matter (PM) Mass Emissions

A raw particulate sampling probe was fitted close to and upstream of the raw gaseous sample probe in the exhaust. In order to measure PM mass, a sampling probe was inserted into the end of the dilution tunnel (>10 diameters downstream) and directed to a PM sample splitter that allowed up to three samples to be collected. For the fire testing, we used two lines with 47 Gelman filter holders, one for collecting PM on a Teflon® filter and the other for collecting PM on a quartz filter. Thus the flow in the dilution tunnel was split into two fractions, a smaller flow for measuring PM mass and PM properties and a much larger flow that was vented outside the vessel. Note with the partial dilution approach for measuring gases and PM that it is critical for the dilution ratio be determined very accurately.

UCR collected simultaneous Teflon® and quartz filters at each operating mode and analyzed them according to standard procedures. The simultaneous collection of quartz and Teflon® filters allowed an internal quality check of the PM mass. Teflon® (Teflo) filters used to acquire PM mass weighted following the procedure of the Code of Federal Regulations (CFR) (40 CFR Part 86). Briefly, total PM were collected on Pall Gelman (Ann Arbor, MI) 47 mm Teflo filters and weighed using a Cahn (Madison, WI) C-35 microbalance. Before and after collection, the filters were conditioned for 24 hours in an environmentally controlled room (RH = 40%, T = 25° C) and weighed daily until two consecutive weight measurements were within 3 μg.

PM samples were collected in parallel on 2500 QAT-UP Tissuquartz Pall (Ann Arbor, MI) 47 mm filters that were preconditioned at 600°C for 5 h. A 1.5 cm^2 punch was cut out from the quartz filter and analyzed with a Sunset Laboratory (Forest Grove, OR) Thermal/Optical Carbon Aerosol Analyzer according to the NIOSH 5040 reference method (NIOSH 1996). All PM filters were sealed in containers immediately after sampling, and kept chilled until analyzed.

3.3.4 RFL Trials: Real-Time PM Emissions by AMS

The Aerosol mass spectrometer (AMS) was a key instrument in the proposal, providing the first real time data about: 1) organic components including HOA (hydrocarbon-like organic aerosol, linked to primary combustion sources) and OOA (oxygenated organic aerosol, linked to secondary aerosol sources; 2) elemental composition (O:C, H:C) and 3) direct linear detection of sulfate, nitrate, ammonium, chloride and organic aerosol species. The AMS was the only instrument capable of providing quantitative size and chemical mass loading information in real-time for non-refractory sub-micron aerosol particles. The AMS was intended to be mounted on the instrument platform and provide organic aerosol quantification and analysis with a fast response, up to 100 Hz.

The AMS schematic is shown in Figure 3-15. It couples size-resolved particle sampling and mass spectrometric techniques into a single real-time measurement system. Aerosol particles in the size range 0.04 to ~1.0 micrometers are sampled into a high vacuum system where they are aerodynamically focused into a narrow beam (~1 mm diameter). The particle beam is directed onto a resistively heated surface where volatile and semi-volatile chemical components are thermally vaporized and detected with 70eV electron impact ionization quadrupole mass spectrometry. Particle aerodynamic diameter is determined from particle time-of-flight (velocity) measurements using a beam chopping technique. This approach provides universal detection of chemical species that vaporize (in <1 sec) at 200 to 900C (typically 600 C). This non-refractory

fraction includes the majority of atmospheric components, with the notable exception of elemental carbon and crustal oxides (dust). Some inorganic components (e.g., sea-salt) require vaporization at higher temperature (900 C).

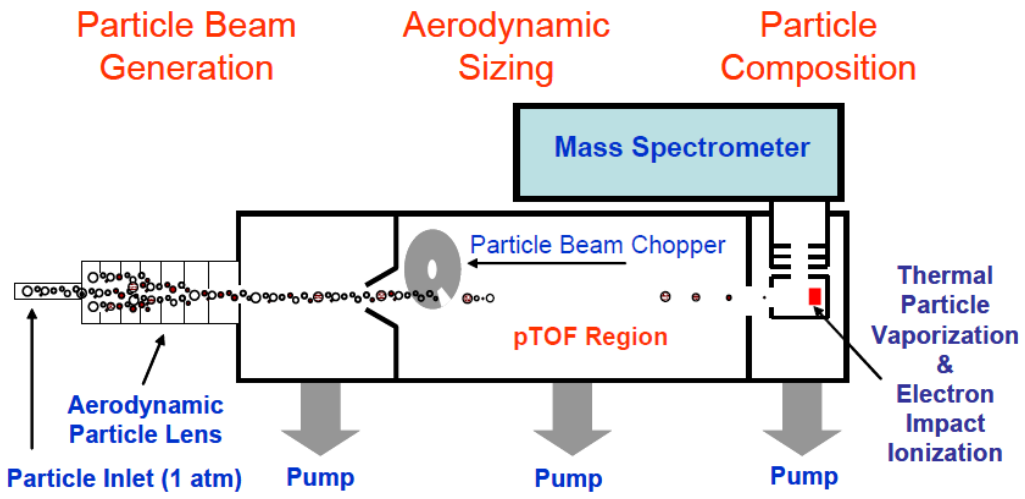

Figure 3-15 Schematic of an Aerosol Mass Spectrometer

3.3.5 RFL Trials: Real-Time PM Emissions by EEPS

An **Engine Exhaust Particle Sizer Spectrometer** (EEPS) Model 3090 from TSI was used for measuring the size distribution of particles. The Engine Exhaust Particle Sizer spectrometer (EEPS) measures particle emissions in the sub-micrometer range from 5.6 to 560 nm with data collected at 10Hz. The EEPS spectrometer displays measurements in 32 channels total (16 channels per decade) and operates over a wide particle concentration range, including down to 200 particles/cm^3. This instrument allowed us to monitor a continuous time resolved size distribution of the particles

3.3.6 RFL Trials: Real-Time PM Emissions by DustTrak™

In addition to the PM mass filter-based measurements, UCR recorded data with a nephelometer (TSI DustTrak™ 8520) as the combustion process is highly transient and that information is not captured with filter samples. Nephelometers are fairly simple and compact instruments with excellent sensitivity and time resolution. Nephelometers measure light scattered by aerosol introduced into their sample chamber. However, scattering per unit mass is a strong function of particle size and refractive index. If particle size distributions and refractive indices in the exhaust strongly depend on the particular engine and operating condition, this may not be an effective way to measure exhaust particle mass. UCR has shown that mass scattering efficiencies for both on-road diesel exhaust and ambient fine particles have values around $3m^2/g$. For this project, a TSI DustTrak™ 8520 nephelometer measuring 90° light scattering at 780nm (near-infrared) was used. While the instrument displays its measurement as mass density (i.e., units of mg/m^3) the output was calibrated against the federal reference method, namely the particulate mass on the Teflon filters.

3.3.7 RFL Trials: Real-Time PM Emissions by DMM

According to the brochure the DMM is currently the most advanced PM mass measuring equipment available, measuring both solid and volatile particles with outstanding sensitivity and a fast time response. The instrument was used for measuring both number and mass concentration of particles down to concentrations below ambient levels. The minimum detectable concentration is as low as 1µg/m^3, and the data is still reported in real time, time resolution being 1Hz and time constant 2-3s. The dynamic range is also exceptionally wide, maximum concentration is 1000 µg/m^3, even higher for short periods of time. A schematic of the various sections of the instrument is shown in Figure 3-16.

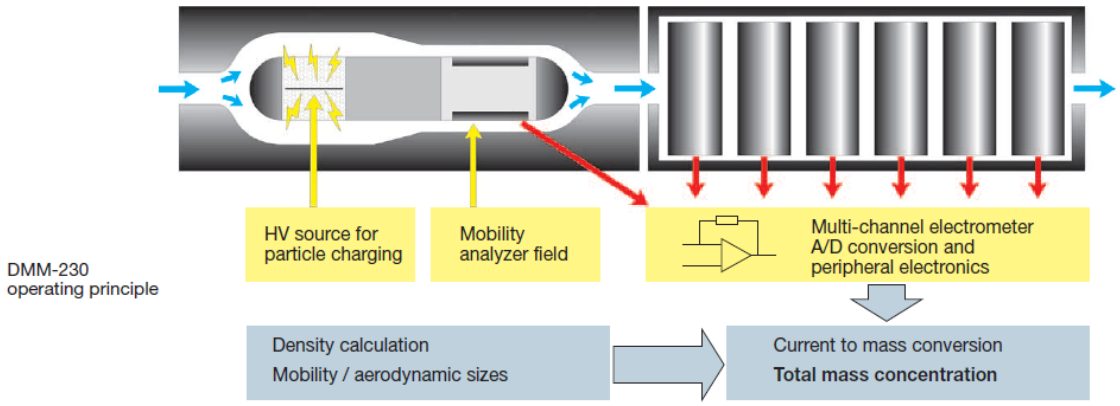

Figure 3-16 Schematic of the Dekati® Mass Monitor

3.3.8 RFL Trials: Real-Time PM Emissions by SMPS

Scanning Mobility Particle Sizers (SMPS) are a high resolution nanoparticle sizer that is the researcher's choice for nanoparticle size characterization. The SMPS measures the size distribution and concentration of particles in the size range of 2 nm to 1 μm using differential mobility analysis. The SMPS can measure a wide concentration range from 1 to 107 particles/cm^3 and can measure both uni- and multi-modal samples.

The method is based on the principle associated with a particle migrating through an electric field is fundamentally related to particle size; no size calibration is necessary. In a Differential Mobility Analyzer (DMA), an electric field is created and the airborne particles drift in the DMA according to their electrical mobility (Figure 3-17). Particle size is then calculated from the mobility distribution. This method is independent of the particle zeta potential.

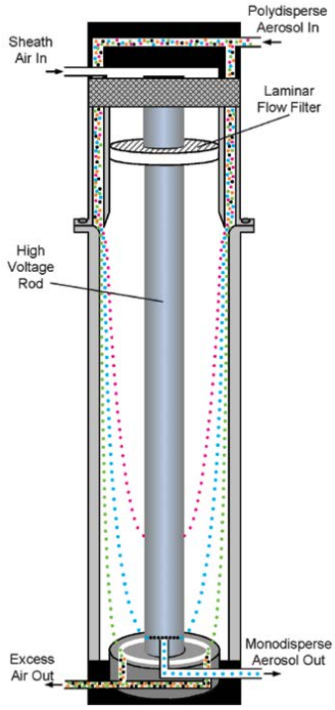

Figure 3-17 Differential Mobility Analyzer

3.4 Measurements at US Forest Service Missoula Lab (MFSL)

The next phase of the project moved to the combustion laboratory at the USDA Forest Service's Missoula Fire Science Laboratory (MFSL) in Missoula, MT. The facility, shown in Figure 3-18 measures 12.5 m by 12.5 m and is 22 m high. The combustion products from the fuel bed is exhausted via a 3.6 m diameter hood attached to a 1.6 m stack located in the center. The stack extends from 2 m above the floor to all the way up through the ceiling. Air velocity in the stack was set at 1.5 m/s or 3 m/s by controlling the exhaust fan speed. The lab is slightly pressurized with pre-conditioned outside air to precisely control the temperature, and relative humidity. This design ensures entrainment of all the produced emissions, making the conditions ideal for determining emissions factors.

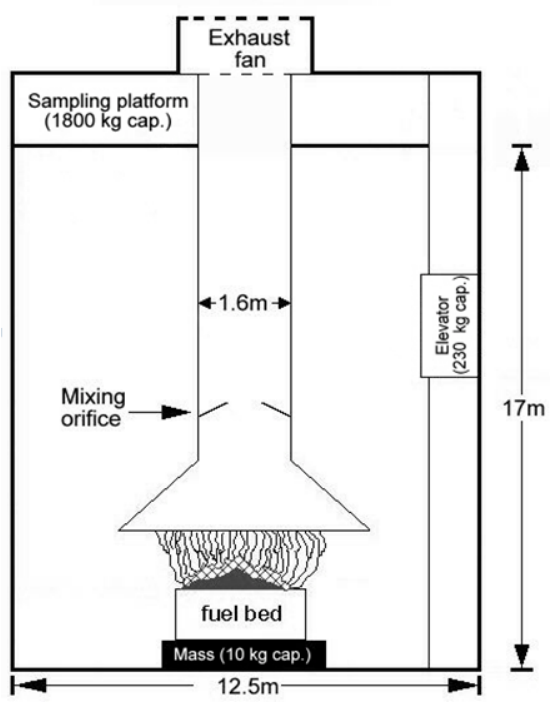

Figure 3-18 Design of Missoula Combustion Lab

An actual photo of the fuel bed and hood arrangement is seen in Figure 3-19 . The fuel type shown in the figure is excelsior, which is made of shredded aspen (*Populus tremuloides*) wood. This fuel has been used in laboratory fire spread experiments as a reference for decades. The fuel bed frame is placed on an electronic balance for continuous measurement of fuel mass. Nearly all fires are ignited with a propane torch; sometimes an isobutanol starter is needed.

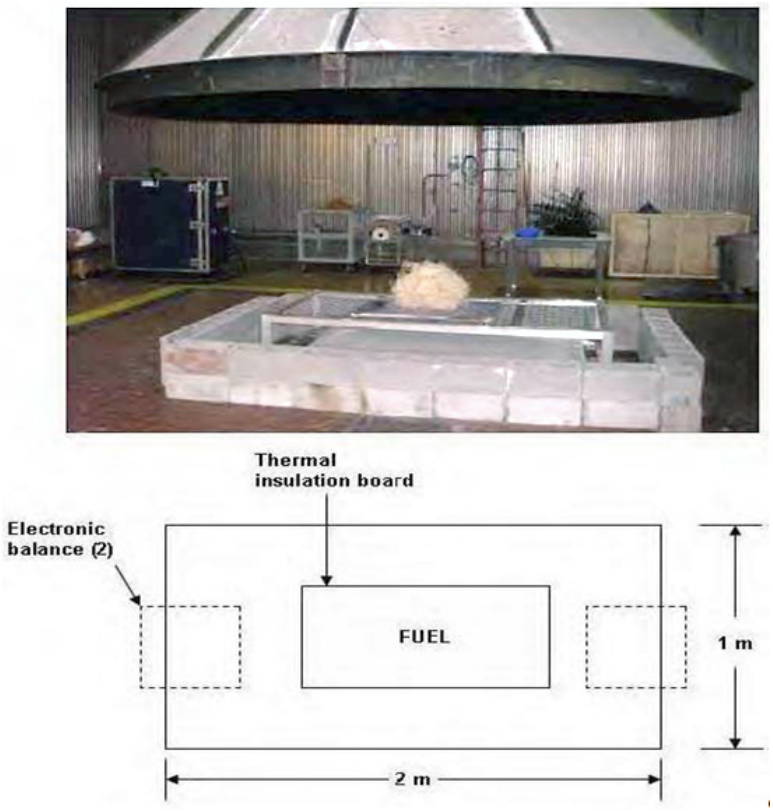

Figure 3-19 Picture of Fuel Bed and Hood to Collect Emissions at MFSL

3.4.1 Design of Fuel Bed

Ideally the fuels burned at MFSL would have the same properties as in nature and burn like in the wild. Living fuels, such as shrubs and grasses, tend to be oriented vertically in the wild, and have about 70% moisture. However, after several weeks of storage at MFSL the fuel moisture is about 10% moisture, Hosseini et al 2010. To simulate the natural arrangement in the wild, the fuels in the original beds were vertically oriented in a frame; see Figure 3-20. However, average fuel consumption of the vertically oriented chamise/scrub oak fuel beds was ~30% and burning times were short. As a result the fuels were laid horizontally on the frame; see Figure 3-21. Average fuel consumption of horizontally oriented fuel beds increased to ~90% (Hosseini et al., 2010) and burning time increased appreciably.

Figure 3-20 (a) Natural Vertical Arrangement of Fuels (b) Resulted in Low Fuel Consumption

Figure 3-21 (a) Horizontal Arrangement of Fuels (b) Resulted in High Fuel Consumption

Results showed that the fuel burned vigorously for about 120 seconds, followed by ~180 seconds of smoldering as seen in Figure 3-22. Thus time was sufficient to get data both for the flaming and the smoldering regimes.

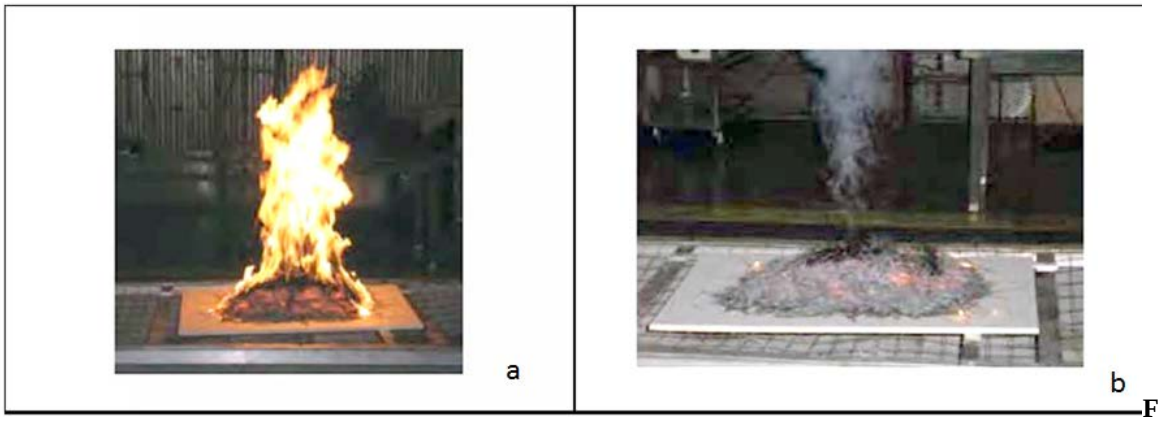

Figure 3-22 Example of (a) Flaming and (b) Smoldering Burns

3.4.2 Schematic of the Instruments at MFSL

Numerous analytical instruments were located on the sampling platform, each with a specific purpose, and the plan for their arrangement is shown in Figure 3-23.

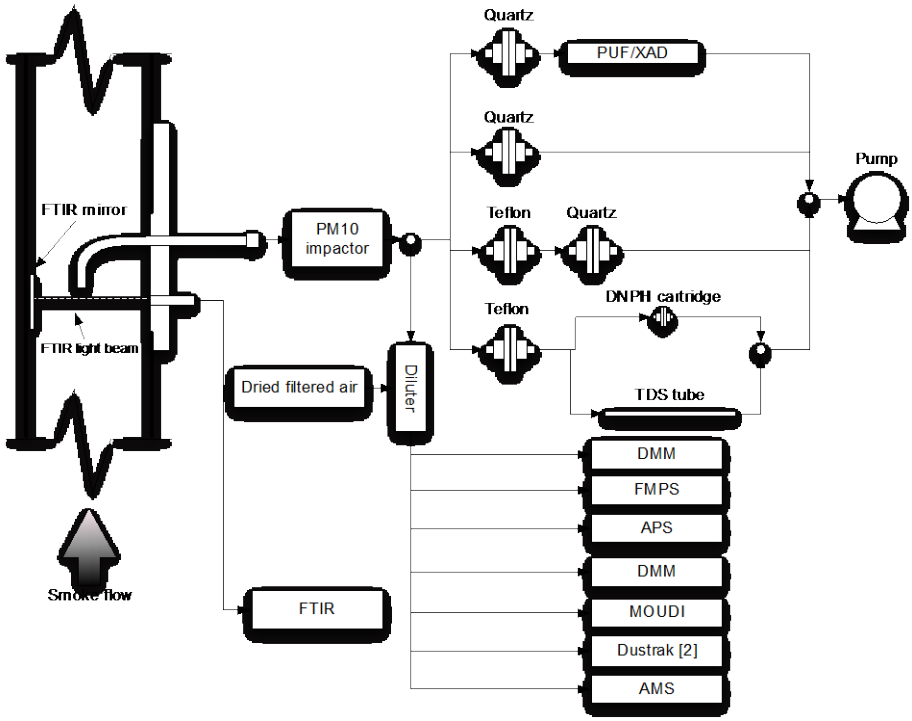

Figure 3-23 Schematic of the Suite of Instruments on Sampling Platform

The MFSL is one of the best, if not premier, laboratories designed for fire behavior and smoke emissions research and is well designed to measure emissions from biomass burning under environmental conditions that simulate actual conditions in the field. As evident in Figure 3-18, the design carries emissions from the fire on a fuel bed through a hood and stack arrangement to the roof. A sampling platform is located 17 m above the floor and has a number of permanently mounted sampling ports on the tunnel. It is reached using an elevator. All instruments for measuring gaseous and particle properties were located on the platform.

A collection of the instruments is shown in Table 3-4 and the resultant measurement from that instrument. This suite represented the largest collection of instruments ever used to measure emissions from biomass burning at the Missoula Lab with a special focus on the characterization of the aerosol. Another important point is that while some of the specialized instruments were used at Missoula before, this was the first time that the instruments were placed on the sampling platform. For example in past cases with the AMS, a 17 meter sampling line was constructed to bring the particles to the floor level. Clearly the quality of the data is significantly compromised as compared to when the sample is collected and analyzed on the sampling platform. Putting the AMS on the sampling platform required disassembly of the AMS on the floor level to fit the elevator and then reassembly on the sampling platform. With this decision, all of the PM monitoring equipment could be co-located on the sampling platform in this project.

Table 3-4 List & Purpose of Instruments on the Sampling Platform

Instrument	Measured Value
Gas concentration	
Five gas analyzer	CO,CO_2, O_2, SO_2, NOx
Open path FTIR (OP-FTIR)	CO2, CO ,CH4, multiple species concentration
Proton Transfer Reaction MS	Multiple hydrocarbon species
Canisters	Multiple hydrocarbon species
TDS,DNPH,PUF/XAD	Selected hydrocarbon species
Aerosol/Particulate properties	
Aerosol Mass Spectrometer (AMS)	Aerosol composition & size distribution
Aerodynamic Particle sizer (APS)	Real time, particle size distribution
Fast Mobility Particle Sizer	Real time, particle size distribution
Scanning Mobility Particle Sizer	Real time, particle size distribution
Micro-Orifice Uniform-Deposit Impactor (MOUDI)	Particle size distribution, composition
Condensation Particle Counter (CPC)	Number of particles
Dekati® Mass Monitor (DMM)	Real time, particle concentration, distribution
DC 2000CE	Particle surface area
Dustrack (DT)	Real time, particle concentration
Filter sampler (FS)	$PM_{2.5}$ mass
Filter sampler (FS)	Elemental & organic carbon

Prior to conducting the primary experiment, several preliminary tests were performed using pine needle fuel beds. Based on the repeatability of PM and other measurements from these preliminary tests, we were conducted a month long campaign of measuring the emissions from southwestern and southeastern fuels (selected by RC-1649 and RC-1647). Figure 3-24 provides an example of the measurements of the PM mass concentration as measured with a DustTrak™ from two similar burns.

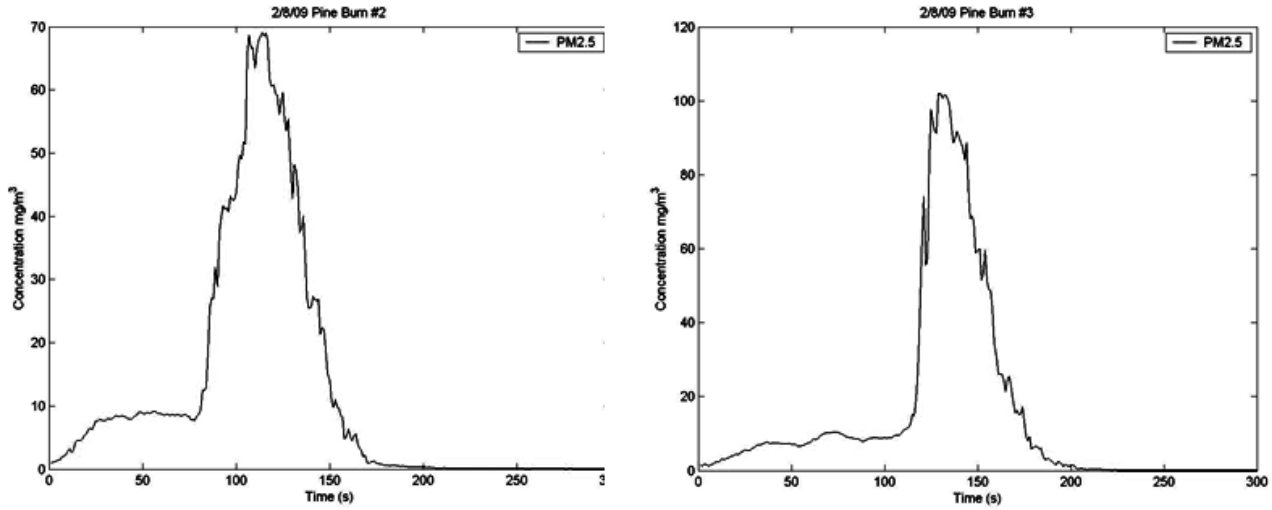

Figure 3-24 Example of Repeat PM Measurements with New Fuel Bed

3.4.3 Test Matrix of Burns at Missoula

As discussed earlier in Section 3.1.3, samples of fuels were harvested at the various participating facilities in January 2009 and shipped to Missoula, MT to be burned in the laboratory phase of the project. Approximately 8-10 kg of each fuel type was shipped in large boxes to maintain as much plant structure as possible. Mean characteristics of the fuel beds are found in Table 3-6. Average moisture content of the fuel beds at the time of burning ranged from 4 to 12% which is similar to fuel moistures in dead fuel beds. The moisture content in live fuel beds in chaparral seldom drops below 50% moisture content. The initial oven-dry mass in the fuel beds was approximately 2 kg. Bulk density of the fuel beds ranged from 5-14 kg m^{-3} and the packing ratio ranged from 0.009 to 0.024. These packing ratios are similar to those reported for laboratory fire spread experiments (Weise et al., 2005); however, they are 1 to 2 orders of magnitude larger than packing ratios observed in the field (Weise et al., 2011). Thus the fuel moisture and packing ratio for the laboratory burns were far from natural fuels. Furthermore as already discussed wet fuels of those arranged in vertical fashion as found naturally resulted in lab fires that were too short and only a small portion of the fuel was burned. Although fuel properties did not match the natural conditions, we also recognized that the heat transfer and burn intensity rates would not match the field conditions during wildfires and proceeded with the laboratory tests. We assumed that the dryer fuels and horizontal burn configuration would result in a more intense fire and provide emission factors closer to those from the flaming and smoldering regimes in field conditions.

During the testing, a total of 77 burns were conducted; however, only 70 of the burns were in wildland fuels pertinent to RC-1647, 1648, and 1649. Fuels were collected from Fort Hunter-Liggett, Vandenberg Air Force Base, and Fort Huachuca as part of RC-1648. Southeastern fuels were collected by RC-1647 from Fort Benning near Columbus, GA and by RC-1649 from Camp Lejeune in coastal North Carolina (Table 3-5). Properties of the southwestern fuel beds are provided in Table 3-6. The fuels collected by the three SERDP projects were burned in a

collaborative effort when all the PM instruments from RC-1648 were at Missoula FSL in order to have a richer data base for the aerosol characteristics. Southeastern fuels included:

- 1-year rough
- 2-year rough
- understory hardwoods, chipped understory hardwoods, pocosin, and pine litter (Burling et al., 2010).

Table 3-5 Wildland Fuels Burned at USFS Missoula Fire Science Lab

Test ID	Fuel Code[3]	Date	Ignition type[4]	Fuel Weight (g)	Installation[5]	Fuel Type
1	chs	2/10/2009	IA/BL	2376.80	FHL	Chamise, Scrub Oak
2	chs	2/10/2009	IA/BL	2442.80	FHL	Chamise, Scrub Oak
3	chs	2/10/2009	IA/BL	2571.9	FHL	Chamise, Scrub Oak
4	chs	2/11/2009	IA/BL	2415.00	FHL	Chamise, Scrub Oak
5	chs	2/11/2009	IA/BL	2303.10	FHL	Chamise, Scrub Oak
6	cea	2/11/2009	IA/BL	2100.60	FHL	Ceanothus
7	cea	2/11/2009	IA/BL	2347.20	FHL	Ceanothus
8	cea	2/12/2009	IA/BL	2401.90	FHL	Ceanothus
9	cea	2/12/2009	IA/BL	2413.40	FHL	Ceanothus
10	cea	2/12/2009	IA/BL	2240.30	FHL	Ceanothus
11	man	2/12/2009	IA/BL	3974.90	AFV	Manzanita
12	man	2/12/2009	IA/BL	4112.00	AFV	Manzanita
13	man	2/13/2009	IA/BL	4102.5	AFV	Manzanita
14	man	2/13/2009	IA/BL	2004.3	AFV	Manzanita
15	man	2/13/2009	IA/BL	3738.20	AFV	Manzanita
16	cas	2/13/2009	IA/BL	2961.00	AFV	California Sagebrush-Artemisia/Ericameria
17	cas	2/13/2009	IA/BL	2961.40	AFV	California Sagebrush-Artemisia/Ericameria
25	cas	2/17/2009	PT	28861.0	AFV	California Sagebrush-Artemisia/Ericameria
26	cas	2/17/2009	PT	28748.0	AFV	California Sagebrush-Artemisia/Ericameria
27	cas	2/17/2009	PT	28793.0	AFV	California Sagebrush-Artemisia/Ericameria
28	cos	2/17/2009	PT	28608.0	AFV	Coastal Sage Scrub-Salvia mellifera Artemisia/Ericameria
29	cos	2/17/2009	PT	28643.0	AFV	Coastal Sage Scrub-Salvia mellifera Artemisia/Ericameria
30	cos	2/18/2009	PT	28618.0	AFV	Coastal Sage Scrub-Salvia mellifera Artemisia/Ericameria
31	cos	2/18/2009	PT	28753.0	AFV	Coastal Sage Scrub-Salvia mellifera Artemisia/Ericameria

[3] See Table 3.1. chg = unknown grass collected as part of mch fuel type (see Fig. 3-6)
[4] IA/BL = isopropanol with butane lighter; PT = propane torch
[5] FHL = Fort Hunter-Liggett (CA), AFV = Vandenberg AFB (CA), FHUA = Ft Huachuca (AZ), Camp Lejeune (NC), FB = Fort Benning (GA)

Table 3-6 Wildland Fuels Burned at USFS Missoula Fire Science Lab (cont.)

Test ID	Fuel Code[6]	Date	Ignition type[7]	Fuel Weight (g)	Installation[8]	Fuel Type
32	cos	2/18/2009	PT	28606.0	AFV	Coastal Sage Scrub-Salvia mellifera Artemisia/Ericameria
33	mch	2/18/2009	PT	3055.0	AFV	Maritime chaparral
34	mch	2/18/2009	PT	3505.5	AFV	Maritime chaparral
35	mch	2/18/2009	PT	3658.9	AFV	Maritime chaparral
36	oas	2/19/2009	PT	3297.5	HUA	Emory Oak Savanna-Quercus emoryi/ Eragrostis lehmanniana
37	oas	2/19/2009	PT	3400.4	HUA	Emory Oak Savanna-Quercus emoryi/ Eragrostis lehmanniana
38	oas	2/19/2009	PT	3364.8	HUA	Emory Oak Savanna-Quercus emoryi/Eragrostis lehmannianna
39	oaw	2/19/2009	PT	7384.4	HUA	Emory Oak Woodland-Quercus emoryi/Pointleaf Manzanita/Leaf litter
40	oaw	2/19/2009	PT	7346.8	HUA	Emory Oak Woodland-Quercus emoryi/Pointleaf Manzanita/Leaf litter
41	oaw	2/19/2009	PT	6898.5	HUA	Emory Oak Woodland-Quercus emoryi/Pointleaf Manzanita/Leaf litter
42	mes	2/20/2009	PT	4236.6	HUA	Masticated Mesquite-Prosopis velutina, Desert Broom-Baccharis sarthoydes
43	mes	2/20/2009	PT	4132.4	HUA	Masticated Mesquite-Prosopis velutina, Desert Broom-Baccharis sarthoydes
44	mes	2/20/2009	PT	4256.6	HUA	Masticated Mesquite-Prosopis velutina
45	1yr	2/22/2009	PT	799.2	CL	1 year rough North Carolina
46	1yr	2/22/2009	PT	906.9	CL	1 year rough North Carolina
47	1yr	2/22/2009	PT	852.4	CL	1 year rough North Carolina
48	2yr	2/22/2009	PT	1042.6	CL	2 year rough North Carolina
49	2yr	2/22/2009	PT	1134.0	CL	2 year rough North Carolina
50	2yr	2/23/2009	PT	802.9	CL	2 year rough North Carolina
51	2yr	2/23/2009	PT	900.0	CL	2 year rough North Carolina
52	cuh	2/23/2009	PT	3243.5	CL	Treated North Carolina
53	cuh	2/23/2009	PT	2480.2	CL	Treated North Carolina
54	litter	2/23/2009	PT	1563.7	FB	pine liter, duff

[6] See Table 3.1. chg = unknown grass collected as part of mch fuel type (see Fig. 3-6)
[7] IA/BL = isopropanol with butane lighter; PT = propane torch
[8] FHL = Fort Hunter-Liggett (CA), AFV = Vandenberg AFB (CA), FHUA = Ft Huachuca (AZ), Camp Lejeune (NC), FB = Fort Benning (GA)

Table 3-7 Wildland Fuels Burned at USFS Missoula Fire Science Lab (cont.)

Test ID	Fuel Code[9]	Date	Ignition type[10]	Fuel Weight (g)	Installation[11]	Fuel Type
55	cuh	2/24/2009	PT	2767.5	CL	Treated North Carolina
56	litter	2/24/2009	PT	1129.5	FB	pine liter
57	uh	2/24/2009	PT	2542.0	CL	untreated North Carolina
58	poc	2/24/2009	PT	5504.1	CL	POCOSIN
59	uh	2/24/2009	PT	2940.4	CL	untreated North Carolina
60	litter	2/25/2009	PT	1288.5	FB	pine liter, duff
61	uh	2/25/2009	PT	1473.7	CL	untreated North Carolina
65	mes	2/27/2009	PT	4163.8	HUA	Masticated Mesquite-Prosopis velutina
66	mes	2/27/2009	PT	3386.6	HUA	Masticated Mesquite-Prosopis velutina
67	chg	2/27/2009	PT	6031.0	AFV	Chaparral, Grass
68	chg	2/27/2009	PT	5973.4	AFV	Chaparral, Grass
69	oas	2/27/2009	PT	3409.4	HUA	OAK SAVANNA
70	oas	2/27/2009	PT	2813.8	HUA	OAK SAVANNA
71	oaw	2/28/2009	PT	5055.6	HUA	OAK WOODLAND
72	oaw	2/28/2009	PT	5180.4	HUA	OAK WOODLAND
73	man	2/28/2009	PT	2077.0	AFV	Manzanita
74	cas	2/28/2009	PT	1993.7	AFV	California Sagebrush-Artemisia/Ericameria
75	chs	2/28/2009	PT	2464.0	FHL	Chamise_ScrubOak
76	cea	2/28/2009	PT	1905.0	FHL	Ceanothus
77	litter	2/28/2009	PT	1231.5	FB	pine liter, duff

[9] See Table 3.1. chg = unknown grass collected as part of mch fuel type (see Fig. 3-6)
[10] IA/BL = isopropanol with butane lighter; PT = propane torch
[11] FHL = Fort Hunter-Liggett (CA), AFV = Vandenberg AFB (CA), FHUA = Ft Huachuca (AZ), Camp Lejeune (NC), FB = Fort Benning (GA)

Table 3-8 Characteristics of Constructed Fuel Beds to Determine Emissions at MSFL (adapted from Table 2, Hosseini et alia, 2010)

Fuel type	N	Moisture content[1] (%)	Fuel bed dry mass[1] (g)	Bulk density[1] (kg m^{-3})	Packing ratio[2]	Consumption (%)
Chamise/Scrub Oak	6	11.9 (8.7, 15.1)	2079 (1951, 2207)	8.6 (5.6, 11.6)	0.015	38
Ceanothus	6	10.2 (9.8, 10.7)	2007 (1821, 2192)	5.8 (3.7, 8.0)	0.010	54
Maritime Chaparral	5	11.2 (5.1, 17.2)	2871 (2699, 3043)	7.5 (7.0, 7.9)	0.013	95
Coastal Sage Scrub	5	9.3 (8.5, 10.0)	2299 (2171, 2427)	6.0 (5.7, 6.3)	0.010	95
California Sagebrush	6	9.0 (7.2,10.9)	2460 (2124, 2796)	6.4 (5.5, 7.3)	0.011	93
Manzanita	6	12.6 (8.4, 16.7)	2906 (2006, 3805)	7.6 (5.2, 9.9)	0.013	94
Oak Savanna	5	14.3 (7.2, 21.3)	2788 (2498, 3077)	7.3 (6.5, 8.0)	0.012	91
Oak Woodland	5	32.8 (7.4, 58.3)	2054 (1622, 2485)	5.3 (4.2, 6.5)	0.009	95
Masticated Mesquite	5	4.3 (0.6, 7.9)	1831 (1372, 2289)	14.3 (10.7, 17.9)	0.024	92

1. Values are mean (lower, upper 95% confidence interval).
2. Packing ratio = bulk density/particle density. Assumed particle density of 593 kg m^{-3} (average from Countryman 1982)
3. Chamise/scrub oak consumption low for the first three burns but increased after redesign of fuel bed.

3.5 Field Measurements: Vandenberg AFB Prescribed Burns (11/2/09-11/11/09)

To validate the lab emission factors and to provide mission-critical data sets documenting actual post emission transformations we made field measurements at the source and downwind on DoD prescribed burns. A set of field experiments were carried out during November 2009.

3.5.1 Installation Description

Vandenberg Air Force Base (ICAO ID: KVBG) is located in Santa Barbara County, California, approximately 150 miles northwest of Los Angeles. The base is home to the Air Force's 30th Space Wing, and is a major launch site for both military and commercial space payloads. Much of the facility's 57 km^2 land area is covered with maritime chaparral and oak woodland species**.** Prescribed burns are used to maintain training areas, promote biodiversity, and reduce the risk of severe wildfire on the base. The SERDP prescribed burn project took place in a wildland area on the northeast end of the base; see Figure 3-25. The area of the burn site was approximately 120 acres, with a slight upward slope.

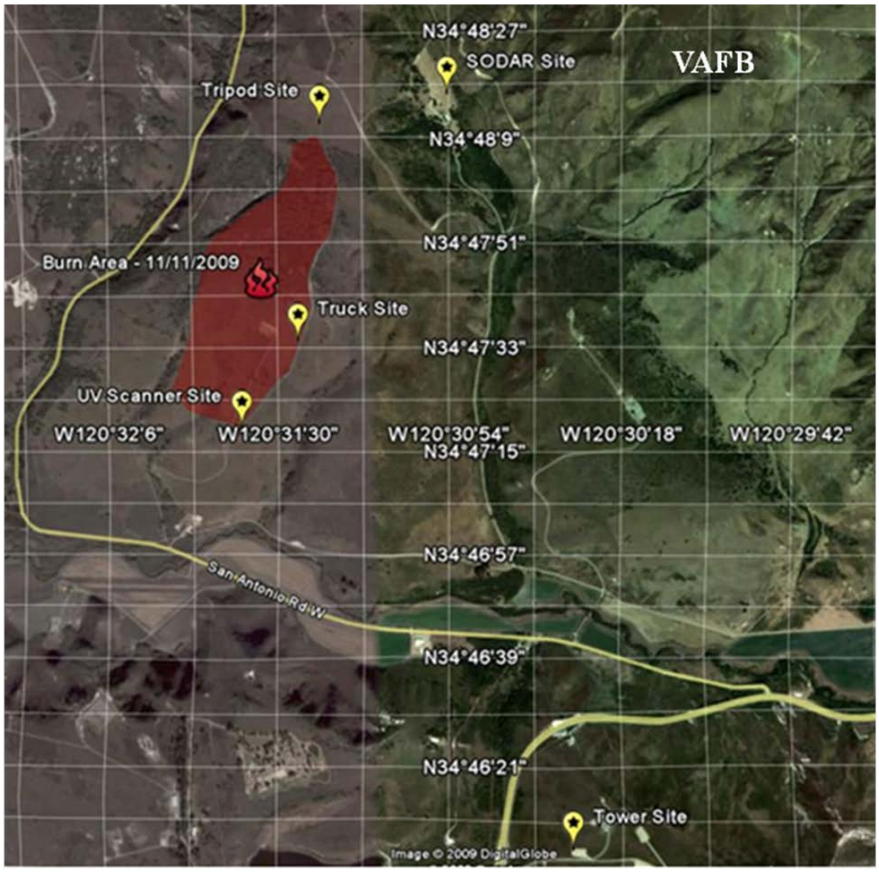

Figure 3-25 Location of Burn Site & Equipment – AFV

3.5.2 Sampling

The field sampling protocol for fuels outlined above was completed in September 2009 at AFV. The prescribed burns scheduled for November 2009 were the Grant Burn with coastal sage scrub

and maritime chaparral. That site is located north of San Antonio Creek. The other planned burn was the Lompoc Terrace Burn with manzanita and that site is located at the southern end of AFV. Approximately 2 months before the burns were to occur; a decision was made to require an EIA and UXO clearance for the Lompoc site making that site unavailable. Other burns planned along the air field in manzanita to eradicate Jubata grass (*Cortaderia jubata*) were made available so fuels were sampled here instead on Lompoc Terrace.

Ten transects 10 m long containing 10 1 m^2 subplots were used to sample fuels at the Grant and Flight Line sites at AFV. A total of 30 transects were installed and permanently marked. Fuel bed height, height to the base of the fuel canopy, species composition, and an ocular estimate of the fuel loading were measured on all 300 subplots. As planned, a 20% sample of the subplot was harvested, fuels were separated into <0.63 cm and 0.63 – 2.54 cm diameter classes and wet weights were determined in the field. Two moisture content samples for each fuel size class were collected and subsequently dried in the laboratory following ASTM D4442 (D07 Committee, 2007).

3.5.3 Laboratory instruments for field measurements

The approach for validating the laboratory data in the field was to use as many of the same instruments in the field as were used in the lab. The set of instruments used in the field are listed in Table 3-7 below and was not exactly the same as used in the lab. These instruments were located either adjacent to the fire line outside of the burn or downwind several kilometers.

Table 3-9 Ground-based Analytical Instruments

	Instrument	#	Purpose	Comment	Source
1.	CSAT3 sonic anemometer	3	Wind, turbulence, temperature, fluxes	2 on 10 m tower and 1 on 3 m tripod	UCR
2.	Net Radiometer – CNR1 Kipp & Zonen	1	Solar and far infrared radiation	Tower mounted	UCR
3.	Krypton Hygrometer – KH20	2	Water vapor fluctuations – latent heat flux	Tower/tripod mounted	UCR
4.	Aerosol Monitor – DUSTTRAK™ 8520 TSI Inc.	3	Particulate matter (PM_1, $PM_{2.5}$, PM_{10}) concentration	Tower/tripod/truck	UCR
5.	Temperature and RH probe – HMP45C-L Vaisala	1	Air Temperature and relative humidity	Tower/tripod mounted	UCR
6.	Infra-red thermocouple – IRTS-P Apogee	1	Surface temperature	Tower/tripod mounted	UCR
7.	Averaging soil thermocouple probe – TCAV-L	1	Averaged soil temperature	Underground, next to tower	UCR
8.	Soil heat flux plate – HFP01SC-L Hukseflux	2	Soil heat flux – bottom boundary	Underground	UCR
9.	Water content reflectometer – CS616-L	1	Soil water content	Ground surface	UCR
10.	Fire Atmosphere Sampling System (FASS)	4	Measure emissions of CO, CH_4, CO_2, C_2-C_4 NMHC, and $PM_{2.5}$ (filters)	Tower	Missoula Fire Lab
11.	Aerodyne AMS (Hi Res)	1	Hi Resolution speciation of OC and aerodynamic sizing	Truck	UCR
12.	SMPS	1	Mobility sizing of PM	Truck	UCR
13.	ELPI	1	Particles	Ground	UCR
14.	UCLA Imaging-DOAS	1	Spatial distribution of column densities of NO_2, HCHO, SO2, and HONO	Ground based/ remote sensing	UCLA
15.	SODAR	1	Wind profiles	Ground	FS
16.	Continuous Flow Streamwise Thermal Gradient CCN Counter	1	Cloud Condensation Nuclei Counter	Truck	UCR
17.	Scanning Mobility Particle SIzer	1	Fine Mode Particle Size Distributions	Truck	UCR

3.5.4 Fire Atmosphere Sampling System (FASS)

In addition to the lab instruments, the FASS towers (Figures 3-26 and 3-27) were dispersed in the middle of the fire area to capture emissions data during the flaming, transition and smoldering phases. Sampling is initiated by real-time CO and CO_2 sensors. FASS captures both canister samples for off-line analysis and real time data (Susott et al., 1991).

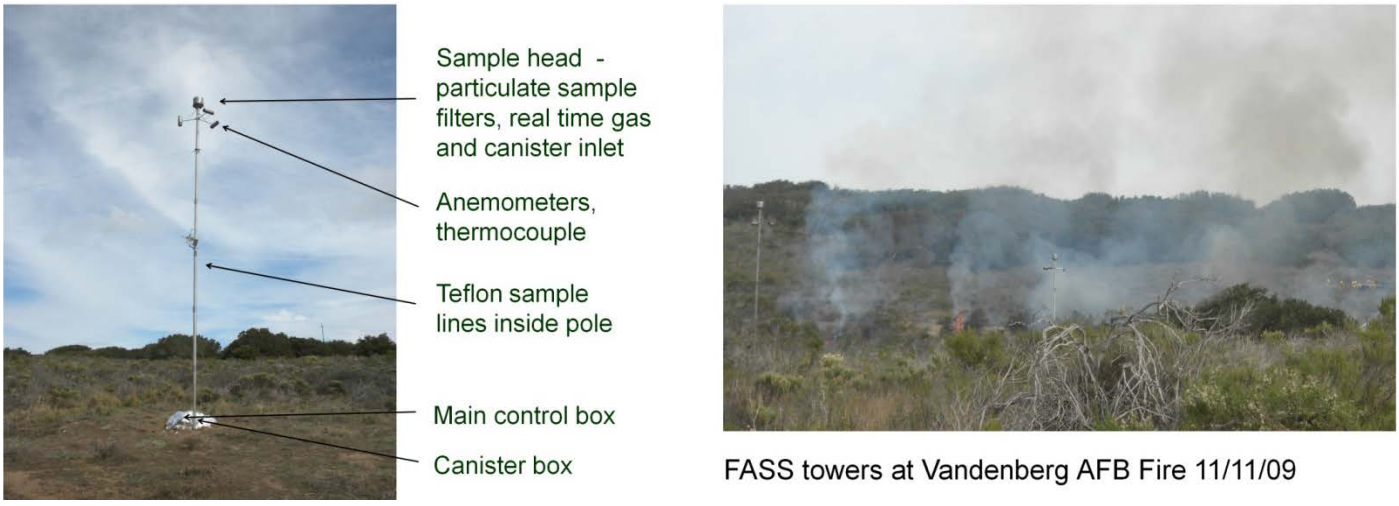

Figure 3-26 Pictures of Fire Atmospheric Sampling System (FASS)

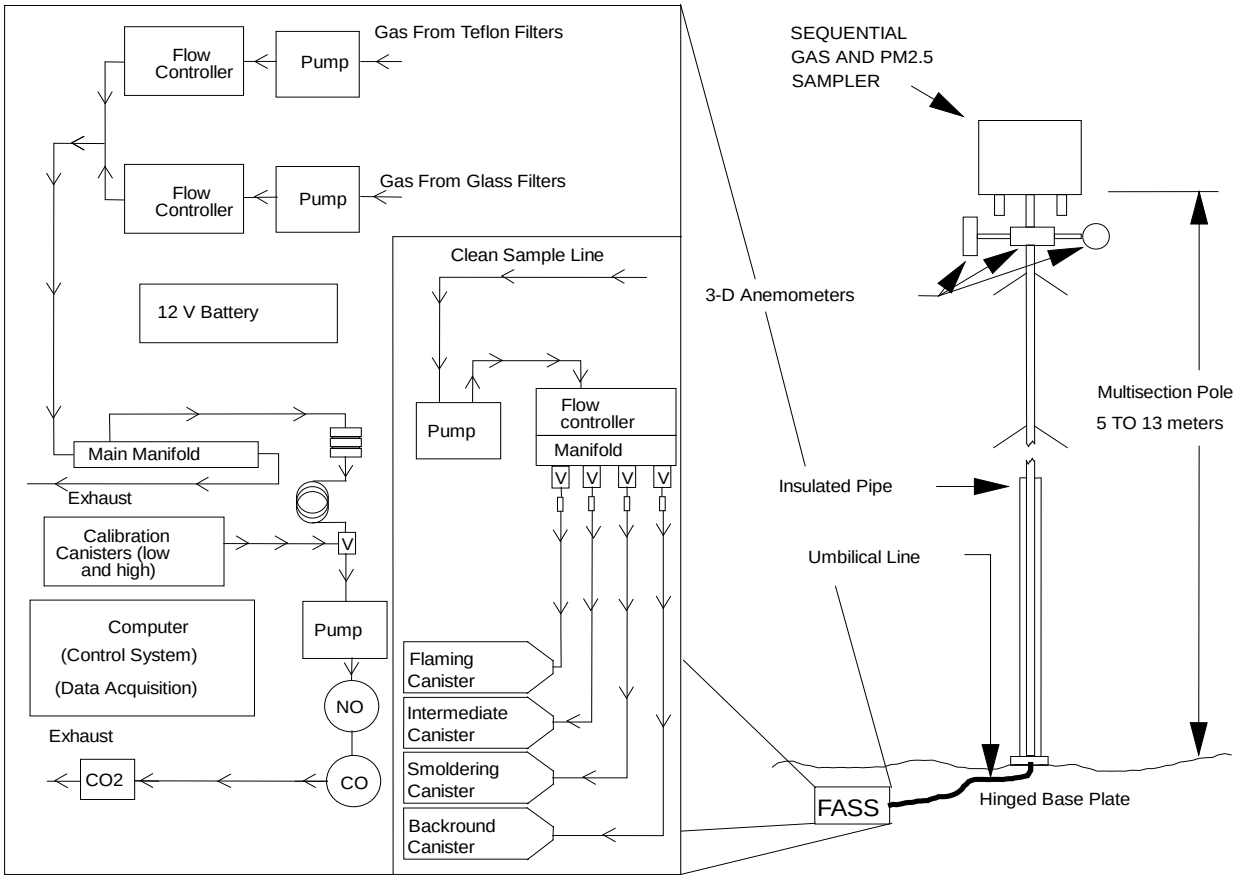

Figure 3-27 Schematic of the Fire Atmospheric Sampling System (FASS) (Fig.3, Ward et al., 1992)

The FASS has been used extensively by the Forest Service's Fire Chemistry research group since 1989 to measure *in situ* trace gases from fires. It consists of the following components:

Sampling head on a tower. The tower is made from hollow, insulated metal poles through which a bundle of Teflon® tubes are threaded up to the sampling head. These connect at the top

to the sampling ports and at the bottom to the main control and canister boxes. The tower is secured by wires staked to the ground. The height of the power is variable, from 10 to 40 feet, dependent on the number of 5 foot sections used for construction. At the top of the tower is the sampling head. It is a 12 inch round metal disk with an insulated cover that contains the sampling port for the canisters, particulate filter cyclones, and real time gas sensors. Also attached to the tower 1 meter below the sample head are 3 anemometers oriented to measure wind speed in three configurations, north-south, east-west, and up-down. Located with the anemometers is a thermocouple to measure temperature.

Main control box contains the electronics to control the sampling, the real time CO and CO_2 sensors, calibration gases for the sensors, pumps for the particulate filters in the sample head, and a memory board to store the data until it is uploaded to a portable computer.

Canister box contains the apparatus for collecting canister or bottle samples. The setup is as follows: A KNF air sample pump draws the sample down the Teflon® tubing from the head. It is filtered through a 15 micron stainless steel fritted filter in the sample head and then by another in the canister box ahead of the pump. The pump pressurizes the system ahead of a Tylan mass flow controller to 35 psia. This pressure is regulated by a adjustable exhaust valve teed off from the main line. The flow controller provides a flow to the sample manifold that has been to fill the canister or bottle to a specified pressure, based on the sample time interval. For example, to sample flaming emission for 10 minutes the flow rate will be half of that for a 5- minute flaming interval. The sample flow from the flow controller proceeds to a sample manifold. The manifold has four solenoid valves that open or close lines to which canisters or bottles are connected. The canisters are evacuated prior to sampling and subsequently pressurized to 25 psia when the sample is collected. The four lines are for background, flaming, intermediate (a combination of flaming and smoldering), and smoldering canister samples.

3.5.5 Instruments for aircraft measurements

In addition to the ground-based instruments, there was a suite of instruments planned for the aircraft to sample and analyze emissions (Table 3-8). Airborne sampling of DoD prescribed fires was conducted to measure emission factors (g pollutant emitted per kg fuel burned) that are essential input for local-global atmospheric models and land management decisions. The airborne data are also needed to reveal the chemical transformations of the particles and gases as they age in the atmosphere. A state-of-the-art chemistry laboratory was installed on a USFS Twin Otter aircraft and used to characterize the particles and gases both near the source and in the downwind plume. Particles were sampled by the Aerodyne Compact Time of Flight Aerosol Mass Spectrometer (c-ToF AMS), Droplet Measurement Technologies Single Particle Soot Photometer (SP2), and a Radiance Research Model 903 integrating nephelometer. Combined, these instruments provided the particle size distribution, particle chemistry (size-resolved at times), and total particle mass. A suite of reactive and stable gases including CO_2, CO, O_3, HONO, hydrocarbons, NOx, oxygenated organics, NH_3, and HCN (a tracer for fires) was measured by an Airborne Fourier Transform Infrared Spectrometer (ATFIR). CO_2 and hydrocarbons were also measured by whole air sampling (WAS) and non-dispersive infrared (LiCor model #7000). An Aircraft-Integrated Meteorological Measurement System with built in GPS logged wind speed, temperature, pressure, and RH as a function of latitude, longitude, and altitude. This allowed accurate aging of downwind samples so that the rates of chemical transformations could be determined. To our knowledge, the SP2 had only been deployed to

measure wildland fires one other time (Pratt et al., 2011). The emissions from two prescribed burns in sagebrush fuel types in Wyoming were measured in 2007.

Table 3-10 Airborne Analytical Instruments

	Instrument	No.	Purpose	Source
1.	Aerodyne AMS(CTOF)	1	Speciation of OC and aerodynamic sizing	Caltech
2.	Fire Lab aircraft package	1	Measure emissions of CO, CH_4, CO_2, C_2-C_4 NMHC. Mass calibrated nephelometer to measure PM2.5	USFS
3.	Airborne FTIR	1	Multiple HC species, CO_2, CO, NO_2, NO..	UM
4.	AIMMS-20	1	Wind velocity, air temperature, RH, atmospheric pressure	USFS
5.	Droplet Measurement Technologies SP-2	1	Measure emissions of BC	U. of Manchester

3.5.6 Prescribed burn plan

There were multiple meetings between the SERDP team members and Vandenberg AFB to coordinate all aspects of the prescribed burn which was made more complicated by the presence of all the ground sampling and aircraft sampling groups. Preconditions included both meeting the conditions of the prescribed burn and complying with the safety elements for the burn. Safety is a key element for all prescribed burns and the final agreements between the SERDP team and Vandenberg required that the personal at the site were properly trained and had the proper Personal Protection Equipment (PPE). Other safety precautions were initiated; for example, a section near the perimeter of the planned burn was bull-dozed free of vegetation to serve as the location of the ground measuring equipment. Airspace access was coordinated by the aircraft pilot and VAF flight control.

All of the agreed conditions were clearly delineated out in the Incident Action Plan; see Figure 3-28. In addition to managing the risk of fire and getting burned, the plan covered training for unexploded ordinance (UXOs) and rattle snakes known to be in that area. Some SERDP funding covered costs of the AFV fire crew who conducted the prescribed burn.

Figure 3-28 Cover Page of Booklet for Prescribed Incident Action Plan at VAF

Due to several complicating factors, the prescribed burn planned for the Lompoc Terrace site did not occur and all energy was focused on the Grant site. The initial test burn to evaluate the potential for a full-scale prescribed burn took place on 5 November 2009. The meteorological conditions for the test burn were as shown in Table 3-9.

Table 3-11 Weather Conditions for 11/5/09 Prescribed Burn

Weather	Scattered clouds
Temperature	65°F
Wind Speed	8 kts
Wind Direction	WSW
Relative Humidity	61%

Ignition of the test burn plot occurred at approximately 1300 PST. Figure 3-29 shows plume development. The test burn failed to propagate. Cool temperatures and high relative humidity resulted in high fuel moisture content that was unfavorable. Vandenberg Fire and research personnel determined that a full-scale burn within the following days would not be feasible, and

the burn was rescheduled for the following week. The poor consumption by the test burn can be seen in Figure 3-30.

Figure 3-29 Test Burn Plume Development over ~ 45 Minutes,11/5/09

Figure 3-30 Post-test Burn Photo Showing Incomplete Fuel Consumption

Vandenberg fire and SERDP research personnel returned to the site on 11/11/09 to attempt the prescribed burn. At approximately 1030 hours the Grant A block was ignited (Figure 3-31). Meteorological conditions at time of ignition were quite different from a week earlier (Table 3-10). The relative humidity was 35% as compared with 61% for the test burn. Live fuel conditions did not change appreciably between 11/5 and 11/11. Meteorological conditions and fine dead fuel conditions were the main difference.

Table 3-12 Weather Conditions for 11/11/09 Prescribed Burn

Weather	Scattered clouds
Temperature	66°F
Wind Speed	5 kts
Wind Direction	SSW to W
Relative Humidity	35%

More favorable fuel and weather conditions allowed the fire to develop, and the entire area at the Grant site was burned. For fire control purposes, a fire line was created separating the burn site into two plots: 1) Grant A was composed primarily of coastal sage scrub and grass fuels and 2) Grant B was composed of maritime chaparral. Grant A was ignited about 1030 hours and firing progressed through the morning with completion around 1230 hours. Conditions remained favorable and Grant B was ignited at 1300 and firing was completed by 1430 followed by mop-up to contain the fire. Major flaming ended at approximately 1500 hours. Aircraft observations recorded smoke plume heights of approximately 5,000 feet at 1245 hours and 6,300 feet at 1445 hours.

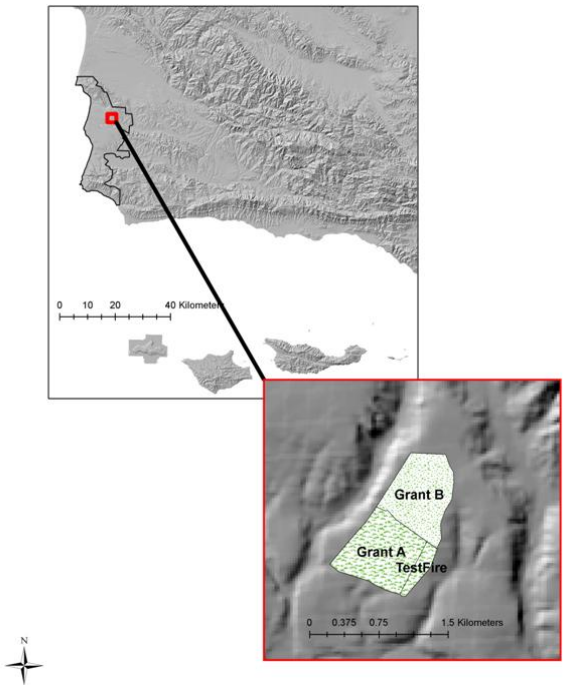

Figure 3-31 Three Components of Prescribed Burn at Vandenberg AFB, Nov 5-11, 2009.

Figure 3-31 a) Fire Ignition by Terratorch b) Smoke Plume Rises


Figure 3-32 a) Flames Spread through Chaparral b) Post-fire Survey of Burn Site

3.6 Field Measurements: Fort Hunter-Liggett Prescribed Burns (11/16/2009 to 11/17/2009)

3.6.1 Installation description

Fort Hunter-Liggett is a United States Army base and training facility in Monterey County, CA. The facility's primary mission is the training of combat support personnel**.** The 668 km^2 base is home to a number of chaparral species**.** Prescribed burns are used at the base to maintain training areas and reduce the risk of severe wildfire on the base. The SERDP prescribed burn experiments took place in a wildland area near the center of the base (Figure 3-33). Based on historical records, November was the best time to plan a prescribed burn at FHL (Table 3-11). To insure that Fort Hunter-Liggett would be able to conduct the burn on the scheduled days, we purchased an air quality permit for research purposes from the Monterey County Air Quality Control Board.

Table 3-13 Average November Weather for Fort Hunter-Liggett (NWS)

High temperature (°F)	74
Low temperature (°F)	51
Precipitation (in)	0.87
Wind Direction (midday)	SSE

Figure 3-33 Prescribed Burn Location and Landscape, Fort Hunter-Liggett

3.6.2 Sampling

Fuel sampling occurred at Fort Hunter-Liggett in October 2009 using the same protocols as used at Vandenberg AFB. While the total burn area at FHL was larger than at AFV, the fuel type was predominantly chamise chaparral with scrub oak. Initial plans were made to repeat the same type of deployment at FHL as had been successfully deployed at AFV. Fuel sampling, ground-based smoke emissions sampling, meteorological sampling including SODAR and atmospheric soundings (SJSU – Clements) as well as heat flux measurements for firefighter safety zone research (Butler – MFSL) were deployed. Due to a breakdown in communication between base personnel, we were unable to deploy the aircraft because of planned jump training associated with the airfield.

3.6.3 Prescribed burn

The prescribed burn site with instrument deployments is shown in Figures 3-34 and 3-35. In Sept 2009, an early winter storm produced nearly 10 inches of rain in the Hunter-Liggett area. As a result, many shrub species broke their summer dormancy and began to absorb the moisture increasing their moisture content. Given the scheduling constraints associated with base activities, aircraft availability, crew availability, fire season, etc., we stayed with the original plan to burn in November. A test burn was ignited on 11/17/09 at about 1200 PST to determine expected fire behavior. A great deal of effort on the part of the FHL Fire Department and cooperating agencies (Los Padres NF, Cal Fire) was expended to ignite the test burn; however, the live fuel moisture was high and cool temperatures resulted in poor to nonexistent burning conditions in the chaparral which did not have a significant dead grass fuel component. The test

burn indicated that the larger fire would not burn so the deployment was cancelled. The meteorological conditions for the day of the prescribed burn are shown in Table 3-12 below.

Table 3-14 Weather Conditions during the Prescribed Burn.

Weather	Clear skies
Temperature	69°F
Wind Speed	<1.5 kts
Wind Direction	WSW to WNW
Relative Humidity	60%

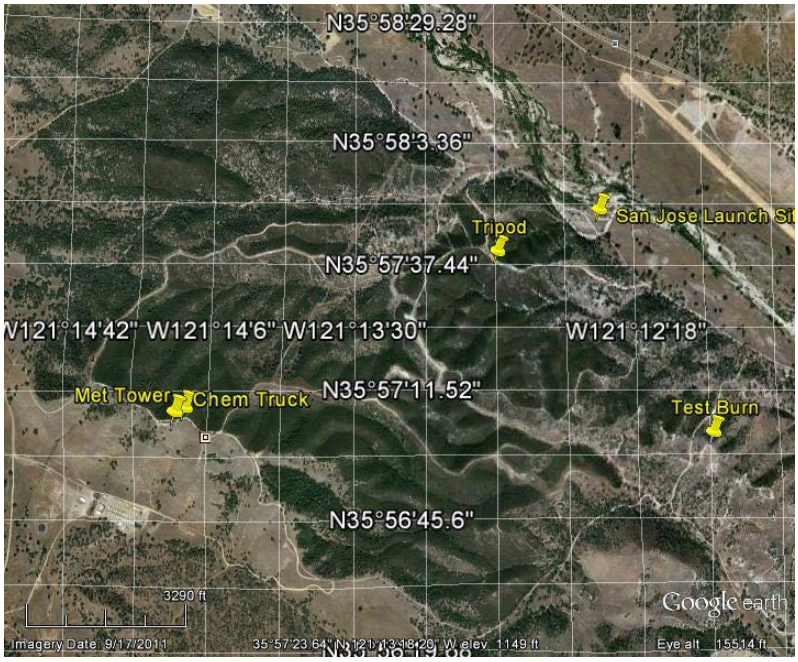

Figure 3-34 Location of the FHL Burn Site and Instruments – 11/17/2009

Figure 3-35 Tower (10m) at Fort Hunter-Liggett during Prescribed Burn, 11/17/09

3.7 Field Measurements: Fort Huachuca Prescribed Burns (February 2010)

3.7.1 Installation description

Fort Huachuca is a United States Army installation under the command of the United States Army Installation Management Command. Fort Huachuca is home of the U.S. Army Intelligence Center and the U.S. Army Network Enterprise Technology Command (NETCOM)/9th Army Signal Fort Huachuca is also the headquarters of Army Military Affiliate Radio System (MARS) and the Joint Interoperability Test Command (JITC) and the Electronic Proving Ground (EPG) Command. Libby Army Airfield is located on post and shares the runway with Sierra Vista Municipal Airport. It is located in Cochise County, in southeast Arizona, about 15 miles north of the border with Mexico and was declared a national landmark in 1976 (Figure 3-36).

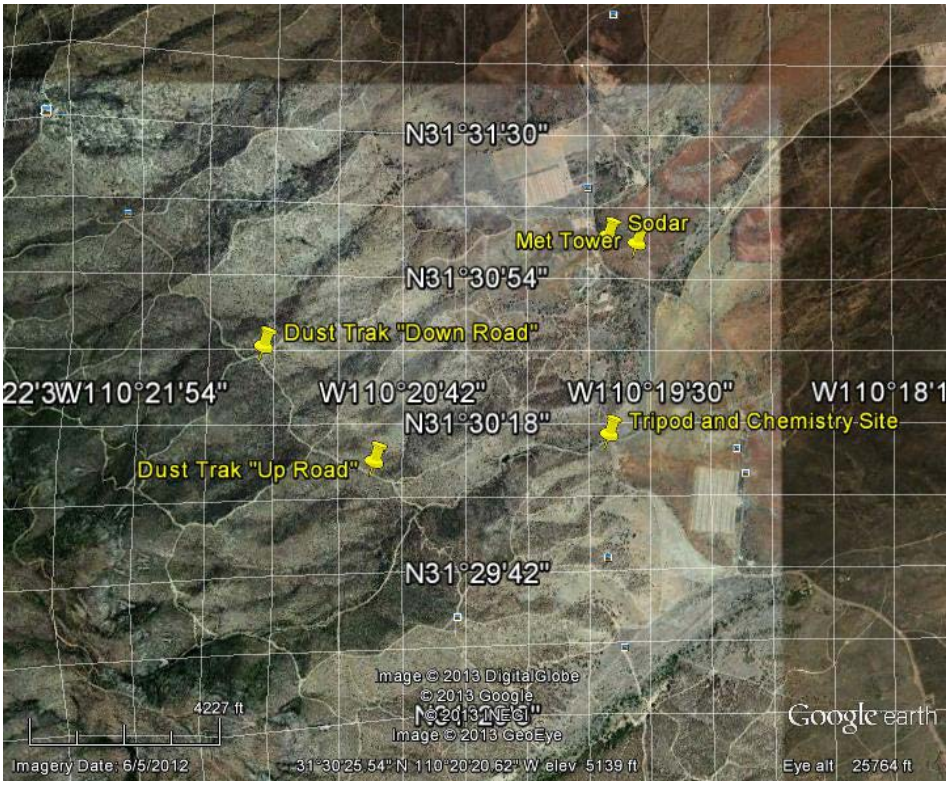

Figure 3-36 Fort Huachuca Burn Location and Measurement Sites

3.7.2 Fuel Sampling

Fuel sampling at Fort Huachuca was modified due to the different nature of the fuels. The Emory oak woodland site (Romeo) was sampled following the same procedures used at Vandenberg and Fort Hunter-Liggett. The oak savanna (T2) and masticated mesquite (Brainard) sites were sampled differently. In the oak savanna, grass and litter samples were collected and dry mass was determined. Grass height was measured. Double sampling was used to estimate grass loading, woody loading < 1", and % dead. Dry mass and depth of the masticated fuels and grass height were measured on the Brainard site.

3.7.3 Prescribed burn

Prescribed burns have been historically conducted in the Huachuca Mountains area in the spring of the year. The 2010-2011 winter was wetter than normal at Fort Huachuca. Due to a variety of constraints and base restrictions that developed late in the planning process for the burns, only the oak savannah site (T2) was available for burning. As a consequence of the abnormally wet winter, the fires on 3/29/2010 failed to spread and mainly grass burned rather than spreading to the oak canopy even though the 880 acre site was located on hilly terrain.

Figure 3-37 Ignition of the Prescribed Burn at Fort Huachuca

Figure 3-38 View of Fort Huachuca Burn Area from Met Tower Location.

3.8 Field Measurements: Ione, California Prescribed Burns (October 2011)

The last prescribed burn was near Ione, California, location of the Cal Fire Academy. Ione is nestled in the oak covered foothills in the Gold Country of Amador County, California. It is located on State Routes 104 and 124, 30 miles Southeast of Sacramento, 30 miles Northeast of Stockton; see Figure 3-39.

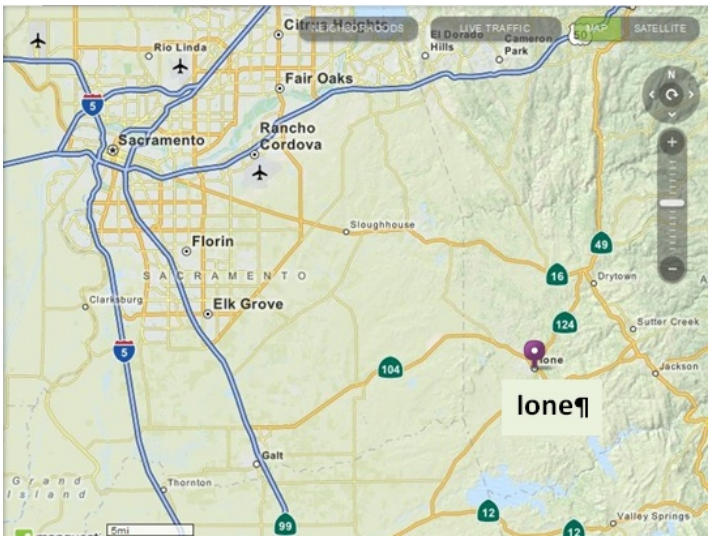

Figure 3-39 Location of Ione California

The prescribed burn near Ione, CA was conducted by Cal Fire in support of studies by the Forest Service San Dimas Technology Development Center. Their goals were to evaluate safety equipment and conditions during a burn-over of fire engines. Due to timing of the experiment, no fuel sampling was performed. However, the prescribed burn offered UCR a chance to measure emissions from a very intense fire and for the team to make the first ground-based measurements of black carbon in real-time with a special instrument designed for measuring black carbon. The burn plot was a slope that had not been burned for more than 10 years on which Cal Fire placed fire trucks on the upslope. The trucks had mannequins with firefighter personal protective equipment that were instrumented to measure the temperature. The principal fuel type was chaparral with scattered oak trees. The fire was very intense as indicated by the flames and melted metal on the vehicle in Figure 3-40.

Figure 3-40 Ione Prescribed Burn Location & Images

3.9 Air Quality Model Development -Methods

3.9.1 U.S. EPA's Community Multi-scale Air Quality Model (CMAQ

U.S. EPA's Community Multi-scale Air Quality Model (CMAQ) was the main method used to develop detailed information about the concentration of air pollutants in a given area with known emissions and weather data. According to the EPA web site, the CMAQ Model is a powerful computational tool used by EPA and states for air quality management in that it can be used to design emission control scenarios to help achieve air quality standards. The National Weather Service also uses the model to produce daily U.S. forecasts for ozone air quality. The CMAQ system simultaneously models multiple air pollutants, including ozone, particulate matter, and a variety of air toxics to help regulators determine the best air quality management scenarios for their communities, states, and countries.

The CMAQ system is complex as shown in Figure 3-41 and requires considerable expertise. Model input includes input emissions inventories, meteorology, and chemical reaction models and geographic dimensions. Research continues to improve the overall system and its components. The overall system has advanced from the CMAQv4.5 to 4.7 to 5.0 over the duration of the project, the last released in 2012. Each of the changes had improved elements within CMAQ. For example, in the original proposal, MM5 was the meteorological model which has been replaced by the Weather Research and Forecast (WRF) model; version 5.0. WRF was used in this project.

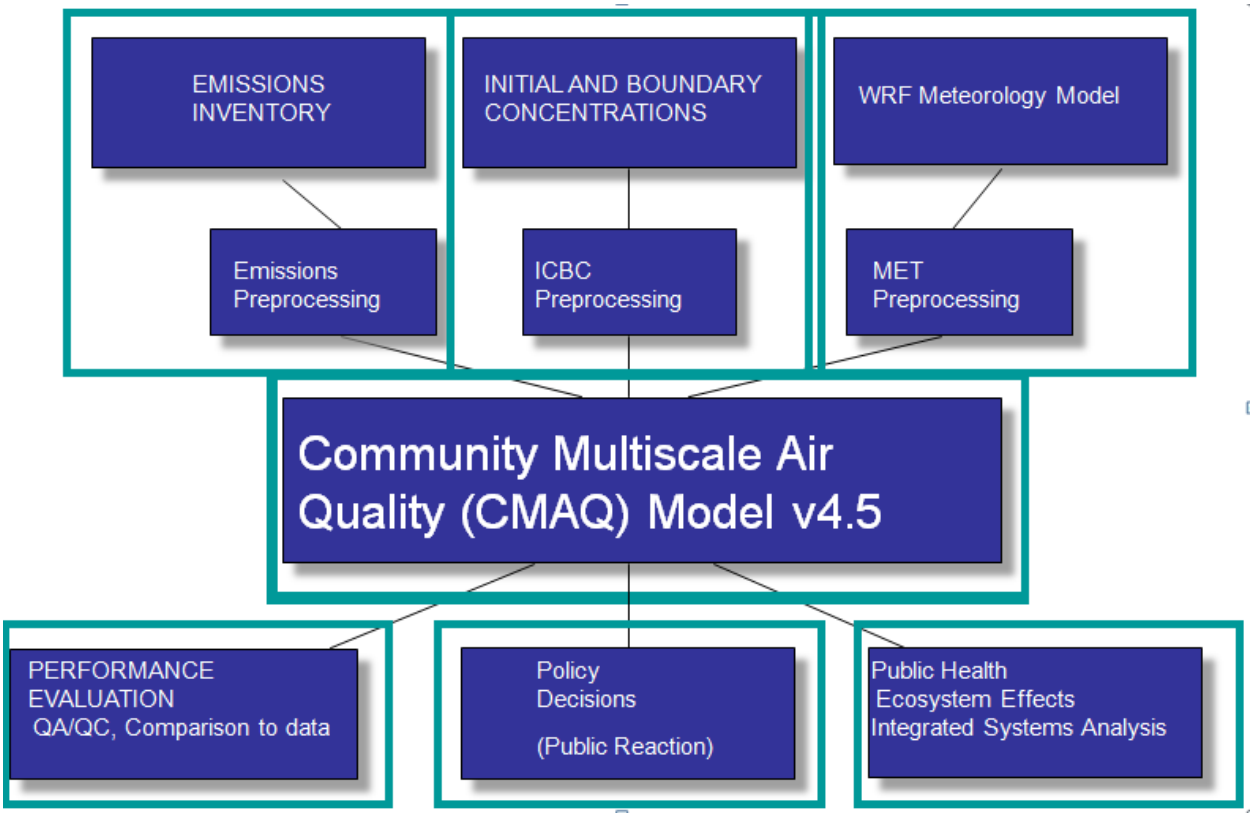

Figure 3-41 Air Quality Modeling Modules and System

3.9.2 BlueSky Framework

The public along with land managers, fire managers and air quality regulators recognized the benefits of prescribed burning and the need for more information about smoke associated with prescribed burning. For example:

- What is the maximum smoke concentration that could be expected downwind areas?
- When is the smoke likely to arrive at a location?
- Will the National Ambient Air Quality Standards be exceeded?
- In what locations should public health alerts potentially be issued?
- Where will visibility most likely be affected by smoke?
- What actions might be taken to mitigate smoke impacts?

As mentioned in the previous section, U.S. EPA's Community Multi-scale Air Quality Model, CMAQ, is the recognized 'gold standard' for modeling local and regional air quality for almost any scenario, including prescribed burns. However, the model is complex and requires considerable skill with computing and with inputs to CMAQ itself in order to produce a credible output. Computer runs can take days for the algebraic equations to converge and produce the desired output of air quality over time. Thus land managers faced with the challenge of reducing fire risk with prescribed burning while meeting air quality standards would need to have access to experts on CMAQ or another reliable method.

Pursuant to the need for an alternative to CMAQ, scientists developed the BlueSky framework to meet the need of accurately forecasting smoke dispersion and settling (Larkin et al.,2009). BlueSky (Figure 3-42) is a framework that contains and combines models and data about weather, fires and fuels, emissions, and terrain. By integrating the individual models into a unified framework, BlueSky is able to predict smoke concentrations and trajectories, and is used to create forecasts helpful to land, fire and air quality managers. The BlueSky Framework allows models chosen by the user to communicate with each other in a modular, user-driven environment. Thus users can combine state-of-the-science emissions, meteorological, and dispersion models to generate results based on the best available models. Most users select the Fire Characteristic Classification System (FCCS) fuel loading map (Ottmar et al., 2007) and Emissions Production Model (EPM), as well as the CALPUFF puff-dispersion model. The National Weather Service (NWS) uses the HYSPLIT dispersion model. BlueSky's main use to date is in modeling $PM_{2.5}$, (Stand et al., 2012) an air pollutant regulated under the National Ambient Air Quality Standards (NAAQS). While BlueSky started as a regional project in the Pacific Northwest it was expanded to provide real-time predictions from large wildfires throughout the contiguous United States and from prescribed fires in some regions.

From the BlueSky web page: What can BlueSky do?

- Lookup of fuels information from fuel maps
- Calculate total and hourly fire consumption based on fuel loadings and weather info.
- Calculate speciated emissions (such as CO_2 or $PM_{2.5}$) from a fire
- Calculate vertical plume profiles produced by a fire
- Calculate likely trajectories of smoke parcels given off by a fire
- Calculate downstream smoke concentrations.

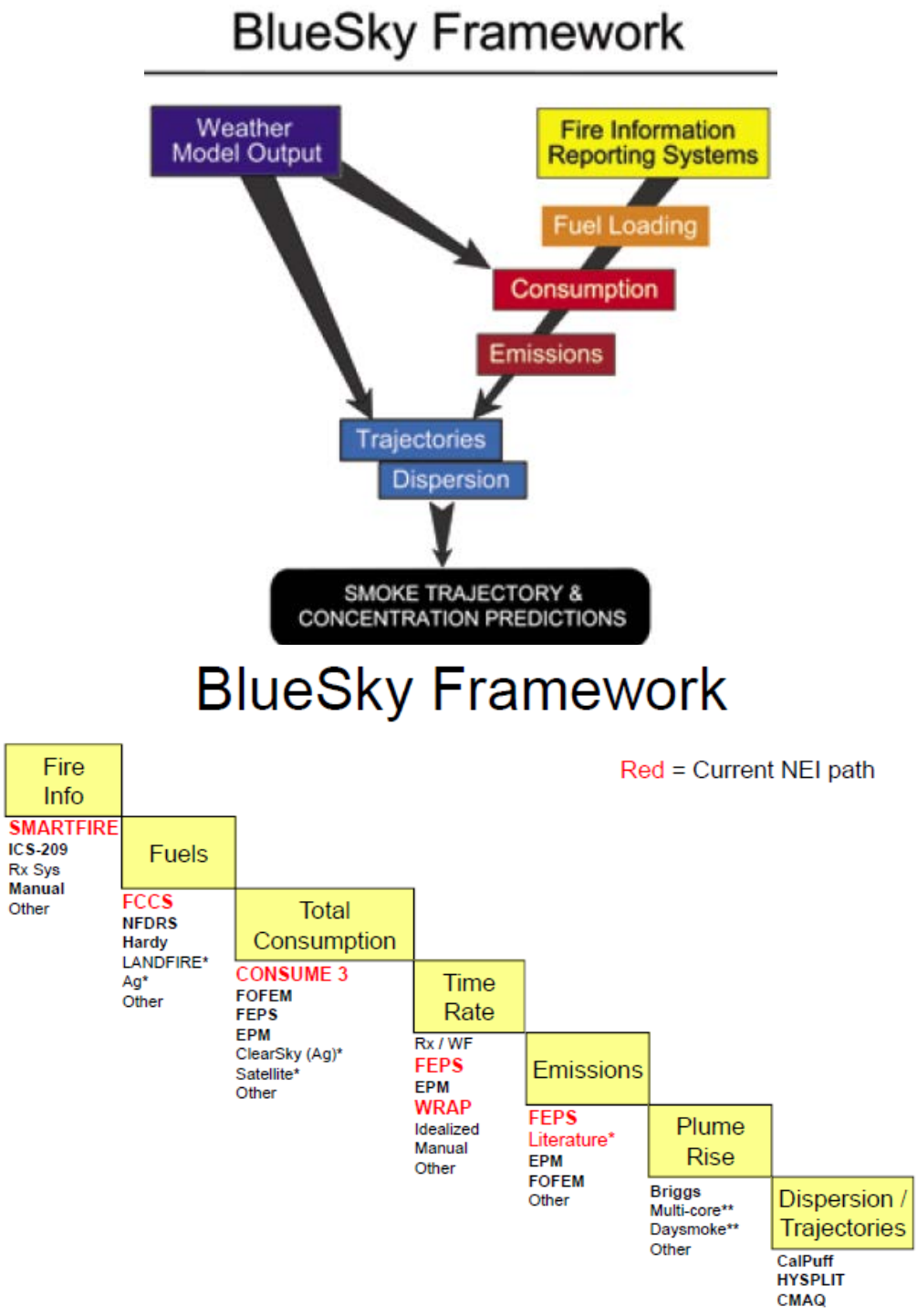

Figure 3-42 Two Schematics of the BlueSky Framework

In closing, the BlueSky Framework integrates data from the latest models on weather, fires and fuels, emissions, and terrain. BlueSky calculates: smoke plume rise, particulate matter concentrations, visibility and chemistry. Its final outputs are forecasts of smoke trajectories and concentrations, with Web displays. More info at http://www.airfire.org/bluesky/

3.9.3 SMARTFIRE Tools

The BlueSky Framework was created through the close collaboration of land management and air quality regulators and scientific researchers as a tool to manage smoke from fire. Today the BlueSky Framework is governed by the BlueSky Consortium with the USDA Forest Service AirFire Team taking the lead responsibility for scientific development. The benefits of the BlueSky Framework are being applied currently by the regional Fire Consortium for the Advanced Modeling of Meteorology and Smoke (FCAMMS) and the National Weather Service (NWS). The BlueSky Framework uses a variety of fire information sources and this organized approach has led to the development of the SMARTFIRE fire information system. SMARTFIRE uses the NOAA Hazard Mapping System satellite to detect fires plus ground reports from systems such as ICS-209 Reports to create a reconciled fire information data feed. SMARTFIRE was developed by the USDA Forest Service AirFire Team and Sonoma Technology, Inc. through a cooperative research agreement funded by NASA.

According to the web site, http://www.airfire.org/smartfire/, the SmartFire fire information system is a framework for aggregating, associating, and reconciling wildland fire information from disparate sources. The current version of SmartFire is Version 2, which includes significant advancements to data processing, associating, and reconciliation algorithms. SmartFire v2 (SF2) can use any number of data sources, associating and reconciling their information to avoid double counting of fires, and selectively utilizing the best pieces of data from each source.

SmartFire v2 is in use for developing the 2011 U.S. EPA's National Emissions Inventory (NEI) for wildland fire. Previous versions of SmartFire were used in prior inventories, with SmartFire v2 first used in the development of version 2 of the 2008 U.S. EPA's NEI. Currently, real-time smoke prediction systems across the U.S. use SmartFire v1 with a change over to SmartFire v2 planned for Spring 2013.

SmartFire is fundamentally a platform or framework for performing the tasks of:

- Gathering fire information from disparate sources including satellite systems and ground based systems, real-time and retrospective systems, and direct fire reports and ancillary data systems;
- Manipulating the fire information from a given source into a hierarchical fire data information structure;
- Associating fire information between difference sources to determine potential overlaps and duplications; and
- Reconciling fire information from multiple sources to provide a single data stream for use in fire emissions inventories, fire models, and smoke and air quality models.

As a framework, SmartFire includes multiple options and settings that will influence the resulting output reconciled fire information data stream. Choices made as to which fire information source to use, which parameters to use, and which reconciliation algorithms to use will fundamentally affect the resulting information. For this reason, when referencing SmartFire data, it is important to specify the full configuration utilized when this data was created.

4 Results and Discussion:

This section provides experimental results for different methods and approaches described in Section 3. In addition the section provides a general view of the results as compared with other studies and insight on the implications for these findings in addressing the project's objectives.

4.1 Improve Characterization of Fuels and Consumption

This area of research was to provide more information on the nature of the wildland fuels relating to fuel types and fuel loadings on the DoD bases in the Southwest with emphasis on the California chaparral and Arizona oak fuel types. The five subtasks are listed in Table 4-1.

Table 4-1 List of Sub-tasks Related to Fuels Characterization & Consumption

1	Identify Southwest fuels, existing data and consumption models.
2	Sample Southwest fuels, measure field & chemical properties.
3	Collect fuel samples & develop beds for lab tests.
4	Field sampling: pre-burn and post burn.
5	Improve existing fuel consumption rates with mass of pollutants emitted during burning.

4.1.1 Existing Fuels Information

Several sources of fuel loading information for chaparral fuels at Fort Hunter-Liggett and Vandenberg AFB and for the oak/juniper woodland fuels at Fort Huachuca are in the literature; see Table 4-2. The Digital Photo Series of Ottmar are often used by land managers to quickly estimate the fuel loading. The photos show representative fuels in nature and accompanying tables provide info on mass/area, size/class and some species data. Note identifier CH1 means chaparral, photo 1 and OJW 1 means oak/juniper woodland.

From our experience, fire behavior models (Rothermel 1972, Albini 1976) are typically used to estimate fuel loading if the vegetation type is not represented in computer programs used to estimate fuel consumption and smoke emissions. Depending on the type of training and background that personnel at DoD have, they may not be familiar with fuel classification systems other than fire behavior/fire danger fuel models and fuel consumption tools such as CONSUME. Several authors have pointed out that use of fire behavior/fire danger fuel models is not appropriate for estimating smoke emissions as the fuel models do not contain larger fuel particles that contribute to smoke emissions produced after the fire front has passed (e.g. Weise and Wright, 2013). While many chaparral stands do not contain these larger fuels, many stands contain a significant litter layer that may smolder. In addition to locating fuel information applicable to the chaparral fuel types at Vandenberg AFB and Fort Hunter-Liggett, we discovered that rather extensive fuel sampling had occurred at Fort Huachuca as part of an effort to prepare a fire management plan in the late 1990s (Danzer 1997, Miller 2003). Due to the turnover in base personnel and changes in fire management responsibility, this information had been lost. We located Jay Miller (2003) and retrieved the spreadsheet data that formed the basis of the publication. This information was shared with Fort Huachuca personnel and also shared with the Forest Service FERA group who is responsible for developing, maintaining and updating the Fuel Characteristic Classification System (FCCS) for possible inclusion of the site

specific data into the FCCS. We are exploring the possibility of sharing the fuels data collected as part of this project with the FCCS system as well.

Table 4-2 Fuel loading Literature Describing Chaparral Fuels at Vandenberg AFB and Fort Hunter-Liggett and Oak Woodland/savanna Fuels at Fort Huachuca

Source	Fuel type	Identifier	Notes
Ottmar et al., 2000	Coastal sage scrub, California sagebrush	CH1, CH2, CH3	Santa Monica Mtns NRA
	Chamise chaparral	CH4, CH5, CH6, CH7, CH8, CH9	Santa Monica Mtns NRA, San Bernardino NF
	Mixed chaparral	CH10, CH11, CH12, CH13, CH14, CH15, CH16	May be similar to FHL chamise/scrub and ceanothus fuel types
Countryman 1970	Chamise chaparral		Based on 16 shrubs
Countryman 1982	Mixed chaparral		Northern California chaparral including manzanita and ceanothus
Riggan 1994	Chaparral		Presents data from southern California and citations to older information
Martin et al., 1981	Manzanita, Ceanothus		
Ottmar, Vihnanek, et al., 2007	Emory oak savanna	OJW 1, 3, 7, 9	Located at HUA, Coronado National Forest
"	Emory oak woodland	OJW 13	"
Folliott et al., 2008	Emory oak savanna		Peloncillo Mtns, SW New Mexico – woody fuels only
"	Emory oak woodland		San Rafael Valley, Huachuca Mtns – woody fuels only
Poulos 2009	Emory oak		Big Bend NP, TX; Maderas del Carmen Protected Area, Coahuila, MX
Danzer 1997	multiple		Report never located.
Miller et al., 2003	multiple		Summary table for 156 sample plots. Original data for this publication retrieved from author and provided to Fort Huachuca fire management.
Hood 2006	Masticated mesquite		Pinyon juniper fuel beds might be applicable
Kane 2007	Masticated mesquite		Measured masticated manzanita and ceanothus species (northern California chaparral)
Busse 2005	Masticated mesquite		Loadings for masticated northern California chaparral

4.1.2 Fuel bed properties

Measured fuel loading and other fuel bed properties for VAF, FHL and FHU are contained in Table 4-3 and Table 4-4. These loadings are for live foliage and woody material < 2.54 cm diameter. As is typical for vegetation data, there was considerable variability in the field. The shrub component of the fuel beds was not continuous resulting in patchiness and thus increased variability in the samples. While we used double sampling on a trial basis to increase sampled size, results presented in these tables are based solely on measured quantities. The oak savannah and oak woodland fuel beds were also patchy. The savannas contained grass between the oak

trees; under the oak trees (typically starting at the drip line), the fuel type was dominated by oak litter. Oak litter and standing grass burn quite differently producing different emissions.

It is important to note that the bulk densities of the field fuel beds are 25 to 50% of the bulk densities of the laboratory fuel beds. Similarly, the packing ratios of the field fuels are also 25 to 50% of the laboratory fuel bed packing ratios. The applicability of lab-based results to field emissions is a point for discussion. Analysis linking the lab and field measurements was performed by Robert Yokelson as part of the joint effort between RC-1648 and RC-1649 and was published recently (Yokelson et al., 2013). Moisture content of the field fuel beds was also appreciably ~50% and much higher than the laboratory fuel beds, ~10%.

Table 4-3 Summary of Field Sampling by Fuel Type for Vandenberg AFB & Fort Hunter-Liggett

Fuel type	N	Fuel loading[12] (kg m^{-2})		Fuel height (m)		Fuel bed depth (m)		Bulk density (kg m^{-3})	Packing ratio[13]	% Dead[7]		Moisture content[14] (%)	
Coastal Sage Scrub (cos)	5	1.3	(0.0, 2.5)	1.22	(0.80, 1.64)	0.77	(0.24, 1.31)	3.1	0.0053	21	(-11, 53)	48.4	43.6
Maritime chaparral[15] (mch)	5	1.6	(0.8, 2.4)	1.26	(0.83, 1.68)	0.73	(0.36, 1.09)	2.9	0.0049	57	(38, 75)	54.3	49.0
Chamise/ Scrub Oak (chs)	11	1.9	(1.1, 2.6)	1.49	(1.24, 1.74)	1.18	(0.92, 1.43)	1.6	0.0027	20	(8, 33)	42.6	42.8

Table 4-4 Summary of field fuel sampling by fuel type for Fort Huachuca

Site	N	Fuel loading (kg m^{-2})			Shrub height (m)	Canopy depth (m)	% Dead	Cover (%)	
		Grass	Litter	Shrub				Grass	Shrub
T2	10	0.19 (0.15-0.23)	0.52 (0.14-0.90)	0.17 (0.07-0.27)	1.35 (0.0-2.8)	0.91 (0.0-1.9)	14	26 (15-37)	16 (0-33)
Romeo	6[2]	0.15 (0.03-0.27)							
Brainard	10	0.18 (0.14-0.21)							

[12] Table values are mean (lower, upper 95% confidence interval).
[13] From Zhou et al. (2006), assumed weighted particle density of 707 kg m^{-3} for chamise and 645 kg m^{-3} for broadleaved fuels. For chamise-scrub oak fuel type, assumed 50% chamise and 50% scrub oak.
[14] Oven-dry moisture content for <0.63 cm and 0.63-2.54 cm diameter live material.
[15] AFV Flightline site also contains jubata grass (*Cortaderia jubata*) with an estimated moisture content of 42.8%.

Another deliverable for the SERDP project was the analysis of the elemental composition of the various wildland fuels on a dry-basis. Elemental analyses of wildland fuel samples taken in the field for the FSL burns are shown in Figure 4-1. Note that carbon is the primary element followed by oxygen, which is not surprising given that plant materials are made of cellulose compounds. Nitrogen and sulfur are <3% by mass.

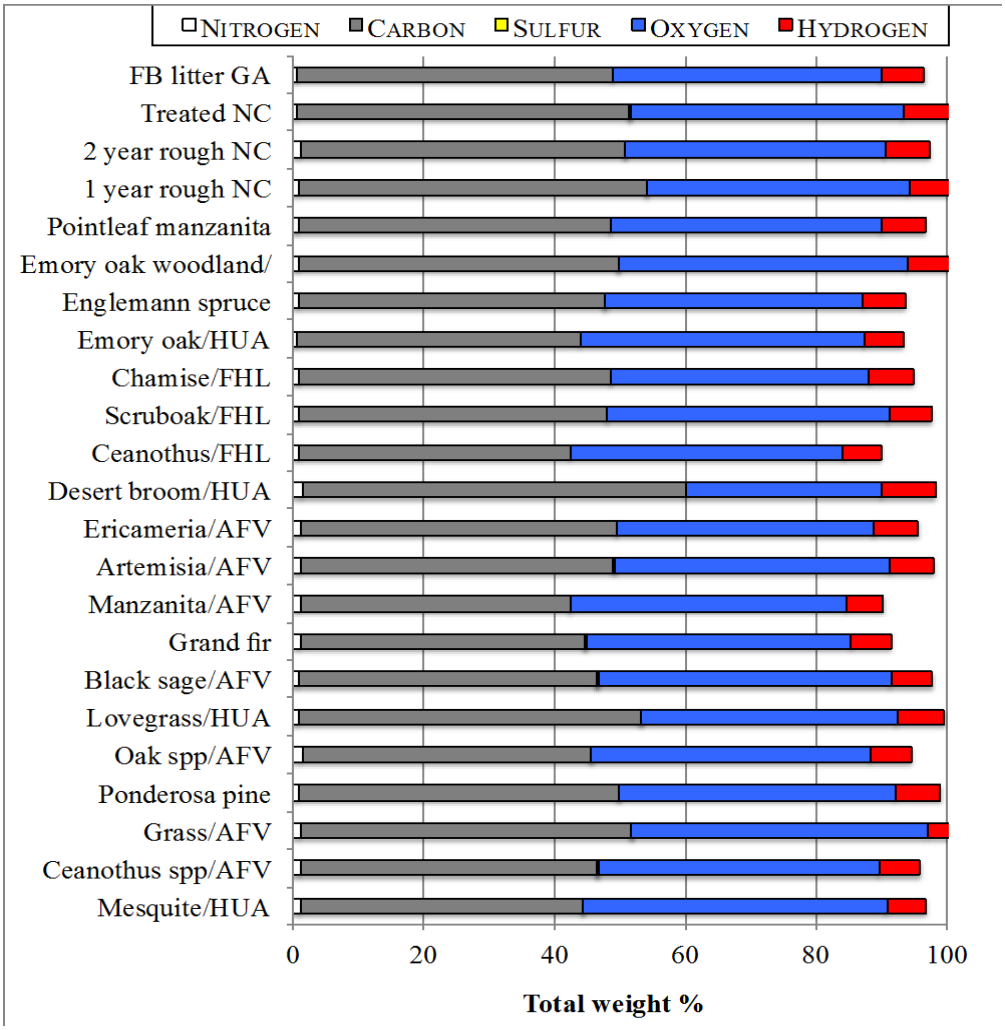

Figure 4-1 Elemental Composition of Wildland Fuels in the SERDP Project

Another analysis was obtained later using the same reduction techniques to produce a sample of about 5 grams for elemental analysis at the University of Idaho. Results are shown in Table 4-5 and are in close agreement with those in Table 5.

Table 4-5 Elemental composition of Fuel Types,

Fuel type	Fuel code	Species names	# of Burns	N wt%	C wt%	S wt%	O wt%	H wt%	Cl mg/kg	K mg/kg	Na mg/kg
Southwestern Fuels											
Ceanothus	cea	Ceanothus leucodermis	6	1.05	43.46	0.01	42.34	6.04	2000	4000	500
Chamise/Scrub oak	chs	Adenostoma fasciculatum, Quercus berberidifolia	6	0.92	47.49	0.00	41.17	6.60	< 50	1100	< 80
California sage	cas	Artemisia californica, Ericameria ericoides	6	1.12	48.11	0.22	40.59	6.69	3000	11000	1600
Coastal sage	cos	Salvia mellifera, Ericameria ericoides, Artemisia Californica	5	1.00	47.92	0.44	41.90	6.66	3000	6900	4100
Maritime chaparral	mch	Ceanothus impressus var. impressus, C. cuneatus var. fascicularis, Salvia mellifera	5	1.10	46.90	0.03	44.18	6.51	3850	6900	1450
Manzanita	man	Arctostaphylos rudis, Acrtostaphylos purissima	6	1.00	41.33	0.20	42.07	5.74	580	4200	460
Masticated mesquite	mes	Prosopis velutina, Baccharis sarothroides	5	1.25	50.96	0.03	44.29	7.08	860	6350	<80
Oak savanna	oas	Quercus emoryi, Eragrostis lehmanniana	5	0.78	52.47	0.03	46.51	7.29	53	2800	< 80
Oak woodland	oaw	Quercus emoryi, Arctostaphylos pungens	5	0.59	43.40	0.00	43.31	6.03	110	4700	< 80
Southeastern fuels											
1 year herbaceous	1yr	Lyonia lucida, Ilex glabra	3	0.82	53.27	0.06	40.00	7.40	160	2000	150
2 year herbaceous	2yr	Lyonia lucida, Ilex glabra	4	1.07	49.68	0.10	39.55	6.90	320	2500	300
Chipped understory hardwood	cuh	Acer rubrum, Persea borbonia, Gardonia lasianthus	3	-	-	-	-	-	-	-	-
Understory hardwood	uh	Acer rubrum, Persea borbonia, Gardonia lasianthus	3	-	-	-	-	-	-	-	-
Pocosin	poc	Lyonia lucida, Ilex glabra	3	-.	-	-	-	-	280	1200	120
Pine litter	lit	Pnus taeda, Pinus echinata, Pinus elliottii, Pinus palustris	5	0.77	49.05	0.02	42.31	6.81	130	1100	< 80

4.1.3 Consumption estimates

Two prescribed burns were successfully conducted at Vandenberg AFB (Grant) and one was conducted at Fort Huachuca (T2). The 8 ha test burn at VAF was conducted on 5 November 2009 and resulted in very little fuel consumption. Therefore no fuel transects were located in the test burn.

The remainder of the VAF area (108 ha) was burned on 11 November 2009 and eight of the ten transects were contained within the burned area. Three transects were in the maritime chaparral (mcp) fuel type and five were located in the coastal sage scrub (cos) fuel type. The pre and post-burn fuel loadings by size class are contained in Table 4-3. Fuel moisture samples were not collected at the time of post-burn sampling because the majority of the remaining material was charred and dead. We assumed that the moisture content of the dead aboveground material was equal to the mean 10-hr fuel stick moisture content (6%) at the Vandenberg AFB RAWS for the 3-day period 1/5-1/7/2010 when the post-burn sampling occurred.

Data from the nearest remote automated weather station (5.6 km), the Vandenberg station, (VDBC1, 34.7586N, -120.4861W), indicated that 10 hour fuel moisture content averaged about 7 percent during the burn. Measured live fuel moisture content collected in chamise fuel type near the burn site on 2 November 2009 before the burn was 70% and 64% for new growth and old growth, respectively. Assuming equivalent amounts of old and new growth leads to a site average moisture content of 67%. The Grant prescribed burn consumed nearly 90% of the above-ground material < 0.63 cm in diameter and nearly half of the material 0.64 to 2.54 cm in diameter (Table 4-6). Combining the total fuel consumption (Table 4-7) with the respective areas (Grant A – coastal sage scrub, 55 ha; Grant B – maritime chaparral, 53 ha) yields a total fuel consumption for the Grant burns of ~1,000 Mg (metric tonnes) or 1 Gg. Due to the high variability and relatively low sample size, the 95% confidence interval for this estimate includes a wide range.

Table 4-6 . Pre and Post-Burn Fuel Loading by Size Class for Grant Prescribed Burn, Vandenberg AFB, 11 Nov 2009.

	Fuel Loading (kg m^{-2})							
	Pre-burn			Post-burn			Consumption (%)	
Fuel Type	n[1]	<0.63	0.64-2.54	n	<0.63	0.64-2.54	<0.63	0.64-2.54
Coastal Sage Scrub (cos)	5	0.431	0.831	3	0.056	0.437	87	47
Maritime chaparral (mcp)	5	0.606	0.957	3	0.084	0.484	86	49

[1] Number of transects sampled. Each transect contained 10 1-m^2 subplots, 2 of which were harvested pre-burn and 2 post-burn.

Table 4-7 Fuel Loading Estimates and Associated 95% Confidence Intervals for Grant Prescribed Burn, Vandenberg AFB, 11 Nov 2009

		Fuel loading (kg m^{-2})					
Fuel type	N	Pre-burn		Post-burn		Consumption	
Coastal Sage Scrub	5	1.3	(0.0, 2.5)	0.47	(-0.20, 1.15)	0.79	(-0.78, 2.37)
Maritime chaparral	5	1.6	(0.8, 2.4)	0.54	(-0.84, 1.93)	1.13	(-1.18, 3.43)

Surface fuels at the Fort Huachuca T2 site (356 ha) were more sparse in comparison to the chaparral fuel types at Vandenberg and Hunter-Liggett with % cover < 30%. Litter from the oaks comprised nearly 60% of the fuel loading. The bulk density of the shrub fuel bed was estimated to be 0.19 kg m^{-3} which produced a packing ratio of 0.0003 using the particle density for broadleaved fuels. Estimated live fuel moisture content was 53% and 46% for the < 0.63 cm live material and the 0.64-2.53 cm live branches. These moisture contents excluded dead attached branches which were initially identified as living. The moisture content of the combined dead aerial and ground woody fuels < 0.63 cm and 0.64-2.54 cm was 7%, respectively. The burn was marginal with little fire spread into the shrub component of the site. The primary fuel that was consumed was the grass fuel. Fuel consumption was estimated by subtraction from pre burn and post burn fuel sampling at the T2 site and is presented in Table 4-6. All live and dead fuels were added to calculate the total loading for each transect. If the calculated fuel consumption for a transect was < 0 and was greater than -10% of pre-burn loading, the calculated consumption was set = 0. This occurred on 1 transect. As can be seen in Table 4-8, the variability was quite large as indicated by the large 95% confidence intervals. Even though litter was the largest component of the fuel bed (Table 4-9), only the consumption of the grass was significantly different from 0 again reflecting the large variability in both the fuel bed and the burn. Estimated total fuel consumed in the grass only class was 498 Mg.

Table 4-8 Estimated Fuel Consumption for the Emory Oak Woodland/savanna Prescribed Burn at Fort Huachuca, Feb 2010.

Site	N	**Fuel loading (kg m^{-2})**		
		Pre-burn	Post-burn	Consumption
T2	10	0.88 (0.41, 1.36)	0.59 (0.19, 1.00)	0.38 (0.07, 0.69)

Table 4-9 . Estimated fuel consumption by size class for the Emory oak woodland/savanna prescribed burn at Fort Huachuca, Feb 2010.

Size class[1]	N	**Fuel loading (kg m^{-2})**		
		Pre-burn	Post-burn	Consumption
Litter	10	0.52 (0.14, 0.90)	0.34 (0.11, 0.58)	0.24 (-0.05, 0.53)
Grass	10	0.19 (0.15, 0.23)	0.05 (-0.01, 0.10)	0.14 (0.08, 0.20)
< 0.63 cm	10	0.08 (0.02, 0.13)	0.07 (0.01, 0.14)	0.04 (-0.00, 0.06)
0.64-2.54	10	0.09 (0.02, 0.17)	0.16 (0.00, 0.31)	0.03 (-0.01, 0.08)

[1] Woody fuel size classes include both live and dead stems.

Comparing the measured with calculated fuel consumption using potentially applicable fuel models is challenging given the wide disparity in the wildland fuel parameters when measured in the field and when measured in the lab. For example, as shown in Table 4-10 the fuel loadings

observed in the lab and in the field differ by 100% and this difference creates uncertainty when calculating the expected fuel consumption. We present the fuel loading observed in the laboratory burns with the estimated field loadings and chose a fire behavior fuel model and an FCCS fuel model that might represent those fuel types. Notice the variation in the fuel types which could all be classified as fuel model 4. None of the observed fuel loadings are close to the loading and depth of fuel model 4. CONSUME was used to estimate consumption using the observed fuel moisture content. Given the wide variability in the sampling data, the predicted consumption is similar to the observed consumption.

Table 4-10 Properties of Lab & Field Fuels and Predicted Consumption

Fuel type	Loading (kg m^{-2})		Depth	NFFL Model[1]			FCCS Fuel bed			Consumption (kg m^{-2})	
	Lab	Field	(m)	ID	L	D	ID	L	D	Actual	Predicted
Chamise/scrub oak (chs)	4.9	1.9	1.2	4	3.6	1.8	44	1.0	0.7		
Ceanothus (cea)	3.6						44	1.0	0.7		
Maritime chaparral (mch)	4.5	1.6	0.7	4	3.6	1.8	44	1.0	0.7	1.13	0.45
Coastal sage scrub (cos)	3.6	1.3	0.8	2	0.8	0.6	51	0.8	1.1	0.79	1.11
Manzanita (man)	4.6	1.8	0.8	4	3.6	1.8	44	1.0	0.7		
California sagebrush (cas)	3.8						51	0.8	1.1		
Emory oak savanna (oas)	4.4	0.2		1	0.2	0.3	43	0.1	0.3		
Emory oak woodland (oaw)	3.2	0.7	0.9	4	3.6	1.8	43	0.5	1.2	0.38	

1. ID = fuel model number (1-13 for NFFL models (Albini, 1976); FCCS fuel bed number (1-216 (Riccardi et al, 2007), L = loading (kg m-2), D = depth (m).

4.2 Improved Emission Factors & New Test Methods

The measurement of emission factors was a key deliverable in the proposal submitted by the RC-1648team. Table 4-11 summarizes the work and shows goals and what was completed.

Table 4-11 Improved Emission Factors & New Test Methods

Proposed	Actual
Criteria pollutants: CO, NO_x, SO_x ,$PM_{2.5}$ mass	CO, NO_x, SO_x ,$PM_{2.5}$ (mass, number, diameter)
Other gases : CO_2, CH_4 and THC	CO_2, CH_4 and selected light hydrocarbons
Toxics: aldehydes, ketones, NH_3 and BTEX, SVOCs, PAHs	Aldehydes, ketones, BTEX, PAHs
Ions	SO_4, NO_3, Cl, Br, Na, NH_4, K, Ca
Elements (K, Cl…),	38 elements; primary were K, Cl, Na …
PM (EC, OC) Secondary PM	PM (EC, OC), levoglucosan (marker for biomass burning), Secondary O_3 and PM in atmospheric reactor, Black Carbon

The research was carried out in a number of steps or sub-tasks as indicated in Table 4-12.

Table 4-12 List of Sub-Tasks for the Emission Measurement Portion of the Project

1	Test and calibrate new PM/aerosol instruments at Riverside Fire Lab
2	Exploratory studies of primary and secondary PM in UCR atmospheric reactor
3	Measure gas/PM emissions from burns of chaparral in FS fire science lab
4	Measure gas/PM emissions from burns of oak woodlands in FS fire science lab
5	Measure gas/PM emissions from burns of long-leaf pine in FS fire science lab
6	Measure gas/PM emissions from prescribed burns of chaparral and oak savannah/woodlands
7	Create emission rate data in EPA AP-42 format for gaseous, PM, metals and reactive gases
8	Compare AMS biomass markers in lab with field & aircraft data.
9	Extend exploratory studies of secondary reactions in UCR atmospheric chamber. Measure black carbon.
10	Collect data during intense fire associated with prescribed burn of chaparral at California site.

4.2.1 RFL: Test and calibrate new PM/aerosol instruments

RFL was used to test whether specialized instruments designed for atmospheric levels of pollution with emissions levels could be used during biomass burning. Exploratory trials showed that the super-sensitive instruments were adaptable for biomass burning, thus enabling real-time characterization of multiple gases and PM properties during flaming and smoldering regimes at MFSL.

As mentioned in the methods section, the SERDP project work and goals at RFL were expanded when the Forest Service asked for measurements of emissions from burning silvicultural piles

covered by polyethylene plastic. The project mixed different weights of plastic with manzanita wood (*Arctostaphylos sp.*) and found that inclusion of polyethylene plastic at levels found in silvicultural piles had no effect on the measured emissions of the 195 detectable with the UCR instrument suite. The full results of that work are presented in the paper Hosseini et al (2014) *Effect of low-density polyethylene on smoke emissions from debris pile burning.* Basically the new project provided the UCR team with a chance to gain experience at adapting the very sensitive equipment used in the atmospheric chemistry lab to the very high concentrations seen near fires and time to improve the planned protocols for the Montana deployment before arriving there. As is customary in the literature, the emission factors were plotted against MCE and fitted to a linear relationship (Figure 4-2). However, note the narrow range of MCE so equation is of limited use.

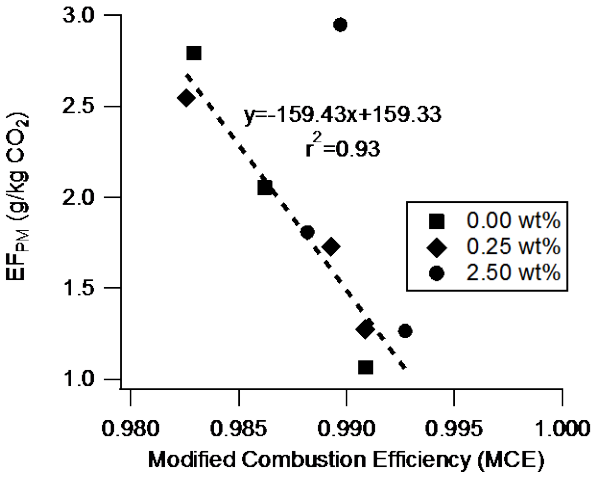

Figure 4-2 PM Emission Factor vs. Modified Combustion Efficiency vs. % Polyethylene

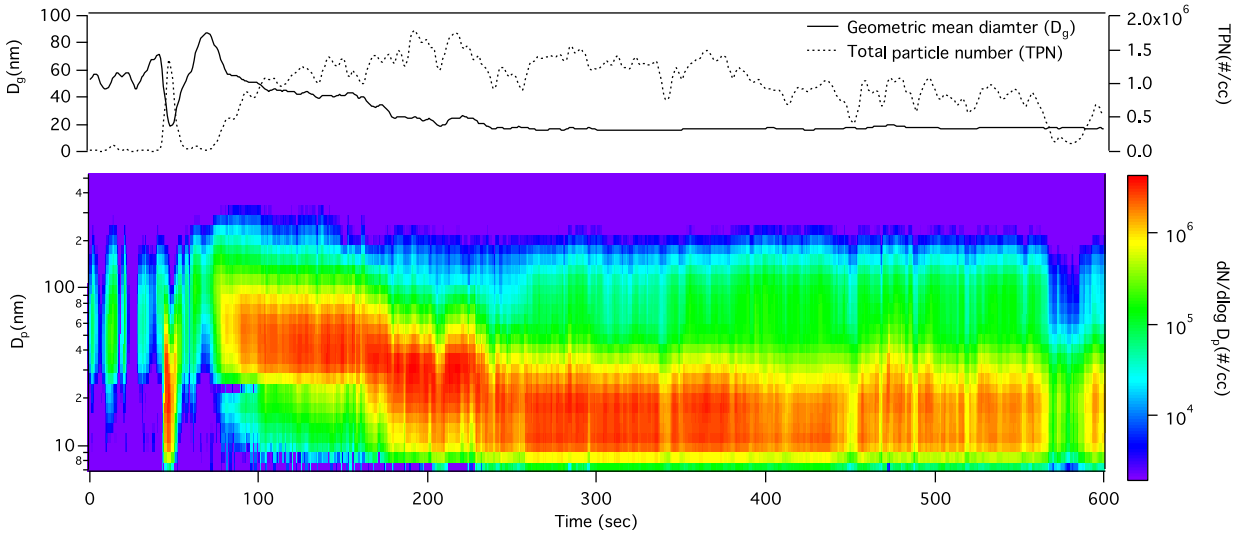

Figure 4-3 Example of Particle Size and Number Data from Manzanita/Polyethylene Fire

Table 4-13 Selected Emission Factors from Manzanita wood (g/kg-CO_2)

Species	Manzanita	Other ref. (g/kg fuel burned)
MCE	0.987±0.002	0.948±0.007, 0.930±0.029
CO	13.5±2.4	64.3±8.0
NO_x as NO	1.53±0.09	2.67±0.21
PM mass	1.97±0.50	3.61±1.17, 23.5±25.9, 3.3-11.4, 2.5-9.0, 0.1-2.5, 5.1-9.5
EC	0.379±0.062	0.51±0.18 , 0.35±0.31, 0.22-3.56, 1.4-3.2
OC	0.91±0.24	0.85±0.71, 14.8±17.3, 2.34-8.37, 43.7-56.0

Note the data for the PM emission factor are expressed as gm per kg of CO_2 vs. reference data that is expressed as g per kg of fuel burned (Table 4-13). Given that we assumed manzanita wood is 41.3% carbon, the conversion factor is: (413 gC/kg manzanita) * (44 g CO_2/12g C) = 1.5 kg CO_2/kg-fuel. For example a PM mass of 1.97g/kg CO_2 is 2.97g/kg-fuel when comparing. The first data point of 3.61 was for manzanita and is close, given the range of reported values. Values from this work showed the expected trend, when plotted against the Modified Combustion Efficiency (MCE) provide the expected relationship. Comparative comments are difficult to make given the very wide range of the reported values. Comparative values for CO were much lower so CO values were watched in the MFSL experiments.

Continuous data provided for PM in Figure 4-3 showed analysis of PM could be followed from flaming to smoldering something that was not possible before when a single filter was used. This finding was encouraging. Other data follow in Tables 4-14, 4-15, and 4-16 from the multi-component analysis of the selected gases and polycyclic aromatic hydrocarbons (PAHs).

Table 4-14 Emission Factors for Carbonyl from Manzanita (g/kg-CO_2) & Other Fuels

Species	Manzanita	Other ref. (mg/kg fuel burned)
Acetone	50±18	366 , 749, 73.9±16.2
Formaldehyde	206±77	113-245, 422, 1165, 174.8±52.5
Acetaldehyde	127±55	301-425 , 86 , 1704 , 92.7±21.9
Propionaldehyde	19.9±8.5	80-150 ,7.6, 255, 7.5±15.1
Crotonaldehyde (butenal)	12.5±5.0	276
MEK	3.9±1.3	8.3 , 215
Methacrolein	23.5±10.3	1.8 , 23
Butyraldehyde	5.4±1.9	19-36 , 96, 52.1±18.2
Benzaldehyde	8.4±3.3	12
Valeraldehyde	4.0±1.1	7-18 ,1.1 , 85.9±37.4
Tolualdehyde	4.5±2.7	0.9
Hexanal	120±47	34.6 , 89.0±37.5
Acrolein	33±14	46-91 , 63
Sum	618±109	

Table 4-15 Emission Factors for PAHs from Manzanita (mg/kg-CO_2) & Other Fuels

Species	Manzanita	Other ref. (mg/kg fuel burned)
Particle-phase Poly Aromatic Hydrocarbons (PAH)		
Naphthalene	71±23	21-54, 18.34±14.05, 38.1±31.9
Acenaphthylene	43±33	5-9, 1.01-2.66, 14.2±12.2
Acenaphthene	0.82±0.45	0.41-0.89, 0.18-2.51, 0.2±0.1
Fluorene	3.4±1.7	2.15-3.50, 0.05-0.92, 0.2±0.1
Phenanthrene	10.5±7.0	1.99-3.94, 5.8±1.8
Anthracene	1.15±0.48	0.32-1.27, 6.3±1.4
Fluoranthene	1.02±0.21	0.52-2.86, 1.2±0.2
Pyrene	1.03±0.20	0.45-1.47, 1.1±0.5
Benz(a)anthracene	0.039±0.018	0.21-0.40, 0.04±0.06
Chrysene	0.029±0.010	0.75-1.14, 0.21-0.34, 0.04±0.05
Benzo(b)fluoranthene	0.059±0.025	0.40-0.79, 0-0.05, 0.09±0.12
Benzo(k)fluoranthene	0.008±0.002	0.29-0.67,0-0.13, 0.02±0.01
Benzo(a)pyrene	0.032±0.006	0.25-0.71, 0.03±0.03
Indeno(1,2,3cd)pyrene	0.013±0.001	, 0.03±0.04
Dibenzo(a,h)anthra.	0.013±0.006	0.05±0.07
Benzo(ghi)perylene	0.043±0.016	0-0.002
Sum	132±41	
Gas-phase Poly Aromatic Hydrocarbons (PAH)		
Fluorene	0.056±0.015	27.4, 73-269, 0.04±0.06
Phenanthrene	0.122±0.035	10-17, 99.1, 0.21±0.20

Species	Manzanita	Other ref. (mg/kg fuel burned)
Anthracene	0.0101±0.0024	19.3, 1-50, 0.04±0.03
Fluoranthene	0.095±0.021	1.75-3.99, 19.3, 286-1083, 0.22±0.14
Pyrene	0.116±0.031	1.49-3.39, 25.5, 1.87-2.70, 222-1080, 0.74±0.84[f]
Benz(a)anthracene	0.112±0.040	0.31-0.56, 3.5, 127-249, 0.23±0.08
Chrysene	0.096±0.033	0.28-0.61, 4.1, 107-253,0.18±0.16
Benzo(b)fluoranthene	0.26±0.12	0.51-1.05, 6.1, 36-157, 0.67±1.00
Benzo(k)fluoranthene	0.081±0.036	0.51-1.05, b.d., 3.23±2.91
Benzo(a)pyrene	0.18±0.08	0.15-0.34, 0.09±0.10
Indeno(1,2,3-cd)pyrene	0.21±0.10	0.07-0.19, 3.6, 39-164, 0.06±0.03
Dibenzo(a,h)anthra.	0.04±0.01	b.d., 3-11, 0.02±0.01
Benzo(ghi)perylene	0.28±0.13	0.07-0.22, 2.6, 0.44, 25-70, 0.11±0.07
Sum	1.66±0.23	

Table 4-16 Emission Factors for Light Aromatic Volatiles from Manzanita (mg/kg-CO_2) & Other Fuels

Species	Manzanita	Other ref. (mg/kg fuel burned)
Benzene	105±70	225-110, 1500**,** 383, 411.8± 67.1
Toluene	25±20	130-320, 740, 158, 148.9± 22.9
m & p-xylene	6.6±6.0	41-72, 125, 60, 34.8± 4.3
o-Xylene	2.20±1.76	16-27, 20, 18, 9.0 ± 4.2
Styrene	9.2±8.0	40-117
Indane	0.016±0.008	0-0.12
Sum	148±74	

Hosseini et al (2014) provides emission factors from burning manzanita wood of many other hydrocarbon compounds, including alkanes, cycloalkanes, alkenes, cycloalkenes, diolefins, and monocyclic aromatic hydrocarbons, that were desorbed from the collection tubes. The key finding of the testing at RFL was that we were able to successfully adapt the atmospheric instruments to work with concentrated emissions from biomass burning. This demonstration provided confidence that the proposed protocols would work at Montana when all the outside members arrived for the testing.

4.2.2 MFSL Burns

One of the most important goals of the SERDP project was the publication of new and improved emission factors to: 1) update values in the EPA's AP-42 tables and 2) provide new values as input into the air quality models.

The approach was to select representative wildland fuels from the southwest and southeast and burn then at MFSL on a platform under a hood. Seventeen meters above the fire bed well-the mixed exhaust was sampled with a suite of traditional and state-of–art instruments to measure the concentrations of gaseous and PM constituents in the emissions leaving the fire. Concentrations were measured starting with the flaming phase and continuing to the smoldering phase. Some concentrations were collected as one sample for the duration of the burn and other concentrations were measured continuously with sophisticated instruments. The sophisticated instruments

allowed a number of first-ever continuous measurements to be made for some gaseous species and PM characteristics. As mentioned earlier, there were a total of seventy-seven burns of sixteen different fuels carried out (Table 4-17).

Concentration data with flow rates in the exhaust stack are used to compute emission factors. Emission factors can be computed as the emission ratios for any point in time during a fire (Yokelson et al., 1996), but in this paper we present only fire-integrated emission ratios. Since the emissions from the various combustion processes (e.g. flaming and smoldering) are different, a useful quantity describing the relative amount of flaming or smoldering combustion is the modified combustion efficiency, MCE, defined as (Yokelson et al., 1996):

$$MCE = (\Delta CO_2)/ (\Delta CO_2 + \Delta CO)$$

Higher MCE values are indicative of more complete combustion to CO_2 in the flaming regime and lower MCE values are for the incomplete combustion found in the smoldering regime. As with emission ratios, MCE can be computed for any point in time during a fire (Yokelson et al., 1996), but in that paper only the MCE values integrated for the whole fire were computed in order to compare with other values.

Table 4-17 Summary of Vegetation Burned and Fuel Elemental Analysis

Fuel Type	Species Names	Fuel Code	Location[1]	# Burns ([2])	C-content (%)	N-content (%)
SW Fuels						
ceanothus	*Ceanothus leucodermis*	cea	FHL CA	6(5)	51	1.1
chamise/scrub oak	*Adenostoma fasciculatum, Quercus berberidifolia*	chs	FHL CA	6(5)	53	0.82
California sagebrush	*Artemisia californica, Ericameria ericoides*	cas	VAFB CA	6(6)	50	1.2
coastal sage scrub	*Salvia mellifera, Ericameria ericoides, Artemisia californica*	cos	VAFB CA	5(3)	50	1.04
maritime chaparral	*Ceanothus impressus var. impressus, C. cuneatus var. fascicularis, Salvia mellifera*	mch	VAFB CA	5(5)	51	1.15
manzanita	*Arctostaphylos rudis, Arctostaphylos purissima*	man	VAFB CA	6(6)	53	0.71
masticated mesquite	*Prosopis velutina, Baccharis sarothroides*	mes	FHUA AZ	5(5)	48	1.3
oak savanna	*Quercus emoryi, Eragrostis lehmanniana*	oas	FHUA AZ	5(5)	49	1.0
oak woodland	*Quercus emoryi, Arctostaphylos pungens*	oaw	FHUA AZ	5(4)	51	0.86
SE Fuels						
1 year rough	*Lyonia lucida and Ilex glabra*	1yr	CL NC	3(3)	55	0.72
2 year rough	*Lyonia lucida and Ilex glabra*	2yr	CL NC	4(4)	53	1.0
chipped understory hardwood	*Acer rubrum, Persea borbonia, Gordonia lasianthus*	cuh	CL NC	3(3)	54	0.44
understory hardwood	*Acer rubrum, Persea borbonia, Gordonia lasianthus*	uh	CL NC	3(3)	50[3]	-[3]
pocosin	*Lyonia lucida and Ilex glabra*	poc	CL NC	3(3)	54	0.72
pine litter	*Pinus taeda, Pinus echinata, Pinus elliottii, Pinus palustris*	lit	FB GA	5(5)	53	0.58
Other Fuels						
Duff (black spruce forest)	*Picea mariana*	duf	AK	1(1)	42	1.1
Englemann Spruce	*Picea engelmannii*	spr	MT	2(2)	53	0.88
ponderosa pine needles	*Pinus ponderosa*	ppn	MT	1(1)	53	0.48

[1] FHL – Fort Hunter Liggett; VAFB – Vandenberg Air Force Base; FHUA – Fort Huachuca; CL – Camp Lejeune; FB – Fort Benning.
[2] Number in brackets is the number of burns sampled by OP-FTIR.
[3] The nitrogen and carbon contents of the understory hardwood sample of Camp Lejeune were not determined. A reasonable estimate of 50% was used for the carbon content of this fuel type.

Table 4-18 Selected Fuel Bed Properties at Montana Fire Lab

Fuel type	*n*	Moisture content (%)	Fuel bed dry mass (g)	Bulk density (kg/m^3)	Packing ratio[a]	Consumption (%)
Southwestern U.S.						
Chamise/Scrub Oak **(CHS)**	6	11.9	2079	8.6	0.015	38
Ceanothus **(CEA)**	6	10.2	2007	5.8	0.010	54
Coastal Sage Scrub **(COS)**	5	9.3	2299	6.0	0.010	95
California Sagebrush **(CAS)**	6	9.0	2460	6.4	0.011	93
Manzanita **(MAN)**	6	12.6	2906	7.6	0.013	94
Oak Savanna **(OAS)**	5	14.3	2788	7.3	0.012	91
Oak Woodland **(OAW)**	5	32.8	2054	5.3	0.009	95
Masticated Mesquite **(MES)**	5	4.3	1831	14.3	0.024	92

[a] Packing ratio = bulk density/particle density. Assumed particle density of 593 $kg\,m^{-3}$ (average from Countryman, 1982)

4.2.3 MFSL Results – Gaseous emission factors

The emissions factors for the gases are mainly described in a publication in Atmospheric Chemistry and Physics by Burling et al.: *Laboratory measurements of trace gas emissions from biomass burning of fuel types from the southeastern and southwestern United States.* As pointed out in the publication, smoke emissions were measured with a large suite of state-of-the-art instrumentation including an open-path Fourier transform infrared (OP-FTIR) spectrometer for measurement of gas-phase species. The OPFTIR detected and quantified 19 gas-phase species in these fires: CO_2, CO, CH_4, C_2H_2, C_2H_4, C_3H_6, HCHO, HCOOH, CH_3OH, CH_3COOH, furan, H_2O, NO, NO_2, HONO, NH_3, HCN, HCl, and SO_2. Those species measured by the OP-FTIR associated with flaming combustion include CO_2, NO, NO_2, HCl, SO_2, and HONO while those associated with smoldering combustion include CO, CH_4, NH_3, C_3H_6, CH_3OH, CH_3COOH, and C_4H_4O (furan).The species C_2H_2, C_2H_4, HCOOH, and HCHO can be associated with both flaming and smoldering combustion (Lobert et al., 1991; Yokelson et al., 2008).

Emission factors for these species are presented for each vegetation type burned. Concentrations of the multiple gaseous constituents were continuously monitored and later converted into emissions factors based on the mass of the dry fuel burned. For example, carbon dioxide is the primary emission from biomass burning and constitutes a significant amount of the global greenhouse gases released. Emission factors for CO_2 range between 1600 to 2250 g per kg fuel. As is evident, chamise released the most CO_2 and oak savanna and oak woodland released the lowest amount. Similarly, CO emissions from chamise correspond to a maximum and emissions from oak woodland and oak savanna were the lowest. Error bars as shown in Figures 4-4 and 4-5 are at one standard deviation and show some differences. However, at 95% confidence interval, the error bars would overlap. Lab burns have many uncontrolled variables and that leads to variations expressed as a large value for the standard deviation and coefficient of variation, the underlining cause of the peaks to overlap.

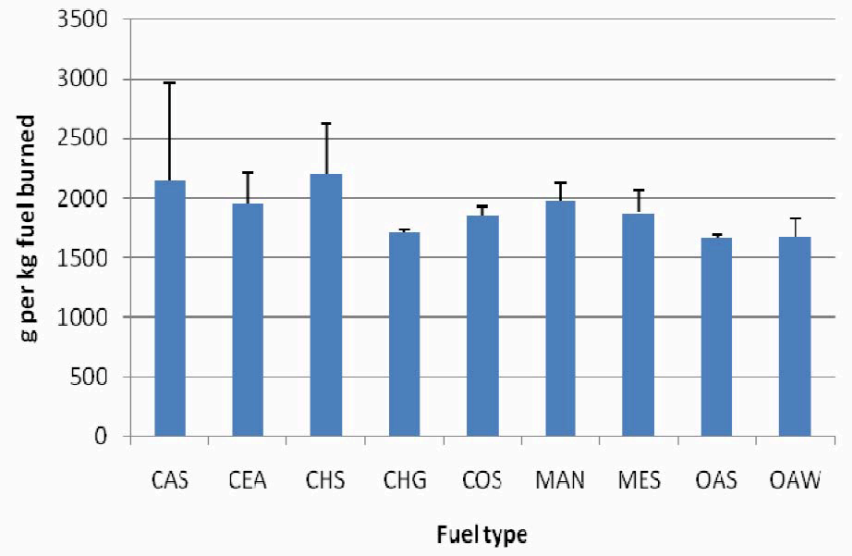

Figure 4-4 Carbon Dioxide Emission Factors for Different Southwestern Fuel Types

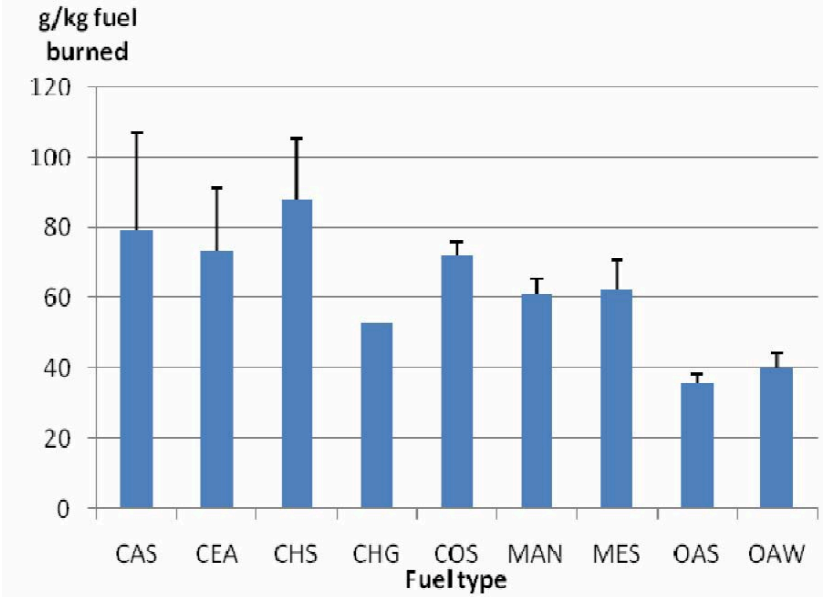

Figure 4-5 Carbon Monoxide Emission Factors for some Southwestern Fuel Types

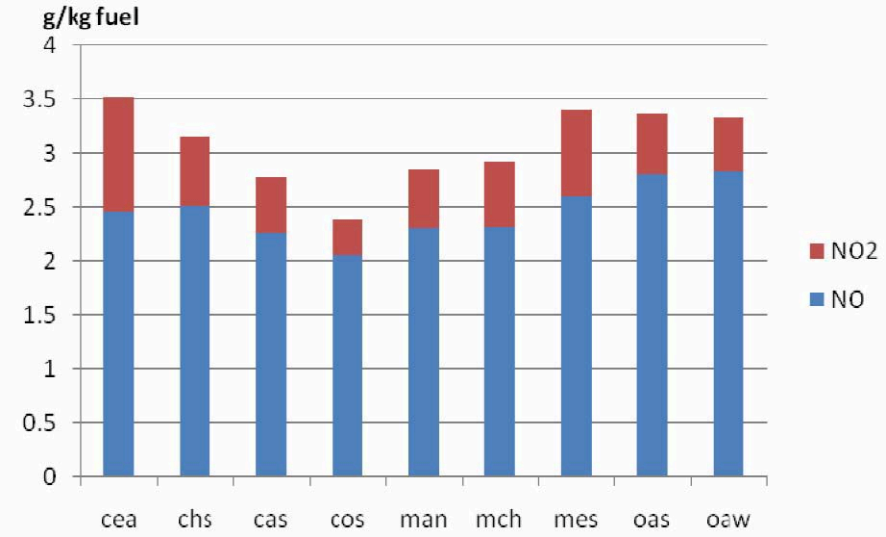

Figure 4-6 Nitric Oxides Emission Factors for some Southwestern Fuel Types

NO_x emission factors are shown in Figure 4-6. The data show that ceanothus, mesquite, oak savanna, and oak woodland produce the highest amount of NO_x per kg of fuel burned and coastal sage the lowest emissions factor. The NO_x data are divided into emission factors for NO_2 and for NO. Results show that the NO emission factor is about 90% of the total NO_x emissions.

Emission factors were determined for a number of trace gases using the FTIR data. Some of these data are plotted in Figure 4-7 to Figure 4-9 for various gases of interest. Noteworthy is the high value for the emission factor of nitrous acid (HONO) as this was an unexpected finding and significant since HONO is a significant molecule in the kinetic path leading to the formation of ozone.

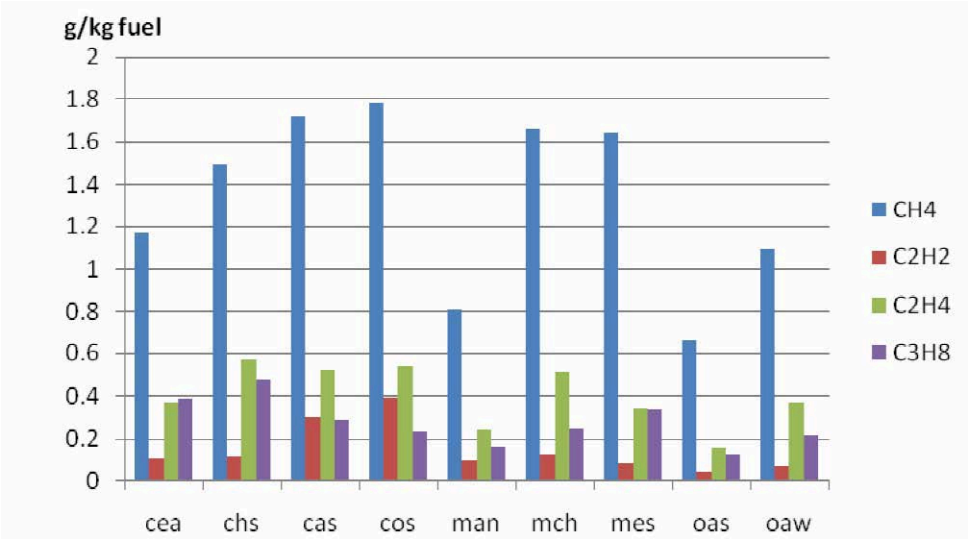

Figure 4-7 Emission Factor for Light Paraffins for some Southwestern Fuel Types

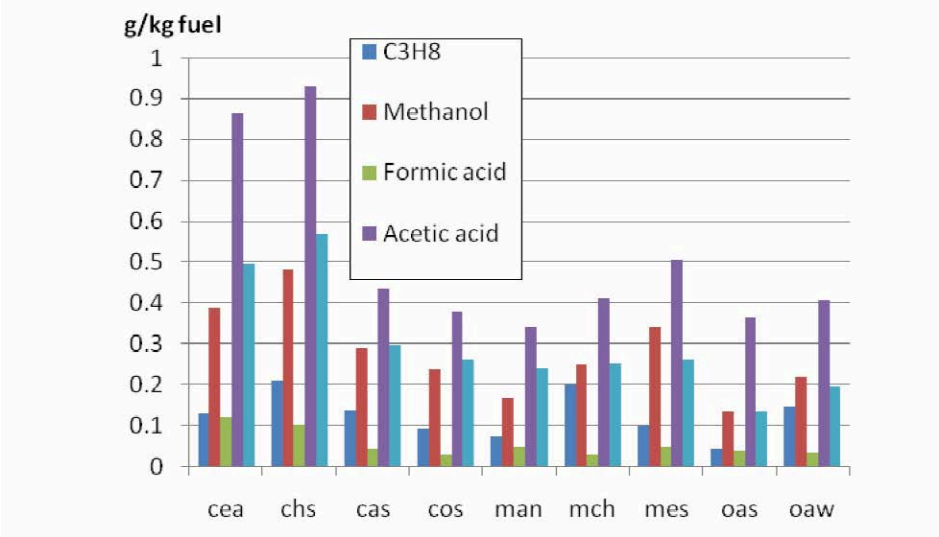

Figure 4-8 Emission Factor of Selected Oxy-Hydrocarbons for some Southwestern Fuel Types

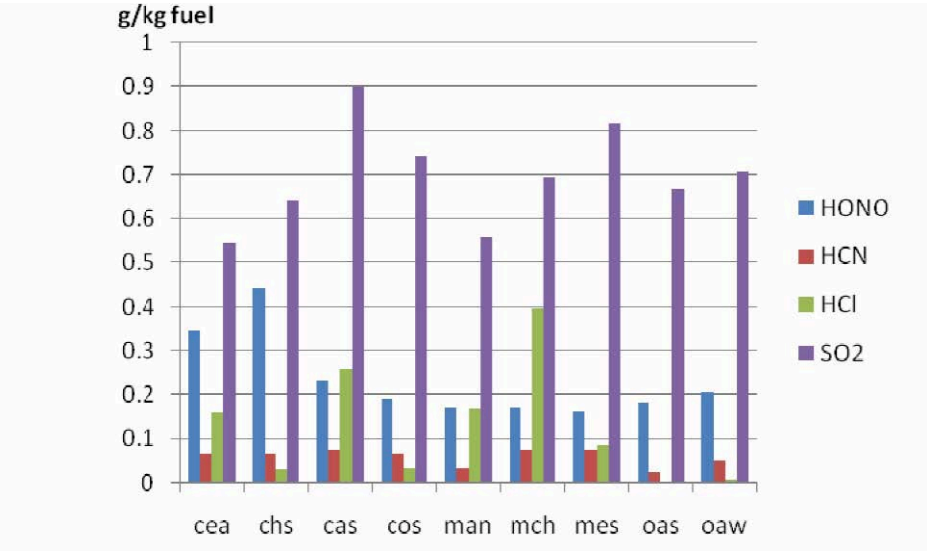

Figure 4-9 Emission Factor for Selected Compounds for some Southwestern Fuel Types

Gas-phase nitrous acid (HONO), an important OH precursor and ozone initiator, was detected in the smoke from all fires. The HONO emission factors ranged from 0.15 to 0.60 g per kg of fuel and were higher for the southeastern fuels. The fire-integrated molar emission ratios of HONO (relative to NO_x) ranged from approximately 0.03to 0.20, with higher values also observed for the southeastern fuels. The majority of non-methane organic compound (NMOC) emissions detected by OP-FTIR were oxygenated volatile organic compounds (OVOCs) with the total identified OVOC emissions constituting 61±12% of the total measured NMOC on a molar basis. These OVOC may undergo photolysis or further oxidation contributing to ozone formation. Elevated amounts of gas-phase HCl and SO_2 were also detected during flaming combustion, with the amounts varying greatly depending on location and vegetation type. The fuels with the highest HCl emission factors were all located in the coastal regions, although HCl was also

observed from fuels further inland. Emission factors for HCl were generally higher for the southwestern fuels, particularly those found in the chaparral biome in the coastal regions of California.

Fire-integrated emission factors and emission ratios to CO and CO_2 were determined for all fires. We use mass-based EF and molar ER in this discussion when appropriate for comparison purposes. The fire-integrated emission factors for all fuels sampled in this study are shown in Table 4-19 for the southwestern fuels and Table 4-20 for the southeastern fuels, respectively. These are averages of the replicate samples. More than 100 other NMOC and inorganic acids were also measured along with the particle emissions, and are being reported separately (including Roberts et al., 2010;Veres et al., 2010; and Warneke et al., 2010). While only a small percentage of the total carbon sources, these additional NMOC are often reactive and very important in plume chemistry.

Table 4-19 Emission Factors (g kg^{-1}) of Gas-phase Species for Southwestern Fuels. (Burling et al., 2011)

	FHL cea[2]	FHL chs	VAFB cas	VAFB cos	VAFB man	VAFB mch	Chaparral average	Chaparral (Radke et al., 1991)	FHUA mes	FHUA oas	FHUA oaw	FHUA average
MCE	0.946(0.011)	0.939(0.010)	0.944(0.005)	0.939(0.004)	0.948(0.007)	0.952(0.001)	0.945(0.005)	0.946(0.021)	0.954(0.001)	0.971(0.004)	0.965(0.004)	0.963(0.009)
CO_2	1762(25)	1801(14)	1739(9)	1724(6)	1837(15)	1769(15)	1772(41)	1687(53)	1688(5)	1733(8)	1786(6)	1736(49.1)
CO	63.9(13.4)	74.9(13.1)	65.6(5.3)	71.1(4.8)	64.3(8.0)	56.4(1.9)	66.0(6.4)	61.0(23.4)	52.3(1.6)	32.7(4.5)	40.6(4.3)	41.9(9.9)
CH_4	1.17(0.51)	1.49(0.28)	1.72(0.33)	1.78(0.20)	0.81(0.49)	1.66(0.30)	1.44(0.38)	2.30(1.35)	1.64(0.31)	0.66(0.26)	1.10(0.31)	1.13(0.49)
C_2H_2	0.111(0.038)	0.122(0.076)	0.307(0.111)	0.394(0.115)	0.101(0.037)	0.130(0.025)	0.194(0.125)	0.20(0.12)	0.090(0.036)	0.039(0.004)	0.073(0.023)	0.067(0.026)
C_2H_4	0.369(0.251)	0.574(0.138)	0.526(0.130)	0.545(0.068)	0.246(0.116)	0.514(0.121)	0.462(0.128)		0.344(0.065)	0.163(0.050)	0.371(0.120)	0.293(0.113)
C_3H_6	0.132(0.101)	0.208(0.039)	0.136(0.072)	0.093(0.038)	0.074(0.070)	0.200(0.075)	0.141(0.055)	0.43(0.17)	0.100(0.041)	0.045(0.022)	0.146(0.065)	0.097(0.051)
CH_3OH	0.386(0.242)	0.480(0.072)	0.292(0.117)	0.238(0.047)	0.170(0.085)	0.249(0.037)	0.303(0.112)		0.341(0.066)	0.133(0.039)	0.218(0.078)	0.231(0.105)
HCOOH	0.123(0.099)	0.104(0.030)	0.045(0.022)	0.032(0.002)	0.050(0.047)	0.032(0.010)	0.064(0.039)		0.051(0.036)	0.040(0.009)	0.035(0.012)	0.042(0.008)
CH_3COOH	0.864(0.524)	0.928(0.148)	0.434(0.098)	0.377(0.012)	0.342(0.169)	0.414(0.084)	0.560(0.263)		0.506(0.061)	0.366(0.089)	0.407(0.159)	0.426(0.072)
HCHO	0.496(0.349)	0.569(0.188)	0.296(0.077)	0.263(0.050)	0.240(0.167)	0.254(0.036)	0.353(0.142)		0.264(0.048)	0.134(0.031)	0.198(0.069)	0.199(0.065)
C_4H_4O (furan)	0.142(0.132)	0.116(0.084)	0.051(0.024)	0.036(0.012)	0.064(0.048)	0.048(0.010)	0.076(0.043)		0.039(0.016)	0.024(0.021)	0.047(0.019)	0.037(0.012)
NH_3	0.540(0.190)	0.512(0.242)	0.734(0.431)	0.522(0.103)	0.411(0.250)	0.769(0.164)	0.581(0.140)	0.90(1.14)	0.717(0.262)	0.269(0.102)	0.580(0.130)	0.522(0.230)
NO	2.466(0.193)	2.506(0.290)	2.260(0.242)	2.060(0.256)	2.311(0.205)	2.327(0.101)	2.322(0.160)		2.611(0.158)	2.807(0.167)	2.832(0.226)	2.750(0.121)
NO_2	1.061(0.474)	0.650(0.140)	0.523(0.103)	0.330(0.008)	0.552(0.096)	0.601(0.169)	0.620(0.242)		0.790(0.039)	0.566(0.077)	0.496(0.087)	0.617(0.154)
NO_x (as NO)	3.158(0.243)	2.930(0.366)	2.601(0.268)	2.276(0.261)	2.672(0.209)	2.719(0.140)	2.726(0.300)	5.11(2.27)	3.126(0.154)	3.176(0.163)	3.156(0.215)	3.153(0.025)
HONO	0.345(0.161)	0.442(0.098)	0.230(0.042)	0.189(0.058)	0.170(0.039)	0.171(0.032)	0.258(0.112)		0.160(0.029)	0.182(0.042)	0.204(0.033)	0.182(0.022)
HCN	0.063(0.048)	0.064(0.036)	0.074(0.025)	0.063(0.006)	0.033(0.016)	0.073(0.009)	0.062(0.015)		0.072(0.019)	0.024(0.013)	0.049(0.006)	0.048(0.024)
HCl	0.159(0.062)	0.030(0.011)	0.258(0.168)	0.035(0.030)	0.167(0.094)	0.397(0.164)	0.174(0.139)		0.086(0.032)	0.002(0.007)	0.007(0.012)	0.032(0.047)
SO_2	0.545(0.204)	0.641(0.090)	0.902(0.139)	0.743(0.031)	0.559(0.070)	0.693(0.043)	0.681(0.133)		0.817(0.107)	0.666(0.068)	0.708(0.088)	0.730(0.078)
ER(CO_2) Σ NMOC[3]	1.708	2.042	1.563	1.545	0.850	1.311	1.503		1.243	0.618	1.015	0.959
ER(CO_2) Σ OVOC[3]	1.193	1.305	0.708	0.605	0.504	0.610	0.821		0.770	0.405	0.533	0.570
Σ OVOC/Σ NMOC[3]	70%	64%	45%	39%	59%	47%	54%		62%	66%	53%	60%

[1] Value in brackets corresponds to (1σ) standard deviation.

[2] See Table 1 for fuel codes.

[3] NMOC and OVOC data includes only those species measured by OP-FTIR and are given as molar emission ratios (mmol mol^{-1}).

Table 4-20 Emission Factors[1] (g kg^{-1}) of Gas-Phase Species for Southeastern and Additional Fuels (Burling et al., 2011)

	FB lit[2]	CL 1yr	CL 2yr	CL poc	CL cuh	CL uh	Camp Lejeune average	Camp Lejeune (Yokelson et al., 1999)	AK duf	MT spr	MT ppn
MCE	0.894(0.017)	0.934(0.015)	0.927(0.006)	0.953(0.011)	0.959(0.003)	0.954(0.012)	0.945(0.014)	0.926(0.001)	0.827	0.934	0.959
CO_2	1710(39)	1859(42)	1780(19)	1874(27)	1891(7)	1739(23)	1828.6(66)	1677(8)	1219	1785	1856
CO	128.6(19.8)	84.0(18.2)	88.8(7.4)	59.4(13.7)	51.9(3.3)	53.6(13.7)	67.5(17.5)	85.9(2.7)	162	80.6	51.0
CH_4	4.25(1.87)	3.25(1.07)	3.47(1.35)	1.69(0.55)	1.55(0.44)	1.35(0.37)	2.26(1.01)	4.46(1.03)	9.60	4.00	1.21
C_2H_2	0.138(0.029)	0.527(0.486)	0.207(0.091)	0.098(0.022)	0.065(0.012)	0.088(0.010)	0.197(0.192)		0.112	0.565	0.085
C_2H_4	1.048(0.339)	1.969(1.556)	1.059(0.385)	0.450(0.143)	0.280(0.070)	0.428(0.097)	0.837(0.700)		1.73	2.14	0.502
C_3H_6	0.500(0.236)	0.551(0.364)	0.442(0.136)	0.176(0.088)	0.108(0.025)	0.162(0.056)	0.288(0.196)	1.26	1.40	0.721	0.201
CH_3OH	1.994(0.687)	0.868(0.424)	1.161(0.404)	0.667(0.294)	0.224(0.036)	0.521(0.112)	0.688(0.353)	2.03	4.07	1.62	0.135
HCOOH	0.460(0.194)	0.227(0.145)	0.280(0.197)	0.224(0.115)	0.033(0.011)	0.119(0.036)	0.177(0.099)	0.59[5]	0.917	0.393	0.079
CH_3COOH	3.688(1.605)	1.853(0.951)	2.743(1.288)	2.119(1.045)	0.337(0.083)	1.276(0.106)	1.666(0.911)	3.11	9.28	2.17	0.188
HCHO	2.024(0.777)	1.277(0.899)	1.088(0.312)	0.846(0.313)	0.209(0.045)	0.633(0.203)	0.811(0.415)	2.25(0.10)	2.28	1.91	0.512
C_4H_4O (furan)	0.486(0.152)	0.091(0.025)	0.132(0.039)	0.124(0.067)	0.041(0.022)	0.139(0.059)	0.105(0.040)		1.25	0.228	0.119
NH_3	0.952(0.337)	0.942(0.212)	1.037(0.162)	0.472(0.132)	0.354(0.006)	0.520(0.162)	0.665(0.304)	0.56	3.41	1.46	0.276
NO	1.860(0.377)	1.980(0.131)	2.257(0.343)	1.148(0.115)	1.365(0.063)	1.849(0.034)	1.720(0.454)		0.738	1.74	2.05
NO_2	0.932(0.403)	1.028(0.256)	1.233(0.311)	1.346(0.220)	0.623(0.098)	0.886(0.040)	1.023(0.286)		0.232	1.58	0.865
NO_x (as NO)	2.468(0.490)	2.651(0.053)	3.061(0.261)	2.025(0.079)	1.772(0.126)	2.427(0.033)	2.387(0.509)		0.890	2.77	2.61
HONO	0.241(0.052)	0.603(0.231)	0.515(0.090)	0.402(0.073)	0.146(0.026)	0.425(0.033)	0.418(0.172)		0.037	0.620	0.194
HCN	0.650(0.163)	0.233(0.123)	0.337(0.116)	0.106(0.060)	0.041(0.005)	0.104(0.058)	0.164(0.119)		1.74	0.316	0.105
HCl	0.094(0.045)	−0.012(0.023)	0.032(0.012)	0.177(0.072)	0.057(0.016)	0.045(0.059)	0.060(0.071)		bdl[4]	0.046	0.087
SO_2	1.547(0.324)	1.095(0.099)	1.435(0.176)	0.866(0.081)	0.437(0.013)	0.868(0.156)	0.940(0.365)		2.31	1.50	0.807
ER (Σ NMOC/CO_2)[3]	6.766	4.983	4.513	2.703	0.837	2.171	3.041		17.88	6.84	1.28
ER (Σ OVOC/CO_2)	5.361	2.529	3.121	2.138	0.486	1.601	1.975		14.29	4.00	0.661
Σ OVOC/Σ NMOC	79%	51%	69%	79%	58%	74%	66%		80%	58%	52%

[1] Value in brackets corresponds to (1σ) standard deviation.

[2] See Table 1 for fuel codes.

[3] NMOC and OVOC data includes only those species measured by OP-FTIR and are given as molar emission ratios (mmol mol^{-1}).

[4] bdl – below detection limit.

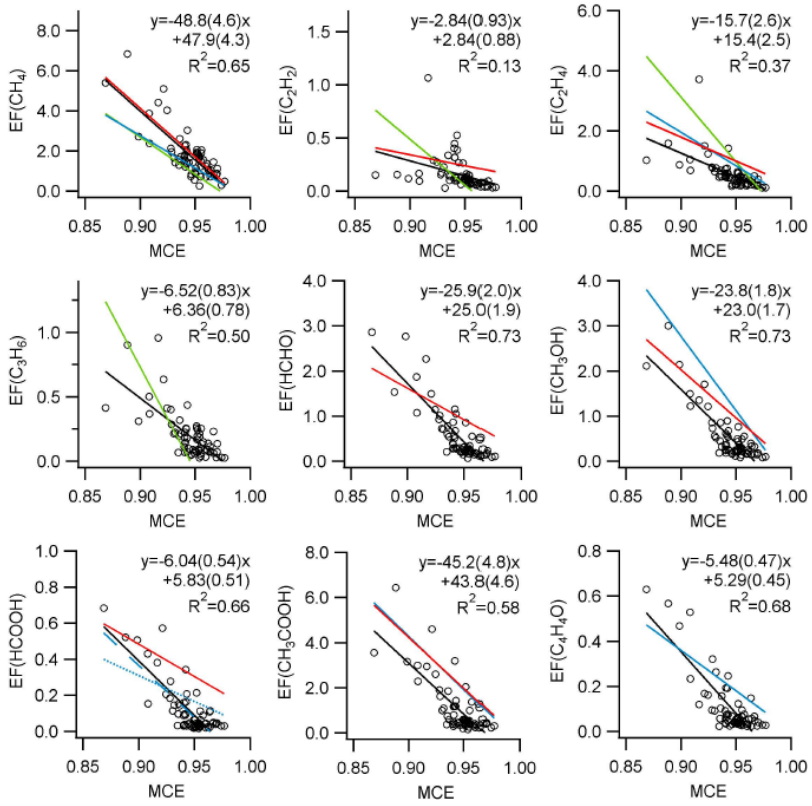

Figure 4-10 Emission Factors as a Linear Function of MCE (g per kg fuel)

Emission factors of organic compounds… Significant emissions of NMOCs were measured in the smoke with the primary compounds being: HCHO, CH_3OH, CH_3COOH with molar OVOC/NMOC ratios of 56% and 69%. The non-methane hydrocarbons are important due to their reactions with oxidants in the plume and activity for photolysis. Figure 4-10 shows the emission factors (g per kg fuel) plotted as a function of modified combustion efficiency (MCE) for carbon-containing gas-phase species measured in this project.

$$MCE = \frac{\Delta CO_2}{\Delta CO + \Delta CO_2} \begin{cases} Pure\ flaming\ if > 0.95 \\ Pure\ Smoldering\ 0.75 - 0.85 \end{cases}$$ where

$$\Delta x = x_{measured} - x_{background}$$

Biomass burning is known as an important source of oxygenated volatile organic compounds (OVOC). All oxygenated organic species detected by OP-FTIR show a linear dependence on MCE characteristic of smoldering combustion, with R^2 ranging from 0.58 to 0.73. EFs agreed well with results previously published in the literature

Emission factors of nitrogen compounds Of particular interest was the observation of elevated amounts of HONO in the emissions of all fires sampled. Emission factors for HONO ranged from 0.15 to 0.60 g kg^{-1} and $\Delta HONO/\Delta NO_x$ ranged from 0.025to 0.20 depending on fuel type burned. The HONO emissions observed could represent a significant source of OH in the plume, contributing to rapid formation of aerosol and O_3 as the plume ages.

In addition to the open-path Fourier transform infrared (OP-FTIR) measurements performed by UM, UCR also took samples during the whole burn with sorption media and analyzed the collected materials off-site using standard methods for selected light hydrocarbons and for carbonyls as described in the methods section. These data are shown in Table 4-21 and Table 4-22.

Table 4-21 Gaseous Emission Factors: Volatile Organics & Toxics (mg/kg fuel)

Location	Fuel type	1,3- Butadiene	Benzene	Toluene	m,p-xylene	Ethylbenzene	o-xylene
FHL CA	cea	25.93	728.24	99.32	21.01	10.60	7.18
	chs	24.86	130.66	66.65	22.11	9.00	7.98
	ave.	25.40±0.76	429.45±422.55	82.99±23.11	21.56±0.78	9.80±1.14	7.58±0.57
AFV CA	cas	15.81±9.51	219.90±134.37	71.65±53.38	24.56±17.70	9.52±7.50	5.71±8.30
	cos	8.54±3.04	279.32±117.85	128.47±108.09	20.78±6.44	6.68±1.62	3.29±0.65
	man	9.12±8.36	92.35±21.78	33.28±7.12	7.77±1.40	4.15±1.12	1.98±0.86
	mch	32.19	170.08	80.98	19.54	11.23	7.85
	ave.	13.03±9.62	183.52±116.95	70.79±63.30	17.40±12.72	7.11±5.00	4.01±5.05
FHUA AZ	mes	5.63±1.70	56.28±34.46	29.56±16.07	10.41±6.49	5.01±3.03	3.81±2.43
	oas	6.72±5.90	37.76±13.51	19.59±12.35	6.16±3.94	2.67±1.79	1.83±0.79
	oaw	5.62±6.24	59.08±77.75	31.54±41.24	7.33±9.47	3.88±5.17	1.58±1.42
	ave.	6.07±4.15	49.43±35.08	25.97±18.88	8.10±5.77	3.85±2.88	2.57±1.88
CL NC	1yr	3.42	20.81	20.92	43.59	11.27	4.55
	2yr	13.10	242.07	215.23	121.40	47.81	46.98
	poc	7.19	85.44	42.92	33.54	8.09	4.31
	cuh	6.73±3.32	78.88±11.01	43.01±2.66	15.22±0.04	7.11±0.13	8.69±1.80
	ave.	7.43±3.88	101.22±83.18	73.02±80.08	45.79±43.99	16.28±17.71	14.64±18.23
FB GA	lit	45.64±35.60	313.05±202.49	389.65±306.28	142.96±91.42	47.46±36.87	48.68±40.67
AK	duf	57.75	703.30	662.53	152.20	79.18	86.01

Table 4-22 Gaseous Emission Factors: Aldehydes and Ketones (mg/kg fuel)

	Fuel type	Form-aldehyde	Acet-aldehyde	Acetone	Acrolein	Propion-aldehyde	Croton-aldehyde	MEK	Butyr-aldehyde	Benz-aldehyde	Valer-aldehyde	Hex-aldehyde
CL NC	1yr	1185.4± 644.2	842.0± 500.3	466.0± 140.3					350.5± 143.6		905.2± 625.9	700.5± 343.7
	2yr	818.2± 81.9	805.0± 239.5	661.5± 84.4		185.2± 62.6		251.5± 32.6	232.1± 29.3		892.7± 353.5	1029.0± 299.2
	poc	558.9	379.5	210.0		73.4		87.3	79.3		500.8	480.0
	cuh	194.1± 42.8	157.3± 49.7	125.7± 7.7		32.6		44.7	64.9		92.1± 29.0	109.9± 32.8
	uh	449.7± 118.5	360.2± 111.6	224.3± 53.7	38.5	79.4± 25.7		98.8± 5.5	123.3± 18.2		294.4± 22.8	393.1± 91.2
	ave.	647.4± 407.5	534.0± 346.5	368.3± 228.4	38.5	105.9± 70.7		138.8± 90.8	186.6± 121.6		550.6± 432.0	597.4± 402.7
FB GA	Lit	1542.9± 576.9	1203.9± 277.4	653.3± 155.9		291.6± 68.5		340.1± 71.4	241.4± 49.5		908.0± 360.0	1485.3± 590.1
FHL CA	cea	368.0± 305.6	244.3± 209.5	189.6± 180.2					162.5± 90.0		291.9± 238.9	255.8± 215.4
	chs	409.3± 135.2	268.9± 25.5	214.4± 31.1		86.6	57.5	314.5	124.9± 41.2		345.4± 48.9	230.5± 93.8
	chg	167.4± 13.0	171.8± 13.6	135.4± 7.2		30.8			71.8± 8.8	47.3± 1.3	56.6± 24.5	72.7± 7.2
	ave.	346.5± 226.0	240.1± 138.0	188.8± 118.8		58.7± 39.5	57.5	314.5	129.8± 69.7	47.3± 1.3	260.9± 195.3	213.3± 161.8
FHUA AZ	mes	220.6± 34.9	147.3± 13.1	117.8± 15.8				44.6± 0.7	65.4± 3.4		88.5± 30.9	106.1± 42.8
	oas	132.1± 37.1	89.7± 33.6	61.7±					36.9± 4.7		48.3± 4.5	61.4± 18.2

	Fuel type	Form-aldehyde	Acet-aldehyde	Acetone	Acrolein	Propion-aldehyde	Croton-aldehyde	MEK	Butyr-aldehyde	Benz-aldehyde	Valer-aldehyde	Hex-aldehyde
				9.2								
	oaw	150.2± 71.0	101.0± 42.0	74.9± 31.8					58.0± 30.5		52.1± 36.3	66.6± 40.2
	ave.	185.3± 56.6	124.2± 34.8	95.8± 31.0				44.6± 0.7	56.4± 17.2		71.5± 32.5	87.4± 40.7
MT	fir	971.3	551.9	289.4					294.8		226.2	253.6± 0.0
AFV CA	cas	228.6± 53.8	141.7± 54.8	106.1± 51.0					72.6± 19.8		76.6± 17.7	76.8± 23.2
	cos	215.7	126.8	115.4					69.6		75.5	85.9
	man	178.9± 33.5	97.0± 21.7	76.8± 12.2		29.4			52.4± 12.2		88.7± 32.4	91.8± 31.8
	mch	174.5± 28.6	169.3± 98.7	141.2± 103.4				63.2	74.0± 18.0	71.6	86.4± 12.1	105.8± 57.6
	ave.	204.0± 47.2	131.0± 53.6	103.2± 50.0		29.4		63.2	66.4± 18.0	71.6	82.2± 21.2	86.6± 29.5

4.2.4 MFSL Results – PAH emission factors

One of the project goals was to measure the gas phase PAH emission factors as data were quite limited and these values were of interest to the US EPA as many of the compounds are toxic and also today grouped as part of the brown carbon released by biomass burning. Media were collected at MFSL during the burning and analyzed off line by the standard methods described earlier. As is evident in Figure 4-11, the emission factor varied linearly with MCE, as expected. . Results by fuel type are presented in Table 4-23. Given the variability in the data, no differences in PAH emissions were detected between southwestern and southeastern species. More detail is provided in the PhD Thesis of Dr. Seyedehsan Hosseini.

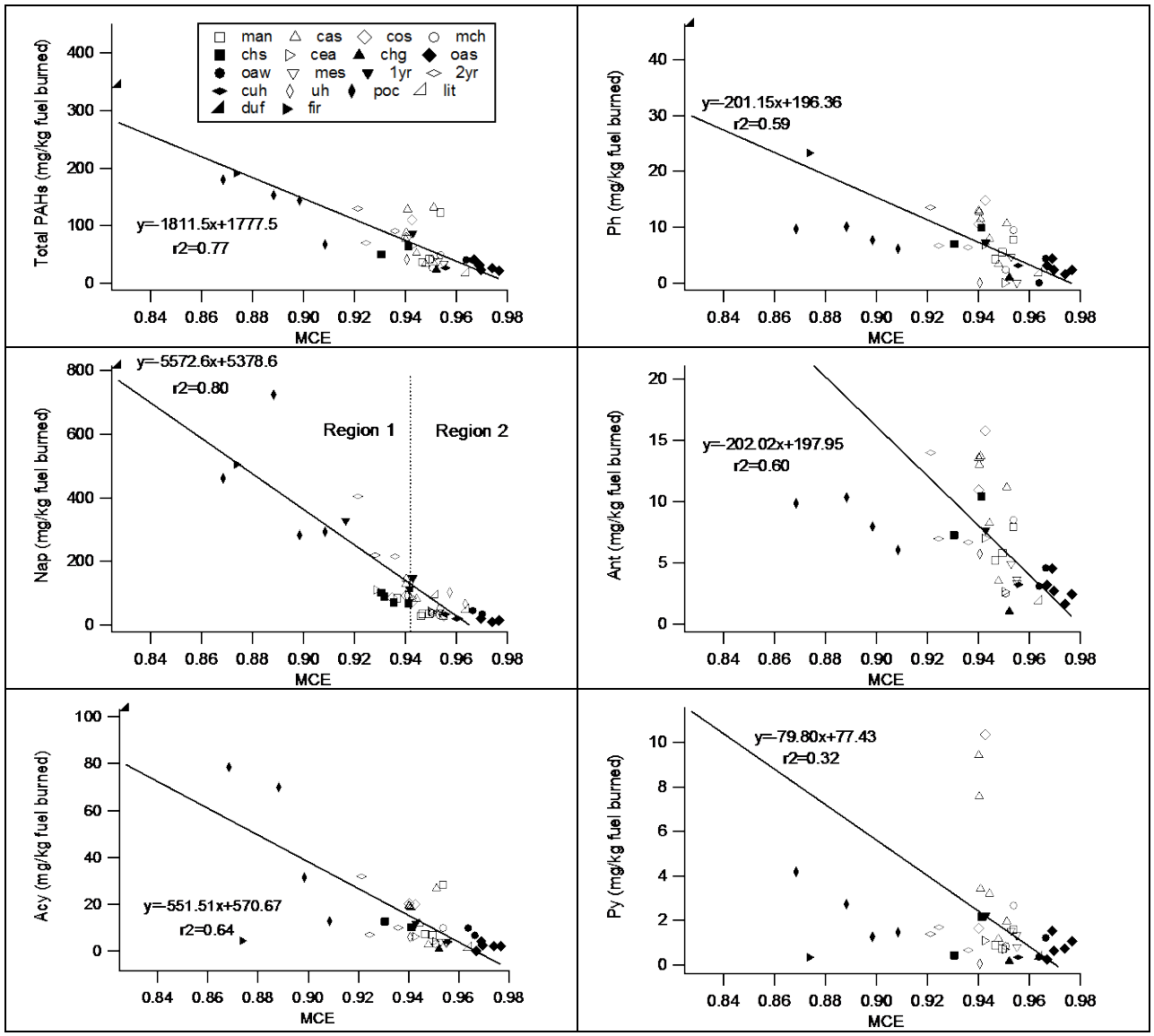

Figure 4-11 Plots of Emission Factor for Various PAH vs. MCE

Table 4-23 Emission factors of Gas Phase Poly Aromatic Hydrocarbons (PAHs) in mg pe kg fuel (average±Stdev)

Region	Fuel code	Nap	Acy	Ace	Fle	Ph	Ant	Fla	Py	B[a]A	Chr	B[b]F	B[k]F	B[a]P	Ind	D[a,h]A	B[ghi]P
AFV CA	cas	38.26± 28.96	16.43± 8.17	1.02± 0.87	0.91± 0.76	9.84± 3.64	10.52± 4.01	3.66± 3.50	4.45± 3.28	0.01± 0.00	0.01± 0.01	0.01± 0.02	0.01± 0.01	0.07± 0.15	0.00± 0.00	0.01± 0.00	0.01± 0.01
	cos	31.67± 3.74	20.21± 0.27	0.63± 0.67	3.19± 3.43	12.65± 2.98	13.36± 3.43	7.42± 2.70	5.99± 6.17	0.01± 0.01	0.01± 0.01	0.01± 0.01	0.02± 0.02	0.01± 0.01	0.00± 0.00	0.00± 0.00	0.00± 0.00
	man	38.09± 31.93	14.17± 12.20	0.25± 0.11	0.21± 0.13	5.84± 1.75	6.32± 1.43	1.18± 0.21	1.06± 0.46	0.04± 0.06	0.04± 0.05	0.09± 0.12	0.02± 0.01	0.03± 0.03	0.03± 0.04	0.05± 0.07	0.00± 0.00
	mch	16.13± 0.71	6.50± 4.85	0.16± 0.06	0.30± 0.40	5.93± 5.04	5.50± 4.26	1.63± 1.27	1.75± 1.29	0.01± 0.00	0.03± 0.03	0.01± 0.01	0.01± 0.01	0.00± 0.00	0.00± 0.00	0.01± 0.00	0.00± 0.00
	Ave.	33.80± 24.25	14.96± 8.50	0.65± 0.71	1.01± 1.51	8.75± 3.93	9.22± 4.20	3.35± 3.22	3.49± 3.37	0.02± 0.03	0.02± 0.03	0.03± 0.06	0.01± 0.01	0.04± 0.10	0.01± 0.02	0.02± 0.04	0.01± 0.01
FHL CA	cea	38.22± 7.05	5.27± 1.43	0.25± 0.04	0.57± 0.17	3.44± 4.85	4.81± 3.09	0.01± 0.01	0.89± 0.27	0.03± 0.03	0.03± 0.03	0.07± 0.06	0.03± 0.02	0.04± 0.05	0.01± 0.00	0.01± 0.00	0.01± 0.00
	chs	24.34± 3.31	11.47± 1.81	0.44± 0.47	1.04± 1.15	8.48± 2.10	8.83± 2.24	1.25± 1.18	1.29± 1.22	0.00± 0.00	0.01± 0.01	0.11± 0.14	0.11± 0.13	0.01± 0.00	0.03± 0.04	0.02± 0.03	0.01± 0.00
	chg	20.47	0.96	0.16	0.15	0.99	1.02	0.14	0.16			0.03			0.01	0.04	0.01
	Ave.	29.12± 9.31	6.89± 4.68	0.31± 0.27	0.67± 0.69	4.97± 4.28	5.66± 3.80	0.53± 0.89	0.91± 0.78	0.01± 0.02	0.02± 0.02	0.08± 0.08	0.06± 0.08	0.02± 0.03	0.02± 0.02	0.02± 0.02	0.01± 0.00
FHUA AZ	mes	23.90± 1.81	3.84± 0.44	0.19± 0.13	0.13± 0.01	1.59± 2.72	3.98± 0.83	0.46± 0.78	1.22± 0.39	0.46± 0.79	0.30± 0.51	0.03± 0.01	0.07± 0.09	0.01± 0.01	0.00± 0.00	0.01± 0.00	0.00± 0.00
	oas	19.33± 9.32	2.24± 1.50	0.20± 0.09	0.29± 0.29	2.75± 1.05	2.91± 1.06	0.53± 0.60	0.84± 0.47	0.03± 0.05	0.02± 0.04	0.06± 0.08	0.01± 0.00	0.02± 0.03	0.03± 0.04	0.04± 0.07	0.00± 0.00
	oaw	24.11± 3.86	8.32± 2.22	0.66± 0.10	0.16± 0.22	2.20± 3.07	3.84± 1.05	0.53± 0.74	0.79± 0.61	0.01± 0.01	0.01± 0.01	0.02± 0.01	0.00± 0.01	0.01± 0.00	0.00± 0.00	0.00± 0.00	0.00± 0.00
	Ave	21.66± 6.85	3.93± 2.73	0.29± 0.21	0.22± 0.22	2.29± 1.86	3.42± 1.03	0.51± 0.60	0.94± 0.46	0.16± 0.43	0.10± 0.28	0.04± 0.05	0.03± 0.05	0.01± 0.02	0.02± 0.03	0.02± 0.05	0.00± 0.00

Region	Fuel code	Nap	Acy	Ace	Fle	Ph	Ant	Fla	Py	B[a]A	Chr	B[b]F	B[k]F	B[a]P	Ind	D[a,h]A	B[ghi]P
CL NC	1yr	54.2	11.96	1.16	0.43	7.28	7.66	1.77	2.22	0.03	0.03	0.05	0.02	0.11		0.01	0.01
	2yr	56.26± 10.71	16.33± 13.59	1.13± 0.91	1.78± 0.80	8.88± 4.03	9.20± 4.14	2.10± 0.80	1.24± 0.53	0.01± 0.02	0.01± 0.01	0.02± 0.00	0.02± 0.01	0.05± 0.05	0.00± 0.00	0.01± 0.00	0.01± 0.00
	poc	11.75	1.56	0.08	0.47	1.8	1.87	0.47	0.36		0.01			0.01			
	cuh	15.05	3.99	0.38	0.13	3.11	3.22	0.65	0.34			0.01		0.01			
	uh	28.91	6.04	0.57	0.2	0.07	5.71	0.01	0.04	0.03	0.02	0.02	0.05	0.03	0.01	0.02	0.01
	Ave	39.81± 21.48	10.36± 10.13	0.80± 0.69	0.94± 0.92	5.56± 4.45	6.58± 3.88	1.31± 1.02	0.95± 0.82	0.01± 0.02	0.01± 0.01	0.02± 0.01	0.02± 0.02	0.04± 0.04	0.00± 0.00	0.01± 0.01	0.01± 0.00
FB GA	lit	62.44± 23.43	48.25± 31.19	1.80± 1.43	3.05± 2.72	8.37± 1.84	8.56± 1.95	0.94± 1.07	2.41± 1.35	0.03± 0.01	0.03± 0.03	0.04± 0.01	0.02± 0.01	0.16± 0.09	0.01± 0.00	0.01± 0.01	0.02± 0.02
AK	duf	88.74	103.4	2.31	7.68	46.46	47.99	22.44	24.97	0.03	0.04	0	0.01	0.04	0.02	0.01	0.01
MT	fir	126.09	4.47	0.49	2.21	23.3	24.46	9.47	0.34	0.01	0.02	0.01	0.02	0.02		0.01	

The full name and the abbreviation of analyzed PAHs are as follows: Naphthalene (Nap), Acenaphthylene (Acy), Acenaphthene (Ace), Fluorene(Fle), Phenanthrene (Ph), Anthracene (Ant), Fluoranthene (Fla), Pyrene (Py), Benzo[a]anthracene(B[a]A), Chrysene(Chr), Benzo[b]fluoranthene (B[b]F), Benzo[k]fluoranthene (B[k]F), Benzo[a]pyrene (B[a]P), Indeno[1,2,3-c,d]pyrene (Ind), Dibenzo[a,h]anthracene (D[a,h]A), Benzo[g,h,i]perylene (B[ghi]P). Empty cells represent below detection limit.

4.2.5 MFSL Results – Quality control, comparing results

UCR & UM independently sampled measured the properties of the emissions from the fires so we were able to check the emission factors to gain confidence in the reported values. For example, both UCR and UM measured NOx and carbonyl emission factors. The best comparison across all the fuels burned was to prepare parity plots as shown in Figure 4-12. For the carbon monoxide, the fit is excellent as results agree within 6%. However, for the formaldehyde, the UM results were 24% greater than the value measured by UCR. Note the excellent coefficient of determination of 98% so there is likely a bias in one of the methods and results. As UCR used an EPA reference method we suspect those results are accurate. In any case, the difference found for this important compound is within the range of existing data.

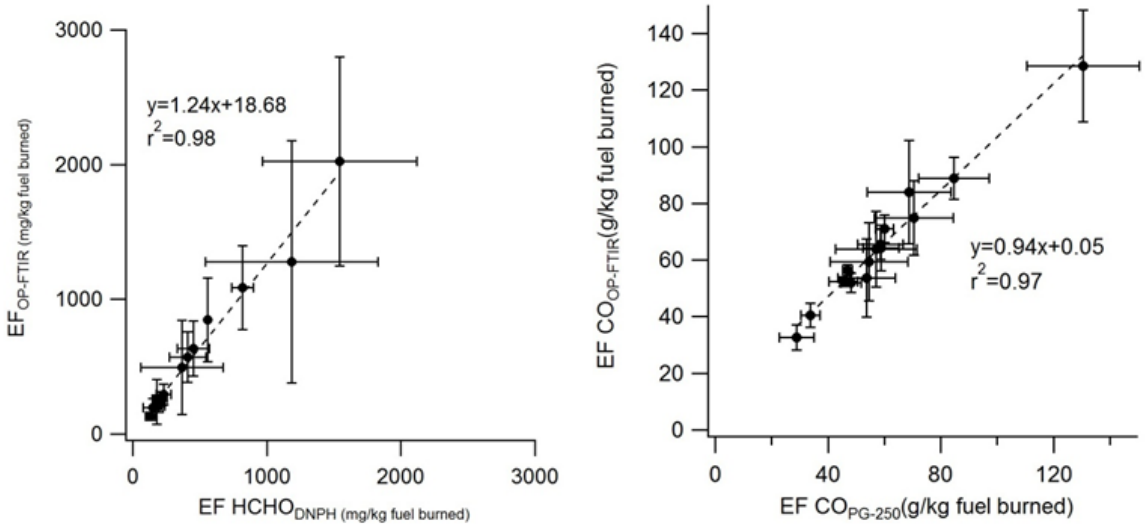

Figure 4-12 Parity Plots Showing Agreement from Independent Measurements

Other cross checks for compounds where both UCR and UM used independent methods to measure the emission factor showed close agreement between the emission factors. For example, spot checks were made of the NOx, PM and several light hydrocarbons and all emission factors were found to be within experimental error of the data.

4.2.6 MFSL Results –Emission Factors for $PM_{2.5}$ Mass & elements

UCR took the lead in determining the $PM_{2.5}$ particulate emissions factors from the various fuels using a suite of instruments. In addition to the sampler system described previously, several particulate phase instruments were also located on the platform at Missoula, including an Aerodyne High Resolution Time of Flight Aerosol Mass Spectrometer (HR-TOF-AMS), an Ultrafine Condensation Particle Counter (UCPC Model 3776, TSI Inc.), a Scanning Mobility Particle Sizer (SMPS), a Fast Mobility Particle Sizer (FMPS Model 3091, TSI Inc.), Aerodynamic Particle Sizer (APS Model 3321, TSI Inc.), a Micro-Orifice Uniform Deposit Impactor (MOUDI), and a Dekati® Mass Monitor (DMM).

A series of data tables follow with various results that were part of the program deliverables. Table 4-24 has values for the emission factors in g/kg fuel for total mass, elemental and organic carbon (EC &OC), potassium (K), chloride (CL), sodium (Na) and sulfur (S). Values for the emission factors are usually plotted against the modified combustion efficiency (MCE) as in

Figure 4-13. As is evident in the figure the $PM_{2.5}$ emission factors can be fitted to a linear expression when plotted against the MCE. Further the plot shows values from this study are in the range for values obtained from other projects.

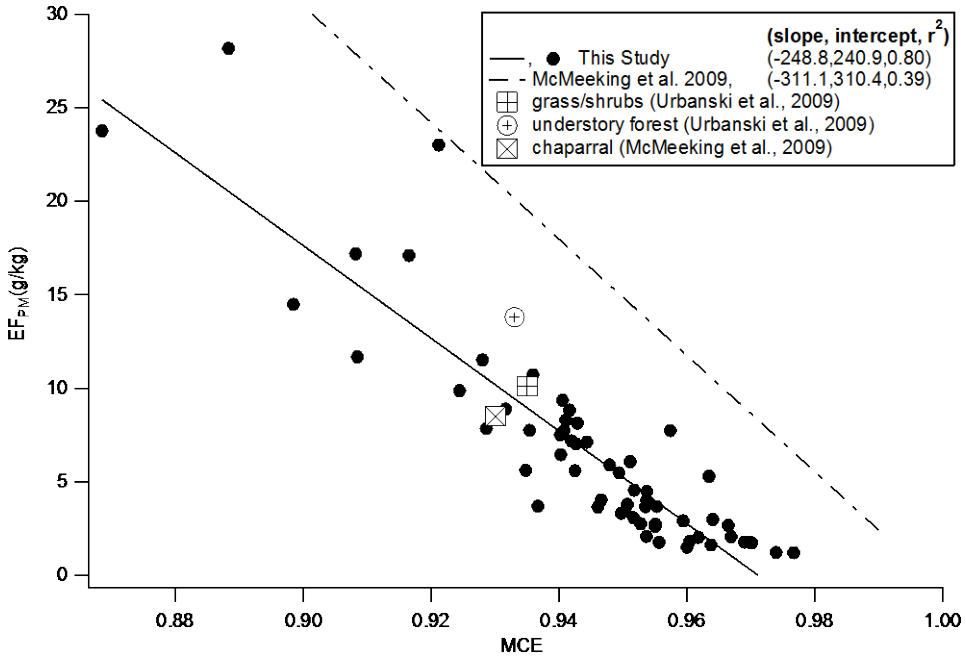

Figure 4-13 Mass of $PM_{2.5}$ as a Function of Modified Combustion Efficiency (MCE)

Other emission factor data were collected for the particle phase PAHs as compared with the gas phase PAH that was reported in the last the section. These data are shown in Table 4-26.

A separate task was measuring the emission factors for the ions and cations captured on the filter samples. These data are shown in Table 4-25. Results show that the primary cations were sodium and potassium, with more potassium, as expected. The major anion was chloride, as expected.

Table 4-24 Emission Factors for total $PM_{2.5}$, EC, OC, K, Cl, Na, S in g/kg fuel

Species/group	MCE	EC/TC	PM2.5	EC	OC	K	Cl	Na	S
Southwest									
cea/FHL	0.953(0.008)	0.40(0.22)	4.62(2.08)	0.64(0.29)	1.16(0.86)	0.607(.065)	0.345(.034)	0.016(.011)	0.025(.004)
chs/FHL	0.941(0.011)	0.39(0.07)	7.38(2.11)	1.36(0.44)	2.18(0.63)	0.535(.245)	0.171(.058)	0.034(.014)	0.061(.031)
cas/AFV	0.944(0.004)	0.58(0.07)	6.87(0.83)	1.54(0.14)	1.16(0.38)	0.725(.057)	0.633(.015)	0.195(.014)	0.049(.001)
cos/AFV	0.939(0.004)	0.62(0.07)	6.36(0.72)	1.54(0.17)	0.97(0.35)	0.664(.575)	0.585(.509)	0.169(.239)	0.053(.046)
man/AFV	0.948(0.007)	0.42(0.14)	3.61(1.17)	0.51(0.18)	0.85(0.71)	0.525(.061)	0.323(.063)	0.218(.043)	0.044(.007)
mch/AFV	0.952(0.002)	0.43(0.15)	4.10(0.34)	0.57(0.12)	0.81(0.35)	0.918(.143)	0.922(.105)	0.253(.042)	0.033(.003)
Chaparral ave.	0.946(0.006)	0.49(0.11)	5.46(1.31)	1.08(0.21)	1.17(0.54)	0.652(.269)	0.471(.320)	0.143(.119)	0.045(.024)
mes/FHUA	0.954(0.002)	0.44(0.01)	2.97(0.42)	0.57(0.09)	0.72(0.13)	0.625(.173)	0.472(.121)	0.001(.000)	0.035(.008)
oas/FHUA	0.971(0.004)	0.52(0.08)	1.61(0.38)	0.50(0.17)	0.44(0.10)	0.169(.039)	0.048(.013)	0.005(.004)	0.027(.009)
oaw/FHUA	0.965(0.003)	0.44(0.14)	2.01(0.47)	0.47(0.13)	0.67(0.33)	0.147(.100)	0.026(.021)	0.007(.006)	0.029(.020)
FHUA ave.	0.963(0.003)	0.48(0.08)	2.21(0.42)	0.49(0.15)	0.58(0.18)	0.297(.248)	0.166(.219)	0.005(.005)	0.030(.013)
Southeast									
lit/FB	0.894(0.016)	0.10(0.06)	19.06(6.78)	1.06(0.63)	10.60(3.64)	0.048(.040)	0.018(.019)	0.039(.015)	0.024(.009)
1yr/CL	0.942(0.001)	0.08(0.03)	11.35(4.99)	0.46(0.17)	5.70(1.04)	0.279(.126)	0.063(.041)	0.054(.020)	0.040(.013)
2yr/CL	0.928(0.007)	0.07(0.03)	13.78(6.19)	0.48(0.18)	6.88(2.63)	0.248(.171)	0.085(.040)	0.089(.072)	0.039(.015)
poc/CL	0.953(0.010)	0.18(0.06)	4.91(2.12)	0.44(0.16)	2.22(1.02)	0.042(.009)	0.011(.003)	0.018(.002)	0.008(.002)
cuh/CL	0.958(0.003)	0.36(0.04)	1.69(0.16)	0.41(0.03)	0.75(0.16)	0.159(.018)	0.108(.027)	0.034(.005)	0.015(.003)
uh/CL	0.954(0.011)	0.32(0.09)	7.46(2.04)	1.51(0.66)	3.07(0.73)	0.282(.073)	0.095(.025)	0.046(.009)	0.047(.015)
Camp Lejeune ave.	0.938(0.008)	0.17(0.06)	10.79(4.12)	0.81(0.37)	5.66(1.85)	0.172(.136)	0.060(.045)	0.047(.037)	0.029(.017)

Note: Numbers in parentheses represent one standard deviation

Table 4-25 Emission Factors for Aerosol-phase of Cations and Anions (mg/kg fuel)

Species/ group	Sulfate	Nitrite	Fluorite	Chloride	Bromide	Sodium	Ammonium	Potassium	Calcium
Southwest									
cea/FHL	-	-	20.29 ± 10.19	481.00 ± 174.81	-	712.99 ± 953.99	-	391.88 ± 93.71	103.24
chs/FHL	140.96 ± 51.17	-	21.67 ± 3.78	177.72 ± 35.86	-	243.26 ± 228.80	-	364.93 ± 160.18	-
cas/AFV	207.65 ± 59.04	-	20.56	1405.99 ± 457.22	-	457.92 ± 177.65	130.3	1192.62 ± 340.16	-
cos/AFV	248.51 ± 26.73	59.96	22.12	1071.73 ± 119.09	-	332.07 ± 44.55	-	1279.42 ± 196.65	-
man/AFV	102.44 ± 18.33	27.32	12.27 ± 8.49	301.03 ± 97.73	8.11	143.00 ± 58.56	-	408.67 ± 101.55	-
mch/AFV	92.50 ± 24.60	-	11.89 ± 4.44	873.76 ± 102.96	-	213.24 ± 47.19	91.44	822.85 ± 86.26	-
mes/FHUA	117.80 ± 15.72	-	16.99 (1)	589.75 ± 124.61	-	186.74 (5) ± 79.91	167.12 ± 7.13	622.48 ± 145.77	-
oas/FHUA	78.97 ± 10.05	-	-	61.40 ± 4.16	-	95.59 (5) ± 17.05	-	119.49 ± 28.40	-
oaw/FHUA	85.24 ± 6.14	-	6.98 ± 2.58	43.41 ± 10.80	-	64.56 (5) ± 13.65	-	143.20 ± 71.74	-
Southeast									
lit/FB	-	-	60.34 ± 29.35	125.43 ± 39.61	-	378.65 ± 149.53	-	-	-
1yr/CL	-	-	-	125.49 ± 14.96	-	402.52 ± 76.58	-	-	-
2yr/CL	-	-	63.04	174.81 ± 60.32	-	356.92 ± 63.81	-	-	-
poc/CL	-	-	12.67 ± 4.99	114.06 ± 12.13	-	116.72 ± 62.64	-	101.47 ± 51.39	-
cuh/CL	-	-	-	33.76 ± 11.11	-	97.48	-	-	-
uh/CL	141.81 ± 10.04	231.32	17.60 ± 1.38	161.29 ± 39.44	-	194.78 ± 36.58	-	245.89 ± 147.55	187.76

Table 4-26 Emission Factors for Particle Phase PAHs in µg per kg fuel & Diagnostic Ratios

Fuel type	cea	chs	cas	cos	man	mch	Chaparral Ave.	mes	oas	oaw	FHUA Ave.
Acy {2}[a,b]	297.2 ± 338.6	144.3 ± 137.5	77.8 ± 42.1	270.8 ± 149.9	19.2 ± 12.6	27.9	139.5 ± 66.2	35.5 ± 26.6	36.1 ± 49.0	82.2 ± 84.3	51.2 ± 33.7
Ace {2}	144.0 ± 97.7	126.8 ± 146.3	26.6 ± 26.9	7.4 ± 4.2	11.0 ± 13.9	3.7	53.2 ± 29.8	25.2±17.7	29.6±39.4	37.9±45.2	30.9±20.8
Fle {2}	329.7±350.1	391.4±476.0	84.2±81.9	20.8±5.2	43.9±53.0	97.4	161.2±99.8	68.4±77.8	145.5±134.5	128.6±156.8	114.2±73.6
Ph {3}	1434.5±1270.8	1055.1±1045.7	301.1±201.6	234.4±53.5	244.6±171.8	133.6	567.2±278.0	116.3±89.9	214.6±160.9	113.5±193.1	148.2±89.0
An {3}	197.5±283.1	78.0±74.5	148.1±166.6	94.5±59.3	156.7±230.4	136.7	135.2±68.7	11.1±9.0	8.7±5.1	79.3±128.9	33.0±43.1
Fla {3}	492.2 ± 171.7	558.3 ± 549.5	1041.9 ± 343.5	1156.1 ± 17.1	176.7 ± 124.8	257.8	613.8 ± 113.7	103.6 ± 96.6	88.5 ± 36.2	181.8 ± 309.3	124.6 ± 108.7
Py {4}	664.2 ± 426.6	738.0 ± 976.6	1480.4 ± 170.2	1433.2 ± 121.3	345.8 ± 162.3	447	851.4 ± 183.0	418.1 ± 420.1	256.3 ± 149.7	273.3 ± 243.0	315.9 ± 169.3
B[a]A {4}	778.9 ± 430.0	338.2 ± 302.4	1524.2 ± 707.5	1550.7 ± 74.4	223.8 ± 119.8	432.5	808.1 ± 148.8	280.1 ± 283.4	134.0 ± 71.6	172.7 ± 161.5	195.6 ± 111.3
Chr {4}	269.6 ± 273.5	225.9 ± 202.9	1478.4 ± 686.8	1425.2 ± 225.6	238.4 ± 167.8	432.5	678.3 ± 136.1	258.1 ± 213.4	133.8 ± 70.2	171.6 ± 159.7	187.8 ± 91.9
B[b]F {4}	216.3 ± 213.1	164.5 ± 182.2	591.8 ± 341.9	823.7 ± 213.2	145.4 ± 108.1	151.9	348.9 ± 83.8	107.8 ± 98.6	37.0 ± 13.8	105.1 ± 116.0	83.3 ± 51.0
B[k]F {4}	1164.6 ± 809.6	256.8 ± 241.8	3232.0 ± 3144.1	2156.5 ± 135.6	537.6 ± 563.0	612.4	1326.7 ± 551.1	228.4 ± 182.6	145.9 ± 43.1	266.6 ± 461.8	213.6 ± 166.2
B[a]P {5}	130.2 ± 80.4	59.9 ± 52.9	713.2 ± 937.3	433.0 ± 37.8	28.2 ± 10.0	75.2	240.0 ± 157.2	29.6 ± 25.8	22.7 ± 1.9	405.7 ± 682.1	152.7 ± 227.5
Ind {5}	104.4 ± 163.9	118.3 ± 123.7	342.5 ± 110.2	582.1 ± 167.1	42.4 ± 28.2	102.3	215.3 ± 48.0	37.3 ± 27.5	23.2 ± 5.3	8.2 ± 12.0	22.9 ± 10.2
D[ah]A {5}	59.0 ± 68.8	12.1 ± 10.5	113.7 ± 59.4	149.9 ± 44.8	13.4 ± 7.5	26.5	62.5 ± 17.0	13.5 ± 9.1	10.7 ± 3.5	8.7 ± 7.8	11.0 ± 4.1
B[ghi]P {4}	199.6 ± 276.0	136.8 ± 119.1	534.2 ± 172.2	993.2 ± 268.1	47.5 ± 31.7	164.6	346.0 ± 73.2	53.9 ± 39.3	34.1 ± 10.7	12.5 ± 20.6	33.5 ± 15.2
Sum	6481.9	4404.4	11690.1	11331.5	2274.6	3102	6547.3	1786.9	1320.7	2047.7	1718.4
Diagnostic ratios											
Fla/(Py+Fla)	0.43	0.43	0.41	0.45	0.34	0.37	0.40	0.2	0.26	0.40	0.28
Ph/(Ph+Ant)	0.88	0.93	0.67	0.71	0.61	0.49	0.72	0.91	0.96	0.59	0.82
Ind/(Ind+Benzo[ghi]P)	0.34	0.46	0.39	0.37	0.47	0.38	0.40	0.41	0.40	0.40	0.40

Abbreviations: Acy(acenaphthylene), Ace(acenaphthene), Fle(fluorene), Ph (phenanthrene), An (anthracene), Fla (fluoranthene), Py (pyrene), B[a]A (benz[a]anthracene), Chr (chyrsene), B[b]F (benzo[b]fluoranthene), B[k]F (benzo[k]fluoranthene), B[a]P (benzo[a]pyrene), B[ghi]P (benzo[ghi]perylene), Ind (indeno[1,2,3-cd]pyrene), D[ah]A (dibenz[ah]anthracene) [b] No. of fused aromatic rings

In addition to the analysis of the filters for the water soluble ions, fifty of the seventy-seven Teflon filters were also analyzed with x-ray florescence for the elements sodium to lead on the periodic table. Data are plotted in Figure 4-14 and the dominant element in 47 of the 50 filters analyzed was potassium. The second most prominent element was chlorine. In the 28 of the 50 burns, the elements K, Cl, Na and S comprised >90% of the inorganic elemental mass. As is evident in the figure, emissions of elements from the southeast fuels were much less than release of elements for the southwestern fuels.

One question is whether the lab results are applicable to wildland fires. For the elements, we believe the lab results are applicable to the field. However, for the carbonaceous materials the laboratory percentage may be overly stated as the combustion and cooling processes in the lab and in wildland fire are different. Nucleation due to cooling is an exponential process while slowing nucleation due to dilution is a linear process. In wild fires, the organic loading during the flaming stages are higher and the relative rate of cooling are faster as compared with dilution. Thus we would expect more nucleation and organic compounds on the filters in wild fires.

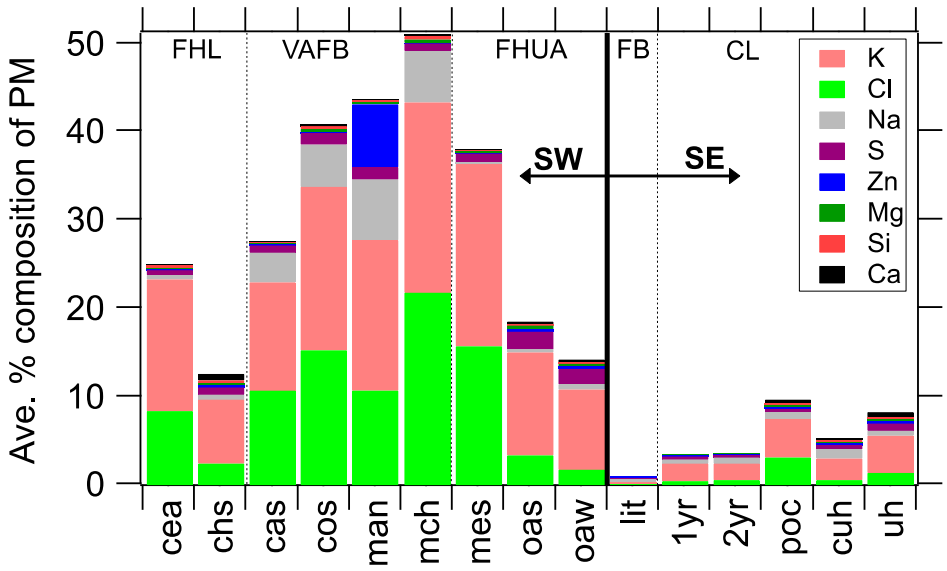

Figure 4-14 Filter Analysis of Elements Released when Burning Different Fuels

In another series of runs, size-resolved, mass emission factors were obtained with the MOUDI equipment. Results are shown as histograms in Figure 4-15. The results showed that most of the mass was in the smaller particle diameters; from 0.056 to 0.100µ and that 1 & 2 year chipped fuels from Camp Legume had particle sizes larger than the chaparral fires. Note that while a wildland fire may spend most of the time smoldering, the results are mass based and most of the mass is released in the flaming regime.

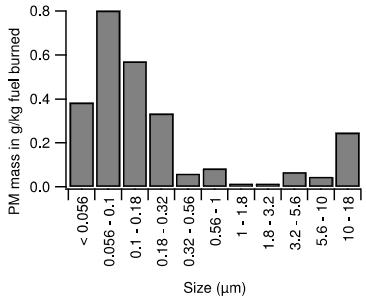

Figure 4-15 (a-f) Size-resolved Mass Emissions with MOUDI Unit g) Parity Check of Data

Data from the MOUDI provided an opportunity to have an independent check of the emission factors captured on the Teflon® filter media. Accordingly the mass emission factor measured using the MOUDI and the filter methods were compared. As is evident from the Figure 4-15(g), the coefficient of determination (R^2) value is near 1; however, the MOUDI PM mass values were about 27% higher than the filter based method as seen in the equation.

Smoke emissions were simultaneously captured on Teflon® and quartz filters. The Teflon® filter was used for the total mass and the quartz filter was processed by the NIOSH methods to measure the elemental and organic carbon contents. Results are in Figure 4-16. Results show a wide range of values for the total carbon as found for the PM mass. Further we see the EC/OC ratio varies over a wide range.

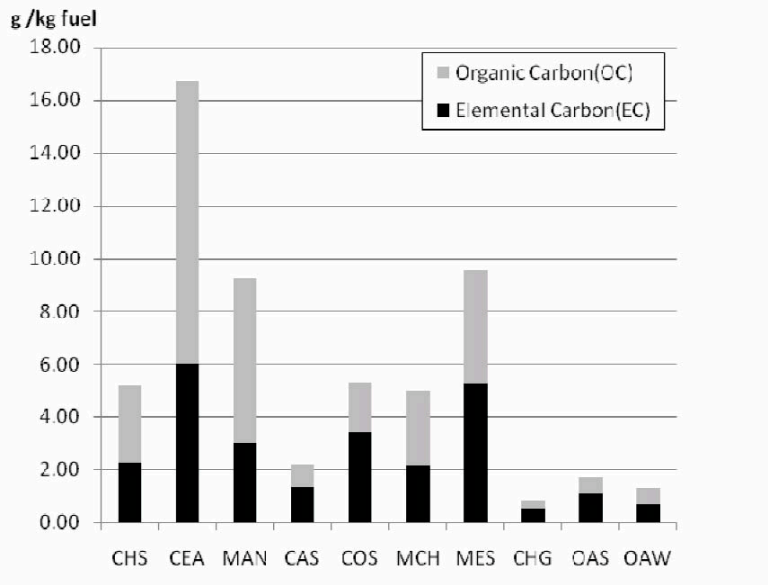

Figure 4-16 Elemental & Organic Carbon for some Southwestern Wildland Fuels

Another set of useful plots are those showing the variation of EC and OC emission factors as a function of MCE. These results are shown in Figure 4-17, again following the unusual protocol of showing a linear fit of EF vs. MCE for the three parameters.

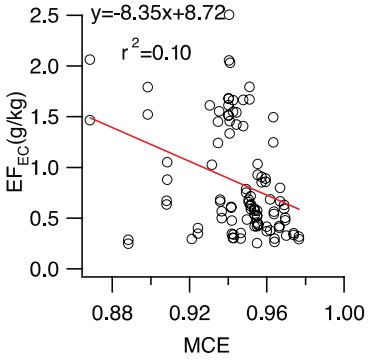

Figure 4-17 Integrate Emission Factors vs. MCE for (a) EC (b) OC (c) TC

During this phase of the work, the goal was to report all emission factors as the integrated values from the whole fire. However, we were interested in measuring the instantaneous PM emission factors in addition to those measured over the whole burn The DMM instrument enabled us to measure instantaneous emission factors Results in Figure 4-18 are a comparison of the $PM_{2.5}$ emission factors measured over the whole fire on one filter as compared with the emission factors obtained by integrating the continuous mass values measured with the DMM instrument. Emission factors ranged from 2 g/kg fuel for the unknown grass growing in maritime chaparral to a maximum of 27 for ceanothus. Except for the mesquite and ceanothus, the results for both methods agree in trend. The reason for difference between the filter mass and integrated DMM values requires further investigation. Considerable variation is evident in both data sets and the

differences are suspected due to the non-homogeneity of the harvested fuel, the geometric properties of the fuel bed and variation in fuel moisture.

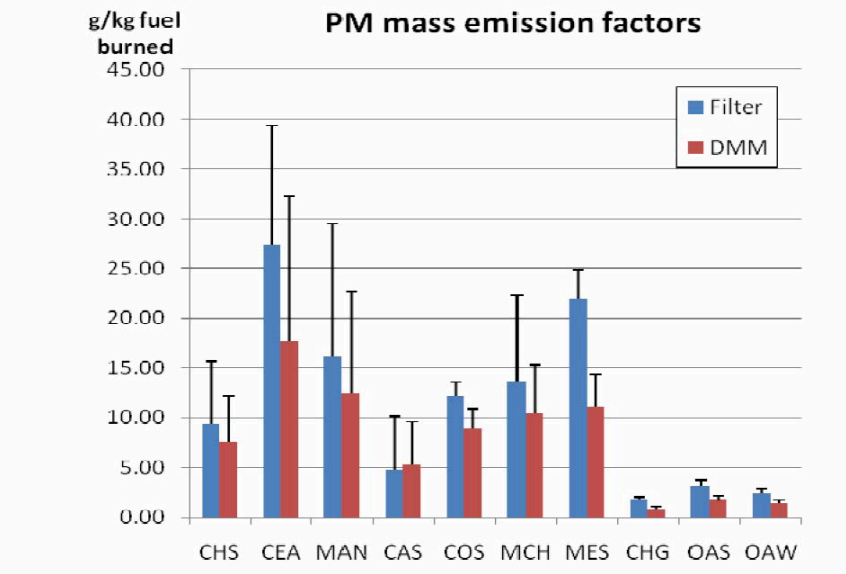

Figure 4-18 $PM_{2.5}$ Mass Emission Factor for Different Plant Species

Particle number and the companion surface area associated with PM is a parameter of interest, especially to health scientists. In this phase of the work, we also compared the particle number measured from a commercial Condensation Particle Counter (CPC) with the instantaneous values from the DMM. Some results are shown in Figure 4-19.

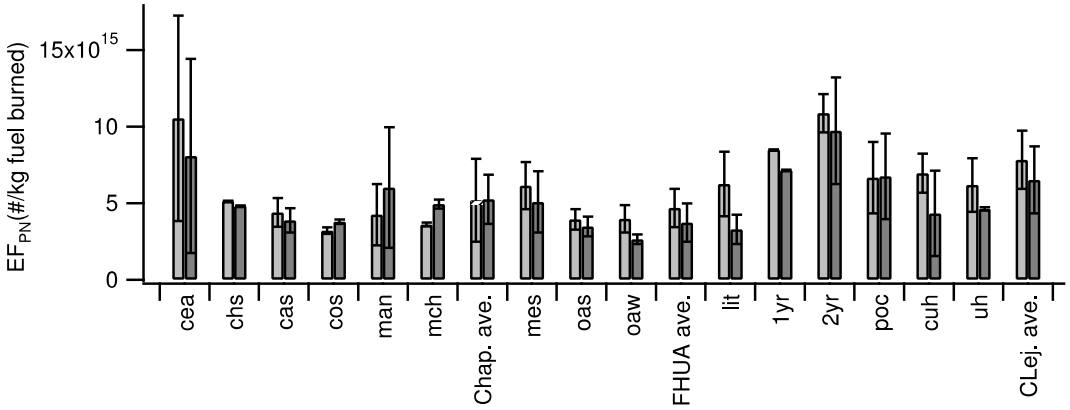

Figure 4-19 Particle Number Emission Factors by CPC and DMM for some Southwestern and Southeastern Fuels

The variation of the emission factors over the range of burn from flaming to smodldering is usually expressed in the literature as a linear function of MCE so a plot of the number of particles versus MCE is plotted in Figure 4-20. As is evident in the figure, the fit for the two independent measurements of the number of particles agree quite well. However, there is considerable scatter in the data, particularly in the smoldering regime and the fit as described by the coefficient of determination (R^2) is poor. For many, the primary interest is the PM mass since that is the metric used by most regulatory agencies but some agencies regulate the number of

particles and this analysis provides an order of magnitude estimate of the number. The figure provides an estimate of the particle number emissions if nothing else is available.

Figure 4-20 Emission Factor for Number of Particles vs. MCE

Often the emissions of CO are checked to determine if they are correlated with the emissions of PM mass. The rationale being that both PM and CO are products from a partial oxidation process. Accordingly we plotted the emission factor of $PM_{2.5}$ mass versus the emission factor of CO in Figure 4-21. The analysis suggests the emission factor for PM mass was reasonably correlated with the emission factor for carbon monoxide as the line is fairly linear and the coefficient of determination is 68%. The results show the PM mass emission factor for all southwestern fuel types were represented by the fitted relationship $EF_{PM}=0.044EF_{CO}$. Note however, the scatter at a value of 60 on the abscissa as the y-value can be 1 or 4. Thus this is only a statistical fit that needs more parameters from the basic fundamental phenomena if one hopes to improve the fit and predictability. It is interesting to note that Ward and Hardy (1991) presented regression equations relating EF for $PM_{2.5}$ and CO to combustion efficiency (CE). Rearranging their equations 2) EFPM2.5 = 67.4 - 66.8*CE and 4) EFCO = 961 - 984*CE yields $EF_{PM2.5} = 2.1 + 0.068EF_{CO}$ which is similar to the fit of this research. A similar equation for PM (no size restriction) can be derived $EF_{PM} = 4.9 + 0.091EF_{CO}$.

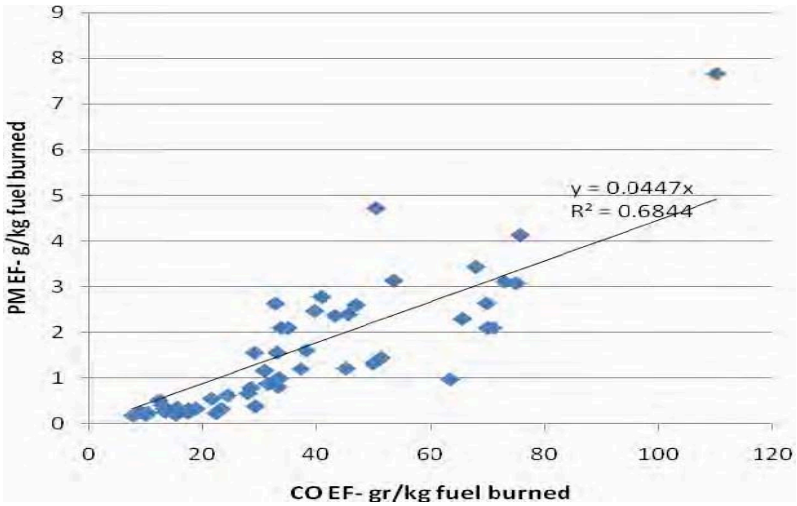

Figure 4-21 Plot of the Emission Factor for CO vs. Emission Factor for $PM_{2.5}$ Mass

4.2.7 MFSL Results – Aerosol Mass Spectrometer (AMS)

A complete description of the AMS equipment and methods can be found in the thesis of Dr. Li Qi. The AMS instrument is capable of measuring all volatile emissions from the fire and the result of average mass spectra of particles for all nine fuels during flaming period are in Figure 4-22. As is evident, the inorganic species such as chloride and sulfate contribute a significant fraction of emissions.

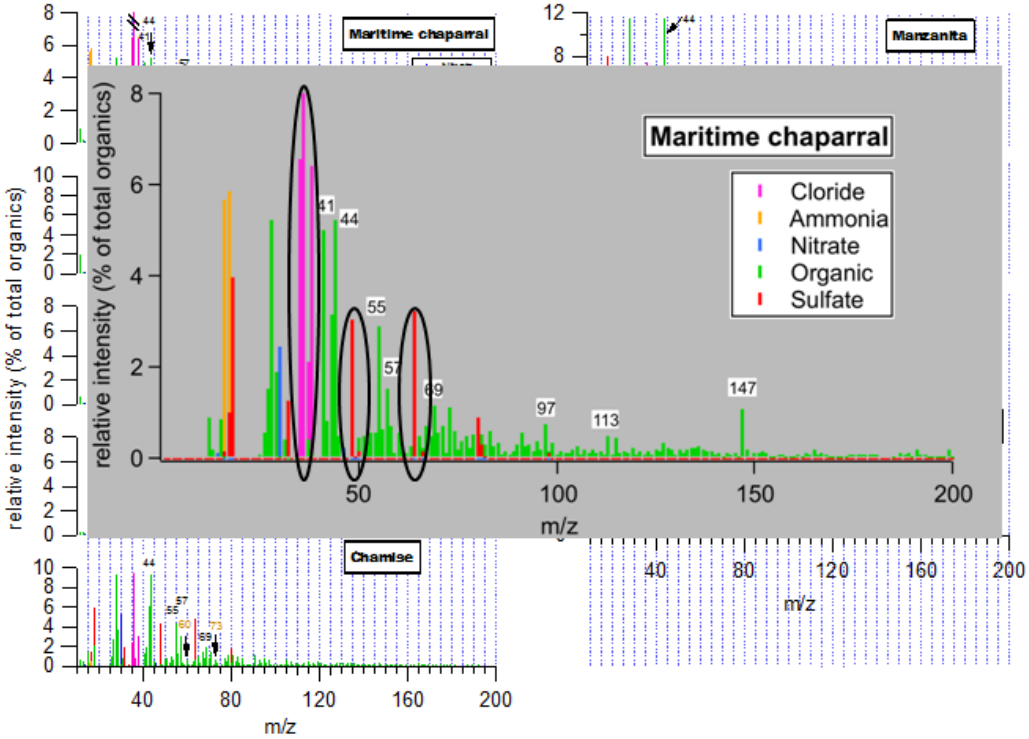

Figure 4-22 Sample Resolution during Flaming Regime

In general, the inorganic species emissions are associated with flaming period and when the fire transitions to the smoldering phase, the organic species dominate. The hydrogen fragment ions dominate the unit mass resolution (UMR) mass spectra with no specific fragment ions attributable to an individual fuel type. Figure 4-23 provides an example of the AMS spectra during the smoldering phase.

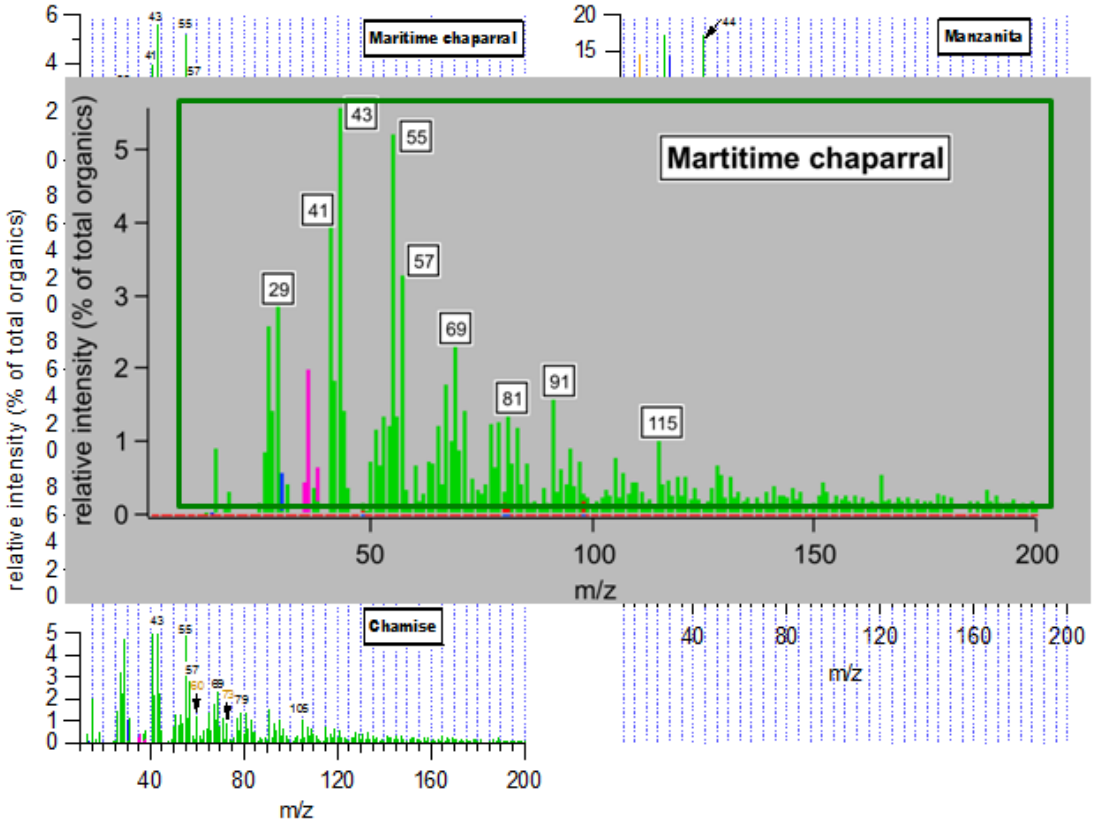

Figure 4-23 Sample AMS Output during the Smoldering Regime

In a series of plots in Figure 4-24 the ratio of organic matter to carbon; nitrogen to carbon and hydrogen to carbon are plotted for all regimes of fire using the data from the Aerosol Mass Spectrometer. From the left, the first chart is for the flaming, the middle chart for the transition/mixed phase and the last chart for the smoldering regime. Statistics shown on the charts are displayed at one sigma. The O/C ratio ranges from 0.20 to 0.48 for flaming; 0.17-0.43 for mixed phase; 0.14-0.37 for smoldering. H/C ratio ranges from 1.435-1.764 over the three processes with smaller standard deviation compared to O/C. N/C ratio varies over a much higher range and with a larger uncertainty. While the charts are intended to compare the trends for the release of various compounds from wildland fuels, the high value for the standard deviation makes it difficult to say that results are significantly different and independent of fuel type. As explained earlier, the standard deviation is high due to uncontrolled parameters in a burn and few replications. Trends show California Sage scrub has the highest values of organic carbon. On the other hand, release of nitrogen is about the same for all fuel sources and independent of the burning regime. Dr Qi in her thesis and soon to be published paper presents more information about the AMS data for all burns at the MFSL.

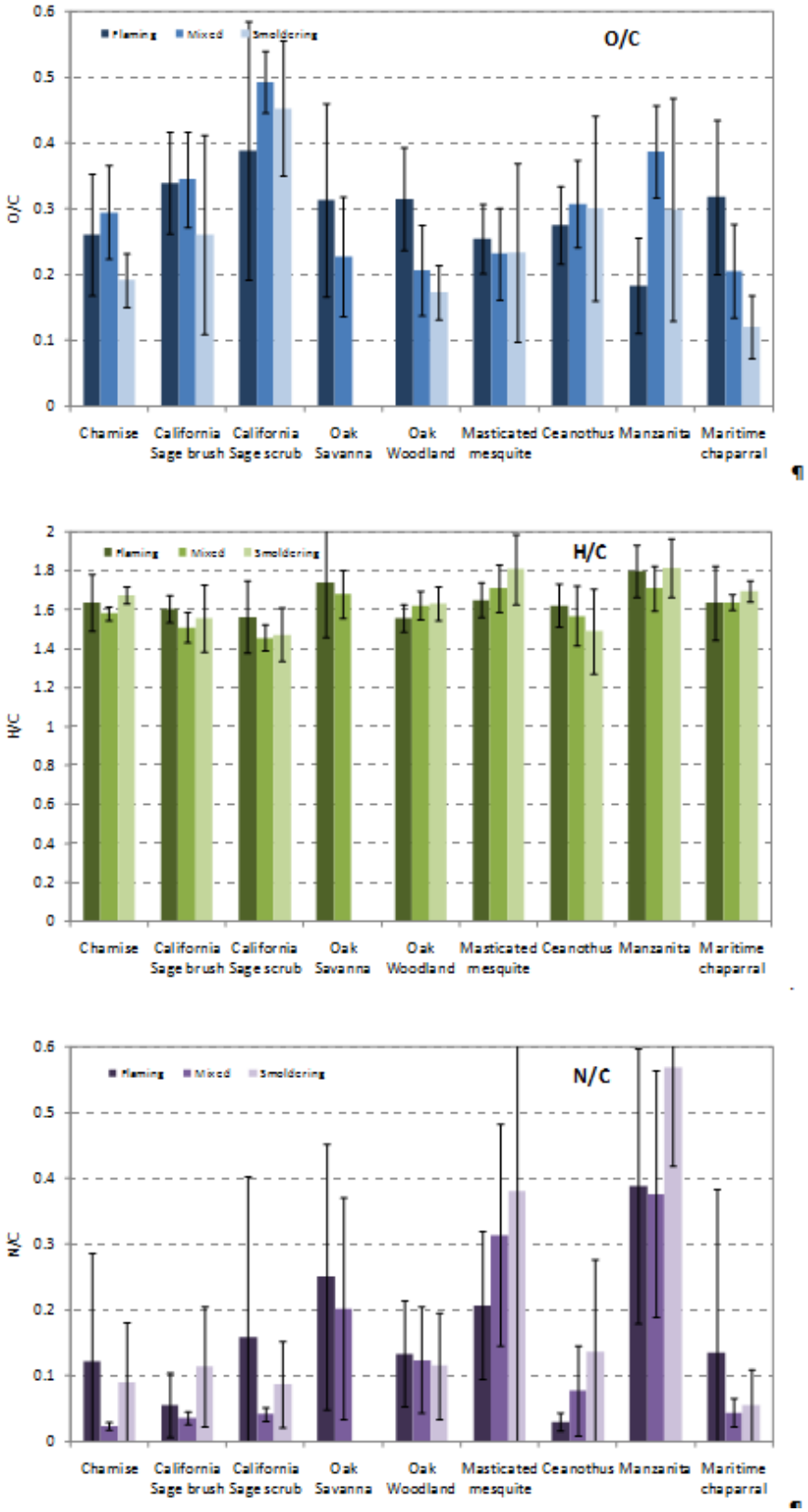

Figure 4-24 Averaged AMS Results showing the Ratio of Various Groups to Carbon (left to right: flaming, transition, smoldering)

Another set of data from the analysis of the AMS data is the elemental composition of the vapor phase. That analysis is in Table 4-27.

Table 4-27 Empirical Formula of Vapor Phase from AMS Analysis for Different Burning Regimes

Fuel type	Empirical Formula		
	Flaming	Mixed	Smoldering
Chamise	$C_1H_{1.62\pm0.07}O_{0.32\pm0.09}N_{0.03\pm0.01}$	$C_1H_{1.61\pm0.04}O_{0.24\pm0.03}N_{0.02\pm0.01}$	$C_1H_{1.67\pm0.04}O_{0.18\pm0.05}N_{0.09\pm0.09}$
California Sage brush	$C_1H_{1.56\pm0.07}O_{0.36\pm0.07}N_{0.03\pm0.01}$	$C_1H_{1.52\pm0.08}O_{0.34\pm0.08}N_{0.04\pm0.03}$	$C_1H_{1.51\pm0.15}O_{0.36\pm0.09}N_{0.08\pm0.04}$
California Sage scrub	$C_1H_{1.43\pm0.09}O_{0.48\pm0.07}N_{0.04\pm0.01}$	$C_1H_{1.48\pm0.19}O_{0.43\pm0.12}N_{0.13\pm0.08}$	$C_1H_{1.61\pm0.25}O_{0.27\pm0.20}N_{0.13\pm0.10}$
Oak Savanna	$C_1H_{1.65\pm0.10}O_{0.35\pm0.07}N_{0.20\pm0.15}$	$C_1H_{1.68\pm0.12}O_{0.22\pm0.09}N_{0.20\pm0.17}$	NA[a]
Oak Woodland	$C_1H_{1.56\pm0.07}O_{0.31\pm0.08}N_{0.13\pm0.08}$	$C_1H_{1.62\pm0.07}O_{0.20\pm0.07}N_{0.12\pm0.08}$	$C_1H_{1.74\pm0.09}O_{0.14\pm0.05}N_{0.19\pm0.15}$
Masticated mesquite	$C_1H_{1.65\pm0.09}O_{0.25\pm0.05}N_{0.21\pm0.11}$	$C_1H_{1.71\pm0.12}O_{0.23\pm0.07}N_{0.31\pm0.17}$	$C_1H_{1.81\pm0.14}O_{0.23\pm0.07}N_{0.38\pm0.18}$
Ceanothus	$C_1H_{1.62\pm0.11}O_{0.27\pm0.05}N_{0.03\pm0.01}$	$C_1H_{1.58\pm0.15}O_{0.30\pm0.07}N_{0.08\pm0.07}$	$C_1H_{1.49\pm0.22}O_{0.30\pm0.14}N_{0.14\pm0.14}$
Manzanita	$C_1H_{1.76\pm0.11}O_{0.20\pm0.05}N_{0.32\pm0.16}$	$C_1H_{1.71\pm0.11}O_{0.38\pm0.07}N_{0.38\pm0.19}$	$C_1H_{1.75\pm0.07}O_{0.37\pm0.09}N_{0.52\pm0.13}$
Maritime chaparral	$C_1H_{1.59\pm0.08}O_{0.35\pm0.07}N_{0.05\pm0.04}$	$C_1H_{1.64\pm0.02}O_{0.17\pm0.05}N_{0.04\pm0.02}$	$C_1H_{1.68\pm0.08}O_{0.15\pm0.10}N_{0.07\pm0.06}$

Levoglucosan is sought after as an important tracer and marker related to biomass burning as it is stable in the atmosphere and does not decay over eight hours of exposure to ambient air and sunlight. Levoglucosan can be identified with high resolution mass spectrometry from its fragments as the m/z 60 only contains $C_2H_4O_2^+$ ion, and m/z 73 includes $C_3H_5O_2^+$ and a nitrogen containing ion. The top charts in Figure 4-25 provide real-time plots of the total organic matter and levoglucosan fragments measured with the aerosol mass spectrometer as a function of time. As is evident, there is a correlation between the release of organic matter and levoglucosan fragments. The bottom charts show the calculated levoglucosan content from the MS fragments versus the organic matter content. Overall, there is a linear relationship. Ceanothus shows good linearity over the whole burn; however, the relationship for manzanita is linear but with a greater variation in the coefficient of determination. Lee et al. (2010) also found that the AMS could be used to identify levoglucosan in smoke from wildland fuels using some similar southwestern and southeastern fuel types.

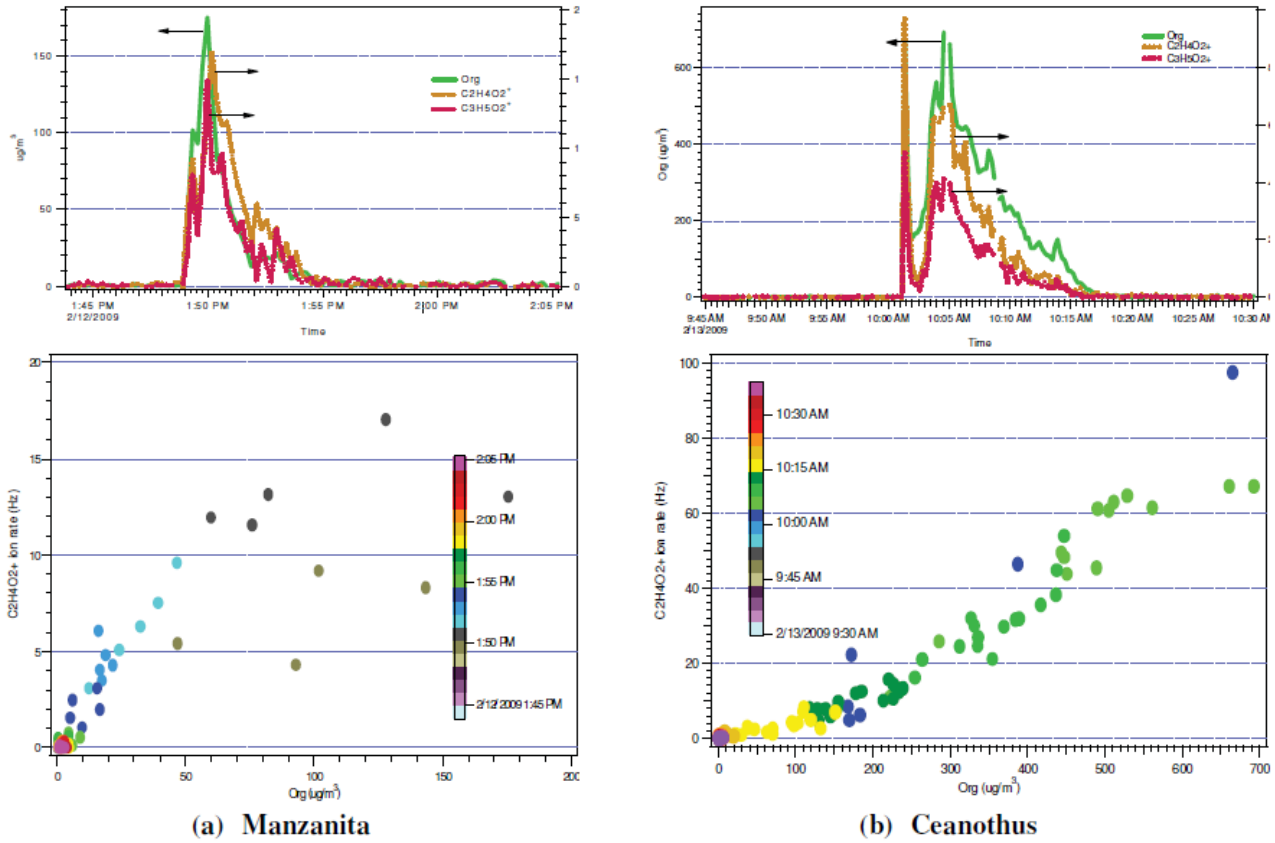

Figure 4-25 Sample AMS Data. Top Charts: Organic Matter (OM) Concentration vs. Time .

Bottom Charts: Levoglucosan (y-axis) vs. OM Concentration (x-axis)

The next chart, Figure 4-26, shows the time evolution of levoglucosan fragment, $C_2H_4O_2^+$, versus total organics throughout flaming, mixed and smoldering phases. To indicate the different phases of biomass burning, the color goes from dark to light as the fire proceeds from flaming to smoldering. Each wildland fuel had a likelihood of releasing levoglucosan; some fuels more than others as the data ranged from 0.75% to 2.46%. Looking at the data as presented one concludes that the coastal sage scrub fuel type had the lowest fraction of levoglucosan and ceanothus had the highest fraction of levoglucosan.

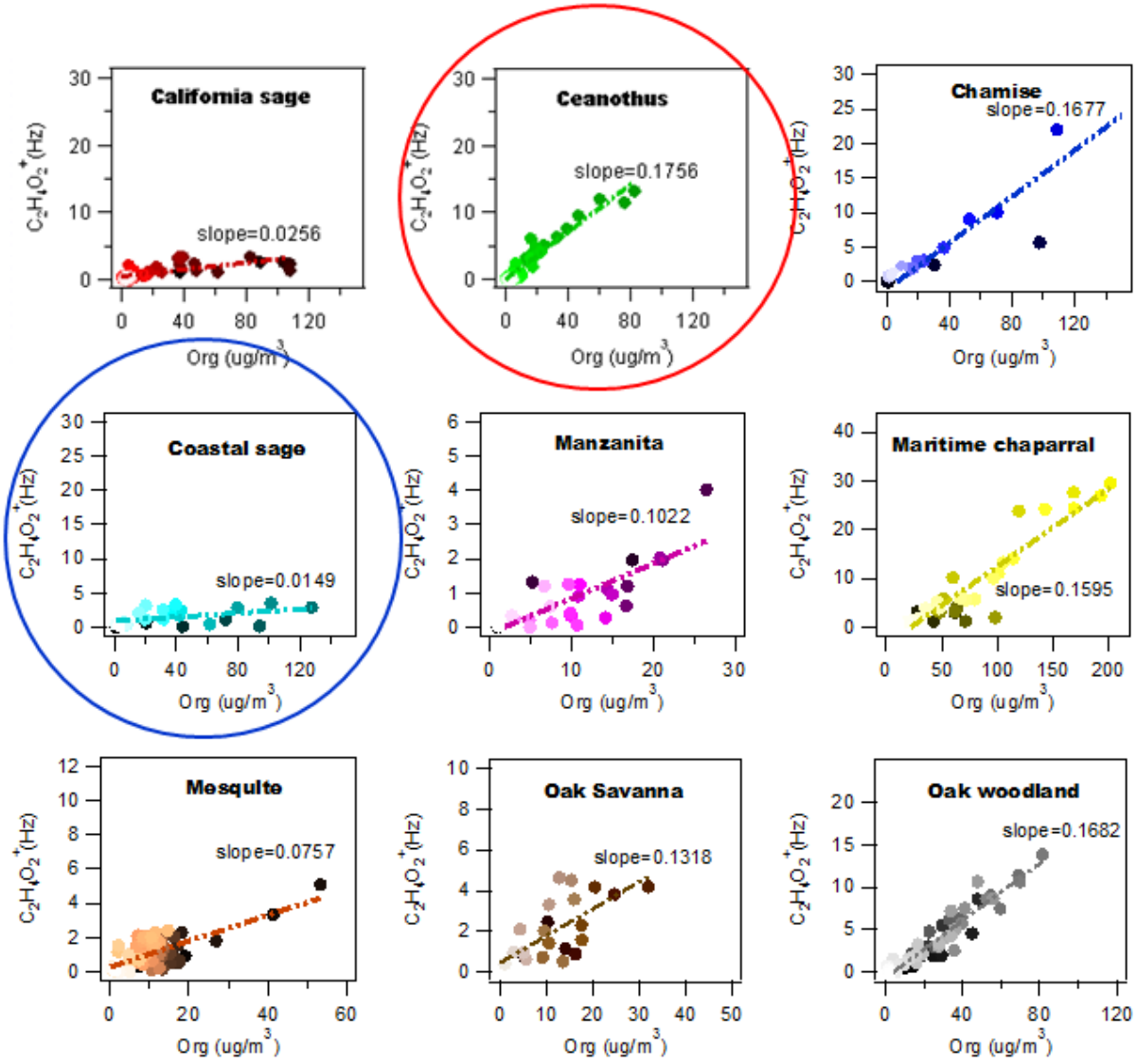

Figure 4-26 Percentage of Organic Matter Released as Levoglucosan

4.2.8 MFSL Results – levoglucosan on filters by GC-MS

In the prior section we discussed measuring levoglucosan in the fire plume with an aerosol mass spectrometer. During the same time as the AMS measurements, UCR took filters for measuring PM mass and these filters were subsequently analyzed for the content of levoglucosan. While the EPA is concerned with toxic air contaminants and PAHs, many scientists studying the course of a fire will follow the release and dispersion of levoglucosan as it is a well-established marker for biomass burning. In this work, we followed the analysis protocols of Schauer; however, analyses proved very challenging as the preparatory methods were not forgiving and difficult to execute. Results for the emissions factors of levoglucosan as a function of the various wildland fuels are in Table 4-28. Note the range of the emission factors for levoglucosan is from about 20 to 1,100 mg/kg with the release of levoglucosan from the eastern fuels being many times higher than fuels from the West. The values from the current study are within the range of values reported by

Schauer et al. (2001) for residential wood burning, average EFs of 1375, 706, and 1940 mg/kg fuel for pine, oak, and eucalyptus, respectively.

Table 4-28 Emission Factors (mg/kg) & Ratios for Levoglucosan (LG) with Various Fuels.

Fuel type	EF_{LG}	LG/PM	LG/OM	LG/OC	EC/TC
Southwest					
cea	187.4±172.2	3.19±2.42	6.24±3.14	4.1±2.1	36±23
chs	234.0±117.7	3.03±1.24	6.44±3.05	4.2±2.0	38±8
cas	25.2±9.3	0.37±0.17	1.46±0.13	1.0±0.1	58±7
cos	19.7±6.4	0.31±0.08	1.53±0.47	1.0±0.3	63±9
man	30.2±10.3	0.79±0.21	3.71±1.13	2.4±0.7	47±9
mch	79.2±42.7	1.64±1.18	6.05±2.86	4.0±1.9	44±18
Chaparral ave.	95.9±35.6	1.56±0.50	4.24±0.90	2.8±0.6	48±6
mes	28.9±10.9	0.75±0.08	2.07±0.37	1.4±0.2	44±1
oas	29.1±13.6	1.80±0.67	4.31±0.91	2.8±0.6	52±8
oaw	58.6±35.1	2.74±1.12	6.53±4.12	4.3±2.7	42±15
FHUA ave.	38.9±13.1	1.76±0.44	4.30±1.41	2.8±0.9	46±6
Southeast					
lit	1089.8±507.2	5.76±1.65	5.76±1.65	3.8±1.1	10±6
1yr	888.0±521.7	6.92±0.33	6.92±0.33	4.5±0.2	8±4
2yr	1272.5±545.9	9.52±1.04	9.52±1.04	6.2±0.7	6±4
poc	208.3±142.2	4.03±1.11	4.03±1.11	2.6±0.7	17±8
cuh	50.2±6.8	3.02	3.02	2.0±0.0	37
uh	337.0±135.7	5.14±3.46	5.14±3.46	3.4±2.3	32±9
Camp Lejeune ave.	641.0±155.1	5.73±0.83	5.73±0.83	3.7±0.5	18±3

4.2.9 MFSL Results – integral vs. instantaneous $PM_{2.5}$ emission factors

Fire is a highly transient process typically going from a short burst of intense flaming to a long period of smoldering as seen in Figure 4-27, pictures of our laboratory burns. Furthermore, during the flaming period, the fuel consumption and emission rates are high and CO_2 is the primary gas. Then there is a transition to the long smoldering period when emission rates are quite low and CO is the primary gas. Trace gases released in the smoldering period are different from the trace gases in the flaming period, as well.

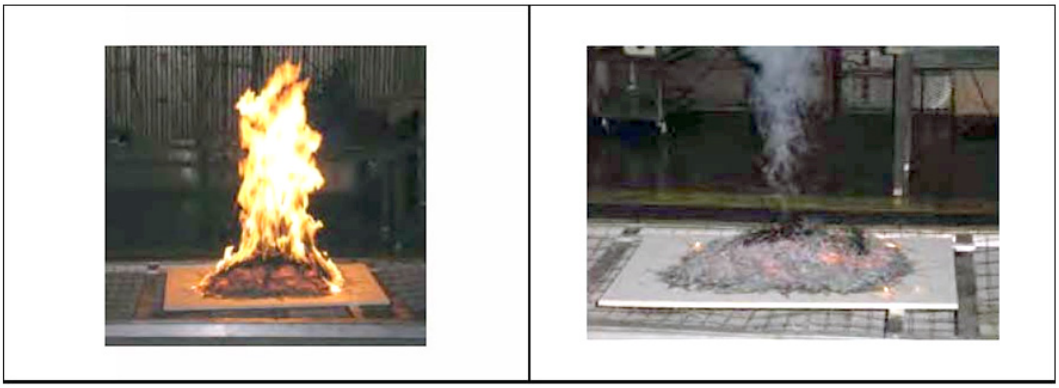

Figure 4-27 Example of Flaming and Smoldering Fire

The transient nature and dynamics of fire can be viewed by simultaneously recording a number of metrics as shown in Figure 4-28. The continuous measurements included CO_2 to show the rate of fuel consumption, the weight of fuel, the number and mass of particles per cc being released and the Modified Combustion Efficiency (MCE) as defined earlier.

$$MCE = \frac{\Delta CO_2}{\Delta CO + \Delta CO_2} \begin{cases} Pure\ flaming\ if > 0.95 \\ Pure\ Smoldering\ 0.75 - 0.85 \end{cases}$$ where

$$\Delta x = x_{measured} - x_{background}$$

Clearly the time series graphs shows a highly transient output and overall process is non-linear especially in the flaming period. One might argue that a linear function could fit the data during the smoldering period, however.

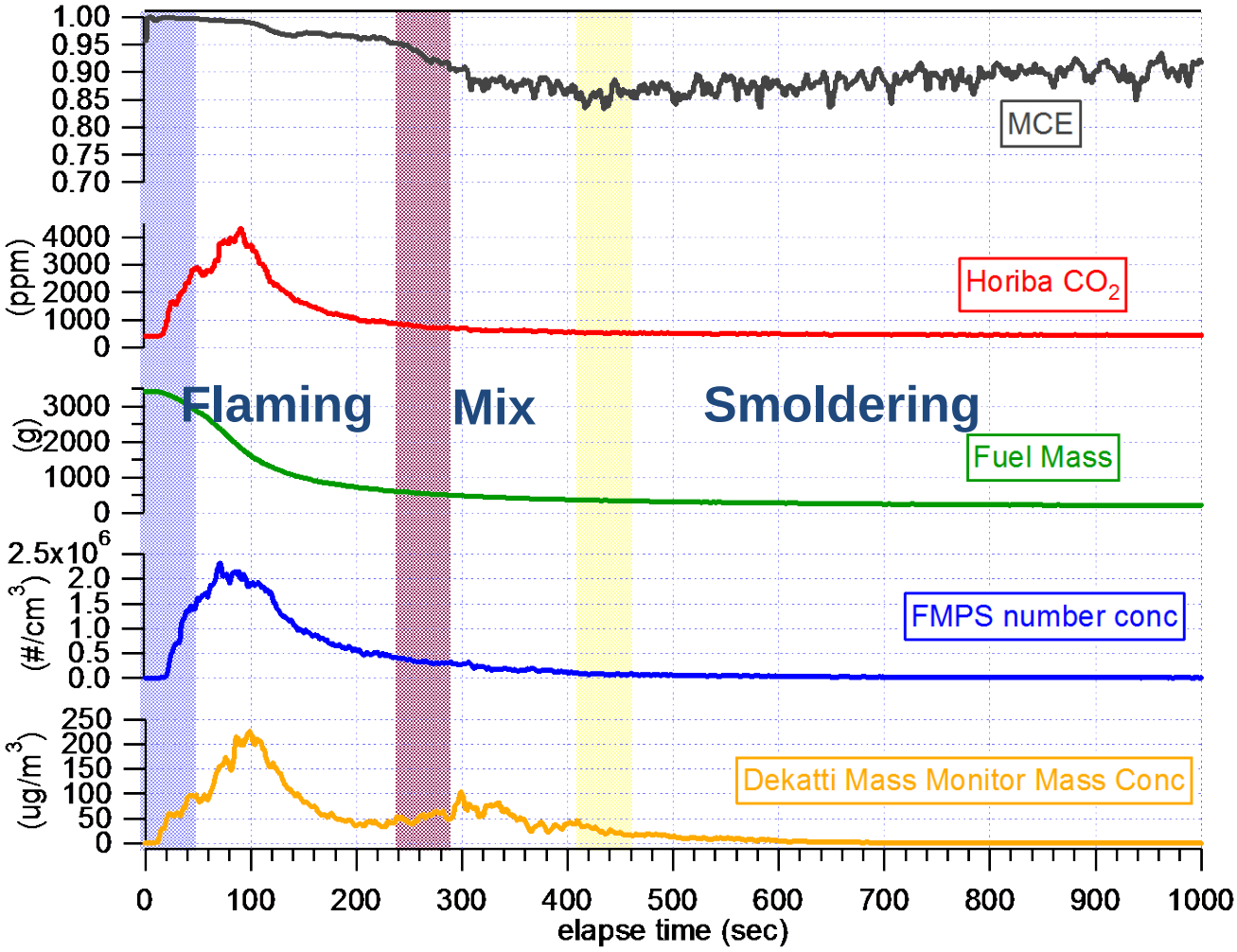

Figure 4-28 Data Stream from a Typical Burn at MFSL

In the experimental design and analysis plan for the data at the MFSL lab, we took one filter per burn and used that data to develop emission factors for a fire that spanned from flaming to smoldering. Normally, data were recorded for up to 2,000 seconds and for about 10% of the time, the fire was in the flaming regime. Thus on a time-weighted basis only about 10% of the data points were from the flaming regime and 90% of the data were from the smoldering regime. What does the single emission factor represent: flaming or smoldering? And is it appropriate to use a single filter to develop emission factors for a whole fire given that the plots of emission factors versus MCE shows the emission factor increases when going from the flaming to the smoldering regime.

Fortunately, while 90% of the data points come from smoldering regime, about 90% of the mass is burned during the flaming regime. Since emissions factors are expressed on a mass basis, we believe the mass data will more properly weight the flaming regime. The question still begging an answer: What are the differences between the emissions factors for the flaming and the

smoldering regime? And would it be more reasonable to develop instantaneous emission factors for the flaming and the smoldering regimes, instead of accepting a single emission factor?

Given the dynamic behavior of fire, the answer to that question would depend on the availability of high-speed continuous analyzers. Such analyzers are now available and would enable us to report the instantaneous emissions factors during the fire and directly compare flaming and smoldering emission factors. Earlier we showed a figure comparing the emission factor determined with a single filter capturing both the flaming and smoldering as compared with the integrated value from a continuous mass analyzer. We concluded there were similar trends and some differences with the DMM not as responsive to the OC mass. See Figure 4-29.

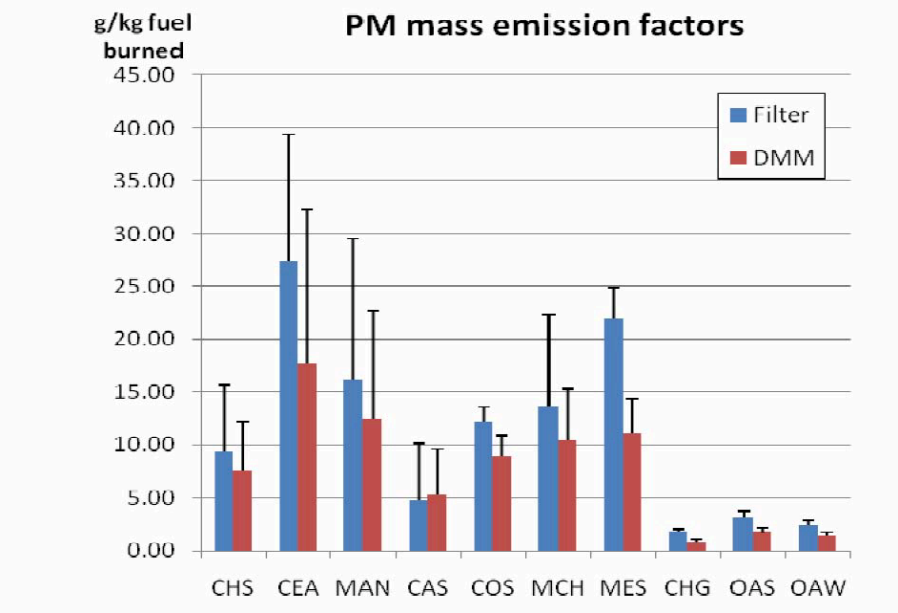

Figure 4-29 PM Emission Factor from a Filter and from DMM

With the DMM we could measure the instantaneous emission factor for PM mass and particle number and this capability is shown in the next two figures. Figure 4-30 shows the averaged PM mass emission factors for each type of fuel during flaming, transition and smoldering phases when calculated based on the overall mass lost. However, values for the smoldering phase, when calculated based on the mass loss in the smoldering phase, show a greater emission factor than for flaming since most of the mass is lost during the flaming phase. See Figure 4-13.

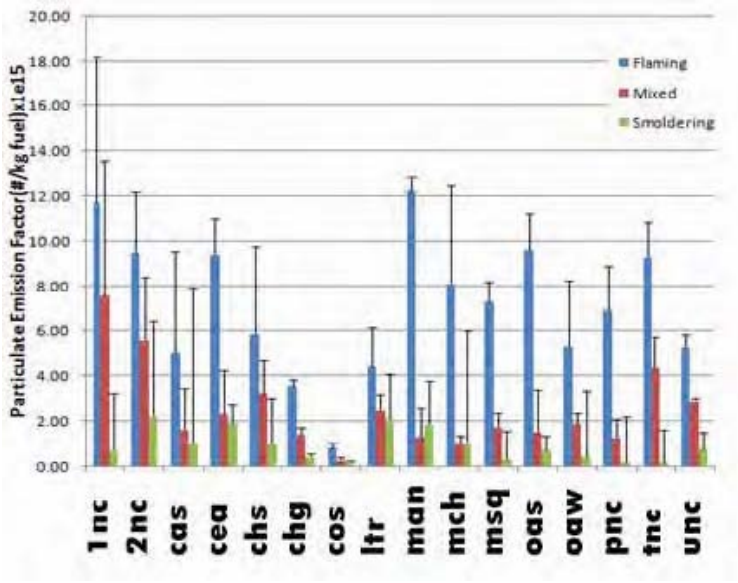

Figure 4-30 Single Burn EFs for Flaming, Mixed and Smoldering Phases for Southeastern and Southwestern Wildland Fuels.

Figure 4-31 shows the particle number emission factors during each of the combustion phases for different plant species when calculated based on the overall mass lost during the burn. While most of the mass is consumed during the flaming phase, the greatest emission factors were in the transitional flaming-smoldering phase. Clearly with these types of differences in emission factors and with today's instruments, we suggest reporting two emission factors; one for flaming and a second one for smoldering.

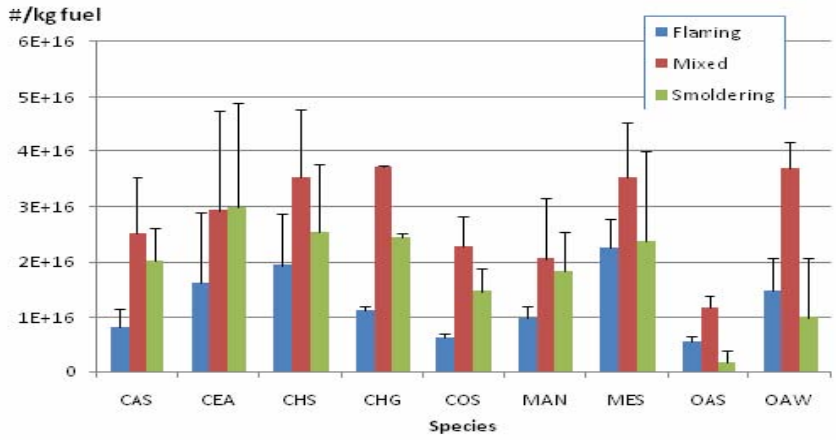

Figure 4-31 Particle Number Emission Factors for Flaming & Smoldering for Southwestern Fuel Types

4.2.10 MFSL Results – Instantaneous particle size distribution

The unique suite of instruments allowed us to make first of a kind measurements for several physical and chemical characteristics of the smoke coming from the fires in near real time. A significant amount of the results with the unique instrument suite were covered in the Hosseini et al. 2010 publication: *Particle Size Distributions from Laboratory-Scale Biomass Fires Using Fast Response Instruments*

In addition to the DMM the equipment included an Aerodynamic Particle Sizer (APS). Sample output from that instrument is shown in Figure 4-32. Note the x-axis is time and the y-axis is the particle size. A third dimension is the color scale ranging from blue to red; for few to many particles. Note all the information that is captured in the 2 minute burst when intense flaming period occurs. Particle size is about 40nm and particle number reaches $>10^6$ (#/cm^3) during the flaming period and then quickly heads towards the background levels. All of this information about the transient nature of the released PM is lost when solely relying on data that results from capturing PM mass on a single filter for the whole burn.

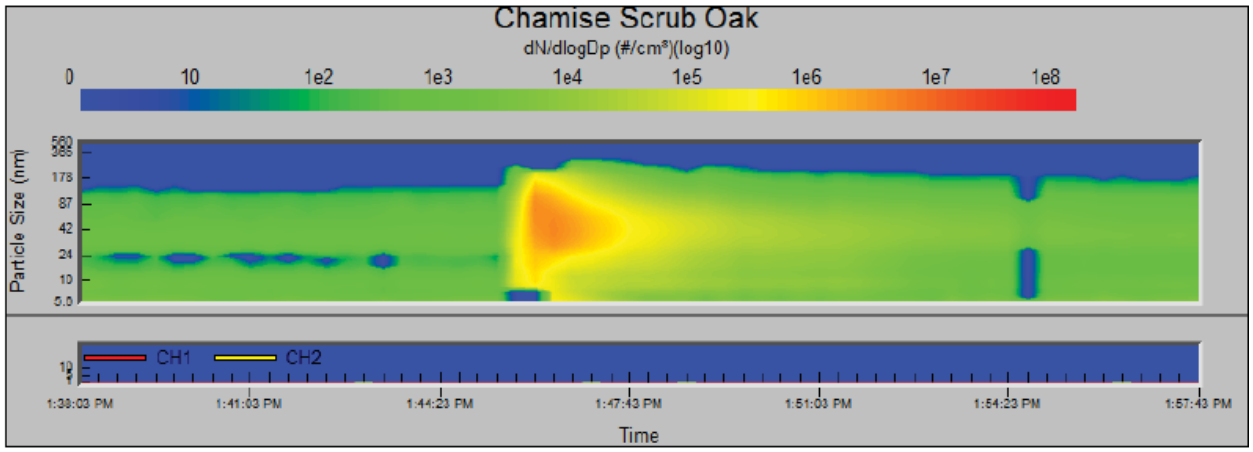

Figure 4-32 Sample APS Output Showing Instantaneous PM Size and Number

Additional specialized instruments on site included a Fast Mobility Particle Sizer Spectrometer (FPMS) and a Condensation Particle Counter (CPC), both described in Hosseini et al. (2010). These instruments enabled measurement of the instantaneous particle size distribution during the laboratory fires. With instantaneous measurements an emission factor can be determined for the flaming and for the smoldering phases rather than assign a single number to the merged phenomena.

Other analyses and graphical representations display the course of the PM emissions during the flaming and the smoldering regimes. For example, Figure 4-33 contains two graphs, typical of all the MFSL burns with the installed instruments. One of the graphs is a log-log graph of the particle concentration, and the other chart is the contour graph. When data from both formats is combined, the resulting information shows in the flaming phase a high concentration of particle emissions starts and encompass a wide size range up to 560nm, which is the upper limit of the FMPS. Mixed flaming-smoldering phase still shows the same size range, but moving to pure smoldering phase lowers the higher end of the size range from 560nm to 200- 300nm, and finally with the lowest particle concentration related to the end of smoldering phase; it peaks around 10nm. FMPS instruments providing real-time data clearly show the significant differences between the flaming and the smoldering phase.

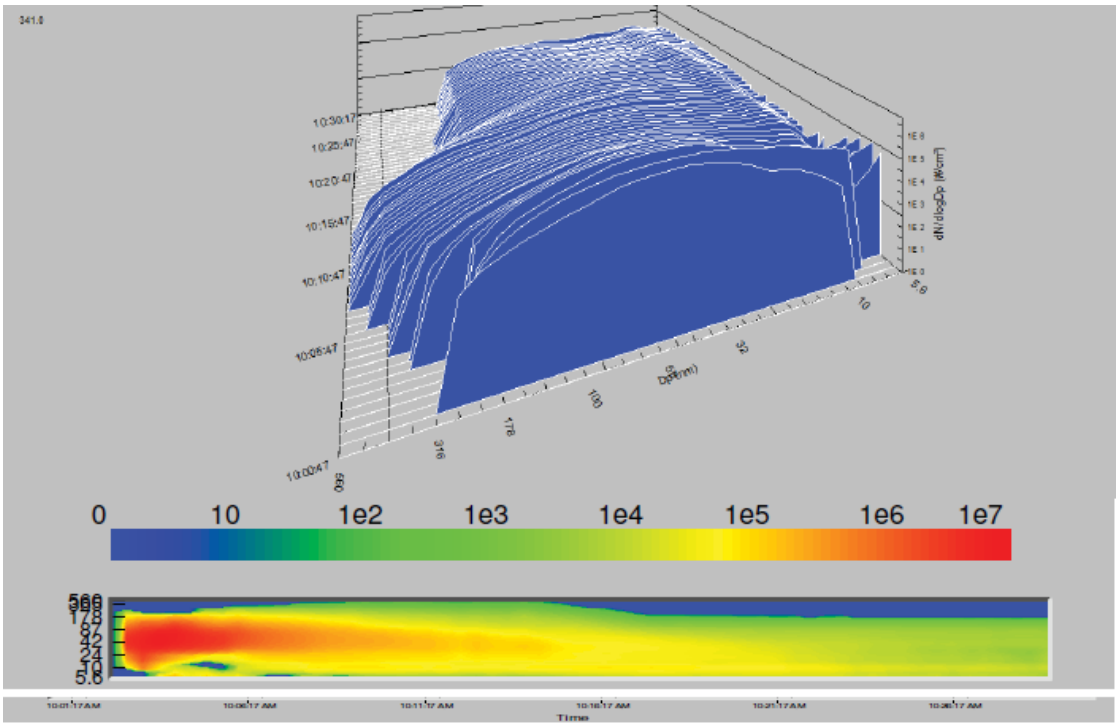

Figure 4-33 Size Distribution Contour for Manzanita .The top graph is a log-log graph as Function of Time; Bottom Graph is (#/cm^3) Contour Graph; x-axis as time & y-axis as Particle Size(nm)

The next series of three plots in Figure 4-34 shows the particle size distribution for various fuels over time and while transitioning from the flaming, transition and the smoldering phases. Basically the particle size distribution measured by FMPS ranged from 7 to 52nm, with the major mode of particle size distribution in the range of 29 to 52 nm. Comparing mass size distribution from FMPS and APS measurements, 51-68 % of particle mass was attributable to the particles ranging from 0.5 to 10 µm for PM_{10}. Geometric mean diameter rapidly increased during flaming and gradually decreased during mixed and smoldering phase combustion. Most of fuels gave unimodal distribution during flaming phase and strong bimodal distribution during smoldering phase. Particle number also varied widely with the combustion phase and was 100 times higher during the flaming phase than during the smoldering phase giving some indications of the stormy nature of the fire during the flaming phase.

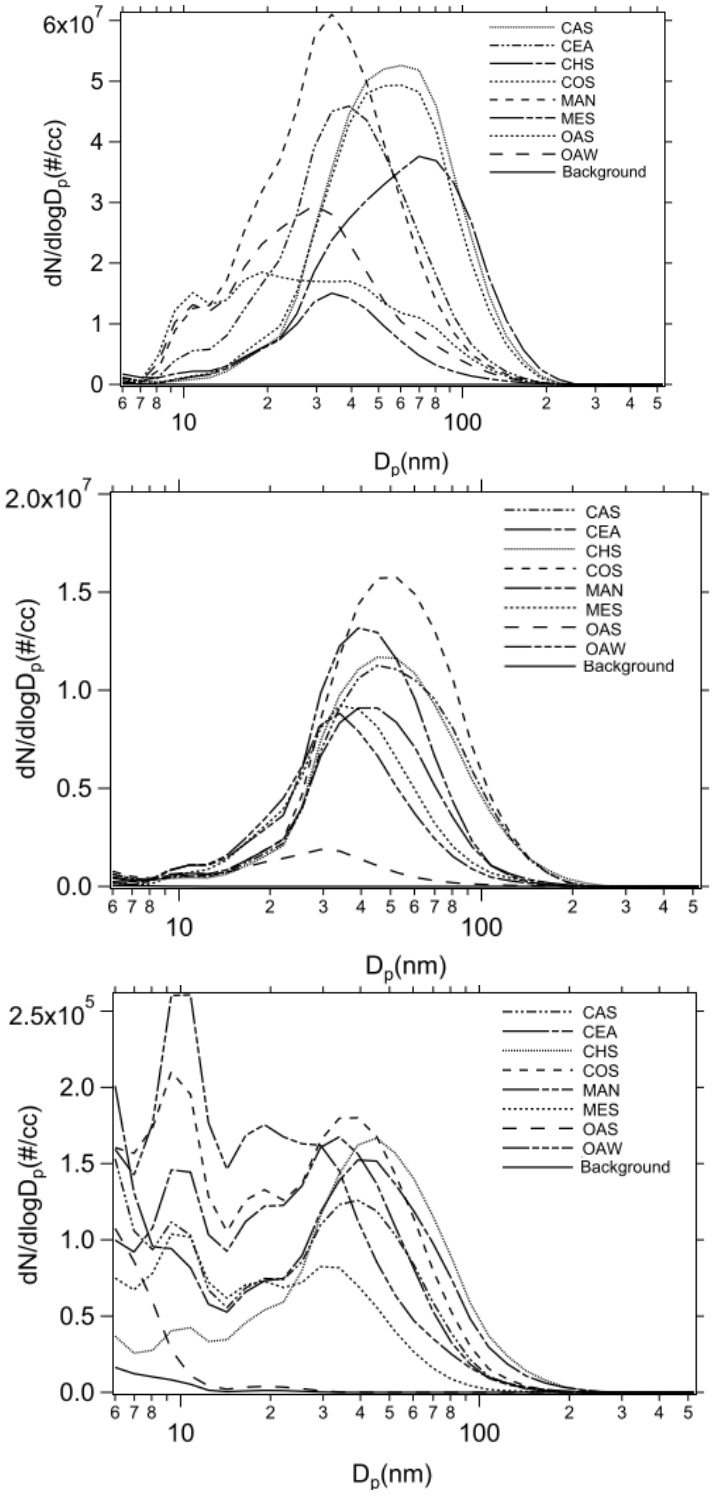

Figure 4-34 Sequence of Particle Size Distributions for: Flaming (top), Trasition (middle) and Smoldering (bottom).

APS data indicated that the sizes of the particles were smaller than 600 nm. The concentration of the particle sizes at the first peak, 10nm, stays about the same level throughout the data set. The highest fraction of the emissions belongs to the strong peak located between 29 and 50nm.

Emissions at this mode decreases up to two orders of magnitude after the flaming mode. These data are shown in Figure 4-35.

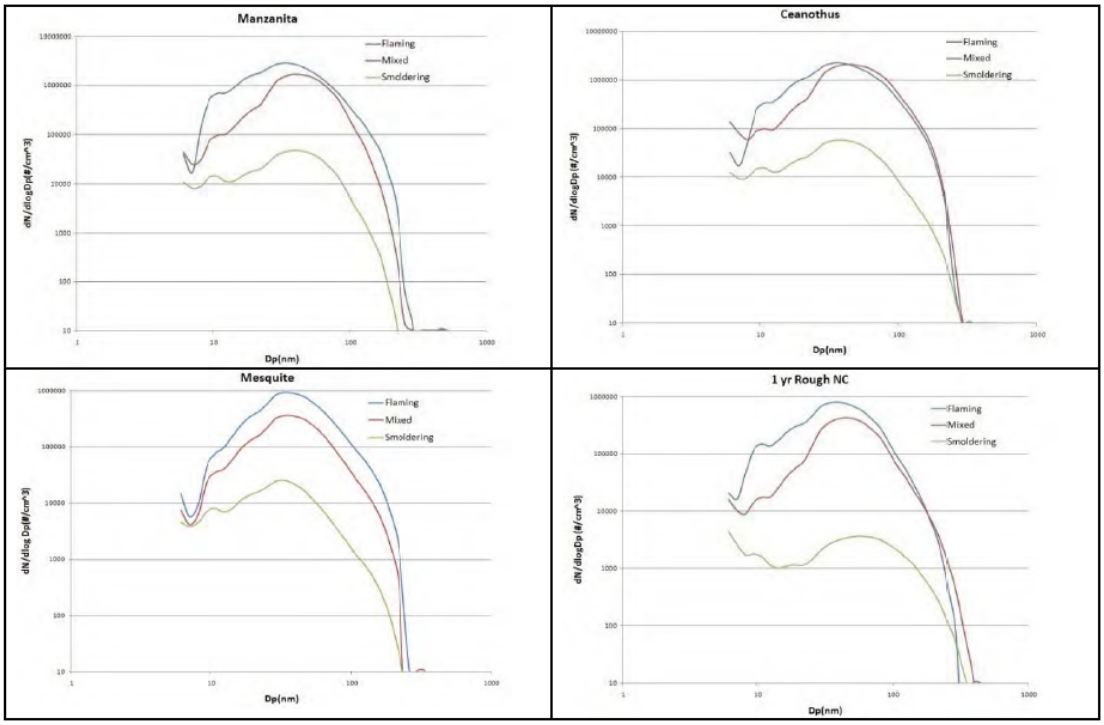

Figure 4-35 Size Distribution Graphs during Different Phases: Flaming to Smoldering (FMPS data)

Other data showing the instantaneous physical characteristics and number of particles released during fire regimes can be learned from the thesis of Dr Hosseini.

4.2.11 Field Results: Vandenberg UCR

There were two days of burning at Vandenberg AFB and since the fire failed to spread on 11/5, no results are reported. On 11 November, the burn was successful and data were collected. Ignition occurred at 1030 PST (UTC – 8). Active flaming lasted until 1500 PST. Recorded plume height by the aircraft was approximately 5,000 ft AGL and approximately 6,300 ft at 1245 PST and 1445 PST, respectively.

UCR Tower data were collected on the wind and temperature fields generated during the fire. Representative data collected from the towers and tripod with various instruments that were identified in Table 3-2. The wind data showed only small perturbations from the mean values and that is not too surprising given that the tower and tripod were a considerable distance away and the burn had to remain within prescription. What is evident is the truck near the burn had a very significant response to the emissions from the fire. There is no response at either the tripod or tower but the truck just downwind of the burn has a 100-fold increase in PM concentrations. These data give a glimpse of the complications of collecting field samples that represent the field fires. Even if you measure a significant response one has to use dispersion modeling to estimate what the conditions were in the fire.

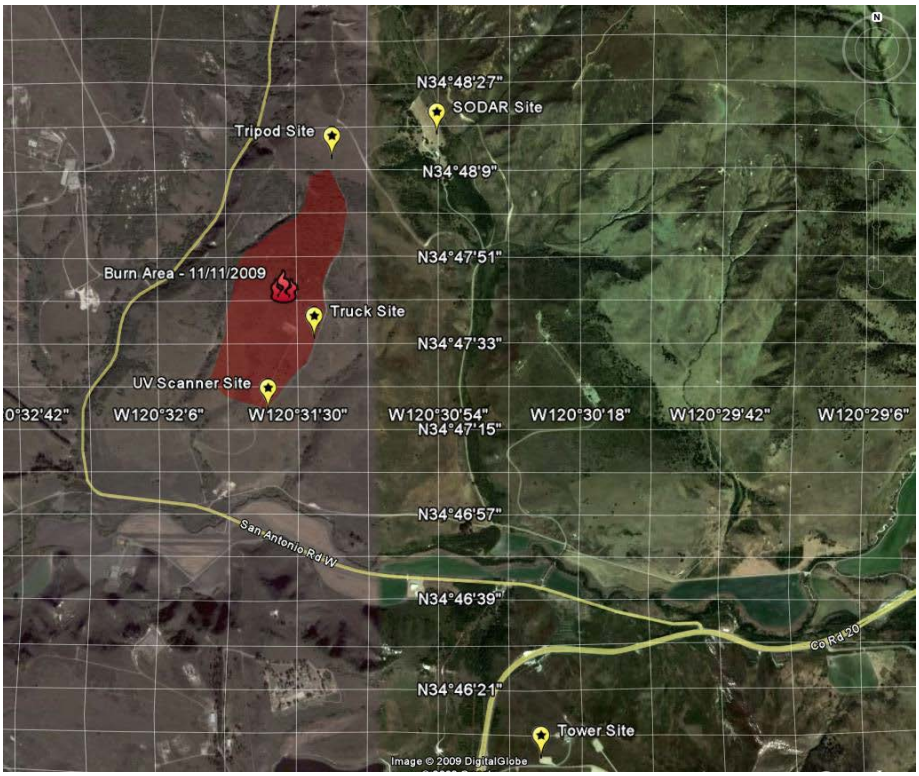

Figure 4-36 Overview of the Burn and Instrument Locations

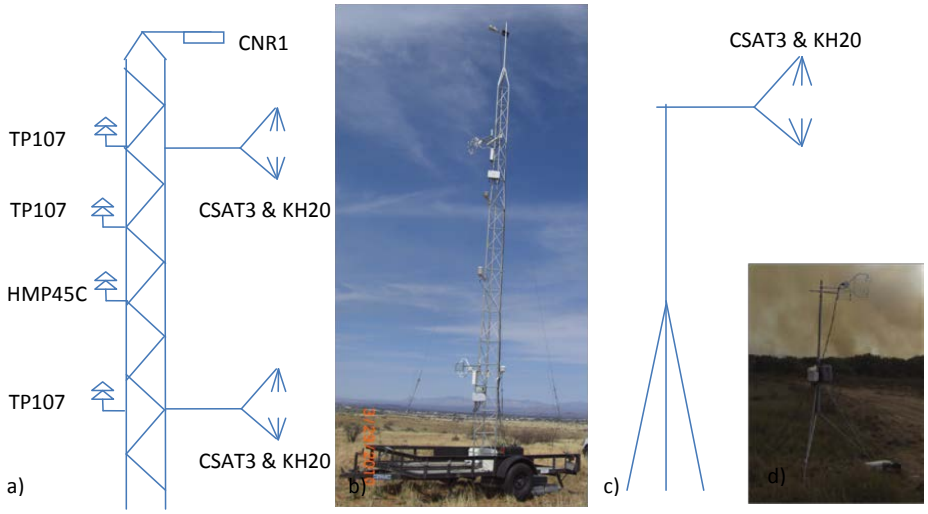

Figure 4-37 Schematic of Tower & Tripod. a) Met tower. c) Tripod.

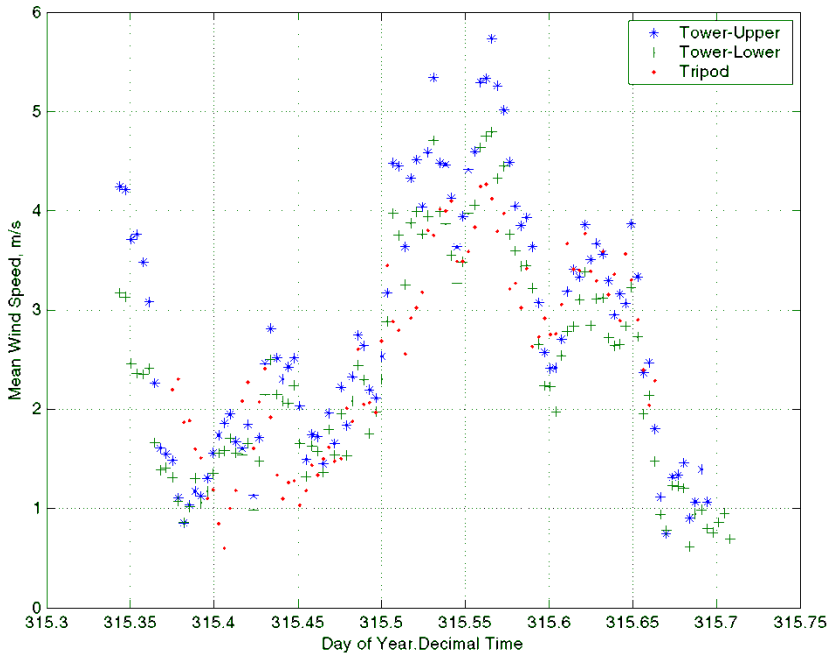

Figure 4-38 Wind Speed at Tower & Tripod Locations at AFV on 11/11/2009

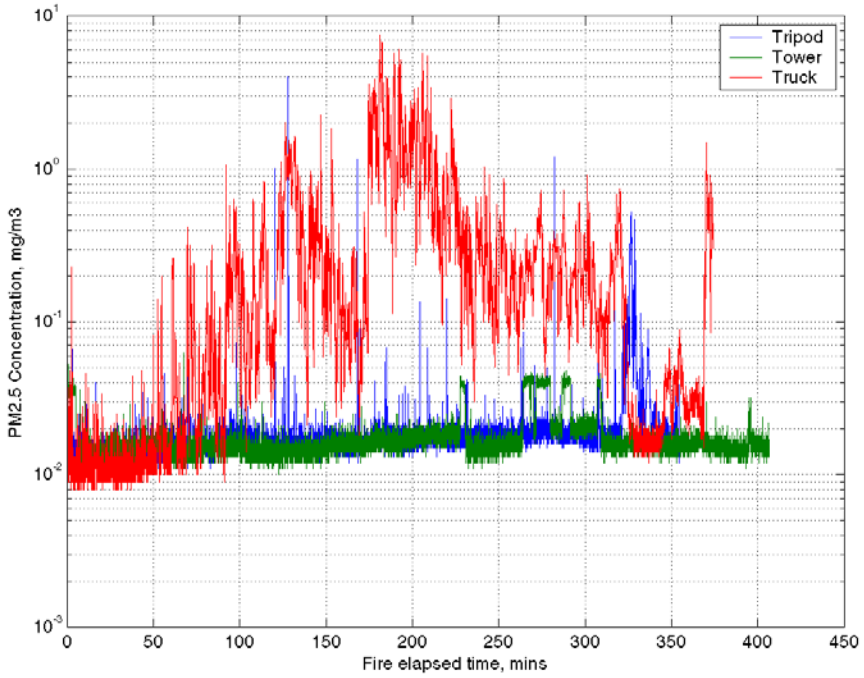

Figure 4-39 Measured PM2.5 Concentration at Tower, Truck & Tripod Locations at AFV

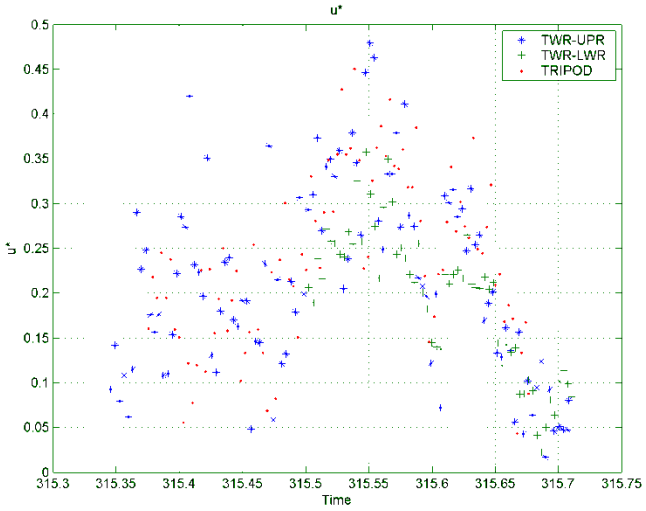

Figure 4-40 Measured Frictional Velocity at Tower and Tripod Locations

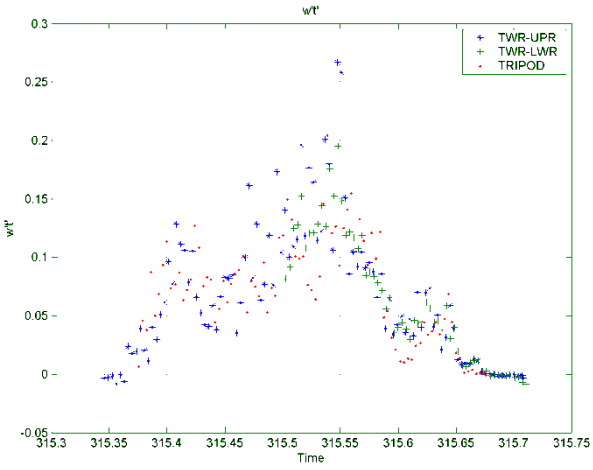

Figure 4-41. Measured Kinematic Sensible Heat Flux at Tower and Tripod Location

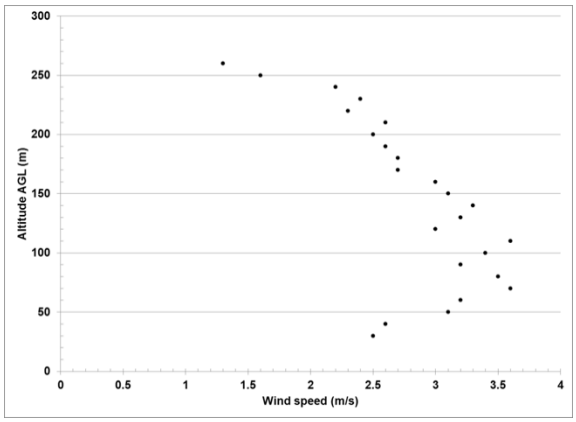

Figure 4-42. SODAR Wind Speed Measurements at noon at AFV

UCR chemical data collected in the truck at the edge of the burn consisted of samples using instruments like those used in the MFSL experiments. Additionally some new ones were added to investigate the interaction between water in clouds and the soot from the fire. The truck was located downwind of the planned burn. As evident in Figure 4-43 the visibility of the bright noon sun was reduced significantly.

Figure 4-43 Maximum Observed Fire Behavior in Grant B Burn at Vandenberg and Truck Sampling Smoke Emissions at 1200 PDT in Grant A Burn

Table 4-29 Sampling Times for Samples taken Vandenberg AFB, CA

	Sample 1	Sample 2	Sample 3	Sample 4
Start sampling	1059 PDT	1213 PDT	1336 PDT	1505 PDT
End sampling	1159 PDT	1324 PDT	1452 PDT	1605 PDT

Table 4-30 Formaldehyde, Acetaldehyde and Acetone in ppb for Samples

(Values in ppb)	Set 1	Set 2	Set 3	Set 4
Formaldehyde	3.85	20.93	25.93	4.23
Acetaldehyde	5.18	19.14	32.74	5.21
Acetone	12.95	71.16	43.40	36.85

Table 4-31 Poly Aromatic Hydrocarbons (PAHs) in the Particle Phase as ng/m^3 Air Sampled.

	Set 1	Set 2	Set 3	Set 4
Naphthalene	706	-	71.4	11.1
Acenaphthylene	131	-	168	78.8
Acenaphthene	5.29	-	29.5	1780
Fluorene	46.4	-	7.74	16.4
Phenanthrene	1130	-	216	242.6
Anthracene	187	-	179	245
Fluoranthene	29.1	-	81.6	2.76
Pyrene	14.8	-	38.5	841
Benz(a)anthracene	0.179	-	23.1	601
Chrysene	1.31	-	22.9	10900
Benzo(b)fluoranthene	N.D.	-	1.38	3760
Benzo(k)fluoranthene	1.01	-	14.3	2850
Benzo(a)pyrene	2400	-	19100	78100
Indeno(1,2,3-cd)pyrene	673	-	287	561
Dibenzo(a,h)anthracene	6830	-	236	4090
Benzo(ghi)perylene	481	-	2420	160

Table 4-32 Analyses of Particulate Matter (PM), Elemental & Organic Carbon for AFV Samples

	Sample 1	Sample 2	Sample 3	Sample 4
PM (µg/m^3)	51.7	139.5	356.3	93.4
EC (µg /m^3)	2.14	6.25	17.40	5.39
OC(µg /m^3)	33.09	88.78	225.79	58.73

To put the PM values in perspective, the EPA National Ambient Air Quality Standard is 12µg/m^3 as the annual mean. From Figure 4-39 PM levels reaching 1,000µg/m^3 on the DustTrak™ were 100-times standards and filter values averaged over an hour were up to 30-times the national standards; very unhealthy and also resulting in the severe loss of visibility. The analysis in Table 4-32 shows that the PM was primarily organic in nature and actually these values would be higher when compensated for the amount of oxygenated compounds.

Table 4-33 X-ray Fluorescence (XRF) Analysis of Teflon filters (µg/m^3)

Element	Sample 1	Sample 2	Sample 3	Sample 4	MDL[1]
Mg	0.624	0.804	0.542	0.544	0.234
Si	3.844	2.826	1.522	1.150	0.131
P	0.019	0.073	0.054	0.031	0.028
S	0.655	2.815	2.606	0.921	0.084
Cl	1.174	8.754	5.626	0.408	0.047
Al	1.218	1.196	0.727	0.643	0.439
K	1.273	10.671	7.378	1.867	0.047
Ca	0.587	1.812	1.703	0.272	0.075
Sc	0.519	0.465	0.376	0.834	0.056
Ti	0.074	0.057	0.034	0.019	0.075
V	n.d.[2]	n.d.	n.d.	n.d.	0.075
Cr	n.d.	0.026	0.098	n.d.	0.056
Mn	n.d.	n.d.	n.d.	n.d.	0.234
Co	n.d.	n.d.	n.d.	n.d.	0.047
Ni	n.d.	0.026	0.073	n.d.	0.047
Cu	0.074	0.094	0.059	0.093	0.047
Zn	0.049	0.115	0.117	0.068	0.028
Ga	n.d.	n.d.	n.d.	n.d.	0.607
Fe	0.804	0.674	0.737	0.365	0.056
Ge	n.d.	n.d.	n.d.	n.d.	0.140
As	n.d.	n.d.	n.d.	n.d.	0.065
Mo	n.d.	n.d.	n.d.	n.d.	0.103
Sr	n.d.	n.d.	n.d.	n.d.	0.065
Se	n.d.	n.d.	n.d.	n.d.	0.140
Br	n.d.	0.188	0.122	0.062	0.075
Rb	n.d.	n.d.	n.d.	n.d.	0.065
Y	n.d.	n.d.	n.d.	n.d.	0.065
Nb	n.d.	n.d.	n.d.	0.074	0.103
Pd	n.d.	n.d.	0.102	n.d.	0.159
Ag	n.d.	n.d.	n.d.	n.d.	0.168
Cd	n.d.	n.d.	n.d.	n.d.	0.159
In	0.136	0.115	0.112	0.185	0.187
Sn	n.d.	n.d.	n.d.	n.d.	0.252
Sb	0.457	0.528	0.376	0.575	0.243
Cs	n.d.	n.d.	n.d.	n.d.	0.523
Ba	n.d.	n.d.	n.d.	0.445	0.626
Pt	n.d.	n.d.	n.d.	n.d.	0.196
Au	n.d.	n.d.	n.d.	n.d.	0.299
Pb	0.136	0.125	0.083	0.192	0.234
Bi	n.d.	n.d.	n.d.	n.d.	0.159
U	0.074	0.063	0.098	0.062	0.178
Sm	0.865	0.736	0.683	0.853	1.243
Tl	n.d.	n.d.	n.d.	n.d.	0.140

Highlighted elements in Table 4-33 show the elements with the highest concentration. High levels of Potassium (K) and Chlorine (Cl) were in agreement with the lab results but the high levels of lead (Pb), antimony (Sb), samarium (Sm), Scandium(Sc) and Indium (In) were unexpected and clearly showing the effect of the localized soil chemistry at the burn site. Antimony is often alloyed with lead to increase its hardness. During discussions with personnel at the AFV site for the prescribed burn we learned that the site was used in the 1950s as a bazooka/rocket test site. Knowing it was formerly a rocket test site provides insight into the practical nature of the working with the host site before a prescribed burn since toxic elements and compounds might be released in addition to the known gases and PM.

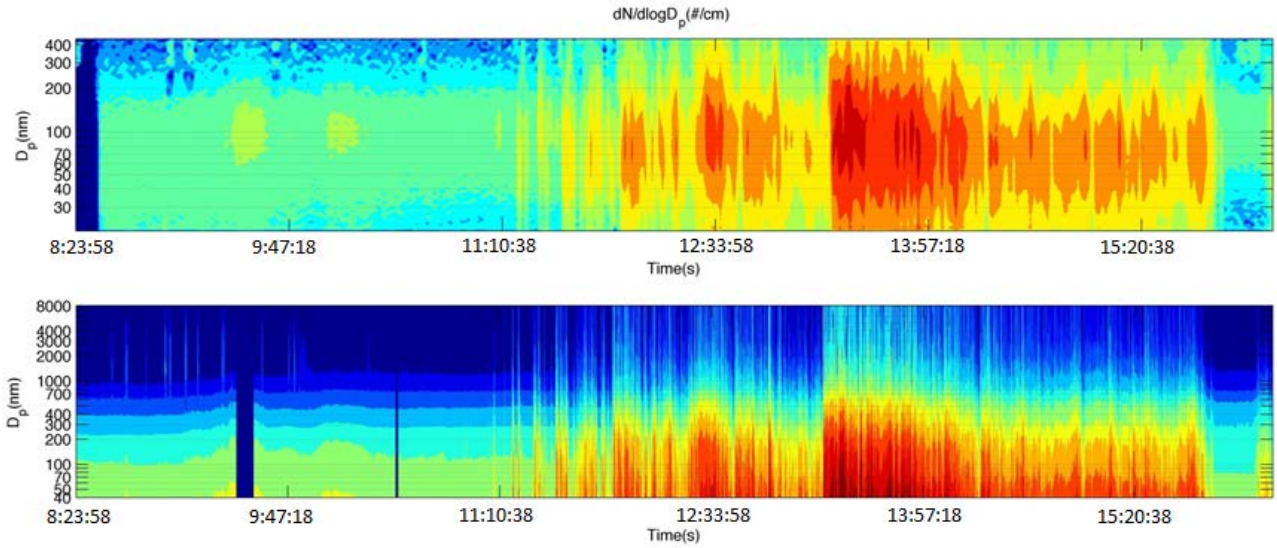

Figure 4-44 Particle Size Distribution with ELPI (top) and SMPS (bottom) Instruments.

Figure 4-44 shows the particle size distribution for the particles reaching the chemistry truck. Clearly both instruments show that the arrival of concentration of particles about the same time and the same intensity for the particle diameter of about 0.1µm or 100 nm.

An experiment to relate particles to cloud formation and climate change was added to the planned emissions measurements at Vandenberg. The science of cloud formation is still developing. One fact is that aerosols, such as those formed in wildland fires, can have a net cooling effect that can counteract the warming form greenhouse gases. Further these aerosols act as Cloud Condensation Nuclei (CCN) to interact with water vapor to form cloud droplets. Small droplets lead to further cooling as clouds reflect solar radiation and as a consequence have a longer lifetime. The main uncertainty in the developing science is the scarcity of data. Thus at Vandenberg UCR added Dr. Asa-Awuku to carry out some measurements of the CCN ability using the aerosols formed in the field fires. Results are shown in Figure 4-45 and show the CCN activity of the aerosol was unchanged during the pre-fire, flaming regime but did decrease during the smoldering regimes.

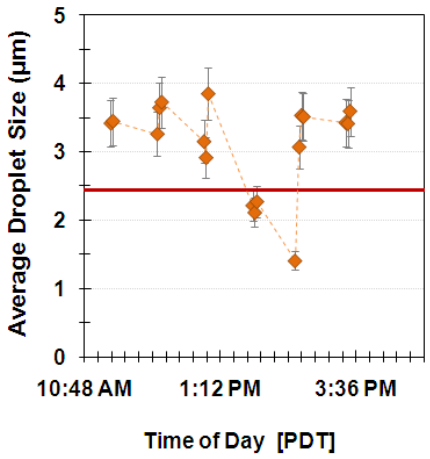

Figure 4-45 Measurements with CCN Counter at Vandenberg, AFB

4.2.12 Field Results: Vandenberg aircraft

At the beginning of the project, some questioned whether the cost of the aircraft was a good investment. This project, like others, clearly showed that the value of having a platform for the sophisticated instruments that could fly through plumes at 500 or 5,000 feet. The instruments included a compact time-of-flight aerosol mass spectrometer (c-ToF-AMS, Aerodyne, Inc.) from Cal-Tech, a single-particle soot-photometer (SP2, Droplet Measurement Technologies) and an airborne FTIR (AFTIR, Yokelson et al., 2007) that was improved as part of RC-1649 and RC-1648. An aircraft platform allowed the capture of fresh emissions from the fire or by following the plume for 10's of miles it was possible to characterize emissions aged several hours in the atmosphere. Several papers were published of the aircraft results so the details are presented elsewhere (Yokelson et al., 2013). For this report, two examples are presented. One of which is the AMS data showing an increase in the nitrate and ammonium ions portion of the aged aerosol. The other figure shows the increase in ozone in the aged plume and the confirmation of the high levels of HONO found in the MFSL experiments. As is evident in Figure 4-47 a number of important changes take time for the transitions to occur and the times are in hours and could not be observed in the short-duration burns in the MFSL even though smoke aging studies have been performed there as well.

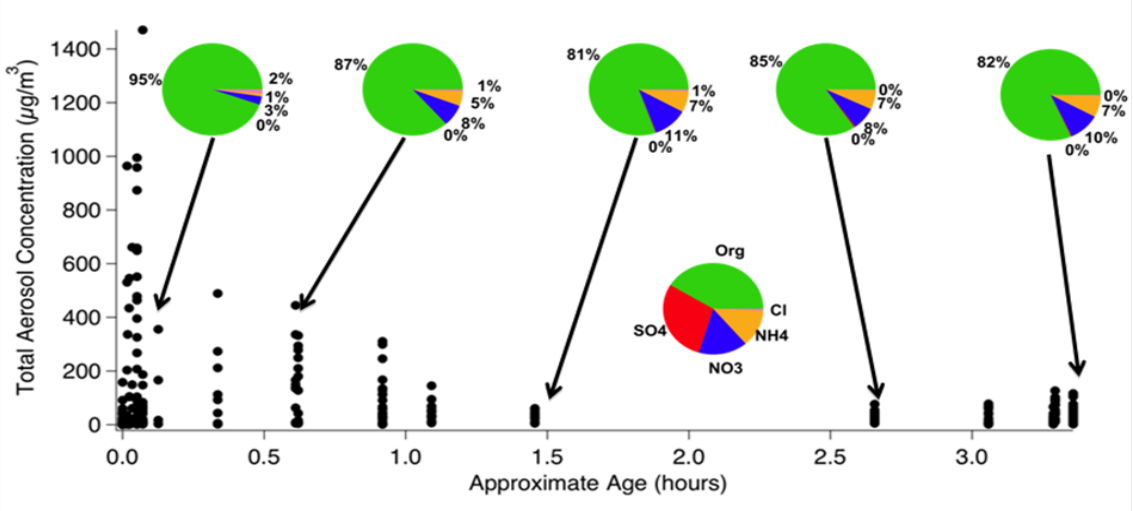

Figure 4-46 In-Plume Aerosol Aging Results from AMS

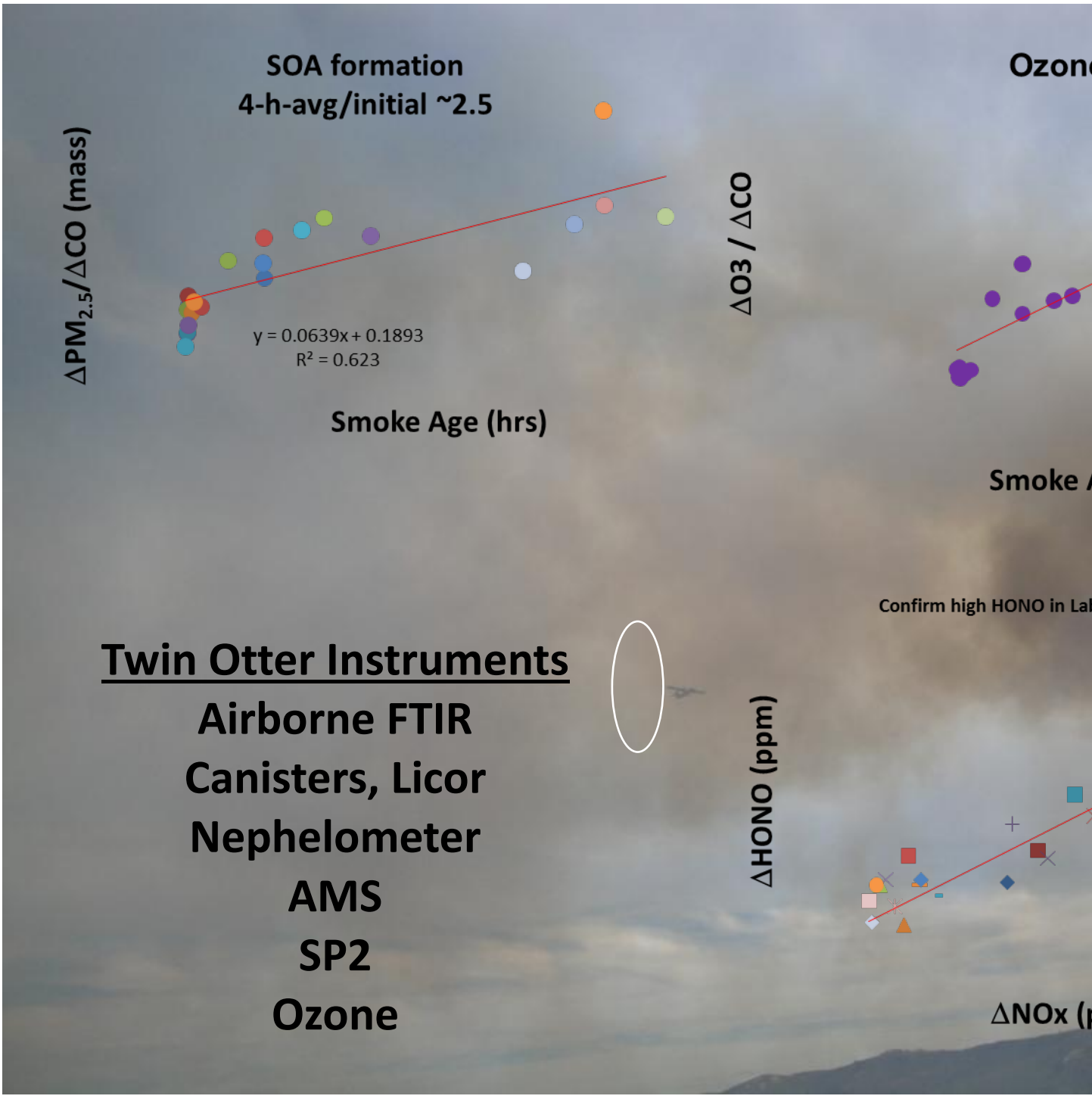

Figure 4-47 Data for Aerosol Samples Aged in the Atmosphere

While the Twin Otter aircraft was deployed in California, smoke from several fires in addition to the Grant Burn was sampled. Two additional prescribed burns in similar fuel types in close proximity to Vandenberg were sampled (Williams and Atmore) as well as two prescribed burns in coniferous forest in the Sierra Nevada (Burling et al., 2011). Detailed results from the Williams fire related to smoke aging and HONO detection were described above and can be found in Akagi et al., 2012. Airborne emissions data for the 5 burns in chaparral fuel types were similar even though the fuels differed somewhat (Burling et al., 2011).

4.2.13 Field Results: Vandenberg US Forest Service's FASS towers

On the Vandenberg AFB burn, four FASS towers were set up within the burn perimeter, in a north/south line along the east edge of the plot within 50 meters of the edge to allow safe access in consideration of buried artillery rounds. The GPS coordinates were Lat. 34° 47.600 N; Long. 120° 31.462 W; alt. 406 ft. The towers were erected to a height of 30 ft. using six 5 ft. sections. The standard sampling times were 10 minutes flaming, 20 minutes intermediate, 30 minutes smoldering. As shown in Figure 3-23 and explained earlier, there are four canisters in the FASS assembly; one canister for each of three phases and a fourth canister for the background values. The background values are subtracted from the measured values in the three canisters collected during the fire. Thus values in Table 4-34 represent the integrated values for the set sampling time above a measured background value. Canisters are triggered into action by detection of an increased carbon dioxide concentration as the fire approaches.

Table 4-34 FASS Data from Vandenberg AFB

Canister	Box	Phase	CO	CO_2	CH_4	C_2H_6	C_2H_4	C_2H_2	C_3H_8	C_3H_6	i-butan	2 buter	- buten	obuten	-butadiene		NMHC	MCE
		Concentration (ppm)																
FC112	32	F	17.38	202	0.88	0.15	0.30	0.09	0.03	0.09			0.02	0.02	0.01		0.71	
FC105	32	I	8.81	113	0.30	0.07	0.17	0.08		0.06							0.37	
FC106	32	S	3.83	26	0.29	0.08	0.08		0.04	0.03	0.01						0.24	
FC222	30	F	18.18	57	0.08	0.06	0.08	0.02	0.02	0.05								
FC399	30	I	67.70	722	5.88	0.69	1.16	0.30	0.17	0.44	0.04	0.02	0.07	0.07	0.07		3.07	
FC161	30	S	13.02	115	1.24	0.18	0.22	0.04	0.05	0.11	0.01		0.02	0.02	0.01		0.67	
FC140	32	F	9.04	121	0.65	0.07	0.27		0.02	0.06	0.07				0.02		0.51	
FC141	32	I	15.99	188	1.18	0.15	0.42		0.04	0.11	0.06	0.02	0.01		0.03		0.85	
FC144	32	S	8.77	113	0.82	0.07	0.21	0.06	0.01	0.05	0.01						0.42	
FC118	37	F	31.22	497	2.06	0.23	0.66	0.20	0.05	0.19	0.02		0.03	0.02	0.05		1.46	
FC123	37	I	13.47	200	1.03	0.11	0.31	0.10	0.03	0.09			0.02	0.02	0.02		0.69	
FC127	37	S	6.92	84	0.49	0.07	0.15	0.05	0.01	0.04							0.33	
		Emission Factor (g/kg)																
			CO	CO_2	CH_4	C_2H_6	C_2H_4	C_2H_2	C_3H_8	C_3H_6	i-butan	2 buter	- buten	obuten	-butadiene		NMHC	MCE
FC112	32	F	91.3	1669	2.65	0.82	1.58	0.42	0.27	0.68	0.00	0.00	0.19	0.24	0.15		4.35	0.92
FC105	32	I	83.4	1686	1.60	0.71	1.57	0.68	0.00	0.84	0.00	0.00	0.00	0.00	0.00		3.80	0.93
FC106	32	S	147.6	1549	6.35	3.36	2.97	0.00	2.14	1.88	1.14	0.00	0.00	0.00	0.00		11.49	0.87
FC222	30	F	278.0	1381	0.70	1.06	1.25	0.32	0.50	1.14	0.00	0.00	0.00	0.00	0.00		4.27	0.76
FC399	30	I	98.3	1649	4.88	1.08	1.68	0.40	0.40	0.96	0.13	0.07	0.21	0.21	0.19		5.40	0.91
FC161	30	S	116.1	1611	6.31	1.74	2.00	0.35	0.68	1.43	0.24	0.00	0.29	0.38	0.20		7.32	0.90
FC140	32	F	79.9	1681	3.30	0.62	2.40	0.00	0.23	0.79	1.30	0.00	0.00	0.00	0.39		5.72	0.93
FC141	32	I	90.1	1663	3.79	0.88	2.38	0.00	0.36	0.94	0.73	0.24	0.16	0.00	0.32		6.01	0.92
FC144	32	S	83.1	1677	4.45	0.76	1.96	0.56	0.18	0.69	0.21	0.00	0.00	0.00	0.00		4.37	0.93
FC118	37	F	68.2	1707	2.57	0.54	1.45	0.41	0.18	0.62	0.07	0.00	0.13	0.11	0.21		3.72	0.94
FC123	37	I	72.7	1697	3.17	0.61	1.66	0.51	0.24	0.70	0.00	0.00	0.21	0.19	0.23		4.36	0.94
FC127	37	S	87.3	1672	3.56	0.92	1.91	0.56	0.28	0.83	0.00	0.00	0.00	0.00	0.00		4.51	0.92
		Emission Factor (g/kg)																
erage by Phase		F	79.8	1686	2.84	0.66	1.81	0.28	0.22	0.70	0.46	0.00	0.11	0.12	0.25		4.59	0.93
		I	86.1	1673	3.36	0.82	1.82	0.40	0.25	0.86	0.21	0.08	0.14	0.10	0.19		4.89	0.93
		S	108.5	1627	5.17	1.70	2.21	0.37	0.82	1.21	0.40	0.00	0.07	0.10	0.05		6.92	0.90

Comparing emission factors from the field FASS canisters with the lab measured values shows that except for butadiene the CO and CO_2 values are about the same, given the wide range of the data that was averaged and observed standard deviation in the data set.

Table 4-35 Emission Factors of Lab & Field in g/kg for COx; mg/kg for butadiene

	CO2	CO	Butadiene
Lab	1750	65	25
Field	1650	90	140

Other data relationships were developed in relationship to CO.

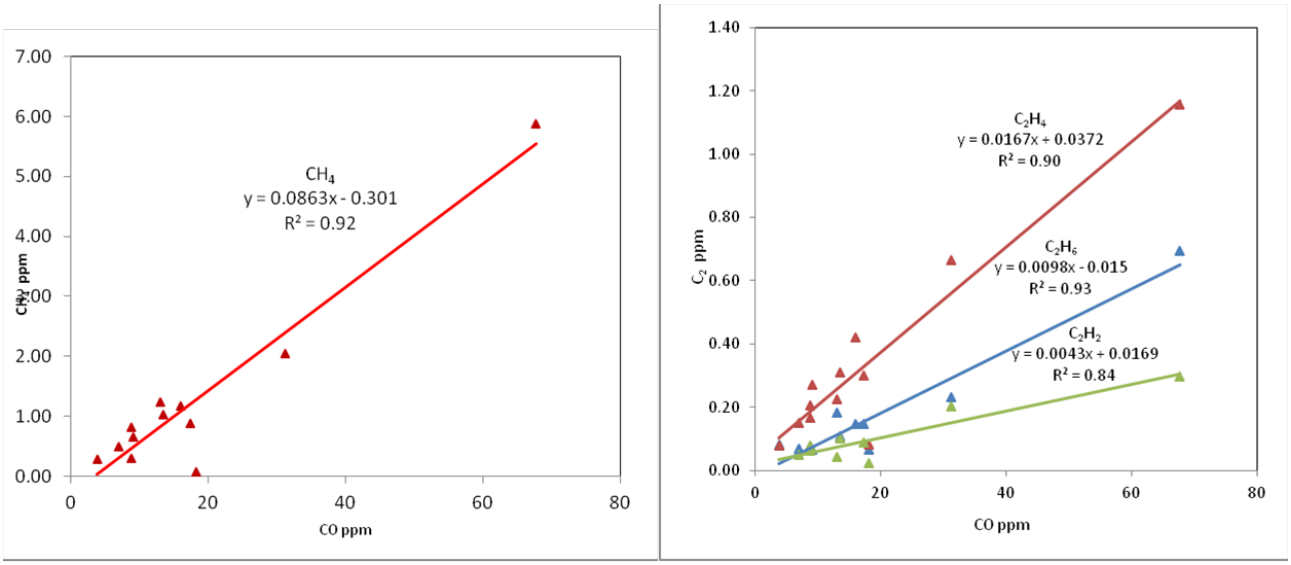

Figure 4-48 Plots of CH4 and C2 Compounds vs. CO

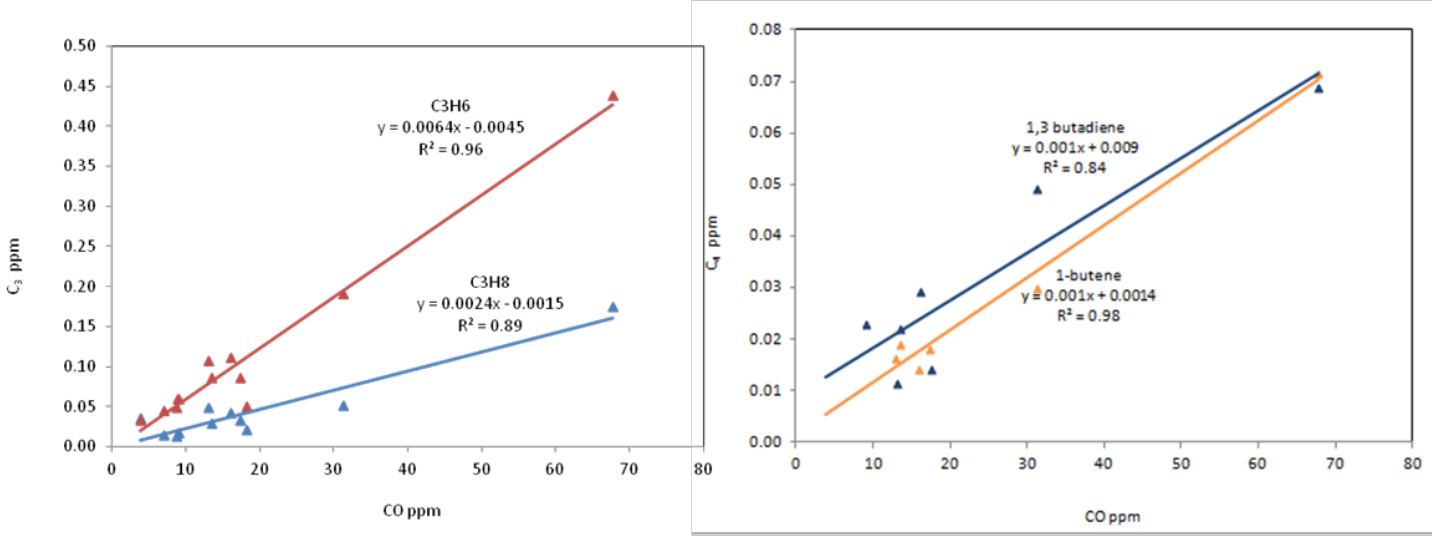

Figure 4-49 Plots of C3 and C4 Hydrocarbons vs. CO

4.2.14 Field Results: Fort Hunter-Liggett

The Fort Hunter-Liggett (FHL) area experienced nine inches of rain about 6 weeks before the prescribed burn. After waiting to deploy and dry weather, the forecast shifted to more rain headed to the area so UCR and the USFS sent their equipment to FHL. Unfortunately with all the rain the live fuel moisture was high and did not burn well enough to generate significant emissions for the instruments on the truck. Some data for wind and $PM_{2.5}$ were collected from the towers and is shown in the following figures. As is evident the $PM_{2.5}$ increased by two orders of magnitude when the plume from the test burn reached the tripod.

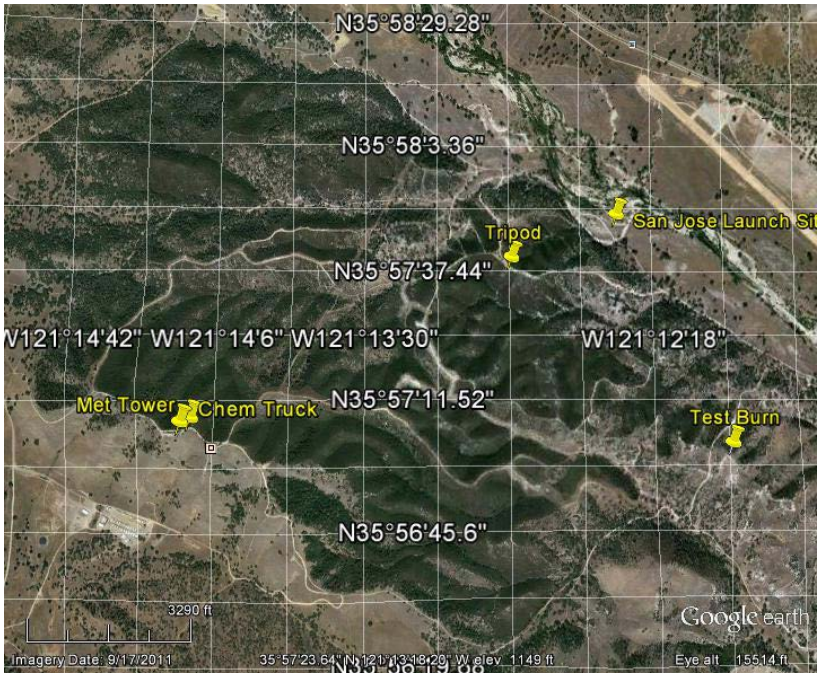

Figure 4-50. Fort Hunter-Liggett Burn Sites and Instrument Location

Figure 4-51. View of the FHL burn area from tower location.

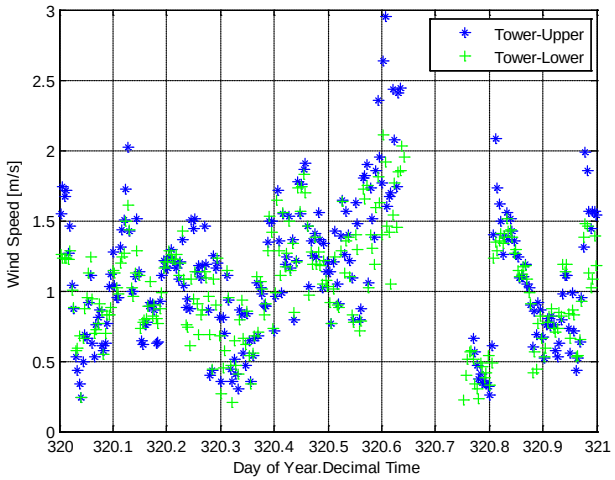

Figure 4-52. Measured Wind Speed at Tower Location at FHL

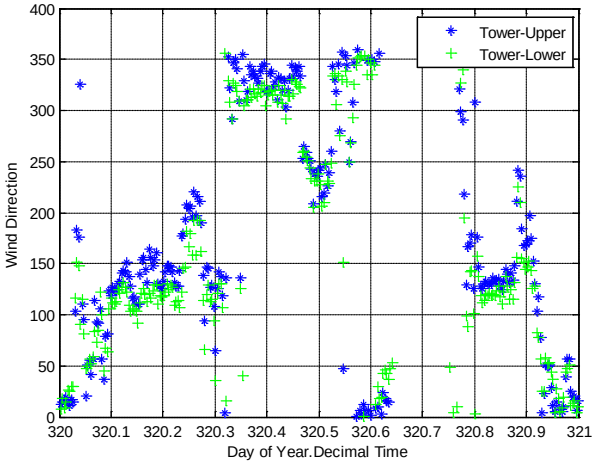

Figure 4-53. Measured Wind Direction at Tower Location at FHL

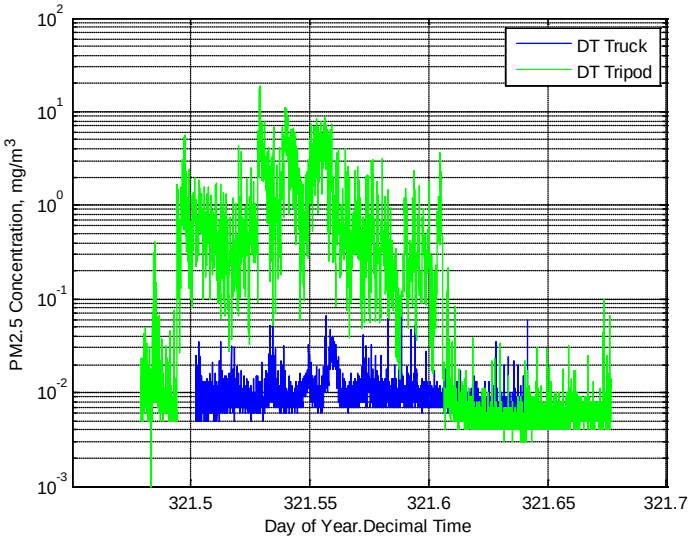

Figure 4-54. Measured PM2.5 Concentration at Truck and Tripod Location at FHL

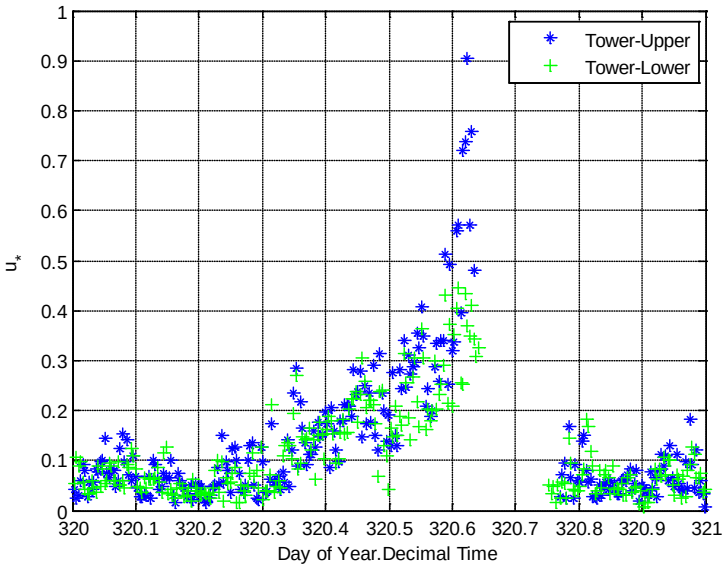

Figure 4-55. Measured Friction Velocity at Tower Location at FHL

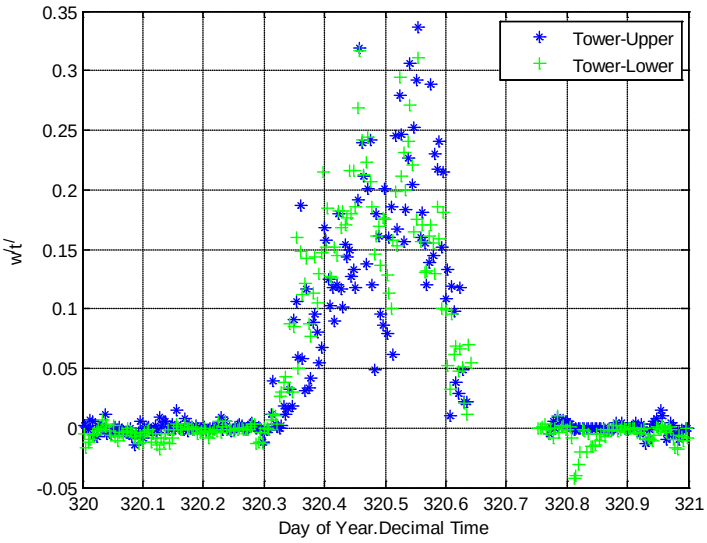

Figure 4-56. Measured kinematic sensible heat flux at tower location at FHL on 11/17/2009.

Instruments located downwind at the tower and tripods detected the emissions from the fire. These data can be used with dispersion modeling to tease out the conditions in the actual fire.

4.2.15 Field Results: Fort Huachuca

UCR deployed a chemistry truck and towers to the FHUA site. Like the FHL site, this site also had wetter than normal rainfall during the winter producing vegetation with higher than desired moisture content. Between weather and other scheduling constraints, the window of opportunity was very narrow and we had only one opportunity to collect data from a prescribed burn. As a consequence of the vegetation moisture content, it was difficult to get the fire to burn continuously and the burn consumed the grass and litter fuels primarily (Table 4-10). Data came from instruments on the towers and is presented below.

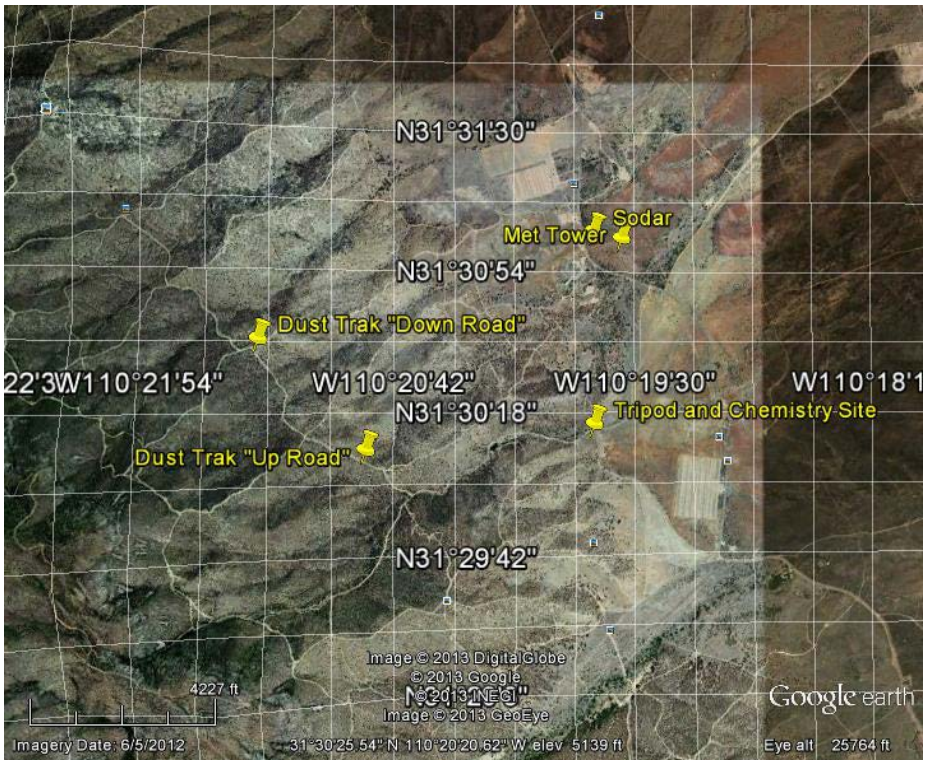

Figure 4-57. Fort Huachuca burn location and measurement sites

Figure 4-58. View of Fort Huachuca Burn Area from Met Tower location.

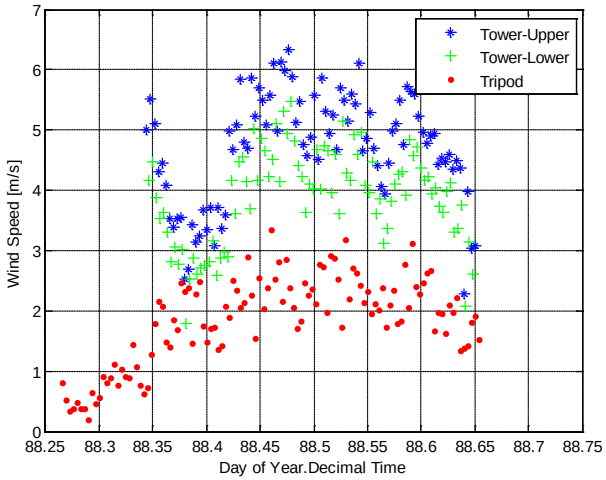

Figure 4-59. Measured Wind Speed at Tower & Tripod location at HUA

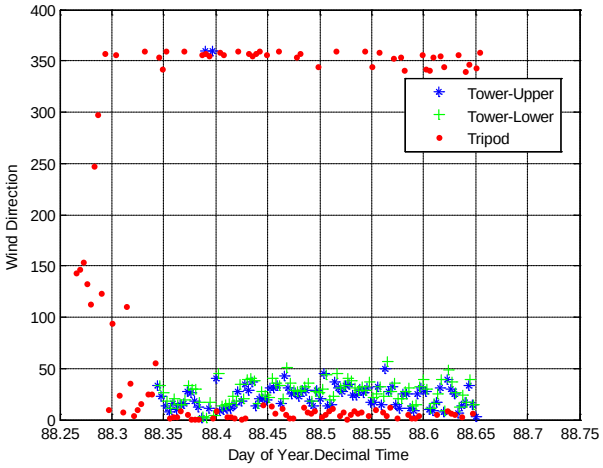

Figure 4-60. Measured Wind Direction at Tower and Tripod location at HUA

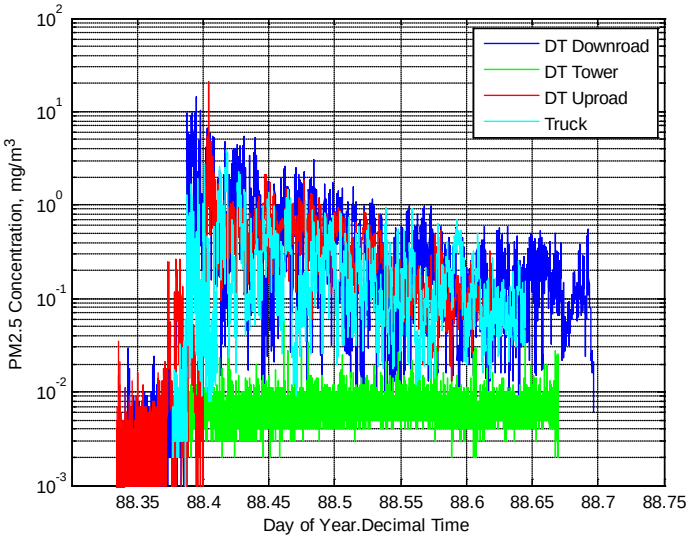

Figure 4-61. $PM_{2.5}$ at Down Road, Tower, Up Road, and Chemistry Truck Locations at HUA

From Figure 4-61 the plume clearly reached those sampling points as the PM concentration increased by 100 times and then slowly decayed back to ambient. Location of the towers, instruments and wind direction are keys when the protocol relies on the wind to carry the emissions from the fire to the sensing instruments. Thus while a significant PM response was recorded at three sites, the fourth site did not show any change in PM levels.

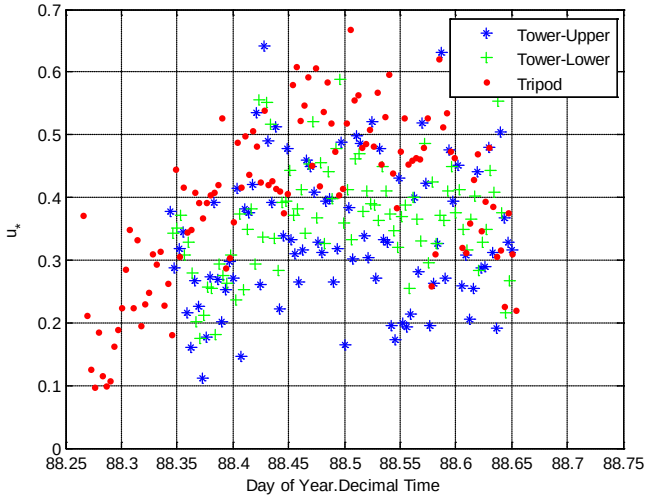

Figure 4-62. Measured Friction Velocity at Tower and Tripod Locations at FH

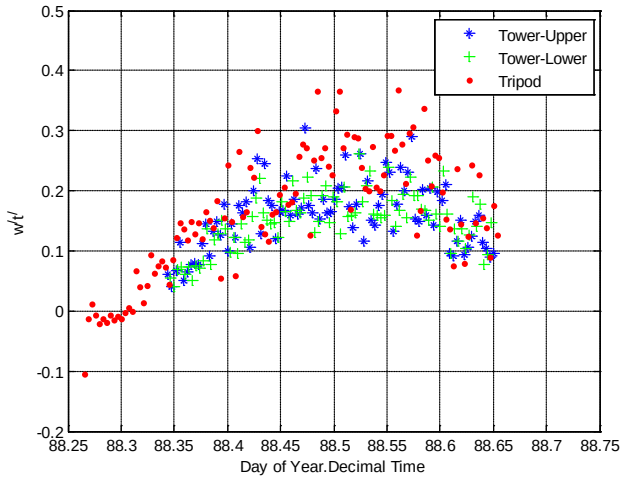

Figure 4-63. Measured Heat Flux at Tower and Tripod Location at FH

4.2.16 Field Results: US Forest Service's FASS towers at Fort Huachuca

At the Fort Huachuca, AZ burn, 4 towers (FASS) were set up: 2 each at locations along a ridge within the burn perimeter. The GPS coordinates of the first two FASS towers (#21, 20) were Lat. 31.505427 N Long. 110.34981 W and the second set (FASS # 22, 27) Lat. 31.501447 N Long. 110.344008 W. The towers were erected to a height of 20 ft. The sampling times were 10 minutes flaming, 10 minutes intermediate, 20 minutes smoldering. One tower (21) did not trigger so was not included in sampling. Tower data follow.

Table 4-36 Tower Data from FASS System at Fort Huachuca

Canister	Tower	Phase	CO	CO_2	CH_4	C_2H_6	C_2H_4	C_2H_2	C_3H_8	C_3H_6	n-butane	t-2 butene	1- butene	isobutene	1,3-butadiene	NMHC	
			Concentration (ppm)														
FC187	20	F	11.9	202	0.65	0.08	0.26	0.08	0.02	0.07			0.01	0.01	0.01	0.54	
FC189	20	I	9.9	117	0.76	0.11	0.20	0.05	0.02	0.06			0.01	0.01	0.01	0.48	
FC205	20	S	6.8	64	0.59	0.08	0.14	0.03	0.02	0.05		0.01	0.01	0.01	0.01	0.36	
FC154	22	F	21.2	399	1.01	0.15	0.42	0.10	0.03	0.11	0.01	0.01	0.02	0.02	0.03	0.89	
FC137	22	I	13.4	176	1.04	0.13	0.24	0.07	0.03	0.08		0.01	0.01	0.01	0.01	0.61	
FC152	22	S	8.4	76	0.83	0.09	0.15	0.04	0.03	0.05		0.01	0.01	0.01	0.01	0.40	
FC136	27	F	12.9	277	0.64	0.10	0.26	0.07	0.02	0.07	0.01		0.01	0.01	0.01	0.57	
FC160	27	I	5.3	119	0.25	0.06	0.13	0.03	0.02	0.04	0.01		0.01	0.01		0.30	
FC167	27	S	16.0	187	1.19	0.16	0.29	0.07	0.04	0.09	0.01	0.01	0.02	0.01	0.01	0.70	
			Emission Factor (g/kg)														
			CO	CO_2	CH_4	C_2H_6	C_2H_4	C_2H_2	C_3H_8	C_3H_6	n-butane	t-2 butene	1- butene	isobutene	1,3-butadiene	NMHC	MCE
FC187	20	F	64.3	1716	2.00	0.49	1.40	0.38	0.16	0.53	0.00	0.00	0.13	0.09	0.16	3.33	0.94
FC189	20	I	89.6	1666	3.92	1.04	1.84	0.42	0.34	0.83	0.00	0.00	0.22	0.15	0.26	5.09	0.92
FC205	20	S	109.8	1624	5.46	1.45	2.28	0.49	0.48	1.16	0.00	0.22	0.36	0.24	0.34	7.02	0.90
FC154	22	F	58.4	1728	1.59	0.43	1.16	0.26	0.14	0.45	0.03	0.06	0.09	0.09	0.17	2.88	0.95
FC137	22	I	81.5	1682	3.61	0.83	1.48	0.41	0.27	0.72	0.00	0.12	0.18	0.18	0.18	4.37	0.93
FC152	22	S	114.4	1616	6.45	1.29	2.00	0.54	0.60	1.04	0.00	0.20	0.27	0.22	0.33	6.48	0.90
FC136	27	F	51.5	1740	1.47	0.41	1.02	0.27	0.16	0.43	0.06	0.00	0.10	0.08	0.11	2.65	0.96
FC160	27	I	49.3	1742	1.31	0.62	1.19	0.29	0.23	0.50	0.12	0.00	0.17	0.16	0.00	3.26	0.96
FC167	27	S	90.6	1666	3.85	0.94	1.62	0.35	0.36	0.76	0.14	0.09	0.19	0.15	0.15	4.75	0.92
			Emission Factor (g/kg)														
		F	58.1	1728	1.69	0.44	1.19	0.31	0.15	0.47	0.03	0.02	0.11	0.09	0.14	2.96	0.95
		I	73.5	1697	2.95	0.83	1.50	0.37	0.28	0.68	0.04	0.04	0.19	0.16	0.15	4.24	0.94
		S	104.9	1635	5.26	1.23	1.96	0.46	0.48	0.98	0.05	0.17	0.28	0.21	0.27	6.08	0.91

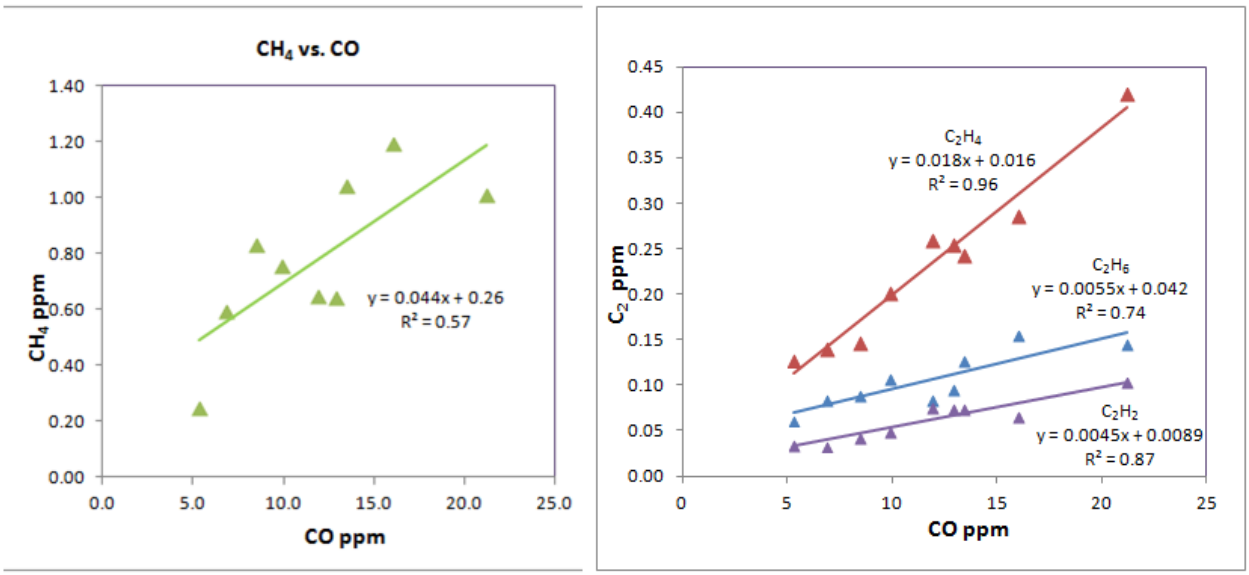

Figure 4-64 Plots of CH4 and C2 Compounds vs. CO

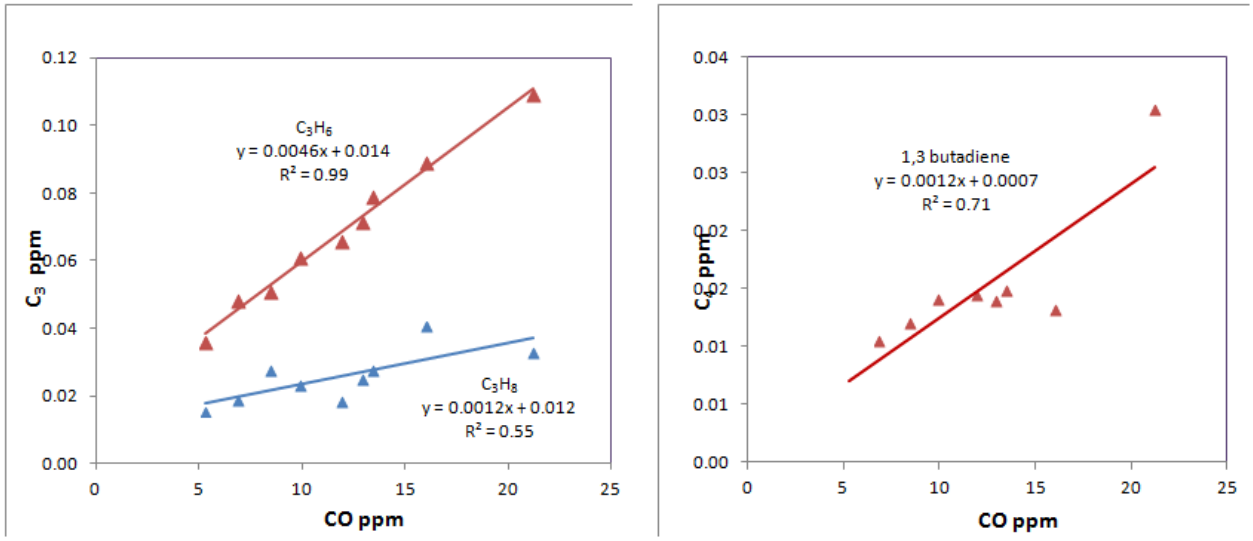

Figure 4-65 Plots of C3 and C4 Compounds vs. CO

The FASS emission factors for CO_2, CO and butadiene were about the same as at Vandenberg but concentrations were lower since the fire was less intense.

4.2.17 Field Results: Ione California

As described in Section 3, the prescribed burn at Ione offered UCR the chance to measure emissions from a very intense chaparral fire and to make the first direct ground-based measurements of black carbon in real-time for chaparral with the MAAP instrument, specifically designed for measuring black carbon. The burn plot was a slope that had not been burned for more than 10 years on which Cal Fire placed fire trucks on the upslope. The trucks had dummies with PPE and imbedded thermocouples. The principal fuel type was chaparral with scattered oak

trees. The fire reached temperatures high enough to melt a portion of the fire truck as evidenced earlier in Figure 3-40. Results show the data collected during the fire.

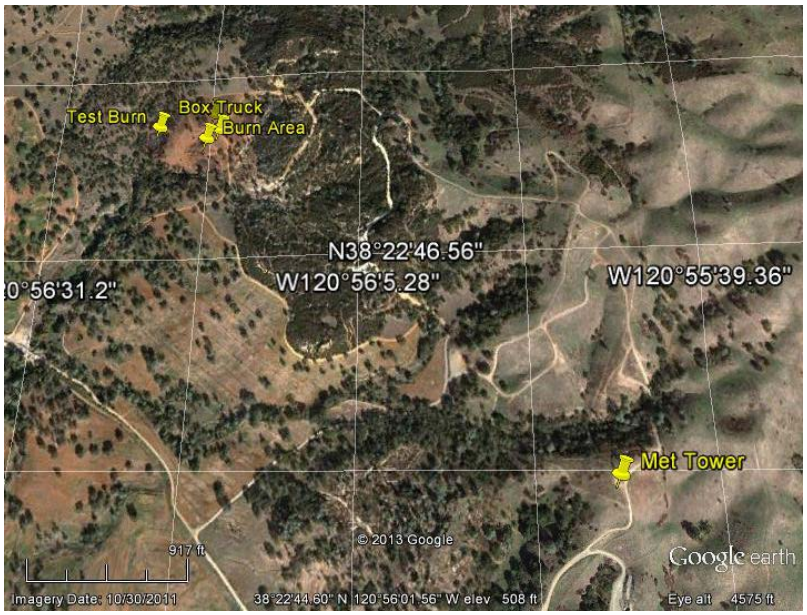

Figure 4-66. Burn and Measurement Sites at Cal Fire Academy, Ione

Chemistry was collected at the box truck as in past field burns. Note the PM levels reached as high as 100mg/m^3 – as compared with a national standard for PM of the annual mean being 12μg/m^3. Thus the instrument was showing instantaneously levels that were 10,000 times the standard, which is probably why the black carbon instrument went off-scale.

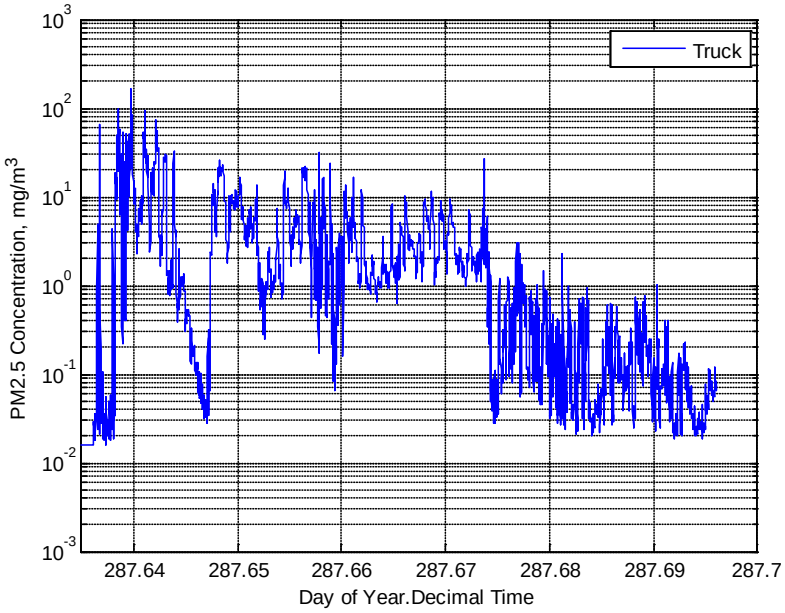

Figure 4-67. Measured $PM_{2.5}$ Concentration at 5m Altitude for Intense Chaparral Prescribed Burn, (Ione, CA)

A number of instruments capable of continuous measurement were positioned on the top of the slope, protected by 1/8 aluminum sheeting and measured PM2.5, black carbon, ozone, NOx, carbon monoxide and carbon dioxide. During the burn, the unprotected plastic cases of instruments were melted.

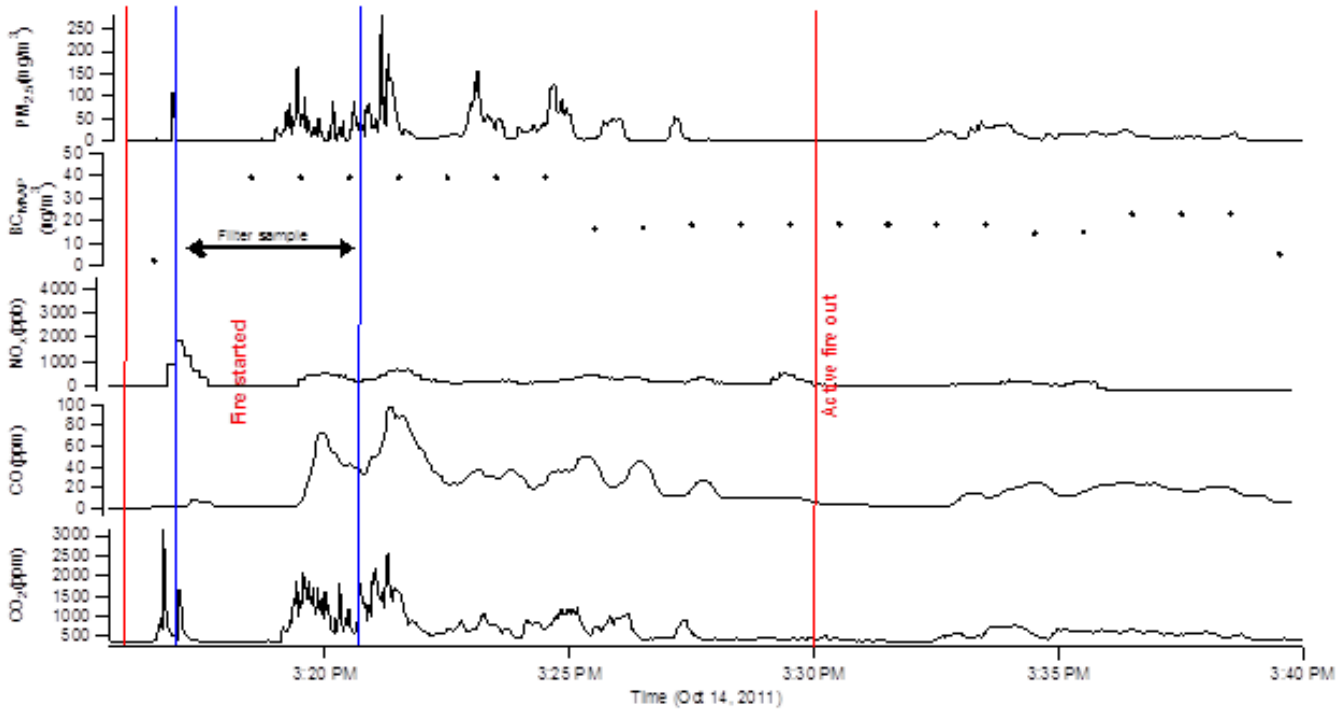

Figure 4-68 Real-time Data for Gases (bottom 3), Black Carbon and $PM_{2.5}$ (top)

Data show:

1. The BC instrument reached its maximum reading at 40µg/m^3 and shut off. These were the highest values seen with this instrument as values closer to 5 were normal in the lab and during the smoldering portion of the laboratory data.
2. The $PM_{2.5}$ reached 250mg/m^3 or 20,000 times the EPA standard. An observation is the BC reached its peak value before the PM values peaked. It took some time to repair the BC instrument before it was reading on scale again as the diagram shows.
3. The NOx values changed only slightly from the ambient which may have to do with scale the instrument was set to.
4. Significant levels of both CO and CO_2 were emitted from the fire simultaneously, different from earlier data that only showed CO_2 in the flaming regime and CO while smoldering. These data might reflect that the fire had both flaming and smoldering taking place simultaneously in different portions of the fuel bed.

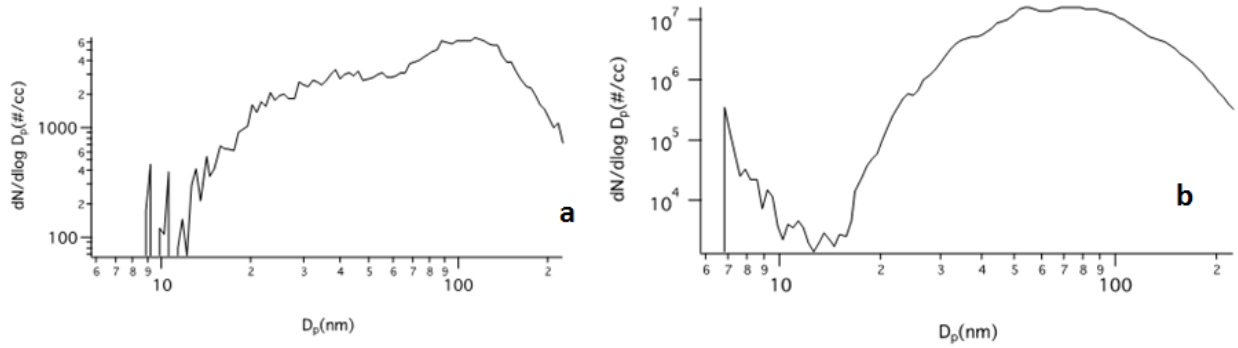

Figure 4-69 Particle Size Data for a) Ambient & b) Rigorous Flaming

Note the SMPs instrument records PM values that are 10,000 greater than ambient levels, a value similar to that seen in the Dust Trak instruments. Also note the PM size is about 70nm or 0.07µm.

Table 4-37 Elemental and Organic Carbon during: 1) Flaming & 2) Smoldering Phases

		Q line		QQ line	
Sample #	**EF TPN**	**EC**	**OC**	**EC**	**OC**
	#/kg CO2	**g/kg CO2**	**g/kg CO2**	**g/kg CO2**	**g/kg CO2**
1	**5.24E+15**	**2.6**	**4.9**	**2.9**	**5.2**
2	**4.73E+15**	**2.3**	**7.3**	**1.6**	**4.1**

One of the interferences in the BC and EC data is the hot fire ignited the tires on the fire trucks and they released copious amounts of BC. Thus we tried to collect the sample before the tires were on fire and to sample close to the smoldering mass; however, there is likely contamination from the tires. In the table above, the EC/OC ratio is significantly different from the lab values as results are rich in EC, perhaps from the tires. Measurements from instruments mounted on the various towers are shown in the following figures.

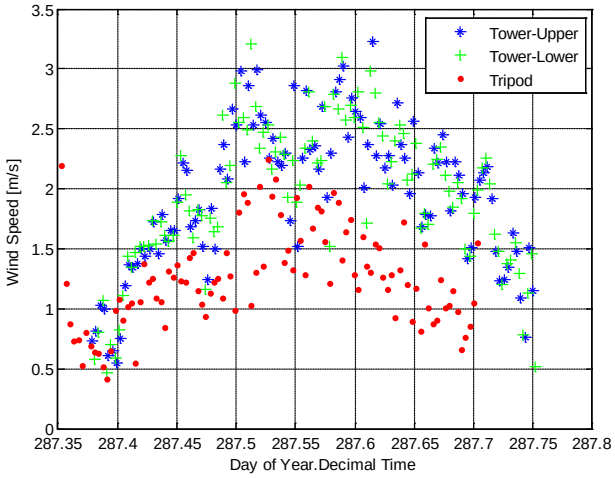

Figure 4-70. Measured Wind Speed at Tower and Tripod Location at Ione

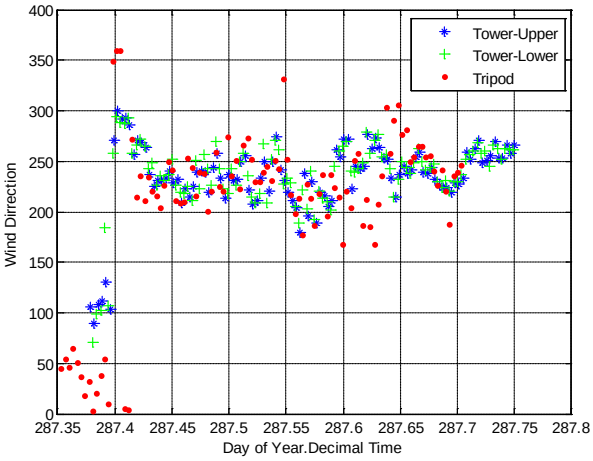

Figure 4-71. Measured Wind Direction at Tower and Tripod Location at Ione

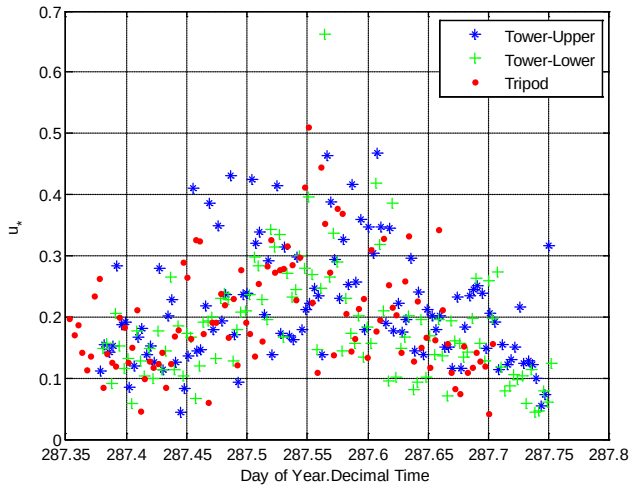

Figure 4-72. Measured Friction Velocity at Tower and Tripod Location at Ione

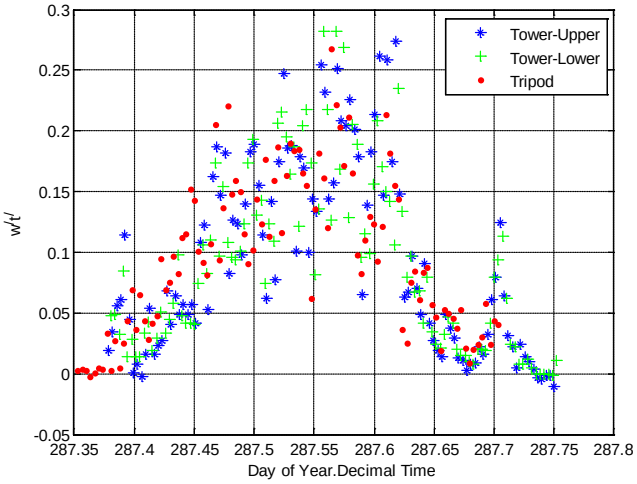

Figure 4-73. Measured Kinematic Sensible Heat Flux at Tower and Tripod Location at Ione

4.2.18 Exploratory Research on Atmospheric Chemistry

One of the elements in the SERDP proposal was to explore the use of an atmospheric reactor to follow the characterization of the emissions from a wild land fires over times much longer than is possible with the reactor platform at MFSL or even by following the emission plumes with an aircraft. MFSL studies are over in minutes and measure only primary emissions, thus providing no information on ozone formation, secondary PM or changes in nature of clouds to form based on aerosol generated in a fire. The benefits from aircraft studies are significant as the plane can follow the plume for a few hours; however, flight time is expensive and limited in time and to daylight hours. The proposed goals were to: 1) study the life cycle of the gases and PM over times longer than possible in MFSL or even in aircraft and 2) study secondary ozone and PM formation. Data for secondary PM are scarce and would be helpful as input into the SOA module for CMAQ. 3) During the Vandenberg studies UCR offered the opportunity to collect data for climate change so a third goal was added, namely, investigating the interactions between the particles and moisture generated by emissions from wildland fires and whether cloud formation was enhanced or diminished.

The atmospheric reactor platform selected for the extended reactions is in Figure 4-74. As is evident the atmospheric reactors allowed control of light intensity, temperature, moisture and a number of other parameters that control atmospheric chemistry. One of the questions investigated with these exploratory studies was whether the laboratory reactors would provide the same information as gathered in the aircraft as the plane followed the plume for 30 or so miles from the fire. If so, then atmospheric reactors should be added to the work carried out by those studying emissions from wildland fires.

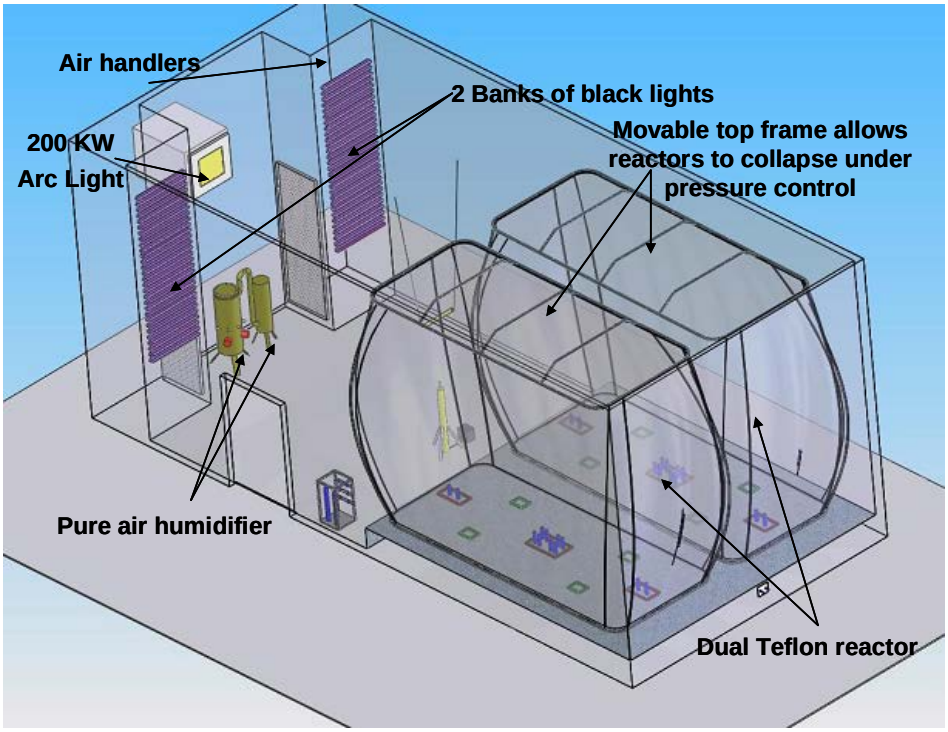

Figure 4-74 Atmospheric Reactor Outfitted with Controlled Conditions

An added element of the work was to build a system that allowed emissions from burning wildland fuels to be injected into the atmospheric reactors at a concentration as dilute as if the air-smoke mixture represented a lofted plume. The proposed design was to burn wildland fuels in a well-ventilated stove with excess oxygen as in nature and then to suck a portion of the exhaust with an injector system into a line that carried the emissions to the bags for subsequent research studies. Figure 4-75 shows the final system that was built.

Figure 4-75 Fuel Burner & Injector System for Conveying Emissions to Atmospheric Reactors

The goals of following atmospheric chemistry pathways and cloud formation required a complex system of reactor design, on-line monitoring instruments and offline analyses. The final system is shown in Figure 4-76.

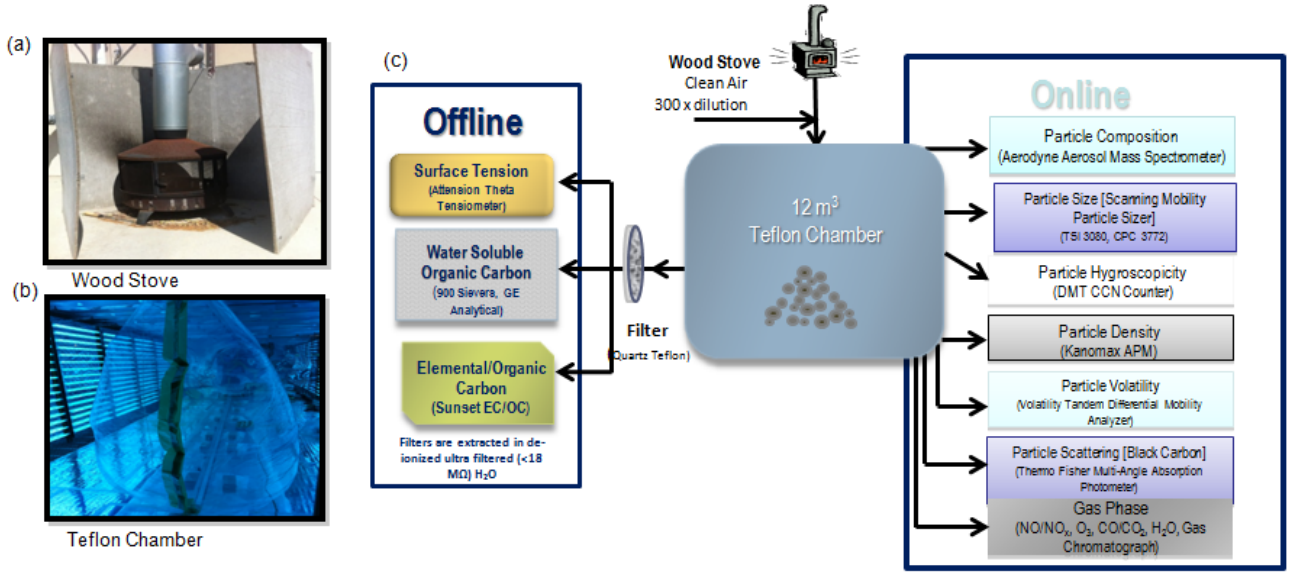

Experimental Set up. Fuel is burned in a wood stove (a) and introduced into the chamber under dilute conditions (b). On and Offline measurement techniques are used to characterize the gas and particulate phase chemical composition and physical properties.

Figure 4-76 Setup for Study of Primary and Secondary PM from Biomass Burning

Some results from the atmospheric reactor studies are shown in the following figures. Figure 4-77 shows some interesting findings. In Figure-77a, the results show that ozone only forms when the mixture of biomass gases and aerosol are exposed to light, as expected. Furthermore plotting the ratio of ozone to carbon monoxide shows similar response for both the laboratory and field data observed with the airplane. These results replicate that ozone is not be formed without sunlight and that atmospheric reactors can play a role in understanding the reaction pathways from the emissions of wildland fires for the chemistry in the plumes in the hours after leaving the fire location.

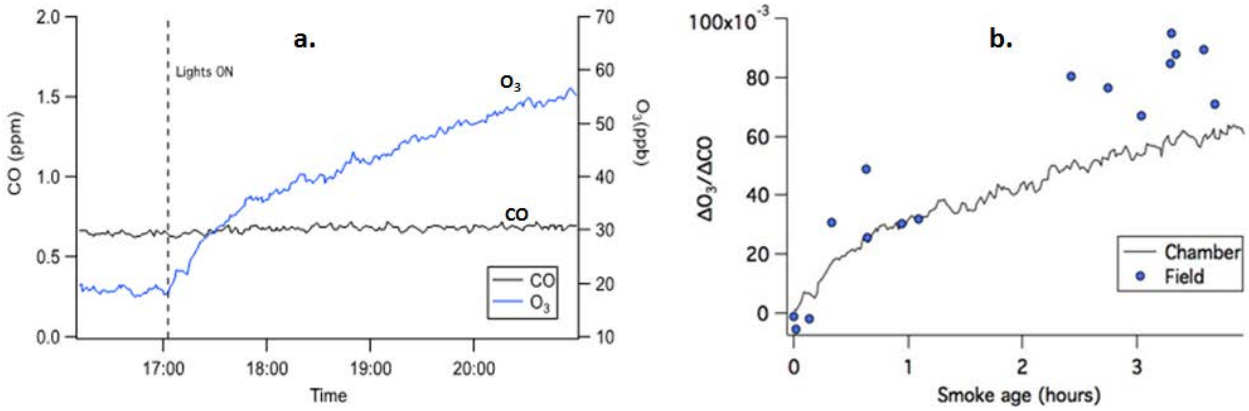

Figure 4-77 a) Ozone Increases with Time b) Lab vs. Aircraft Plume

Other measurements with an SMPS indicated that particle number grew only when the lights were on, similar to the finding for ozone. The results are shown in Figure 4-78.

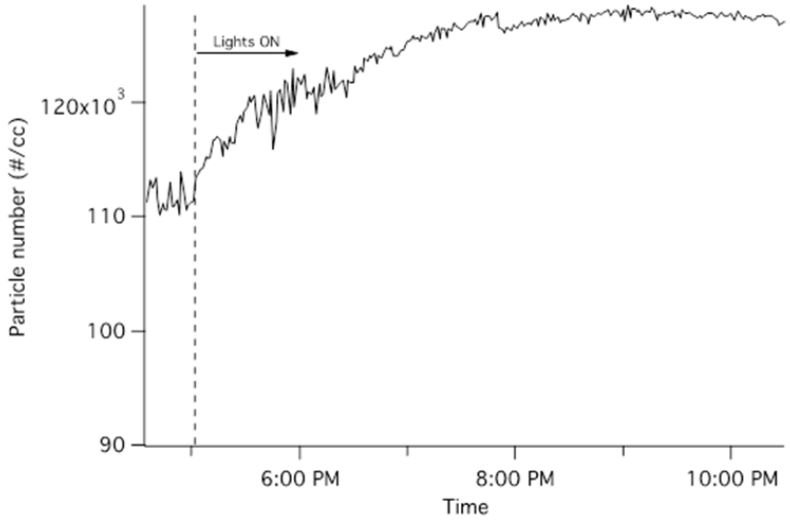

Figure 4-78 Particle Number Increases during Aging Process with Sunlight

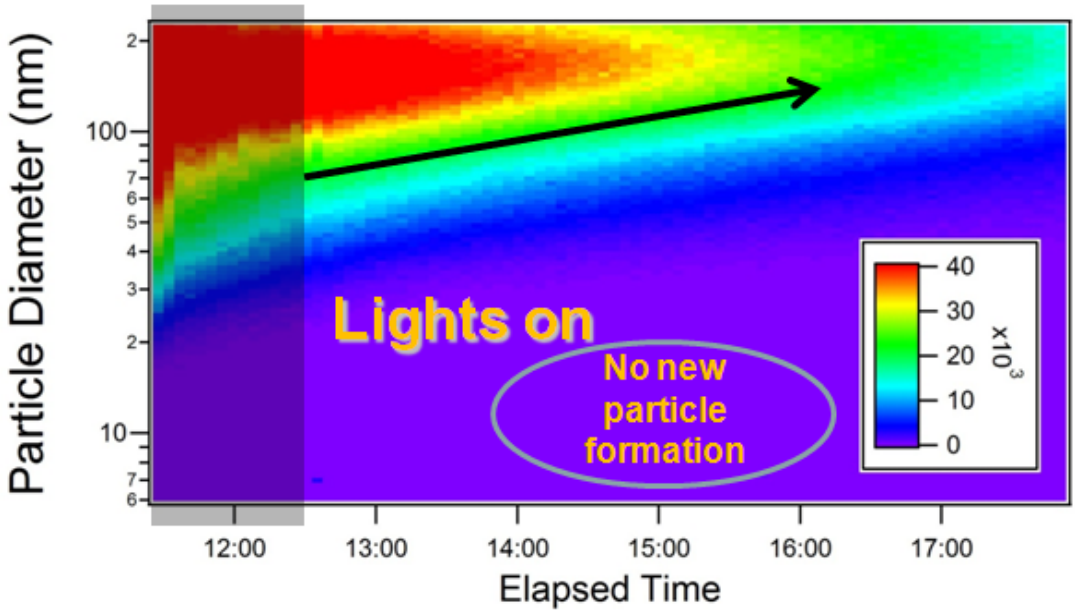

Figure 4-79 Extended Studies on Nature of PM

Further results showed that while the number of particles may initially grow that over the longer times it was growth in particle diameter via coagulation mechanisms that was more important than the growth in particle number. Thus particulate number losses occurred through both the accumulation mode as well as to the walls.

After filing the atmospheric reactor with gases and aerosol generated from burning the wildland fuels, we followed the changes in the solid and organic particulate matter for hours with the AMS instrument and filter samples. Two issues were of interest. One was the lifetime history of organic aerosols after a plume left a fire area as these data cannot be learned from the burns at MFSL given their short time. Understanding the lifetime is of critical importance to people living downwind of fires. Furthermore data on lifetime history of organic species are scarce and especially the development of secondary PM as a result of the atmospheric chemistry. Results from the AMS in Figure 4-80 show the mass concentration of the organic component of the aerosol increases with time. Correction of wall losses can be gained from the decline in the organic matter of the filter samples.

The second issue was how the BC and EC compare as EC is often used as a surrogate for BC and vary with time. Results from the filter samples show that the BC and EC remain approximately constant over time and that the measured BC concentration was higher than the EC measurement for the low levels seen in this test.

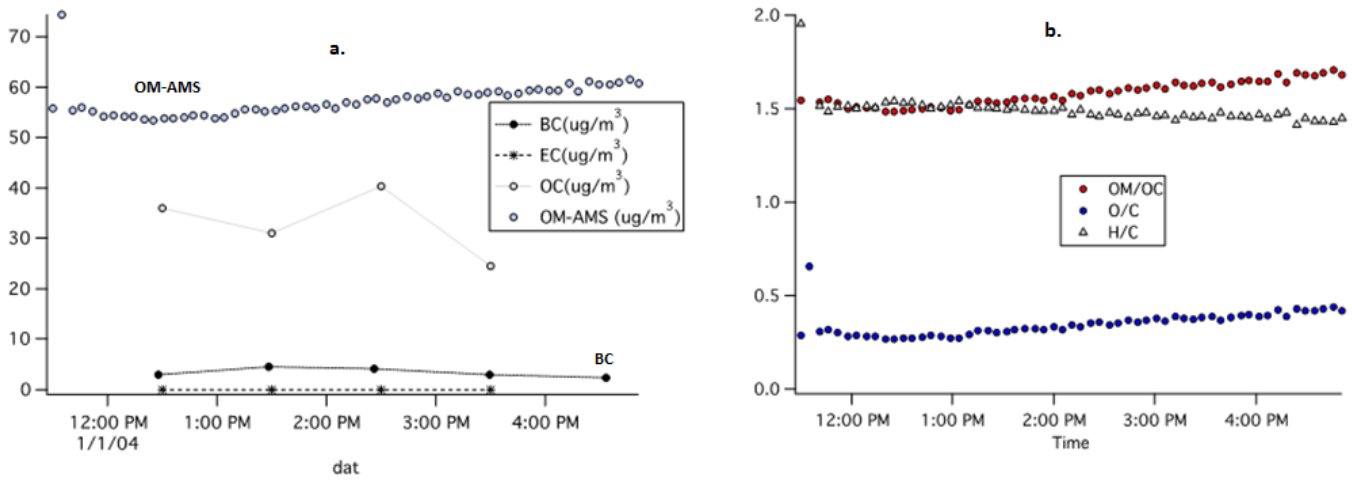

Figure 4-80 Aerosol Evolution during Aging Process, uncorrected for Wall Loses

The plots on the right are all AMS data and show various metrics over time for ratios that are normally followed during atmospheric reactions. These values provide insight into the elemental composition of the aerosol and the changes over time.

The added research topic investigated the interaction of moisture with the aerosol from wildland fires. These data are shown in Figure 4-81. Again we see the nature of the interaction changes are the sun/UV lights are activated. The measure of hygroscopicity is Kappa and the nature of the interaction changes from looking like a (NH4)2SO4 and wetting easily to that of an organic aerosol that does not wet. Further study is required to understand this finding further.

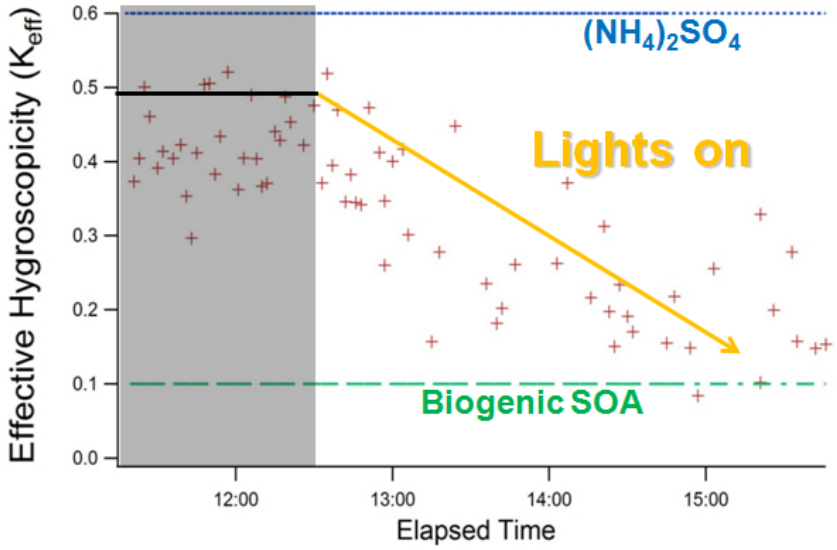

Figure 4-81 Hygroscopicity of Aerosol from Wildland Fires

Data from the exploratory studies were encouraging. What started as an exploratory project with SERDP funding has continued as a project by Dr. Asa-Awuku and her PhD student with outside funding.

4.2.19 Coupling field and lab measurements to estimate emission factors

A question asked by the project's Scientific Advisory Committee was: How relevant were the lab data to the planned prescribed burns in the real world? A final synthesis paper (Yokelson et al, 2013) reviewed both laboratory and field data with the goal of answering their question. The abstract of the article follows.

"An extensive program of experiments focused on biomass burning emissions began with a laboratory phase in which vegetative fuels commonly consumed in prescribed fires were collected in the southeastern and southwestern US and burned in a series of 71 fires at the US Forest Service Fire Sciences Laboratory in Missoula, Montana. The particulate matter (PM2.5) emissions were measured by gravimetric filter sampling with subsequent analysis for elemental carbon (EC), organic carbon (OC), and 38 elements. The trace gas emissions were measured by an open-path Fourier transform infrared (OP-FTIR) spectrometer, proton-transfer-reaction mass spectrometry (PTRMS), proton-transfer ion-trap mass spectrometry (PIT-MS), negative-ion proton-transfer chemical-ionization mass spectrometry (NI-PT-CIMS), and gas chromatography with MS detection (GC-MS). 204 trace gas species (mostly non-methane organic compounds (NMOC)) were identified and quantified with the above instruments. Many of the 182 species quantified by the GC-MS have rarely, if ever, been measured in smoke before. An additional 153 significant peaks in the unit mass resolution mass spectra were quantified, but either could not be identified or most of the signal at that molecular mass was unaccounted for by identifiable species.

In a second, "field" phase of this program, airborne and ground-based measurements were made of the emissions from prescribed fires that were mostly located in the same land management units where the fuels for the lab fires were collected. A broad variety, but smaller number of species (21 trace gas species and PM2.5) was measured on 14 fires in chaparral and oak savanna in the southwestern US, as well as pine forest understory in the southeastern US and Sierra Nevada mountains of California. The field measurements of emission factors (EF) are useful both for modeling and to examine the representativeness of our lab fire EF. The lab EF/field EF ratio for the pine understory fuels was not statistically different from one, on average. However, our lab EF for "smoldering compounds" emitted from the semiarid shrub land fuels should likely be increased by a factor of ~2.7 to better represent field fires. Based on the lab/field comparison, we present emission factors for 357 pyrogenic species (including unidentified species) for 4 broad fuel types: pine understory, semiarid shrub lands, coniferous canopy, and organic soil.

To our knowledge this is the most comprehensive measurement of biomass burning emissions to date and it should enable improved representation of smoke composition in atmospheric models. The results support a recent estimate of global NMOC emissions from biomass burning that is much higher than widely used estimates and they provide important insights into the nature of smoke. 31–72% of the mass of gas-phase NMOC species was attributed to species that we could not identify. These unidentified species are not represented in most models, but some provision should be made for the fact that they will react in the atmosphere. In addition, the total mass of gas-phase NMOC divided by the mass of co-emitted PM2.5 averaged about three (range ~2.0–8.7). About 35–64% of the NMOC were likely semi-volatile or of intermediate volatility. Thus, the gas-phase NMOC represent a large reservoir of potential precursors for secondary formation of ozone and organic aerosol. For the single lab fire in organic soil about 28% of the emitted carbon was present as gas-phase NMOC and ~72% of the mass of these NMOC was unidentified, highlighting the need to learn more about the emissions from smoldering organic

soils. The mass ratio of total NMOC to "NOx as NO" ranged from 11 to 267, indicating that NOx-limited O_3 production would be common in evolving biomass burning plumes. The fuel consumption per unit area was 7.0±2.3Mgha^{-1} and 7.7±3.7Mgha^{-1} for pine-understory and semiarid shrubland prescribed fires, respectively." (Yokelson, et al., 2013).

4.3 Predict Air Quality for Prescribed Burns

This section of the work was aimed at providing an air quality model so DoD sites can calculate the emission impact of criteria and other pollutants on local and regional air quality from prescribed burns. As mentioned in the earlier section the most quantitative tool would be U.S. EPA's Community Multi-scale Air Quality (CMAQ) Model as it is recognized as a powerful computational tool to predict air quality given weather and emissions scenarios, like a prescribed burn. However, the model is complex and requires considerable expertise to run. During the project the lead PI moved to the US EPA and was less available. Notwithstanding the PI leaving, the project took on some tasks that might be more important to the DoD clients.

Table 4-38 List of Tasks for the Air Quality Modeling Area

1	Explore model sensitivity to input of total emissions, emission speciation and plume rise.
2	Validate model performance with new data from controlled burns.
3	Model impact of marine air on emissions.
4	*Compare AQ results using fire emissions from Bluesky framework and SMARTFIRE*
5	*Air quality modeling with CMAQ v4.7 & v5.0*

4.3.1 Model sensitivity to total emissions and plume rise

With the PI leaving extensive sensitivity studies were not undertaken as originally envisioned but a qualitative indication can be gleamed from the air quality modeling carried out in sub-Task 5. As will be learned from sub-Task 5, the air field and met data in that area was complex and contributed more to the outcome than sensitivity of the convective forces in the plume rise and emissions. Basically the perturbations caused by the prescribed burn were small as compared with the established emission and met fields.

4.3.2 Model impact of marine air on emissions.

Early in the project there was a discussion of allocating new resources to the study of air quality near marine environments, specifically as many military facilities are near oceans and the question was raised whether the salt in the marine air would be a significant parameter in the changing the outcome of the local air quality. CMAQ is a tool that allows one to calculate the outcome of a changed scenario, for example, changing from marine air to non-marine air.

The Modeling group applied CMAQ v4.5 with its upgraded aerosol module to handle sea salt in 'aero4' as CMAQ now included fine equilibrium ($PM_{2.5}$) and a non-interactive coarse mode. The results were presented in a SERDP IPR as outlined below.

- Objective: Use existing air quality model data sets to evaluate sensitivity of air pollutants to sea salt in combination with emissions from fires.
- Approach: Use CMAQ air quality model developed for regional visibility study:

  - Extensive fire emissions data base developed by Western Regional Air Partnership for wild fires, prescribed burning and agricultural burning.

- Method
  - Perform base CMAQ simulation including fire and sea salt emissions.
  - Perform sensitivity CMAQ simulation with no sea salt
  - Evaluate differences between the two cases for ozone and secondary fine particulates for areas in which fire emissions were present.
- Results
  - Ozone and other secondary pollutants were insensitive to change in sea salt emissions.
  - Model does not perform well for sea salt aerosols.

Thus the conclusion of the research on the sensitivity of model output to marine air and sea salt indicated the changes were so small that the system was insensitive to the presence of sea salt in the air. Thus mounting an additional major research project to focus on the air quality near marine sources was secondary to models that considered the local air quality to prescribed burns.

4.3.3 Comparison of Fire emissions with BlueSsky and SMARTFIRE models

While BlueSky and SMARTFIRE were not in the original proposal, given their increasing importance in the prediction world, it seemed prudent to examine these options. Thus RC-1648 proposed at the IPR that a portion of the AQ modeling resources be dedicated to reviewing the output of the BlueSky framework and SMARTFIRE using the prescribed burn at Vandenberg AFB as a case study. The approach was accepted with these input data.

- Meteorological Modeling: WRF v.3.3
- Emissions Processing
  - Based on EPA-2002 NEI platform
  - Field data from Vandenberg
  - Fire emissions processed through BlueSky Framework & SMARTFIRE
- Air Quality Model :CMAQ v.4.5

Slides from the IPR follow with results as the findings were presented at the Ninth Symposium on Fire and Forest Meteorology but not published. The first slides present the input data to the models and later slides show the output results.

WRF Domains & Physics

Physics, dynamics & BC conditions	NARR
# vertical layers	38
Grid sizes (km)	36 / 12 / 04 / 1.33
# of grid cells	(70, 94) / (73, 97) / (133, 145) / (211, 229)
Microphysics	WRF single-moment 3-class scheme
Cumulus param	Grell-Devenyi Ensemble Scheme
PBL	Mellor-Yamada-Janic Scheme
Surface layer	Monin-Obukhov Janic scheme
Long-wave radiation	RRTM
Short-wave radiation	Dudhia
LSM	NOAH
fdda	analysis for 36 & 12; obs for 04 & 1.33

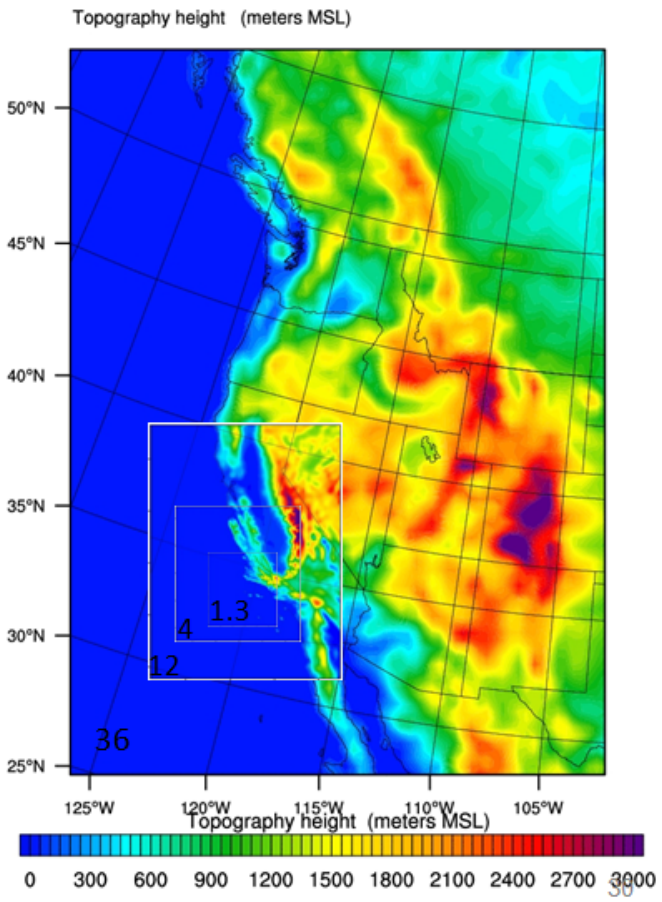

Figure 4-82 Model Setup for the Vandenberg Case Study

The next slide shows the met fields and weather data that was present during the prescribed burn. One of the observations was the hilly terrain near VAF made the representation of the fluid flow (winds) more difficult. These are shown in the next figure.

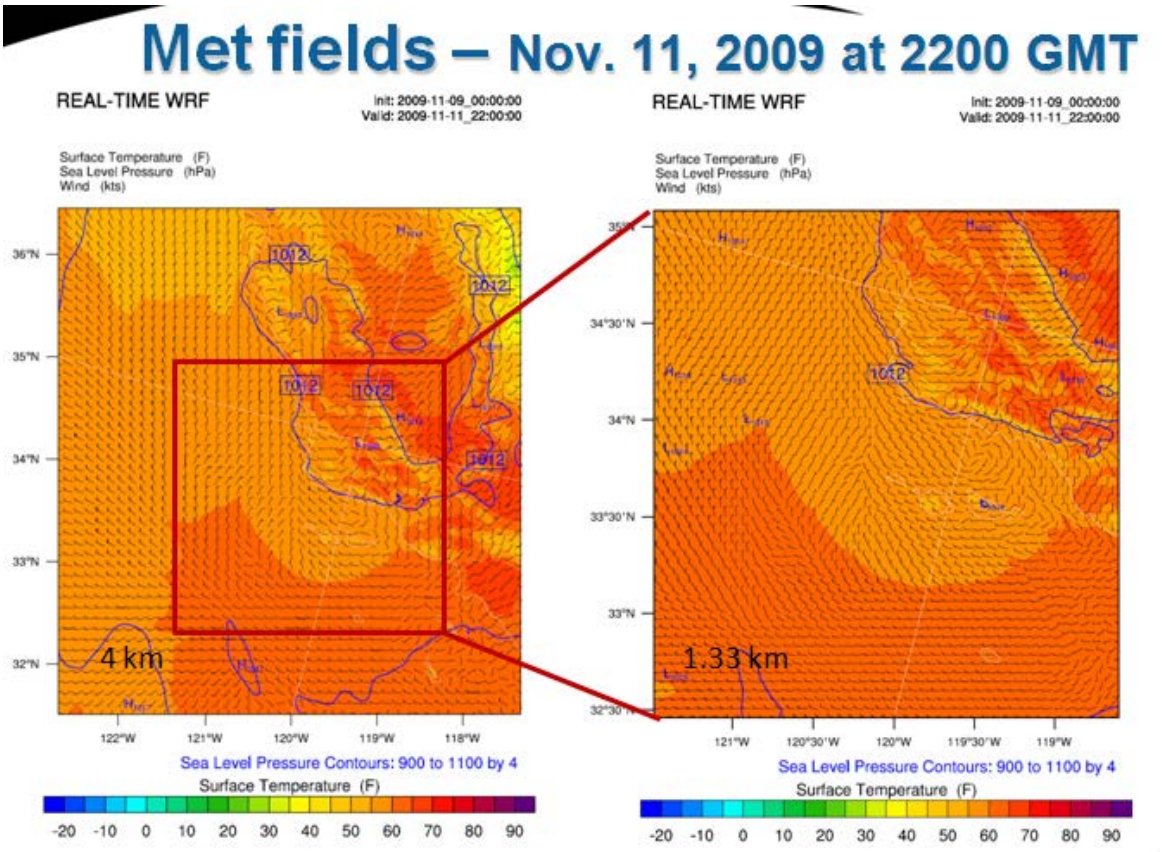

Figure 4-83 Weather Data during the Prescribed Burn

BlueSky Framework

- Input data collected from field study
- Feed into the CONSUME v3.0 stand alone model
- Run BlueSky framework
- Create SMOKE-ready fire emissions
- SMOKE
  - ♦ spatially allocate
  - ♦ speciate VOC

SMARTFIRE

- Obtain directly from STI
  - ♦ Use algorithm (satellite & ICS209 ground report) to generate SMOKE-ready fire emissions
- SMOKE
  - ♦ spatially allocate
  - ♦ speciate VOC
- **Note:** *SMOKE = Sparse Matrix Operator Kernel Emissions*

Figure 4-84 Approach Used for BlueSky and SMARTFIRE Emission Models

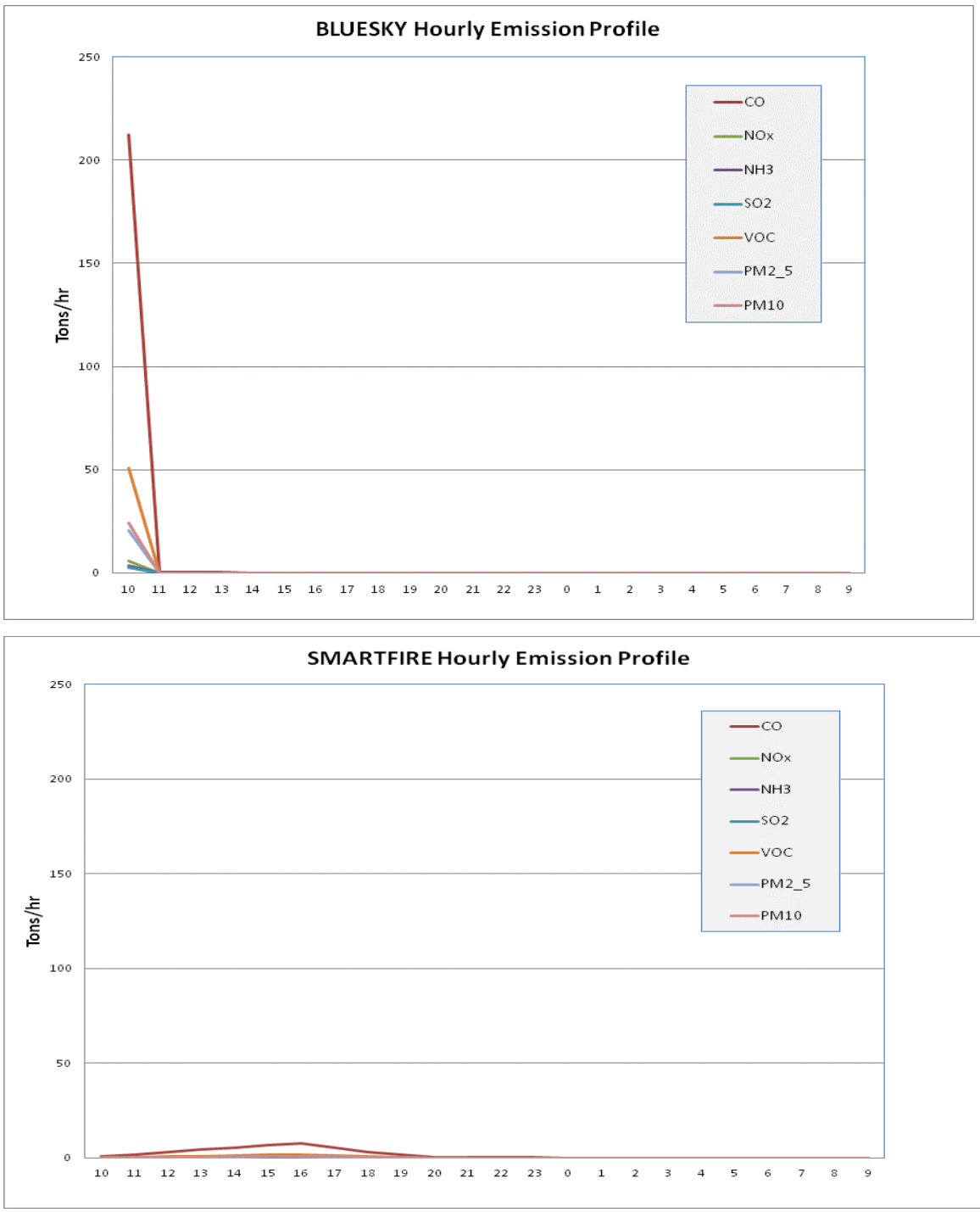

Figure 4-85 Charts Show Emission Rates Used in the BlueSky & SMARTFIRE Models

From Figure 4-85, it is clear that the emissions added to the two models varied in magnitude and in rate. For example, BlueSky added all the emissions at 1100 hours and for SMARTFIRE the emission peaked at about 1600 hours. The model output is sensitive to the magnitude and rate at which emissions are added as will be seen later.

Pollutant	BlueSky Framework (tons)	SMARTFIRE (tons)
CO	213.84	41.10
NO_x	5.83	1.15
NH_3	3.57	0.69
SO_2	2.50	0.49
VOC	51.26	9.86
$PM_{2.5}$	20.64	3.99
PM_{10}	24.36	4.70

Table 4-39 Total Tons of Emissions used in the Modeling

While the charts in Figure 4-85 show the rate in tons per hour at which the emissions added to each model, Table 4-39 shows the total added. The differences between BlueSky and SMARTFIRE in the amount of emissions are significant as are the rates at which the emissions entered the air basin. These differences caused the model output to have significantly different values for ozone and PM over time as the next figures show.

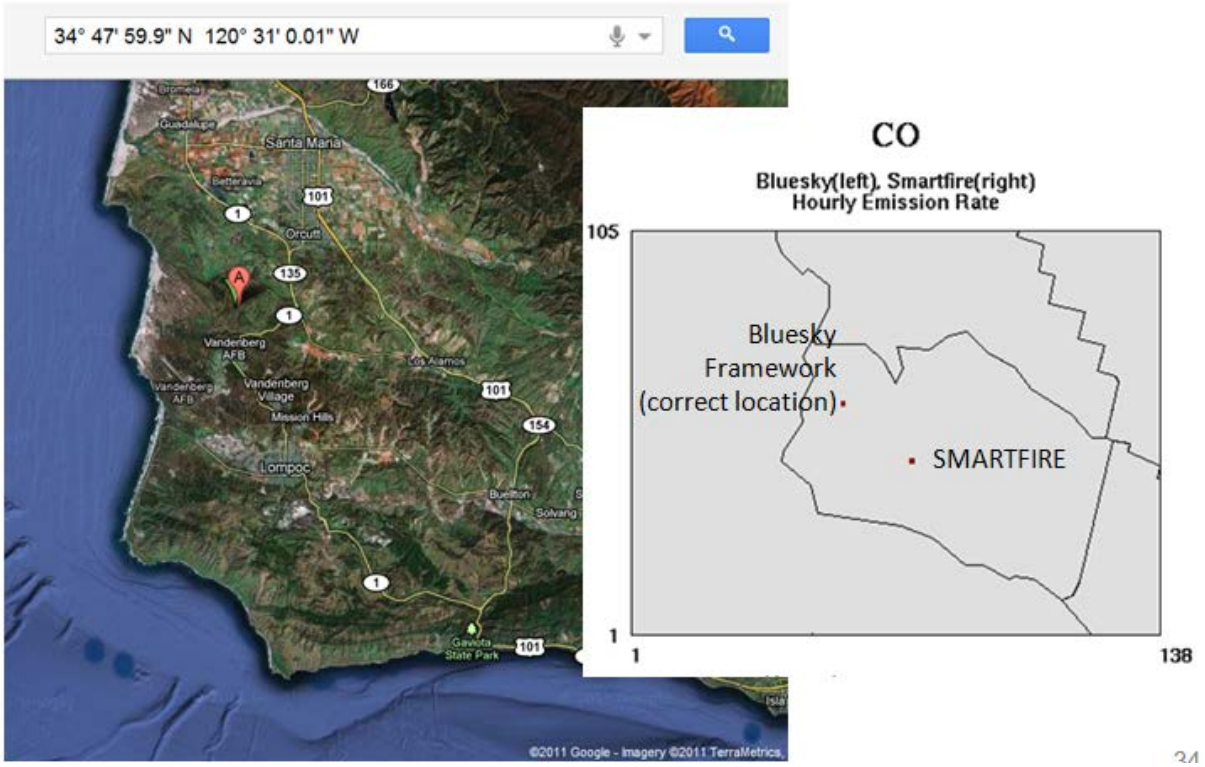

Figure 4-86 Location of Fire ..Note: SMARTFIRE Location Error

Figure 4-86 shows the location of the fire based on the protocol for each method. Note that the satellite inaccurately located the Vandenberg AFB fire on that date. Vandenberg was considerably to the Northwest. Several runs were made including a baseline run in which there was no fire.

- Base case simulation with no fire
- Simulations using current fire emissions factors
  - BlueSky Framework (based on project study)
  - SMARTFIRE
- Evaluate the model performance for these 3 cases using observations during the fire.
- Based on the model performance results,
  - make additional changes in the emissions data to further improve model performance, and
  - do a final model performance evaluation.

Figure 4-87 Air Quality Modeling Approach

Now in addition to differences in the flux of emissions added to the basin there was an error in location that also changed the model output as seen in the sequence of slides to follow.

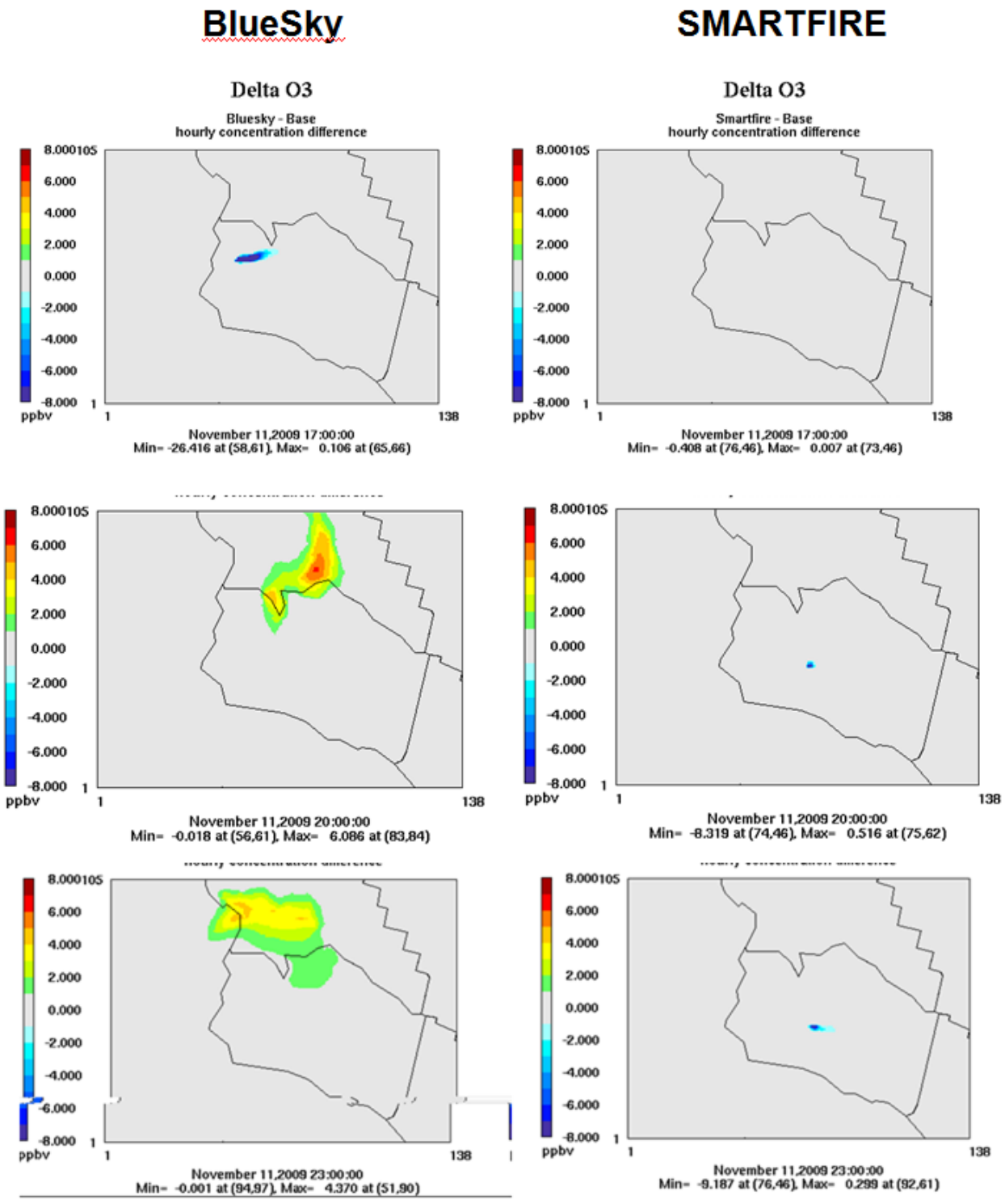

Figure 4-88 Ozone Concentration for BlueSky and SMARTFIRE at Three Times

Notwithstanding the wrong location for SMARTFIRE, the ozone concentrations as a function of time differed substantially between the two models approach, BlueSky and SMARTFIRE. This outcome was expected based on the magnitude and rate of emissions added to the air basin. PM time behavior is shown in the next sequence.

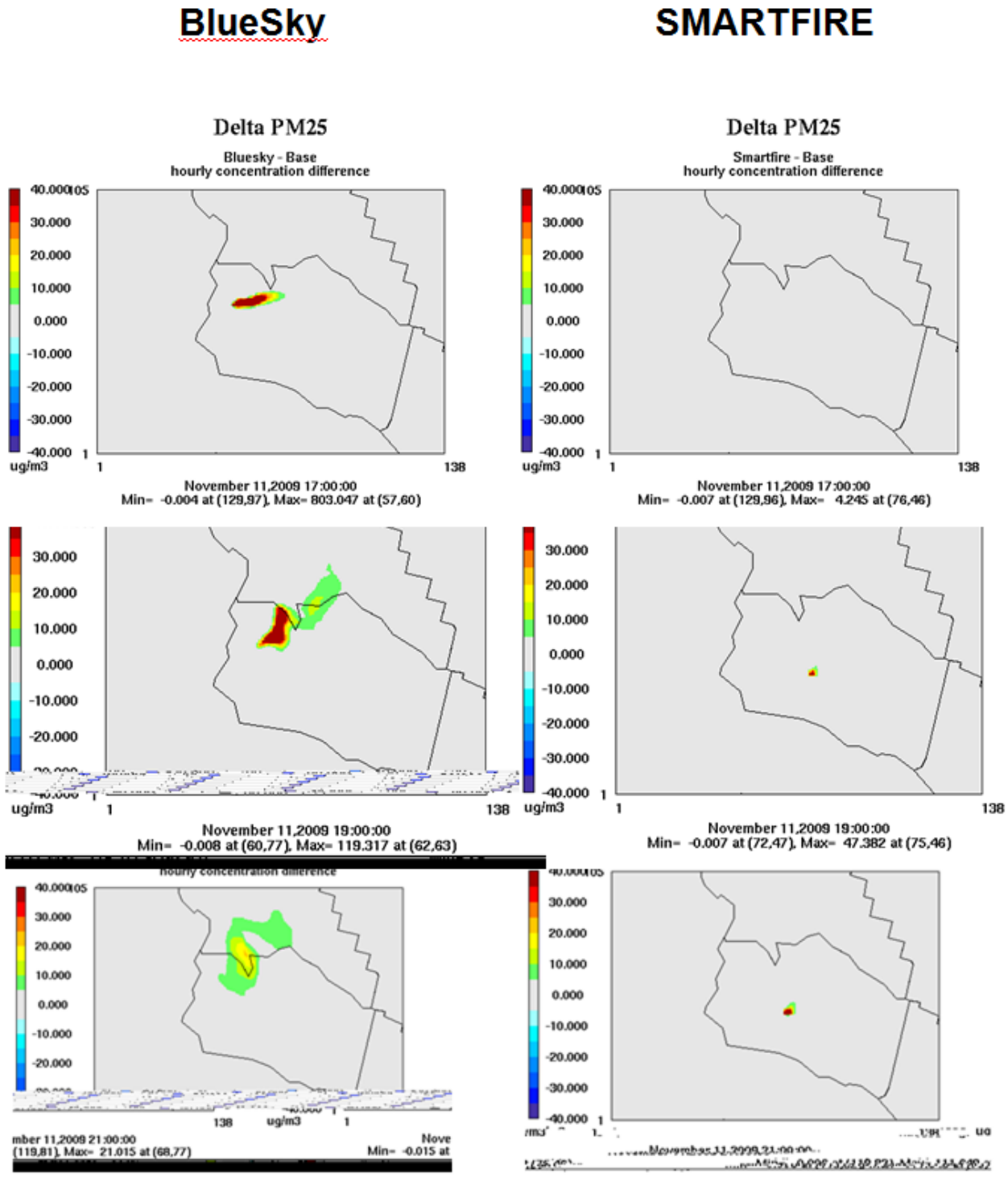

Figure 4-89 $PM_{2.5}$ Concentration Output from BlueSky & SMARTFIRE

Not surprisingly, Figure 4-89 shows the same significant differences in the fine PM ($PM_{2.5}$) modeling as we found for the ozone. Recall that BlueSky used 20.6 tons of fine PM entering the air space as compared with 3.99 tons for SMARTFIRE.

Taken in total the results for this case study showed the BlueSky model was far superior to SMARTFIRE, starting with emissions input into the models, a key driver of the output. Also the location in SMARTFIRE was far to the southeast of the actual fire. The overall observations from this modeling comparison:

- The weather modeling, WRF, was a challenge given the complex terrain near Vandenberg. .
- Placement, emissions amounts and rates significantly affects air quality model predictions. SMARTFIRE location was erroneous
- Using different emission factor inputs, BlueSky Framework generates different hourly emissions rate values.
- Emissions Profiles
    - ♦ BlueSky Framework: Large majority, > 90%, of emissions occurred in early hours (1-2) of fire
    - ♦ SMARTFIRE: Peak emissions occurred later in fire event

4.3.4 Air quality modeling with CMAQ for prescribed burns

In the last task we planned to compare the output of CMAQ v4.7 for the prescribed burn at Vandenberg AFB. Results of the multiple runs of the CMAQ model are presented in Appendix 7 as a series of charts.

In the first series of figures are eighteen input chemicals added to the air basin at 10AM at the start of the prescribed burn to the inventory of chemicals already present in the basin. Note that the model only allowed the addition of chemicals on the hour in a lump sum rather than continuously add emissions in the way that the fire actually burns. Furthermore in the model used, emissions can only be added on the hour even if the fire started on the half-hour.

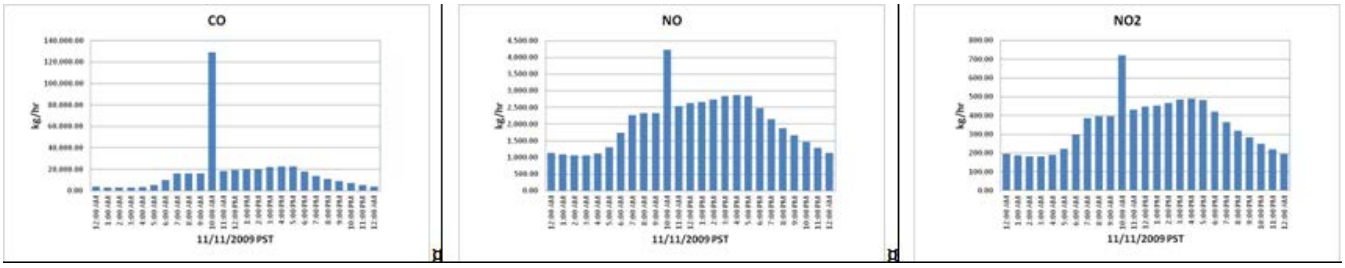

Figure 4-90 Sample Input of Emissions from Prescribed Burn

The second series of charts present CMAQ output for the hourly spatial concentrations near Vandenberg at three different vertical layers between 10am to 2pm PST as a result of the prescribed burn. The altitudes covered were 40 meters, 230 meters and 800meters. Figure 2 was followed by hourly spatial concentrations at three different vertical layers between 10am to 2pm PST for:

1) Carbon monoxide
2) NOx,
3) Ozone,
4) Formaldehyde,
5) Nitrous acid,
6) Particulate organic carbon,
7) Particulate elemental carbon,
8) Particulate sulfate,
9) Particulate nitrate,
10) Particulate ammonia, and
11) Fine particulate ($PM_{2.5}$)

NOx¤	Layer·1·(~40m)¤	Layer·5·(~230m)¤	Layer·10·(~800m)¤
10·am¤	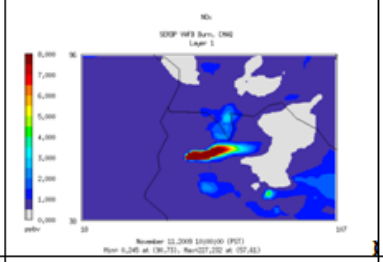	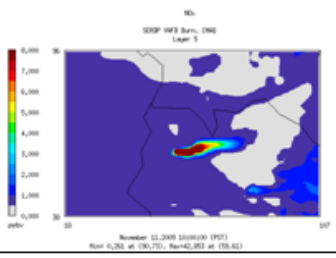	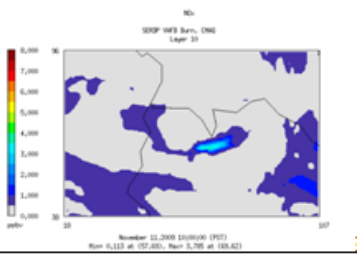
11·am¤	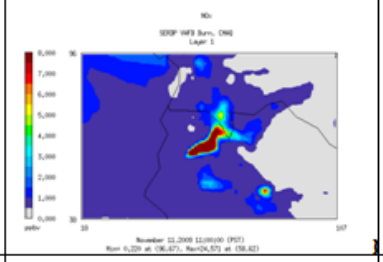	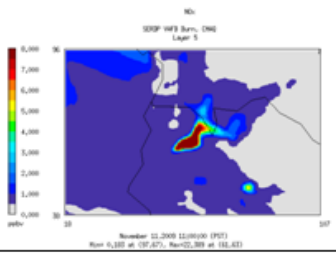	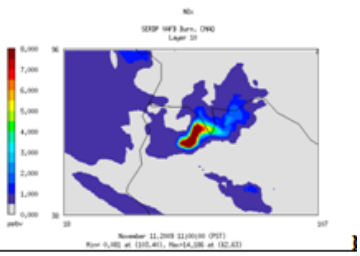
12·pm¤	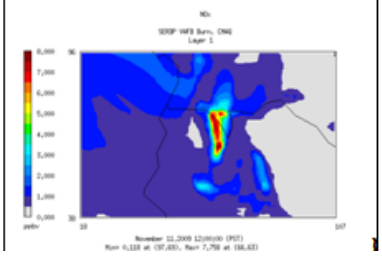	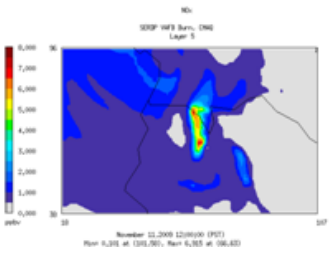	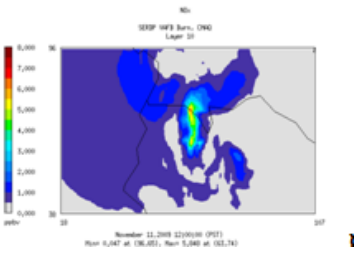

O3¤	Layer·1·(~40m)¤	Layer·5·(~230m)¤	Layer·10·(~800m)¤
10·am¤	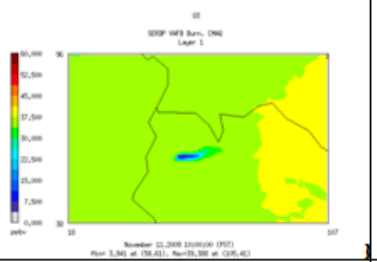	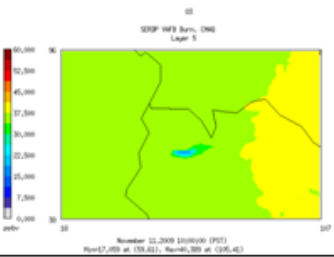	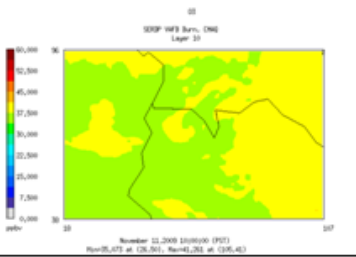
11·am¤	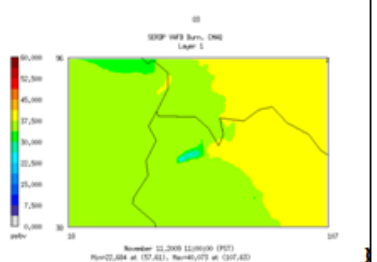	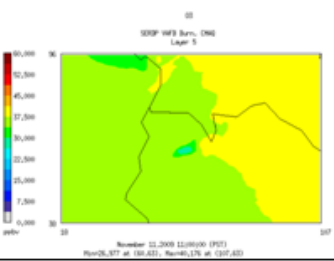	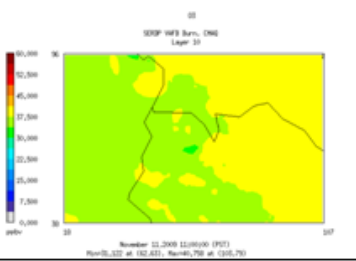
12·pm¤	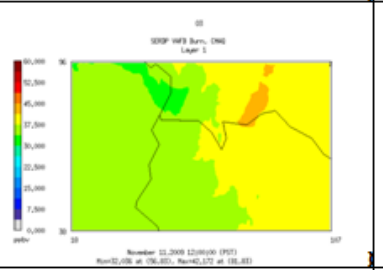	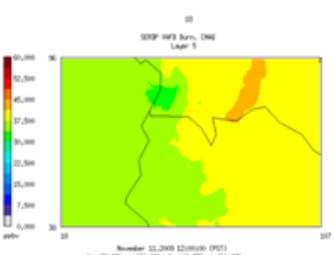	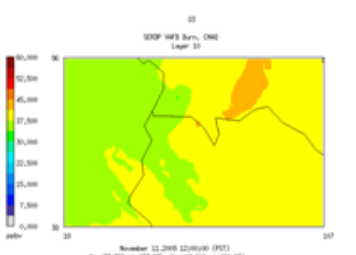

Figure 4-91 CMAX Output Showing Spatial & Temporal Profiles for NOx and Ozone

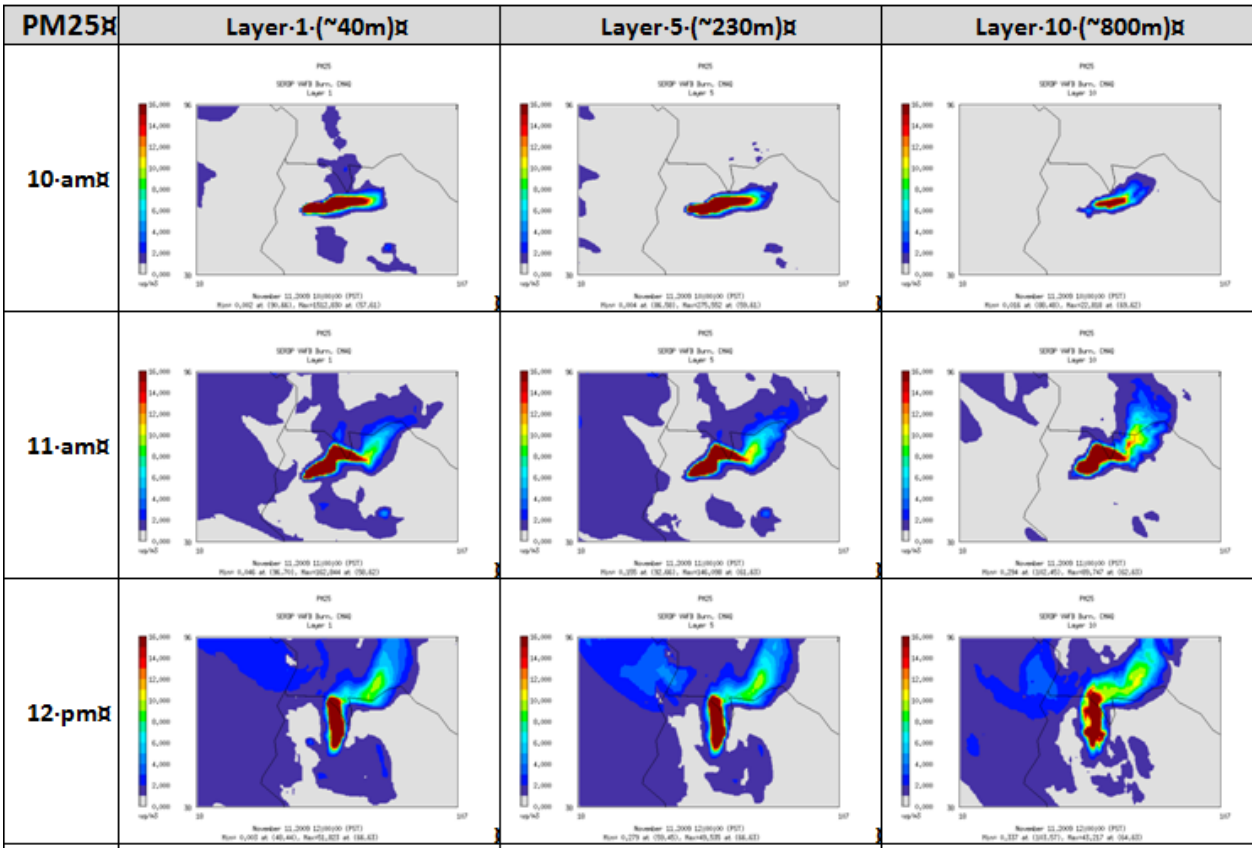

Figure 4-92 Sample Spatial & Temporal Profiles for Fine Particulate Matter

Looking at the model output, it shows that it takes several hours for the ozone to build up and mainly at the higher altitudes. Not surprisingly that the concentration of ozone is low as the intensity of the sun is low in the winter. Other gases like formaldehyde do build at all altitudes and persist for many hours past when the ozone is at a maximum. The fine particulate spatial and temporal charts show that the smoke rises and stays in the area for some time before moving in the north direction.

In another series of charts the model output was examined in the x-y directions from the site of the prescribed burn. A sample chart is shown for NOx in the following chart. This presentation shows the influence of the wind direction at all heights.

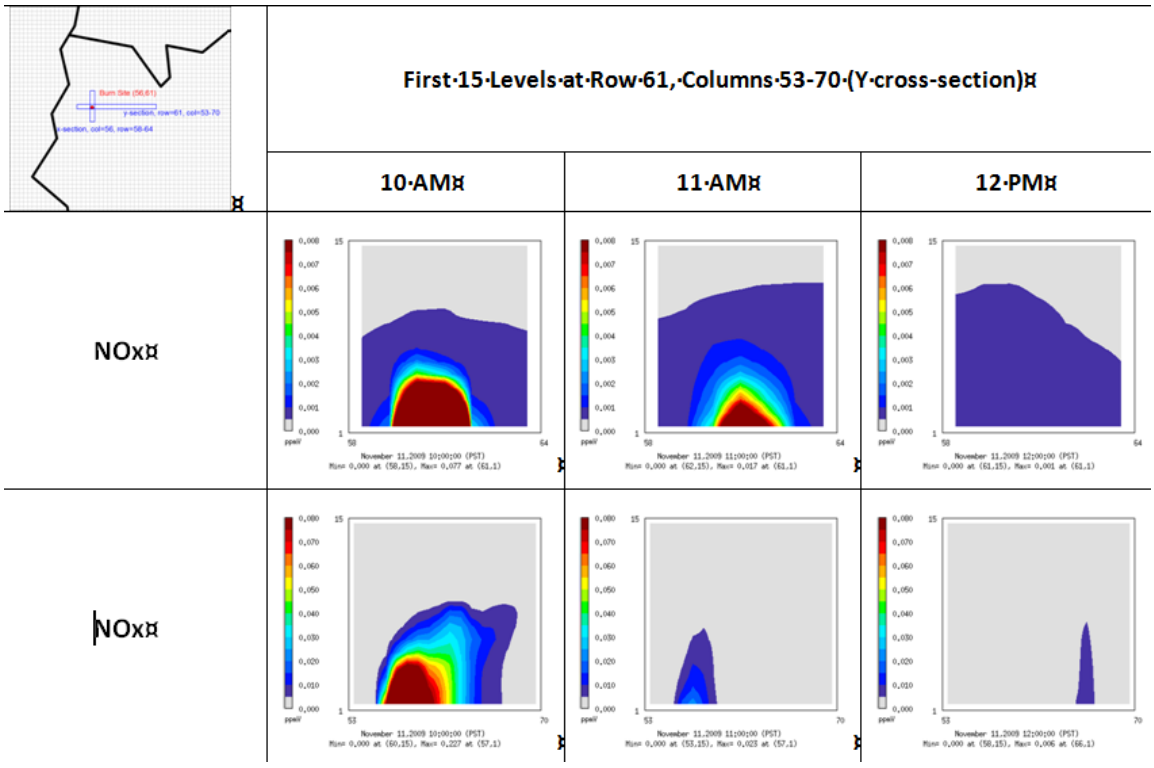

Figure 4-93 Vertical Concentration of NOx: top chart) X-axis and lower) Y-axis

A final set of model output concentrations were compared with the actual measurements either on the ground or in the airplane. Exact GPS positioning of the various sites and aircraft are shown in the following table. Only a few aircraft locations are shown in the table and the complete list of times and locations are shown in the Appendix 7.

Table 4-40 Corresponding Sampling Data to Model Grid Cells

VAFB Burn Location						AQ Model Grid Cells		
sample	local time (hhmmss)	lon	lat	height (m)	Distance (km)	icol	jrow	layer
Burn site		-120.517	34.8000	-	-	56	61	-
AMS Truck		-120.524	34.7928	Ground		56	60	1
FASS Tower		-120.315	34.4760	228		63	31	4
Aircraft Data								
s01	112124	-120.528	34.7928	559	0.94	55	60	8
s02	112823	-120.527	34.7901	214	1.23	55	60	4
s03	113430	-120.528	34.7888	196	1.37	55	60	4
s04	114053	-120.529	34.7899	197	1.29	55	60	4
s05	114752	-120.527	34.7946	236	0.72	56	60	5

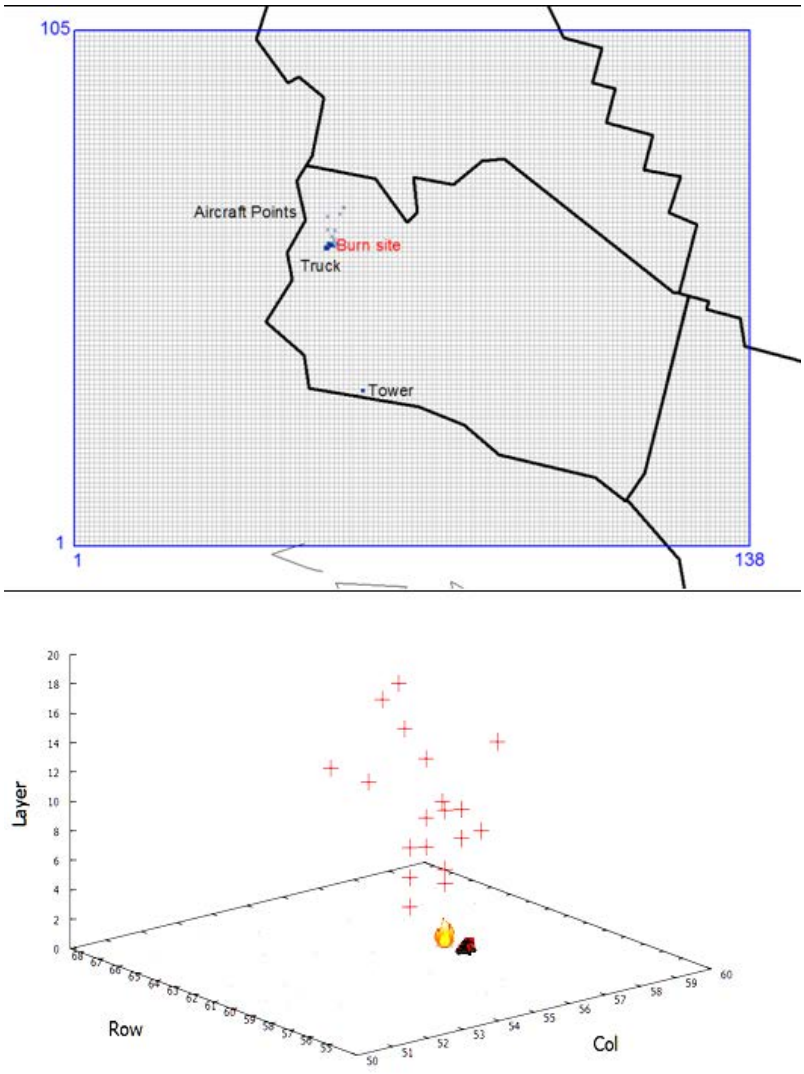

Figure 4-94 . Aircraft sampling (+), AMS-Truck sampling, and Fire Burn Locations Relative to CMAQ modeling grid cells. Top: 2D locations, Bottom: 3D locations

One of the comparisons is made of the particulate organic carbon between the CMAQ model output and the values measured with the AMS on the truck near the prescribed fire. For the exact GPS position of the truck, the chart shows there is a maximum of OC at the start of the prescribed fire. However, this finding is an artifact of the approach used in the model. Recall that all the emissions were entered into the model at 10AM rather that as the emissions were actually released from the fire. As indicated in Figure 4-95, most of the OC arrives at the truck several hours after the fire was ignited. The fire was actually burns of two plots with the second one starting in the afternoon so it looks like the OC from the second block is what reaches the AMS. As an overview, it looks like the model output does not match the ground values except to see a maximum will build and then values return to the background.

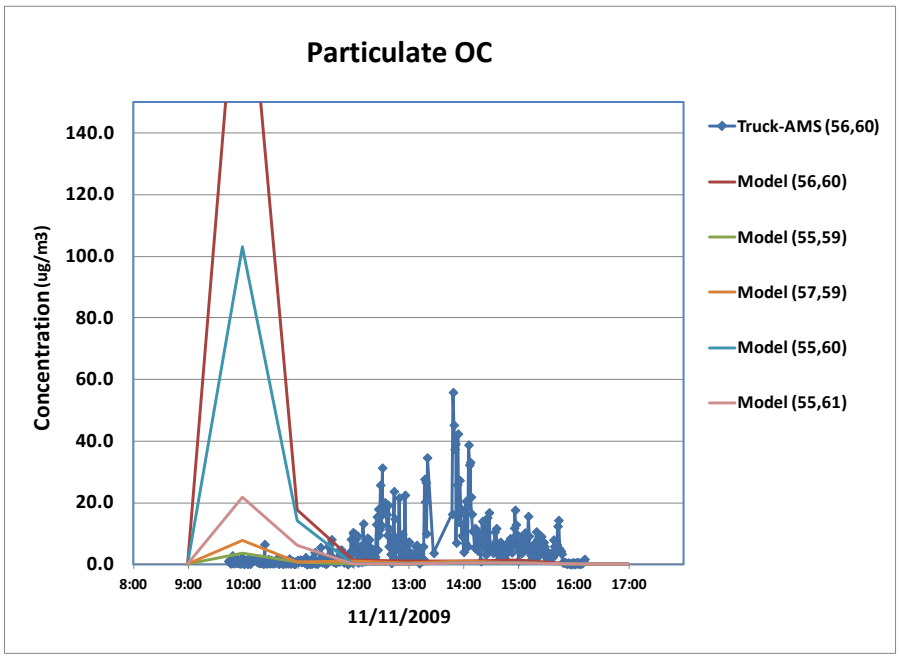

Figure 4-95 Predicted Ground Levels of Particulate Organic Carbon

A comparison of ozone in the airspace where the plane flew with the model output is shown in the following figure. As is indicated the ozone will build to a maximum level and then decay back to the ambient levels. As indicated in Figure 4-96 the agreement was quite good. More figures are included in the Appendix 7 in the back of the report.

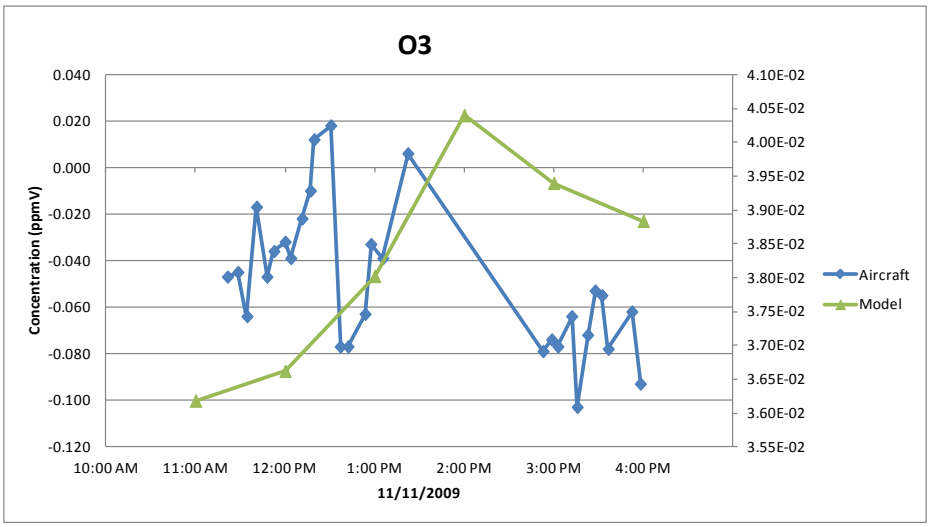

Figure 4-96 Predicted Levels of Ozone Aircraft vs. Model

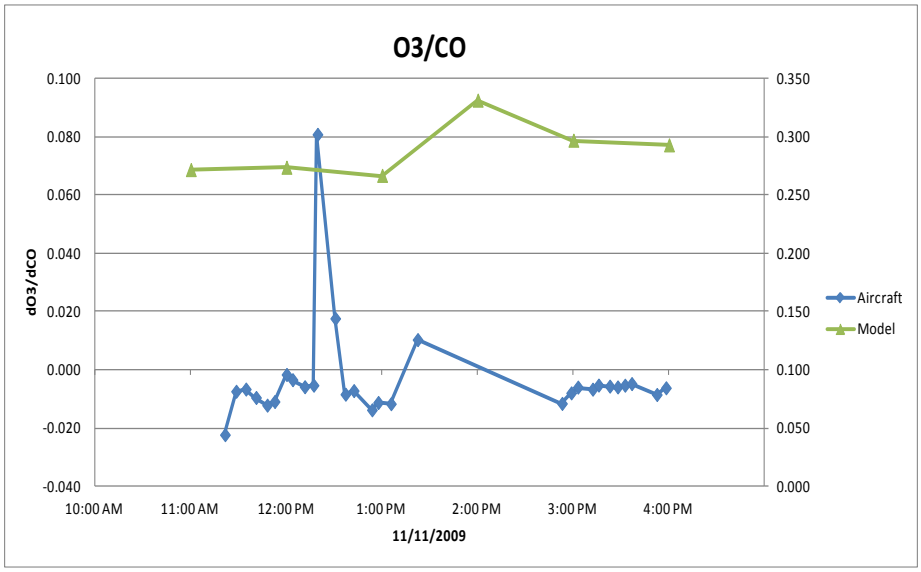

Figure 4-97 Ratio of Species from Aircraft Data vs. Model Results

Another traditional plot of aircraft data is the ratio of the pollutant of interest to carbon monoxide as carbon monoxide is nearly constant in the background. These plots were generated from CMAQ output. The ozone to carbon monoxide ratio from the model is about 2.5 times that of the airplane data (Figure 4-97).

Finally the last of the comparisons is the output functions from the CMAQ and the local Air Quality Stations. These are shown in the plots below (Figure 4-98) with more provided in the appendix. Again with such low ozone concentrations in the winter it is hard to test the robustness of the fit.

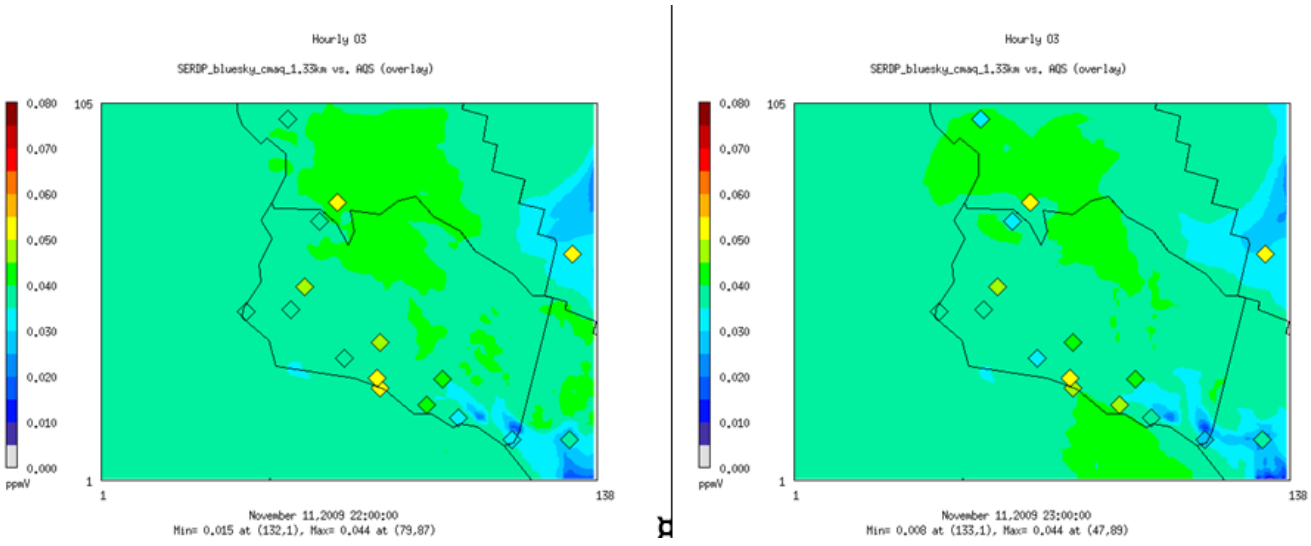

Figure 4-98 O3 AQS Observation in diamonds vs. Model Overlay Plots from 18:00 (GMT) to 23:00 (GMT)

4.4 Novel Approach for Analysis of Flaming/Smoldering Regimes, Black/Brown Carbon and Levoglucosan

Understanding wildland fires and the nature and rate of the emissions is essential given the magnitude of these sources and their increasing role in local and global air quality. For many years the Modified Combustion Efficiency (MCE) has provided a unified and quantitative perspective of the contextual account of a fire, be it wildly flaming or peacefully smoldering. MCE is a proven parameter based on mass balances; however, data regressions of emission factors with MCE often have a large and undesirable coefficient of variation and often have a clump of data in the flaming regime.

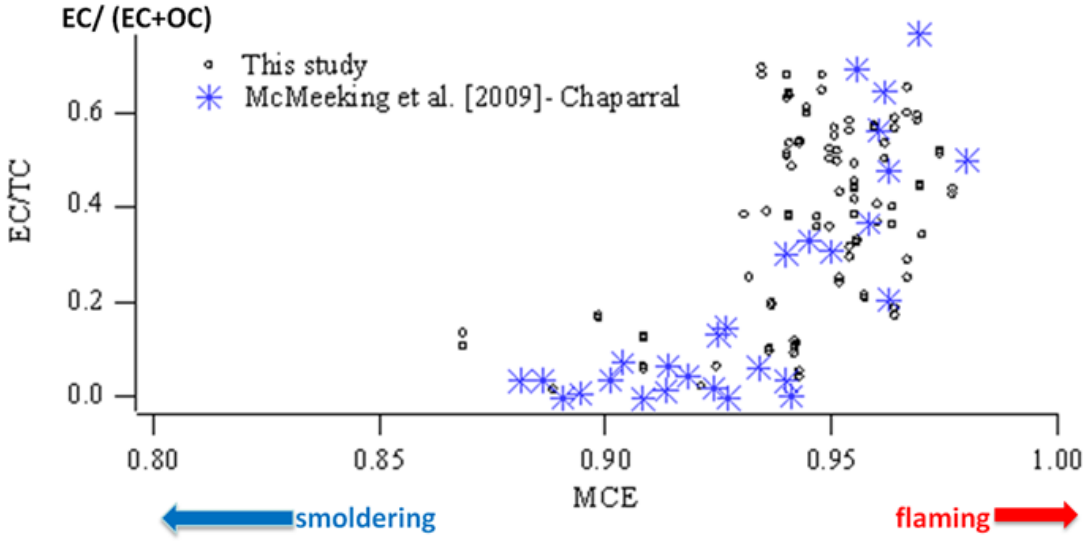

Figure 4-99 Elemental Carbon Emissions are in Flaming Phase (Filter Data)

This research focused on expressing emissions as function of fire intensity in addition to combustion efficiency since it is well known that more intense fires will release significant quantities of graphitic carbon moieties, including black carbon. The research found that the fraction of filterable carbon released as elemental carbon (EC) is a new and useful surrogate for the many complexities associated with fire dynamics. When past emission rates were regressed on this parameter, the data are harmonized and the coefficient of variation was significantly improved. As explained, the new analytical model provides important understanding of soot and its poly aromatic precursors that are in higher levels of concentrations in the flaming phase and the result has implications as to the emission factors of key carbon moieties used in air quality models.

The path to a new model of the chemical compounds released during fires began with an analysis of the earlier data sets from the MFSL that showed the ceaonothus had about four-times the release rate of levoglucosan as did coastal sage, see Figure 4-100. Literature shows that levoglucosan is released when the biomass reaches about 300C so a simple analysis of the data in the figure is that ceaonothus has three-times the amount of cellulose as found in coastal sage. However, analyses show that both have about the same amount of cellulose and hemi-cellulose so the investigation resulted in a deeper analysis.

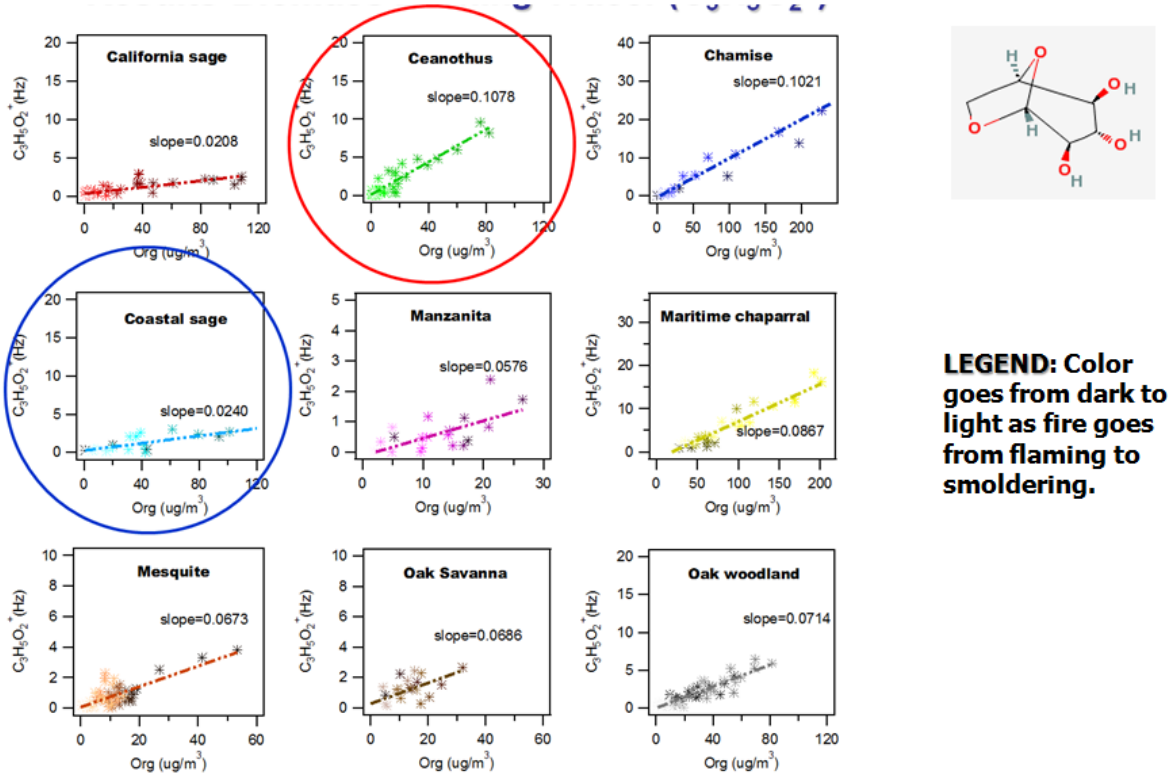

Figure 4-100 Levoglucosan Emissions from Mass Fragments (Aerosol Mass Spec Data)

The deeper analysis focused on a question. Given the same amount of cellulose in each plant, and therefore the same potential for the amount of released levoglucosan, how could the final amount be so different? The answer was certain to be found in a deeper examination of each step in the reaction pathway:

pyrolysis of cellulose → released gases +pyrolysis products + O_2 + heat → final products

Clearly the second reaction where gases are burned and pyrolysis products are further converted into final products is the key to understanding why the amount of levoglucosan differed in the final products. The reaction equation suggests that the pyrolysis products are further oxidized to carbon dioxide, leading to a higher value for the combustion efficiency (CE). In this scenario more of the levoglucosan realized from the coastal sage was oxidized to carbon oxides. However, while the reaction shows excess oxygen is present and that is true on average, there are regions in the emission plume without oxygen and where the poly-aromatic compounds are converted into graphite-like soot compounds. Thus other independent metrics following the course of reactions was needed in order to gain further insight into the fate of the levoglucosan that was released by the coastal sage and lost.

One independent set of data is the fire behavior as indicated in the burn rate. These data are shown in Figure 4-101. From thermodynamics twice as much heat is released in converting carbon to carbon dioxide as compared with carbon monoxide. Thus plotting the concentration of carbon dioxide in the emissions from the MFSL will be indicative of the burn rate and

temperature near the combustion zone. Clearly from these data the coastal sage is more in the flaming regime.

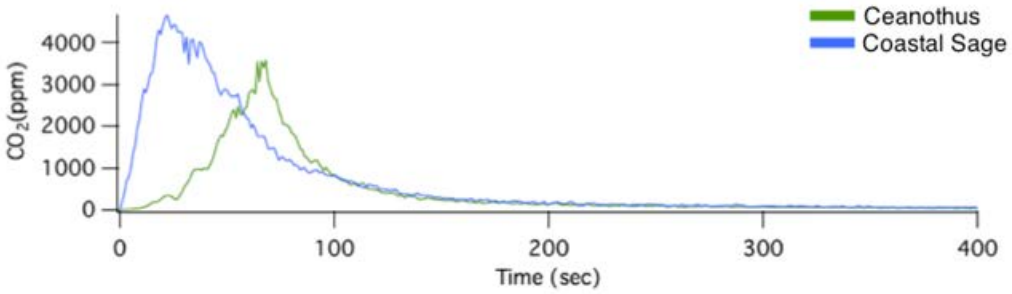

Figure 4-101 Comparing the Fire Behavior for Ceanothus and Coastal Sage

Another indication of the reaction dynamics is the fire intensity which Byram (1959) described as "the most important measure of fire behavior." This relationship is described by Byram's fire intensity equation: I = intensity (kW/m) = Hwr….where

H = heat yield of fuel (J/g)
w= fuel consumed (kg/m^2)
r = spread (m/sec)

Byram comments flame height is an indication and surrogate for fire intensity. From the videos of these two laboratory burns it was evident that the flame height for the coastal sage was considerably higher; hence, a higher intensity. Given that the rate of CO_2 released was higher and that the flame height was higher, it is clear that fire intensity was higher for the coastal sage fire. Higher intensity, faster reactions of pyrolysis products, more oxygen deprived regions and more graphic carbon all occur simultaneously.

Based on the above observations, our hypothesis is: The ratio of filterable graphitic carbon or elemental carbon to total filterable carbon is a measure of fire intensity.

As verification of the hypothesis we reviewed data from the MFSL with literature data and this review is shown in Figure 4-102. Clearly the solid circles from this research showed that the amount of levoglucosan measured in the products depended on the ratio of graphic carbon to the total carbon. The filled square points were data generated at the University of Wisconsin and the other points were from Caltech. Basically all data fit the hypothesis. Note that the ceaenothus from early burn when the fire intensity was very low and before the fuel beds were redesigned. Another observation is the amount of organic carbon is high when the amount of levoglucosan is high…and the amount of elemental/graphic carbon is low.

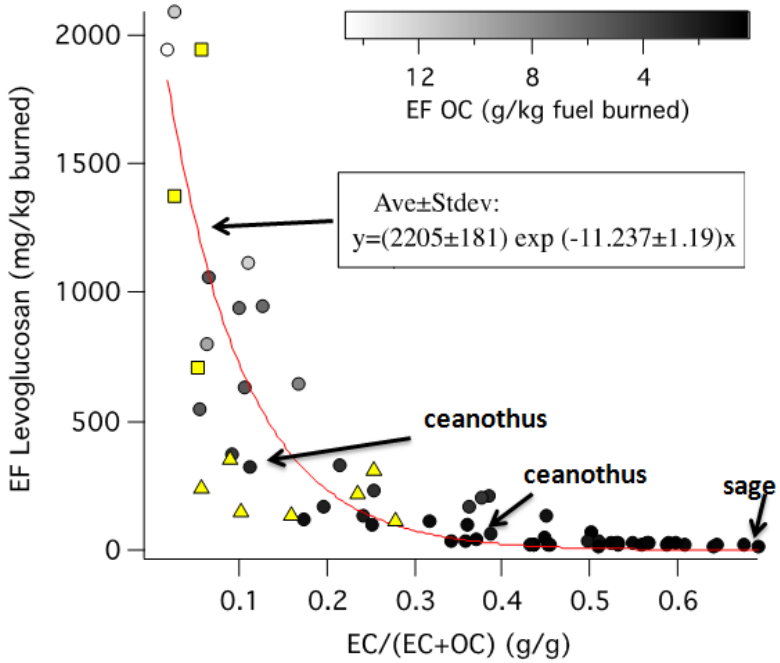

Figure 4-102 Emission Factor Levoglucosan vs. EC/TC Ratio

A more direct test of the hypothesis occurred when all the PAH data from MFSL lab burns were plotted as a function of the traditional EC ratio and also against the new parameter suggested from this work, namely, the ratio of filter elemental carbon to the total filterable carbon. These plots are shown in Figure 4-103 and clearly the new parameter fits the data better. Note the data on the y-axis in the upper graph and the lower graph are exactly the same. The only change is the parameter on the x-axis. Clearly the traditional CE parameter has the same fit as usually seen and is evident in Figure 4-99. The improved fit speaks to analysis that says fire intensity is more important than the combustion efficiency.

The last plot in Figure 4-104 shows another graph where single compounds are plotted against the new parameter. Note an intense fire releases more graphitic carbon and a mild fire will release more levoglucosan. Thus roughly the same amount of levoglucosan is released as pyrolysate and fire intensity will determine how much is found in the products. Note that both the releases of Black Carbon-like and Brown Carbon molecules are associated with high fire intensity.

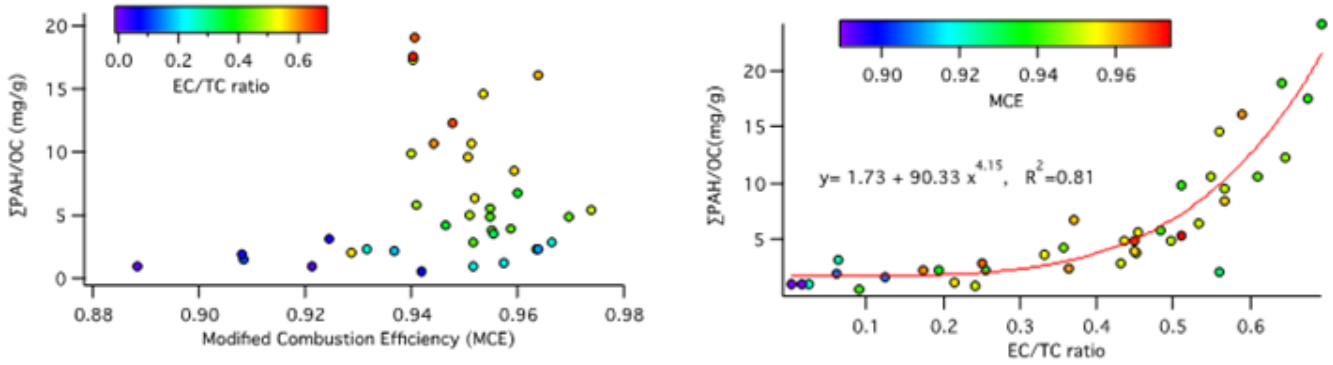

Figure 4-103 Ratio PAH/OC vs. MCE and EC/TC Ratio

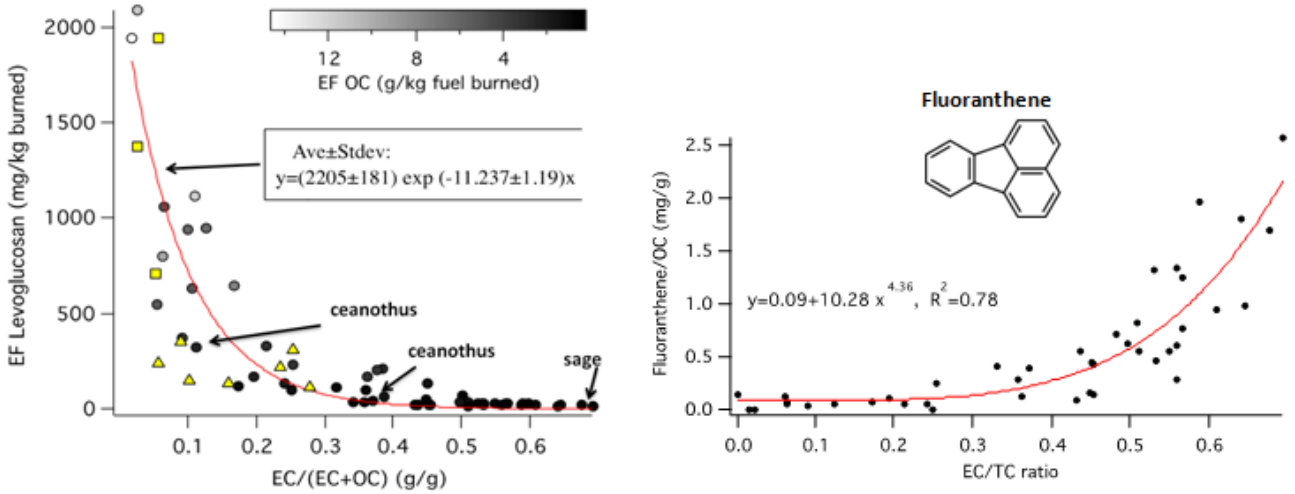

Figure 4-104 Single Compound Emissions Correlate with Ratio EC/TC

5 Conclusions and Implications for Future Research/Implementation

The conclusions, highlights and recommendations for further work in each section follow.

Improved fuel characterization and consumption data. Prior to this research, data for fuel properties and consumption rates during fire for southwestern chaparral and oak woodlands were scarce. Working with four military facilities in California and Arizona the team sampled and characterized their fuel types, including a photographic series, measurements of density, and elemental composition of natural fuels. Fuel loadings were measured in the field before fire and after fire to measure the consumption rates. On completion, the project developed improved data on fuels and fuel-consumption for military bases in the Southwest, as well as the neighboring US Forest Service lands. The new fuels and consumption data will help land managers improve predictions of fuel consumption for chaparral while planning for prescribed burns. The new data are located in a data base established during the SERDP project. Prescribed burns are used as a tool to help control wild land fires.

Improved emission factors and new test methods Much of the funding was spent on improving test methods and determining emission factors from fires with Southwest and Southeast fuel types. Emission data were widely lacking for many of these fuels and the results from RC-1649 and RC-1648 lead to a significant improvement in characterization of the emission factors from burning these fuels. During the project, RC-1649 enhanced the signal to noise ratio of an IR instrument to collect more data and built a data base with new algorithms that allowed them to quantify compounds previously that were not measurable The researchers in RC-1649 quantified the mass contributed by many oxygenated organic compounds for the first time and which represented up to 20% of the emissions. Furthermore they easily quantified HONO, a key precursor to ozone formation. Knowing the amount of these compounds is important as they drive the formation of secondary pollutants like ozone and aerosols that lead to particulate matter. Data were recorded at 1Hz and this approach allowed the continuous determination of the emission factors as the fire transitioned from the flaming to the smoldering regime. Results for the gaseous compounds are reported in peer reviewed journals.

The RC-1648 team focused on characterization of the criteria pollutants and toxic gases from fires, and in addition, RC-1648 provided important first-time measurements of the chemical and physical nature of particulate matter using a suite of real-time instruments. Many of the measuring instruments were designed for the low concentrations found in a normal atmosphere and had to be tailored to work with the much higher concentrations found in the atmosphere associated with fires. The modifications to enable them to work at the higher levels were made at the Riverside Forest Service lab while simultaneously undertaking a project that showed the local air district that covering wood cuttings with plastic does not add to criteria or toxic emissions. This work allows the Forest Service and others to apply for permits with the knowledge that the plastic contributes in a *de minimis* way to emissions. Those results were published in a peer review journal.

Taken in total, over 5 giga-bits of data were collected, analyzed and reported in peer reviewed journals. Additionally under RC-1649 the data from these projects were organized and combined with other data that was harvested from the public literature and from the private literature in the Forest Service. All the gathered data were listed on a searchable Excel spread sheet and deposited on a server to be managed by the Forest Service.

Basically RC-1648 reported measurements in the peer reviewed literature on:

- Criteria pollutant mass: CO, NO_x, SO_x ,$PM_{2.5}$
- Other gases : CO_2, CH_4 and selected light hydrocarbons
- Toxics: aldehydes, ketones, NH_3, BTEX, some SVOCs, PAHs
- Ions: SO_4, NO_3, Cl, Br, Na, NH_4, K, Ca
- Elements: 38 elements were measured with the most abundant being K, Cl, Na …
- PM chemistry: elemental/organic carbon, black carbon, levoglucosan, formation of secondary PM in atmospheric reactors.
- PM physical properties: real-time particle: 1) mass, 2) size distribution and 3) number

Emissions data were collected both in the laboratory and in the field during prescribed burning. One of the difficult things is to compare the emissions in the lab to those in the field because the fuel in the lab has about 20% of the field moisture and is pack considerably tighter in order to maintain the burn for several minutes. One of the peer reviewed papers was an analysis of both conditions and developed a set of emission factors that can be used by people who are estimating the impact of a prescribed burn.

In another area, the project was responsive to SERDP's intention of adding project data to EPA's AP-42: *Compilation of Air Pollutant Emission Factors.* Several discussions were held with the EPA representatives on the IPR and others at Research Triangle Park about the approach to get data accepted. One thing they required was a measure of the confidence limits for the data so whenever gaseous emission factors were measured in both RC-1649 and RC-1648, the values were compared as part of the quality assurance program. Such an approach assists the US EPA to accept and post those values as part of the AP-42's for wide-spread use.

In addition to the planned traditional research, some exploratory research was carried out in a large atmospheric reactor filled with biomass emissions. The reactor allowed us to control many parameters -- such as humidity, sun light intensity, temperature -- in order to investigate particle growth and any increase in ozone concentration. Furthermore the setup allowed the scientists to monitor the cloud forming tendency of particles associated with biomass burning over hours, rather than minutes as carried out at MFSL. Among the noteworthy findings was that ozone only increased when the mixture was exposed to light, and unexpectedly, the light also increased particle growth and reduced the rate of cloud formation.

Finally, a significant advancement in data analysis resulted during this project. For about 30 years, all emissions data during the flaming and smoldering regimes were fitted to combustion efficiency. This project showed the percentage of total filterable carbon that is graphic in nature is a surrogate for fire intensity and provides a better fit as shown in Figure 5-1. Using this parameter enables one to understand the release of black carbon, brown carbon and lighter molecules, like levoglucosan.

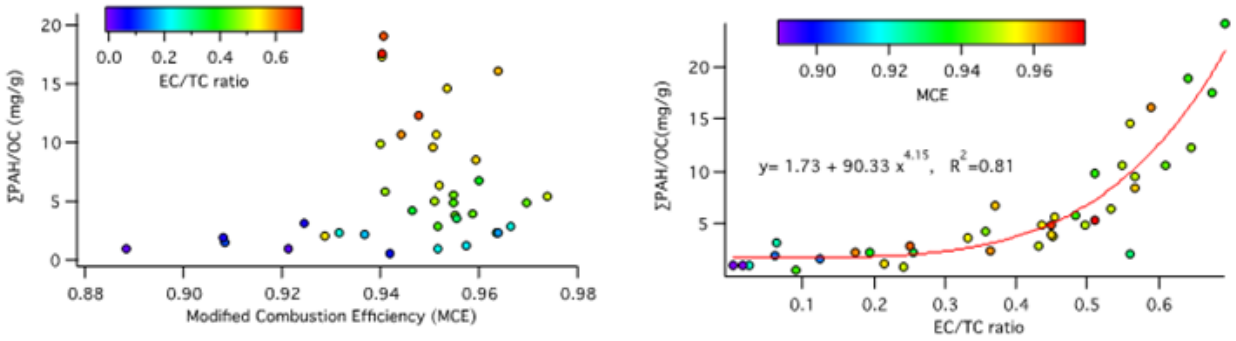

Figure 5-1 New Model Developed Based on Fire Intensity to Explain Emissions

Air Quality Modeling. The work looked at a number of parameters that drive the output result for air quality. One question was the impact of a maritime air mass with higher levels of salt on PM emissions and results from the EPA air quality model showed that the contribution to PM mass was insignificant. A significant effort was made to model the air quality associated with prescribed burning around AFV with current metrological and air quality models. Data are presented in both temporal and spatial formats over three dimensions to represent the history of the emissions from the fire. One problem with prescribed burns is the spatial and temporal resolution of the models only shows trends. Similar trends were observed in the aircraft data but the overlay was far from exact. One problem with the timeframe of the prescribed burns is that the burns were carried out in the winter when sun intensity is low and does not allow much ozone to form. While some data looked promising, running the complex CMAQ model requires experienced scientists to get it to converge with small prescribed burns as the velocity and concentration fields change much less than in a wildfire. Trials comparing BlueSky with SMARTFIRE indicated BlueSky was better and may offer advantages over CMAQ for land managers.

Publications: Many including the award winning presentation at the 92nd American Meteorological Mtg., 16 Journal papers and over 22 conference presentations...with more underway.

Recommendations:

- Emissions factors should be separated into distinct flaming and smoldering regimes rather than both at the same time as was carried out in analysis of the laboratory data. For wildland fires, real world flaming emission rates are high and while smoldering emission rates are low, the burn is over a long time. Neither is represented well by a single emission factor.
- Atmospheric reactors should be used to study the fate of plumes from biomass fires for long periods of time, hours rather than the minutes in lab burns. Many parameters can be controlled in the atmospheric reactors so ozone generation from wildland fires in the summer as well as the winter can be investigated.
- Aircraft present the best platform capable of sampling emissions from prescribed burns or wildfires as they can sample over all altitudes and distances from the fire.

- Field data showed DoD facilities need to analyze soil before prescribed burns as the Vandenberg AFB released significant amounts of lead and antimony and both would be toxic to the personnel near/downwind of the fire.
- A new analytical model was developed for predicting the release of black carbon, brown carbon and lighter molecules, like levoglucosan. More work should be carried out to exploit the links to black carbon and brown carbon.
- Air quality modeling suggest that the BlueSky framework might be more useful to local land managers that the complex US EPA CMAQ.

6 Literature Cited

Albini, F.A. 1976. Estimating wildfire behavior and effects. General Technical Report No. INT-30, USDA Forest Service, Intermountain Forest and Range Experiment Station, Ogden, UT

Busse MD, Hubbert KR, Fiddler GO, Shestak CJ, Powers RF (2005) Lethal soil temperatures during burning of masticated forest residues. International Journal of Wildland Fire 14, 267–276.

Countryman CM. 1982. Physical characteristics of some northern California brush fuels. USDA Forest Service General Technical Report PSW-61, (Berkeley, CA)

Countryman, CM; Philpot CW. 1970. Physical characteristics of chamise as a wildland fuel. USDA Forest Service Res. Paper PSW-66, Berkeley, CA.

Danzer, S.R. 1997. Final report: Fuel inventory on Fort Huachuca - a pilot study, submitted to The Nature Conservancy, Forest Service, and Ft. Huachuca integrated fire management plan.

D07 Committee, 2007. Test Methods for Direct Moisture Content Measurement of Wood and Wood-Base Materials (No. ASTM Standard D4442-07). ASTM International, West Conshohocken, PA.

Folliott, Peter F.; Gottfried, Gerald J.; DeBano, Leonard F. 2008. Fuel loadings in forests, woodlands, and savannas of the Madrean Province. Pp. 271-278 In: Narog, M.G., tech. coord. Proceedings of the 2002 fire conference: mapping fire and fuels in the remaining wildlands and open spaces of the Southwestern United States. Gen. Tech. Rep. PSW-GTR-189. Albany, CA: U.S. Department of Agriculture, Forest Service, Pacific Southwest Research Station.

Fried, Jeremy S.; Bolsinger, Charles L.; Beardsley, Debby. 2004. Chaparral in southern and central coastal California in the mid-1990s: area, ownership, condition, and change. Res. Bull. PNW-RB-240. Portland, OR: U.S. Department of Agriculture, Forest Service, Pacific Northwest Research Station. 86 p.

Hood, S; Wu, R. 2006. Estimating fuel bed loadings in masticated areas. Pp. 333-340 In. Proc. Fuels Management-How to Measure Success, USDA Forest Service Rocky Mountain Research Station Proc. RMRS-P-41.

Hosseini, S.; Li, Q.; Shrivastava, M.; Weise, D. R.; Miller, W.; Cocker, D.; Jung, H. (in press) Effect of low density polyethylene on smoke emissions from debris pile burning. Journal of Air and Waste Management Association

Kane, JM. 2007. Fuel loading and vegetation response to mechanical mastication fuels treatments. MS thesis, Humboldt State University, California.

Larkin, NK , O'Neill, SM, Solomon, R, Raffuse, S, Strand, T, Sullivan, DC, Krull, C, Rorig, M, Peterson, J. 2009. The BlueSky smoke modeling framework. Int. J. Wildland Fire 18:906-920.

Lee , T., Sullivan , A.P., Mack , L., Jimenez , J.L., Kreidenweis , S.M., Onasch , T.B., Worsnop , D.R., Malm, W., Wold , C.E., Hao, W.M., Collett, J.L., Jr. 2010. Chemical Smoke Marker Emissions During Flaming and Smoldering Phases of Laboratory Open Burning of Wildland Fuels, Aerosol Science and Technology, 44:9, i-v

L. Qi, S. Hosseini, H. Jung, D. Weise, D. Cocker III, and Y. Huang. In review. Chemical characterization of particle emissions from controlled burns of biomass fuels using a high resolution time-of-flight aerosol mass spectrometer. Submitted to Atmospheric Environment

Martin, RE; Frewing DW; McClanahan, JL. 1981. Average biomass of four northwest shrubds by fuel size class and crown cover. USDA Forest Service Res. Note PNW-374. Portland, OR: U.S. Department of Agriculture, Forest Service, Pacific Northwest Forest and Range Experiment Station.

Miller, J.D.; Danzer, S.R.; Watts, J.M.; Stone, S.; Yool, S.R. 2003. Cluster analysis of structural stage classes to map wildland fuels in a Madrean ecosystem. J. Env. Mgmt. 68: 239-252.

Ottmar, Roger D.; Vihnanek, Robert E.; Regelbrugge, Jon C. 2000. Stereo photo series for quantifying natural fuels. Volume IV: pinyon-juniper, sagebrush, and chaparral types in the Southwestern United States. PMS 833. Boise, ID: National Wildfire Coordinating Group, National Interagency Fire Center. 97 p.

Ottmar, Roger D.; Vihnanek, Robert E.; Wright, Clinton S.; Seymour, Geoffrey B. 2007. Stereo photo series for quantifying natural fuels: volume IX: Oak/juniper types in southern Arizona and New Mexico. Gen. Tech. Rep. PNW-GTR-714. U.S. Department of Agriculture, Forest Service, Pacific Northwest Research Station. 41 p.

Ott Ottmar, R.D. 2014. Wildland fire emissions, carbon, and climate: Modeling fuel consumption. For. Ecol. Manage. 317, 41-50, doi: 10.1016/j.foreco.2013.06.010.”mar, R.D.

Ottmar, R.D, D.V.Sandberg, C.L. Riccardi, and S. Prichard. 2007. An overview of the Fuel Characteristic Classification System–quantifying, classifying and creating fuelbeds for resource planning. Can. J. of Forest Research. 37: 2383-2393.

Poulos, H.M. 2009. Mapping fuels in the Chihuahuan Desert borderlands using remote sensing, geographic information systems, and biophysical modeling. Can. J. For. Res. 39(10): 1917-1927.

Pratt, K.A., Murphy, S.M., Subramanian, R., DeMott, P.J., Kok, G.L., Campos, T., Rogers, D.C., Prenni, A.J., Heymsfield, A.J., Seinfeld, J.H., Prather, K. A. 2011. Flight-based chemical characterization of biomass burning aerosols within two prescribed burn smoke plumes, Atmos. Chem. Phys., 11, 12549-12565, doi:10.5194/acp-11-12549-2011.

Riccardi, C.L.; Ottmar, R.D.; Sandberg, D.V.; Andreu, A.; Elman, E.; Kopper, K.; Long, J. 2007. The fuelbed: a key element of the Fuel Characteristic Classification System. Can. J. For. Res. 37: 2394-2412.

Riggan, PJ; Franklin, SE; Brass, JA, Brooks, FE. 1994. Perspectives on fire management in Mediterranean ecosystems of southern California. Ch. 8 In Moreno, JM; Oechel, WC (eds). The Role of Fire in Mediterranean-Type Ecosystems. Ecological Studies 107, Springer-Verlag.

Strand, T.M., Larkin, N., Craig, K.J., Raffuse, S., Sullivan, D., Solomon, R., Rorig, M., Wheeler, N., Pryden, D. 2012. Analyses of BlueSky Gateway PM2.5 predictions during the 2007 southern and 2008 northern California fires, J. Geophys. Res., 117, D17301, doi:10.1029/2012JD017627.

Susott, R.A., Ward, D.E., Babbitt, R.E., Latham, D.J. 1991. The measurement of trace emissions and combustion characteristics for a mass fire. Pp. 245-257 in Levine, J.S. (ed.) Global Biomass Burning:atmospheric, climatic, and biospheric implications. MIT Press, Cambridge, MA.

Ward, D.E., Hardy, C.C. 1991. Smoke emissions from wildland fires. Environ. Int., 17(2-3), 117-134, doi: 10.1016/0160-4120(91)90095-8.

Ward, D.E., Hao, W.M., Susott, R.A., Babbitt, R.E., Shea, R.W., Kauffman, J.B., Justice, C.O. 1996. Effect of fuel composition on combustion efficiency and emission factors for African

savanna ecosystems. J. Geophys. Res. – Atmos., 101, D19, 23569-23576, doi: 10.1029/95JD02595.

Ward, D.E., Susott, R.A., Kauffman, J.B., Babbitt, R.E., Cummings, D.L., Dias, B., Holben, B.N., Kaufman, Y.J., Rasmussen, R.A., Setzer, A.W. 1992. Smoke and fire characteristics for cerrado and deforestation burns in Brazil: BASE-B Experiment. J. Geophys. Res. – Atmos., 97, D13, 14601-14619, doi:10.1029/92JD01218.

Weise, D.R., Xiangyang Zhou, Lulu Sun, and Shankar Mahalingam. 2005. Fire spread in chaparral – "go or no-go?" International Journal of Wildland Fire 14: 99-106

Weise, D.R., Wright, C.H. 2014. Wildland fire emissions, carbon and climate: Characterizing wildland fuels. For. Ecol. Manage., 317, 26-40, doi: 10.1016/j.foreco.2013.02.037.

Weise DR, Koo E, Zhou X, Mahalingam S. 2011. A laboratory-scale comparison of rate of spread model predictions using chaparral fuel beds – preliminary results. Proceedings of 3rd Fire Behavior and Fuels Conference, October 25-29, 2010, Spokane, Washington, USA. International Association of Wildland Fire, Birmingham, Alabama, USA. (Available at http://treesearch.fs.fed.us/pubs/38809).

Weise, D.R., Wright, C.H. 2013. Wildland fire emissions, carbon and climate: Characterizing wildland fuels. Forest Ecology and Management, doi: 10.1016/j.foreco.2013.02.037

Yokelson, R.J., Urbanski, S.P., Atlas, E.L., Toohey, D.W., Alvarado, E.C., Crounse, J.D., Wennberg, P.O., Fisher, M.E., Wold, C.E., Campos, T.L., Adachi, K., Buseck, P.R., Hao, W.M. 2007. Emissions from forest fires near Mexico City, Atmos. Chem. Phys., 7, 5569–5584, doi:10.5194/acp-7-5569-2007

Zhou, X.; Mahalingam, S.; Weise, D. 2005. Modeling of marginal burning state of fire spread in live chaparral shrub fuel bed. Combustion and Flame 143(3): 183-198

7 Appendix A

7.1 Supporting Data Air Quality Model Output

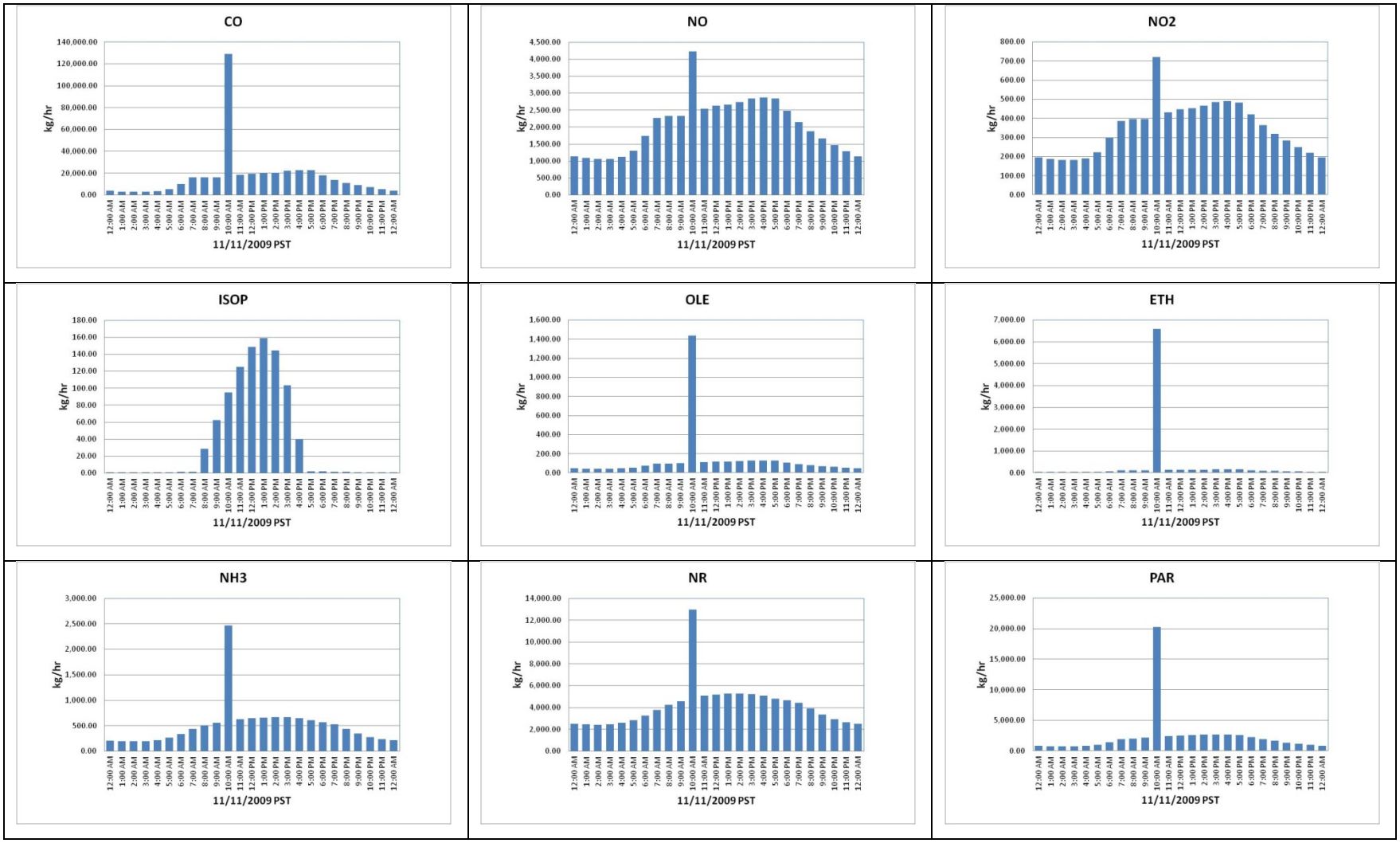

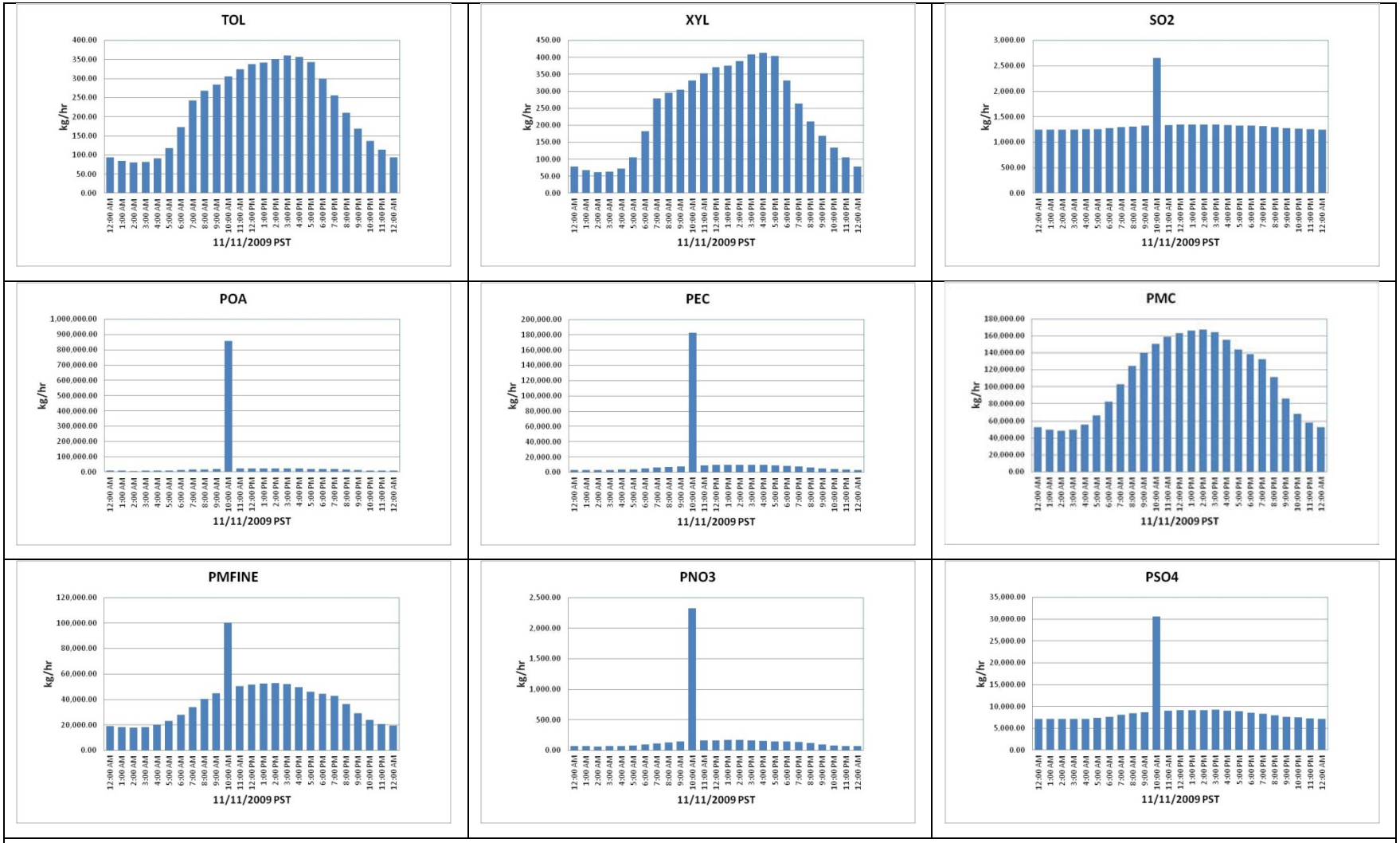

Figure 1. Hourly profiles of domain-wide total emissions for major pollutants on fire burning day.

CO	Layer 1 (~40m)	Layer 5 (~230m)	Layer 10 (~800m)
10 am	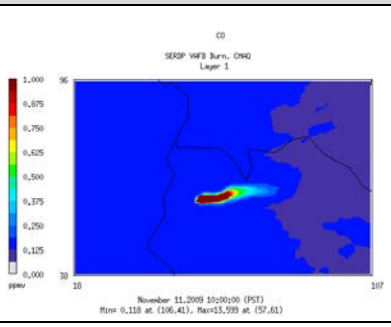	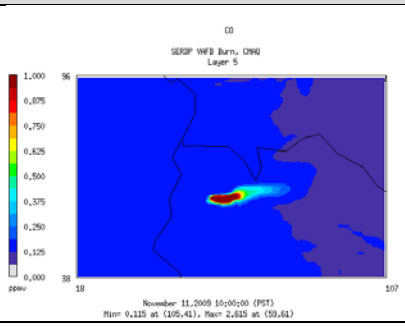	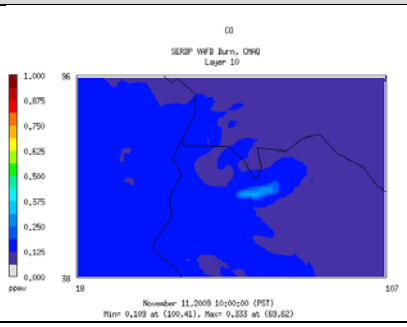
11 am	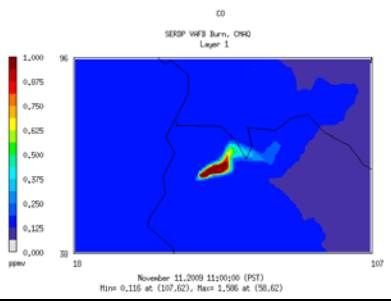	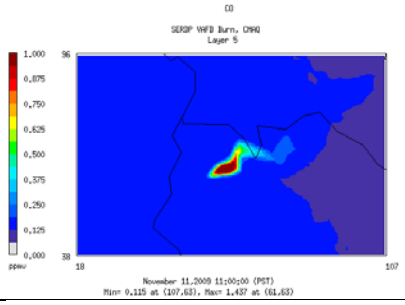	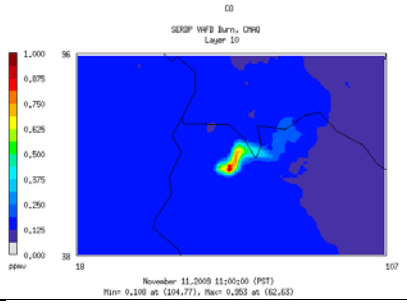
12 pm	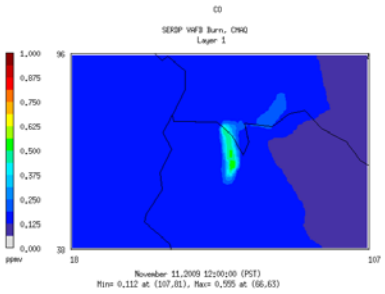	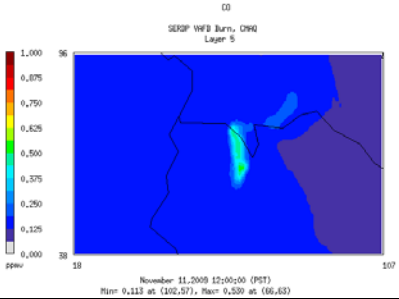	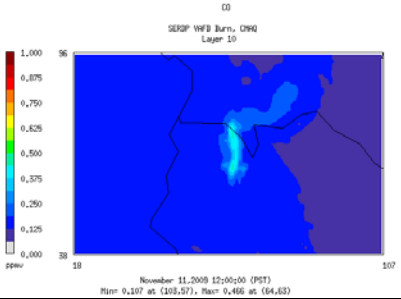
1 pm	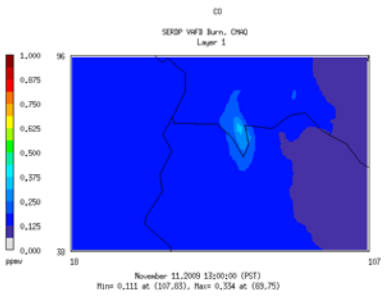	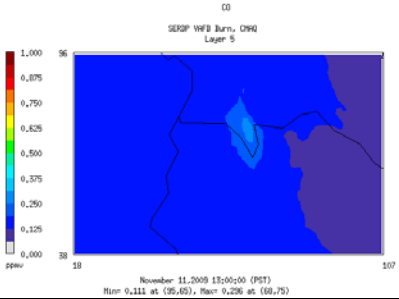	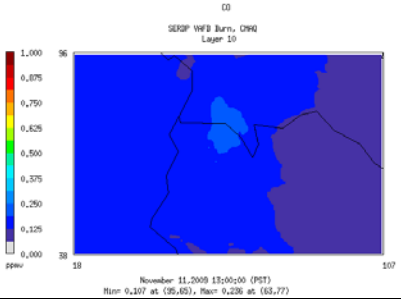
2 pm	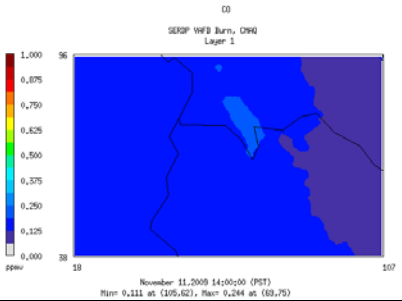	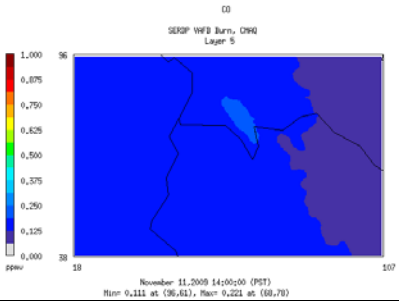	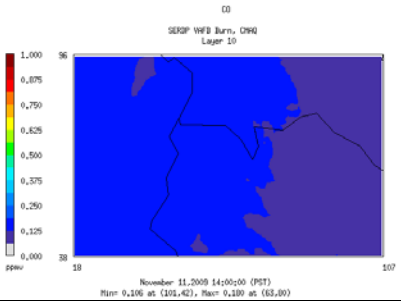

Figure 2a. CO hourly spatial concentrations at three different vertical layers between 10am to 2pm PST.

NOx	Layer 1 (~40m)	Layer 5 (~230m)	Layer 10 (~800m)
10 am	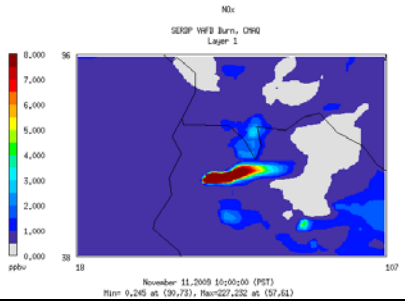	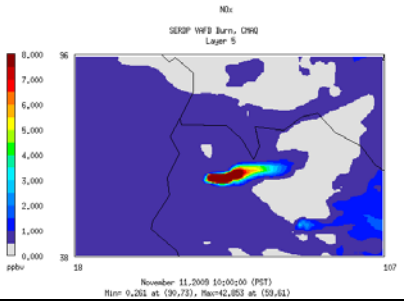	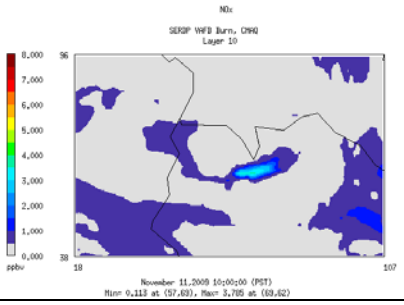
11 am	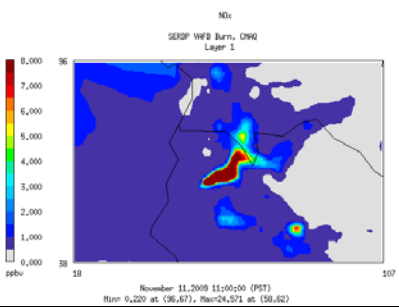	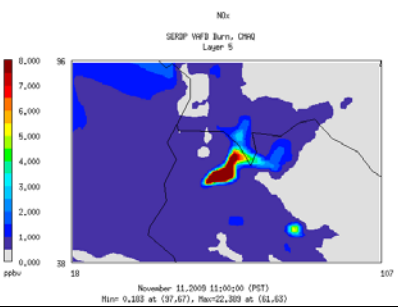	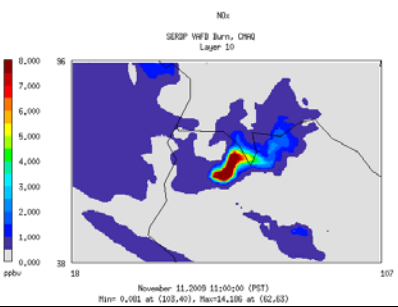
12 pm	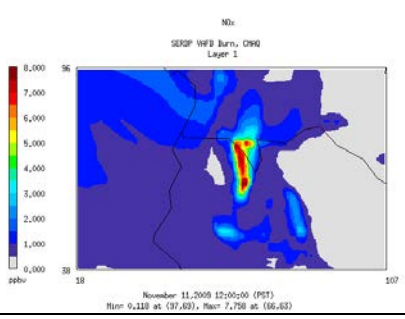	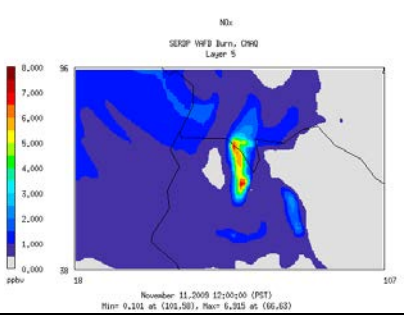	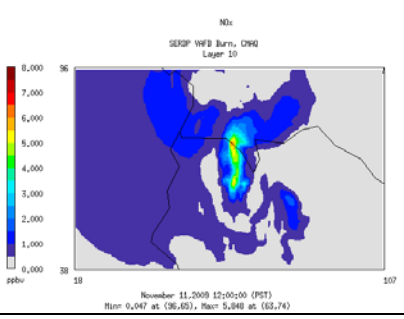
1 pm	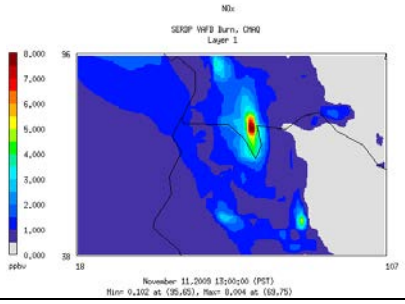	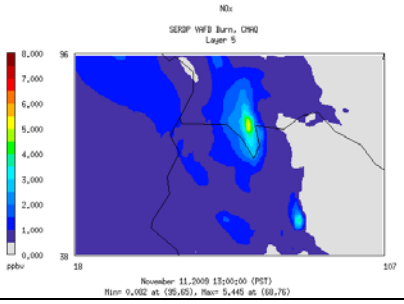	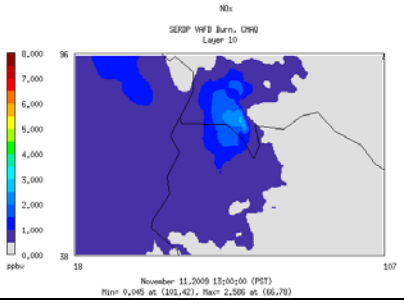
2 pm	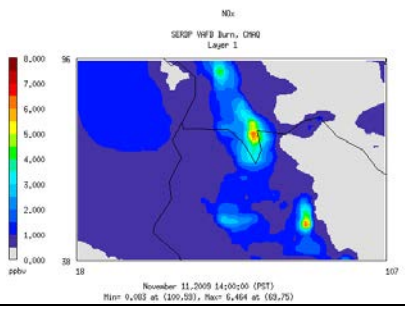	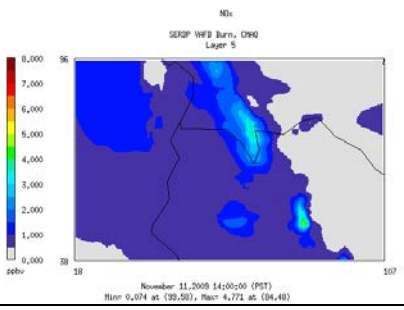	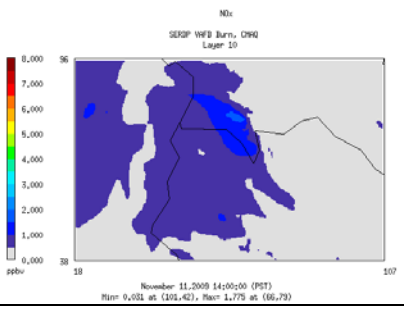

Figure 2b. NOx hourly spatial concentrations at three different vertical layers between 10am to 2pm PST.

HCHO	Layer 1 (~40m)	Layer 5 (~230m)	Layer 10 (~800m)
10 am	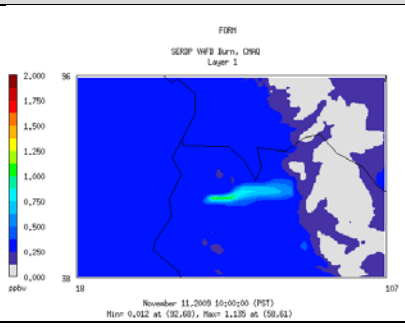	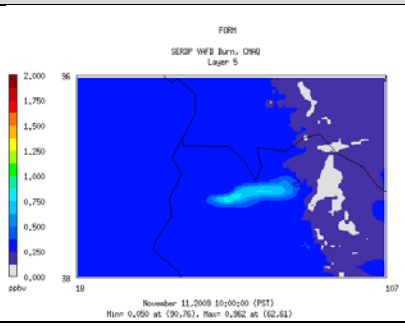	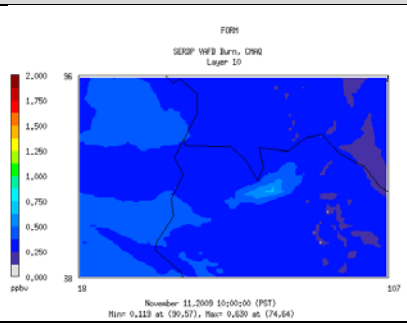
11 am	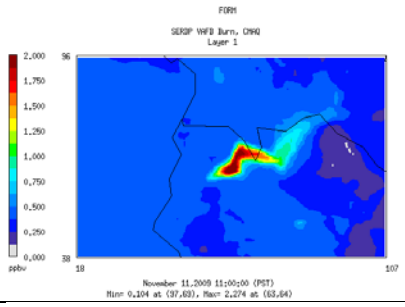	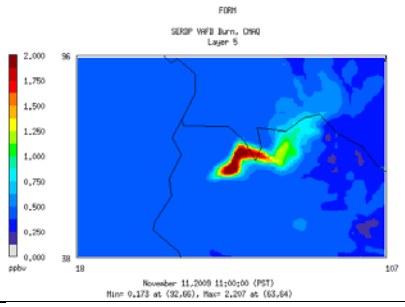	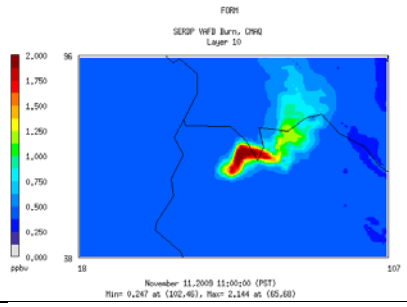
12 pm	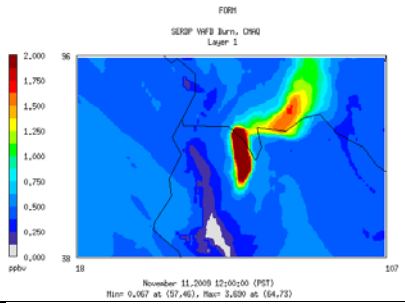	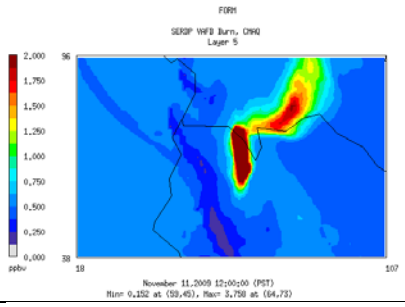	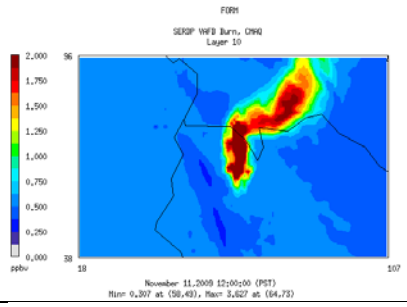
1 pm	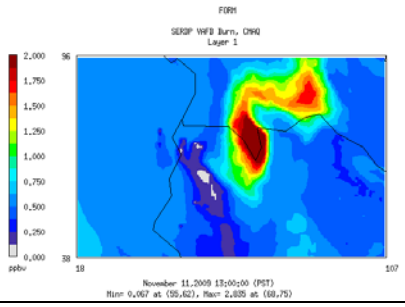	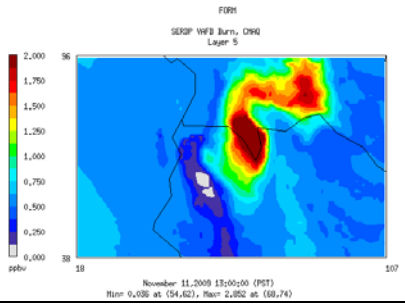	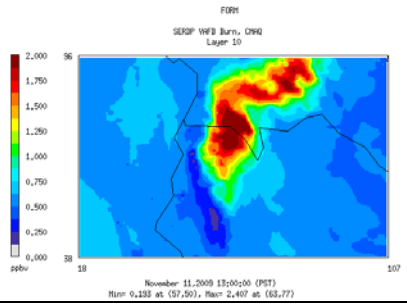
2 pm	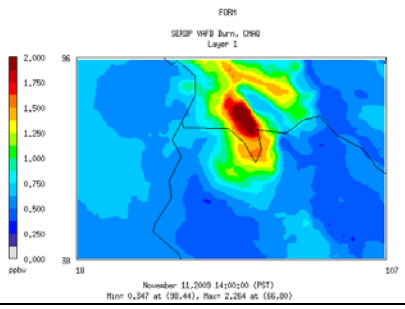	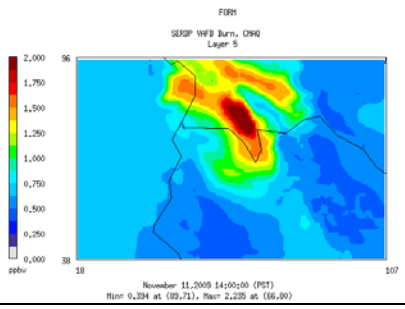	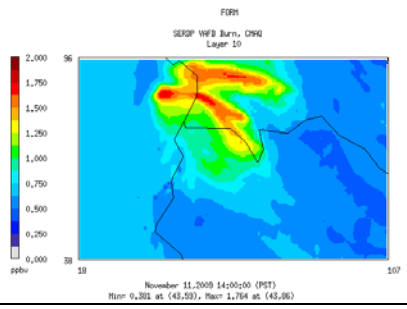

Figure 2d. Formaldehyde (HCHO) hourly spatial concentrations at three different vertical layers between 10am to 2pm PST.

O3	Layer 1 (~40m)	Layer 5 (~230m)	Layer 10 (~800m)
10 am	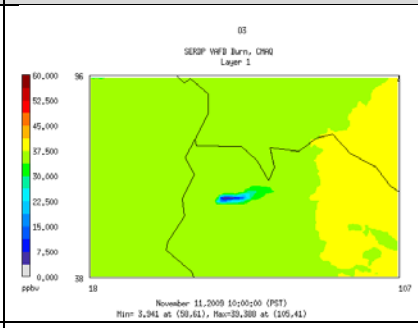	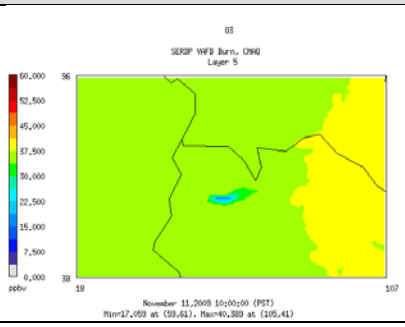	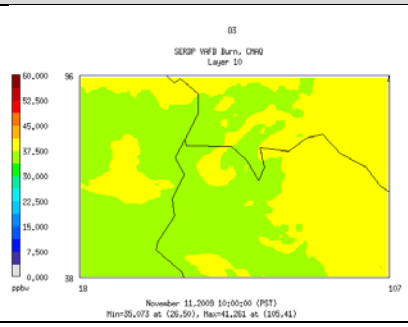
11 am	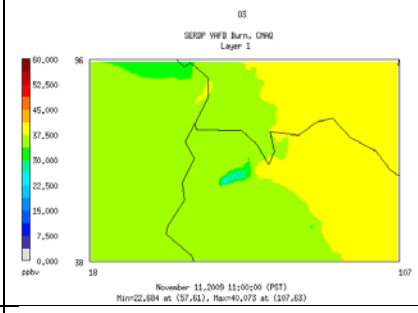	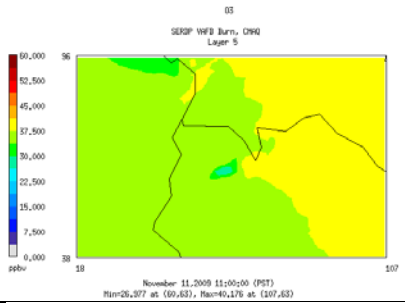	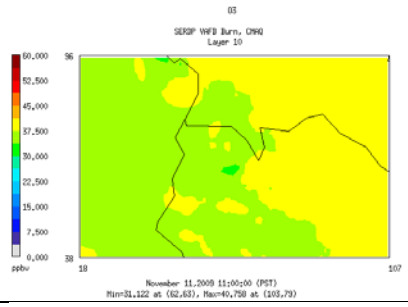
12 pm	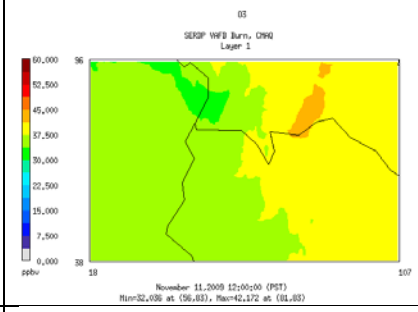	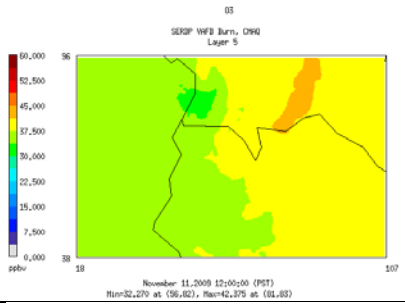	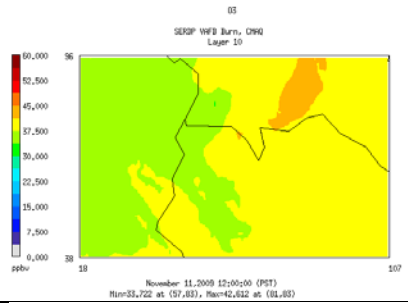
1 pm	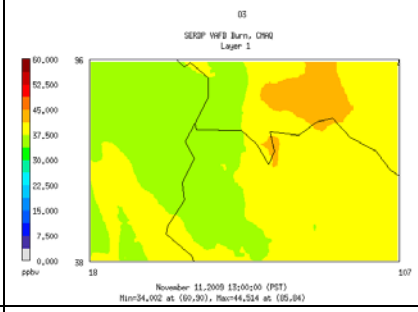	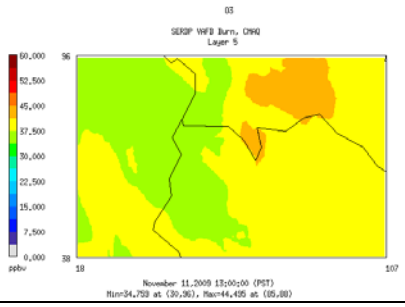	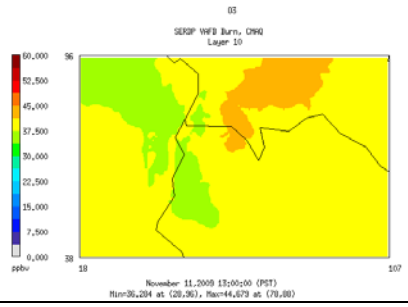
2 pm	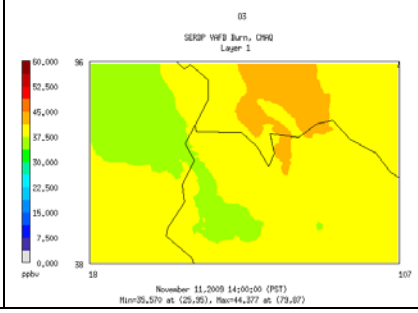	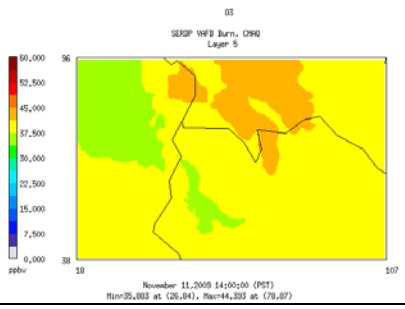	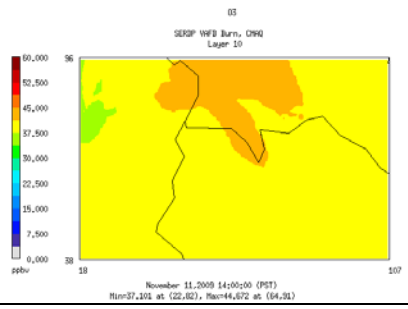

Figure 2c. O3 hourly spatial concentrations at three different vertical layers between 10am to 2pm PST.

HONO	Layer 1 (~40m)	Layer 5 (~230m)	Layer 10 (~800m)
10 am	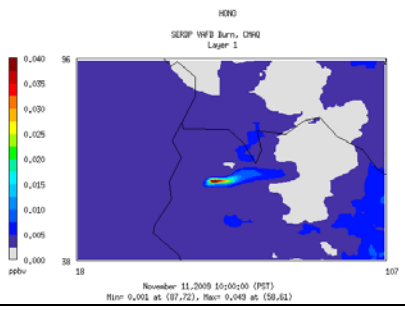	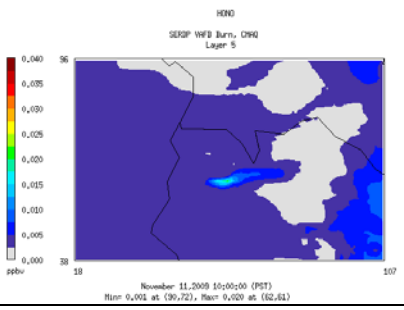	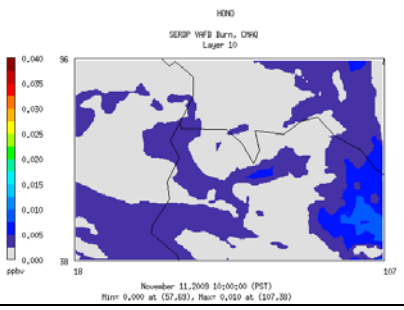
11 am	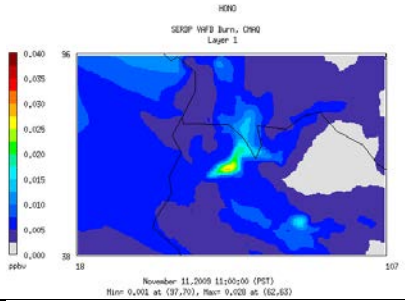	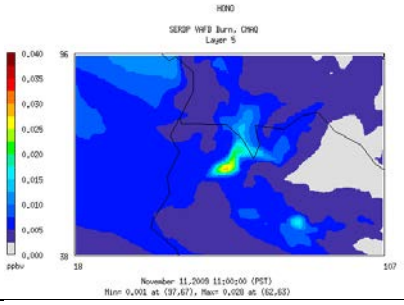	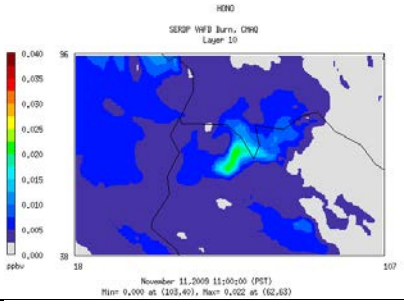
12 pm	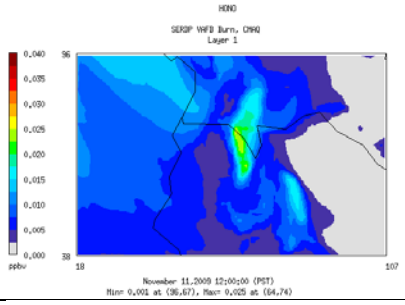	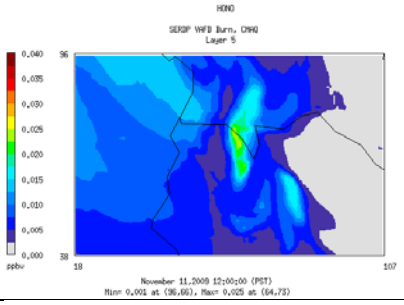	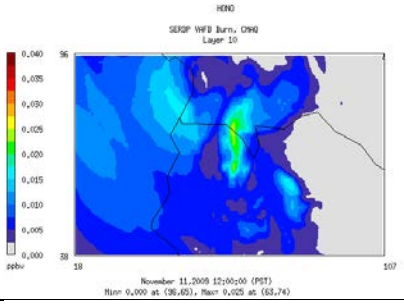
1 pm	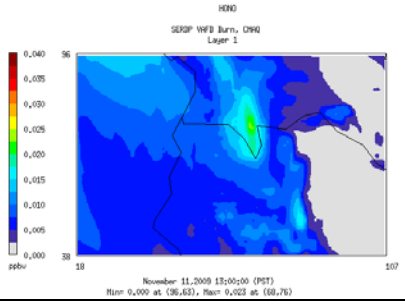	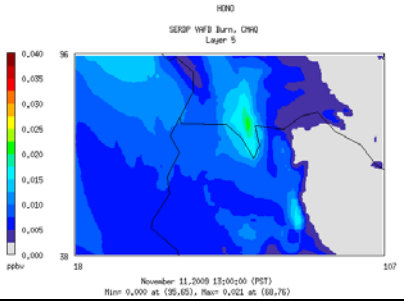	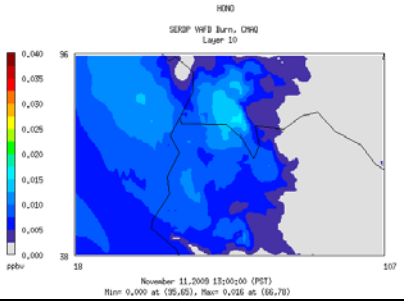
2 pm	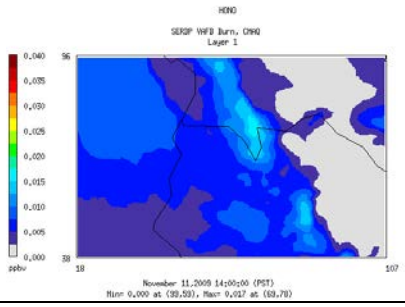	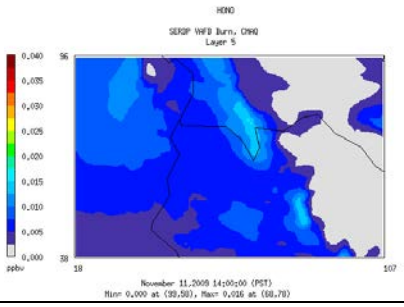	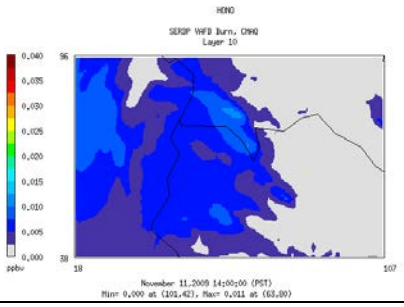

Figure 2e. HONO hourly spatial concentrations at three different vertical layers between 10am to 2pm PST.

OC	Layer 1 (~40m)	Layer 5 (~230m)	Layer 10 (~800m)
10 am	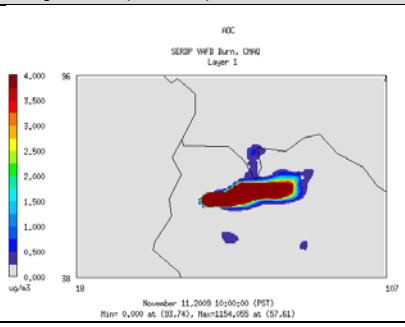	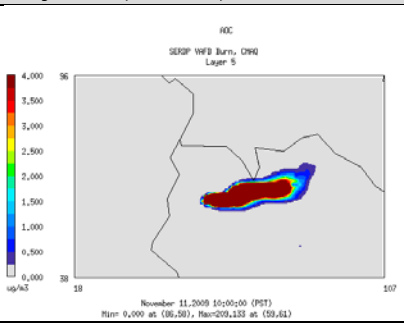	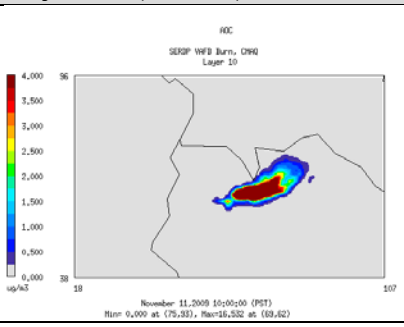
11 am	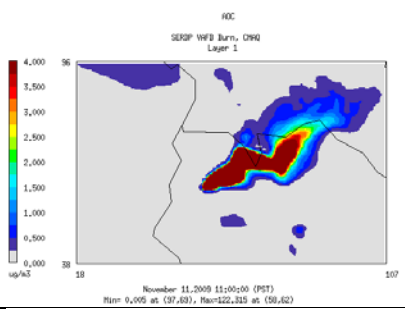	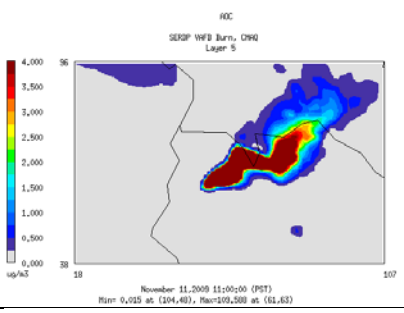	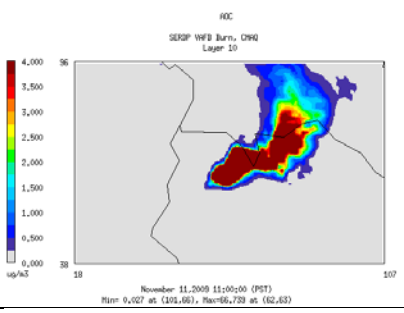
12 pm	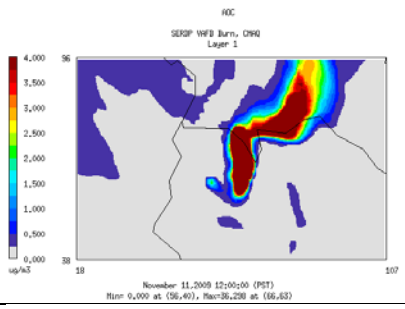	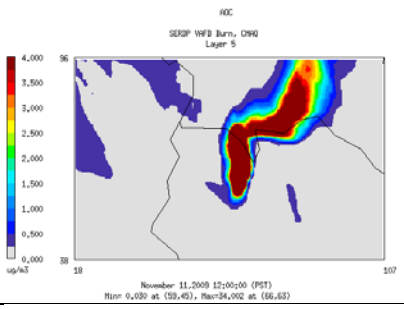	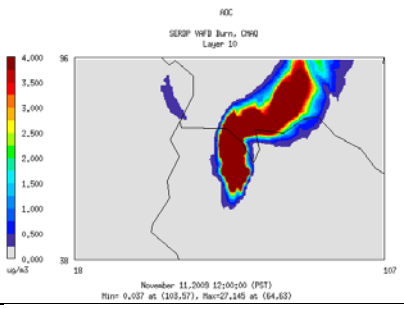
1 pm	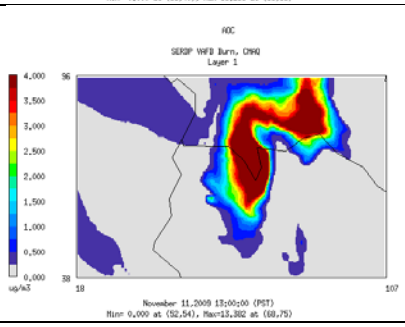	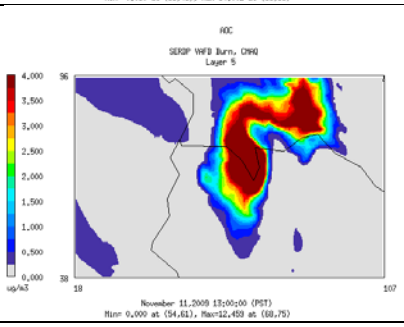	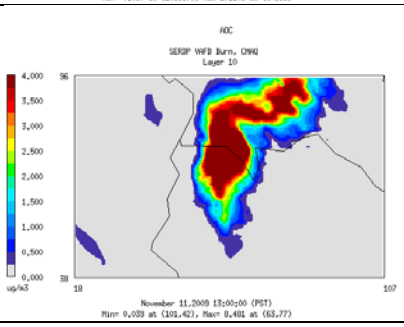
2 pm	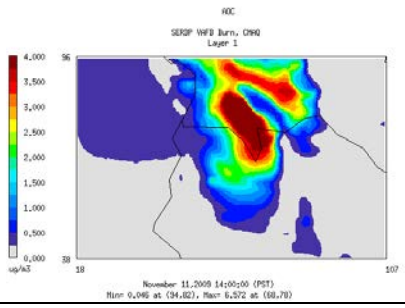	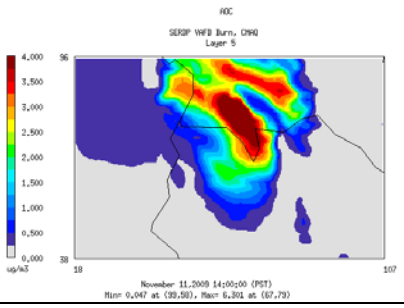	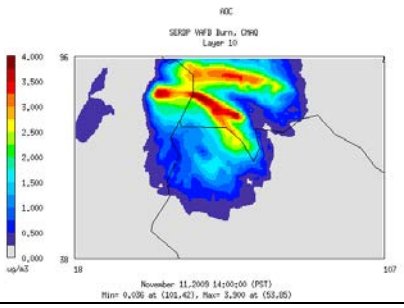

Figure 2f. Particulate Organic Carbon (OC) hourly spatial concentrations at three different vertical layers between 10am to 2pm PST.

EC	Layer 1 (~40m)	Layer 5 (~230m)	Layer 10 (~800m)
10 am	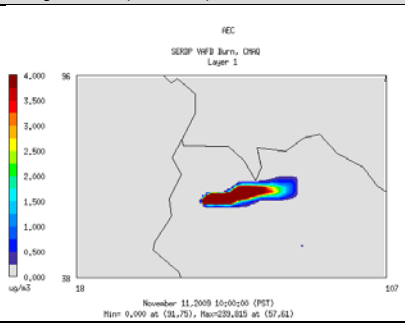	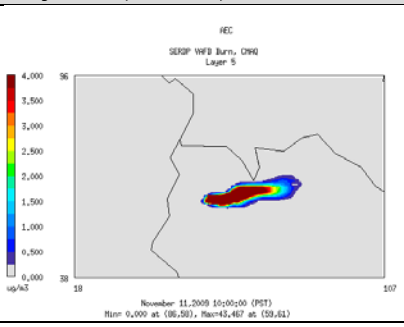	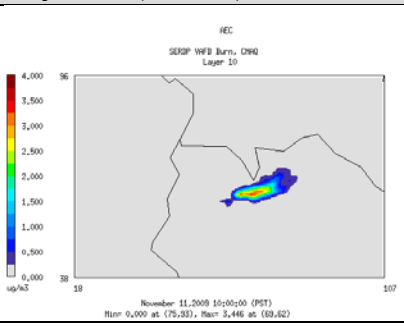
11 am	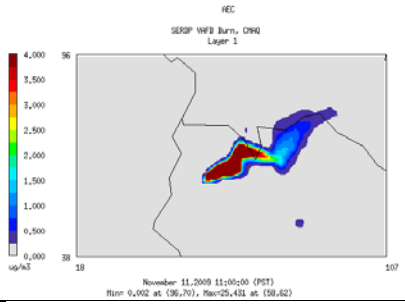	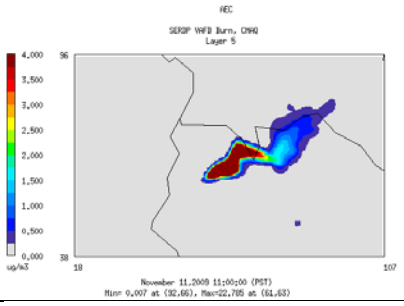	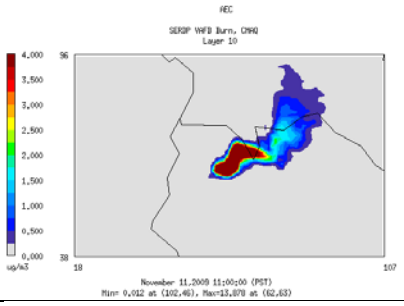
12 pm	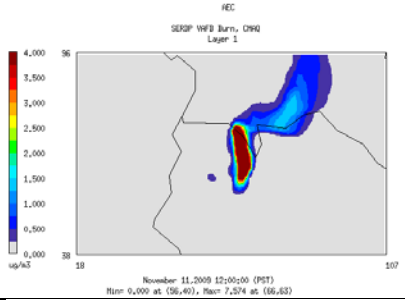	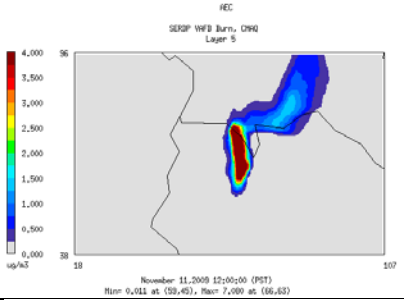	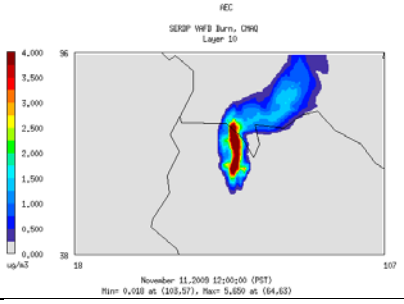
1 pm	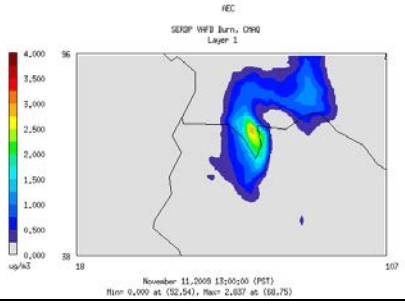	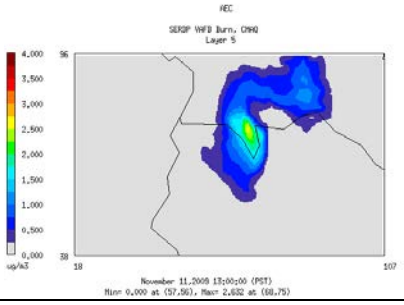	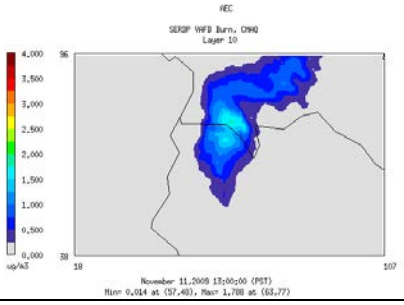
2 pm	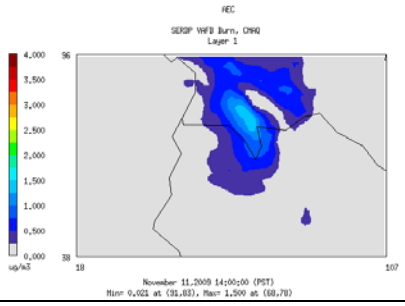	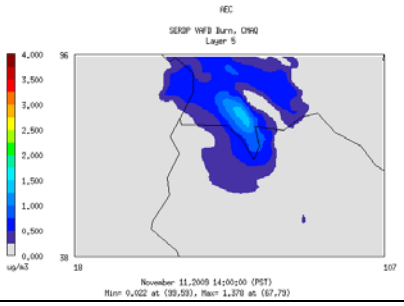	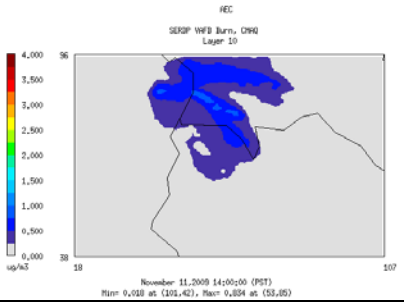

Figure 2g. Particulate Elemental Carbon (EC) hourly spatial concentrations at three different vertical layers between 10am to 2pm PST.

SO4	Layer 1 (~40m)	Layer 5 (~230m)	Layer 10 (~800m)
10 am	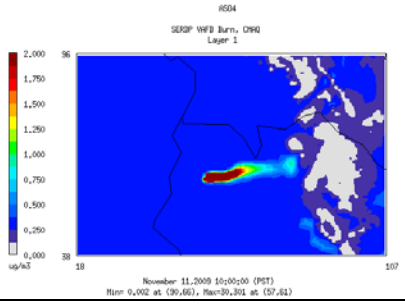	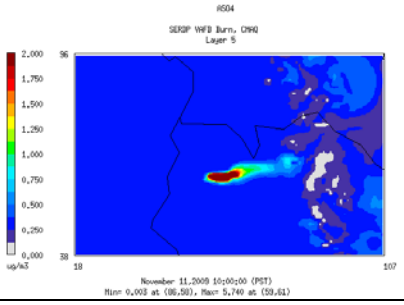	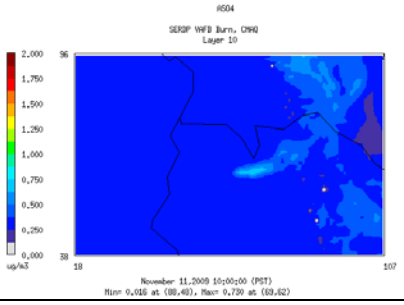
11 am	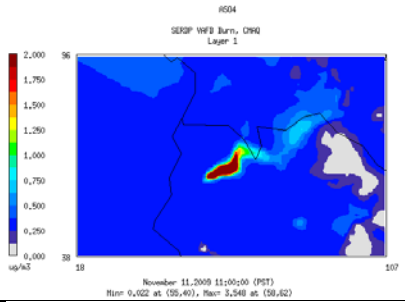	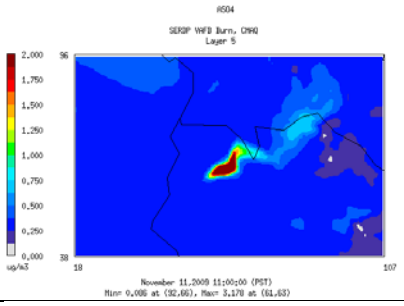	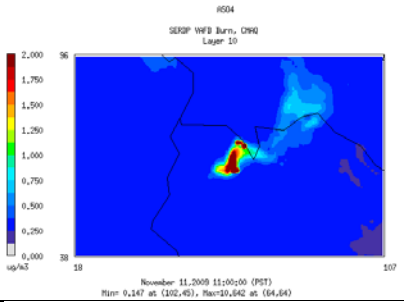
12 pm	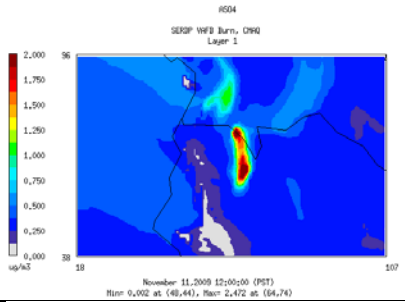	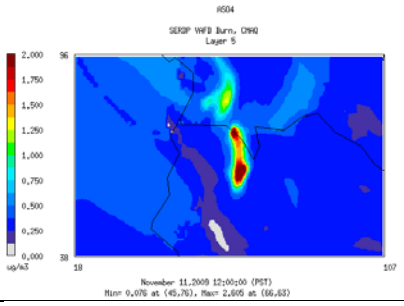	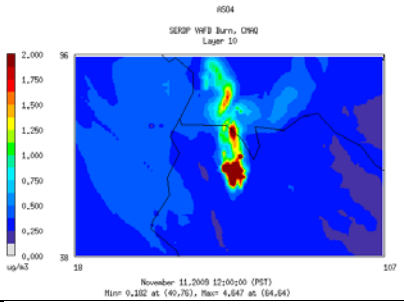
1 pm	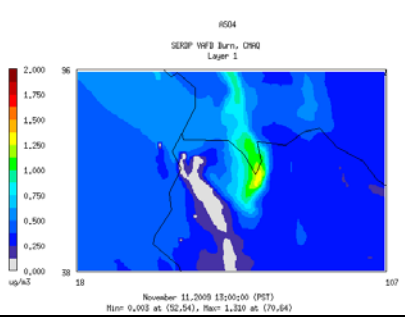	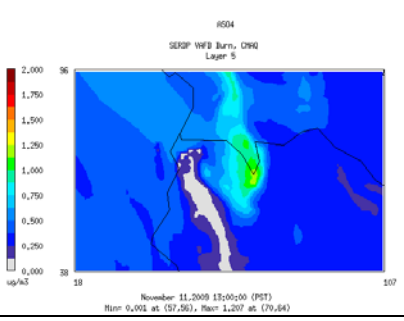	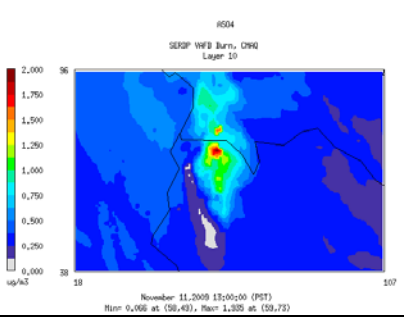
2 pm	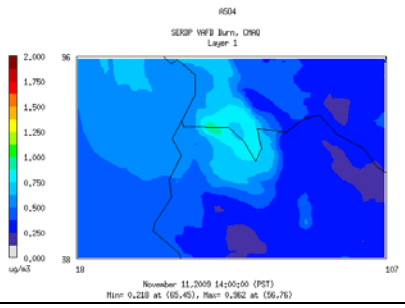	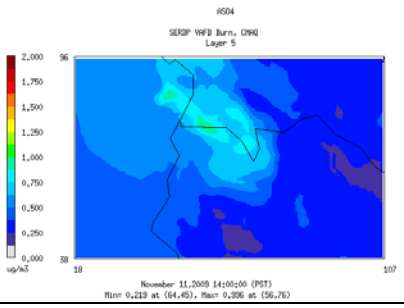	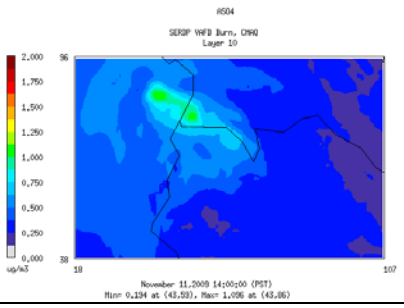

Figure 2h. Particulate Sulfate (SO4) hourly spatial concentrations at three different vertical layers between 10am to 2pm PST.

NO3	Layer 1 (~40m)	Layer 5 (~230m)	Layer 10 (~800m)
10 am	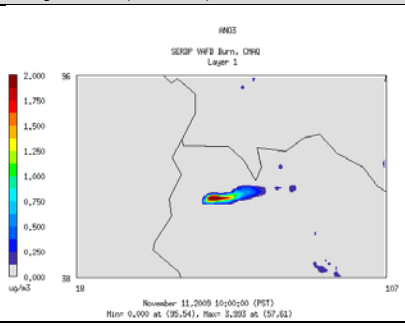	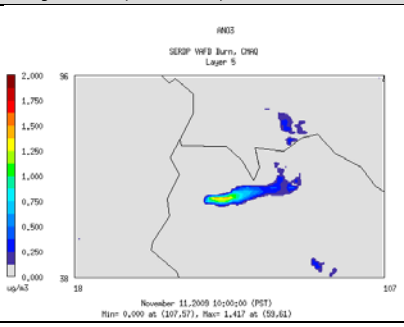	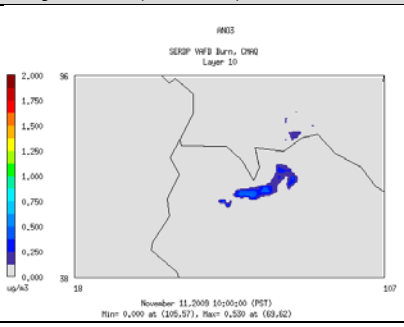
11 am	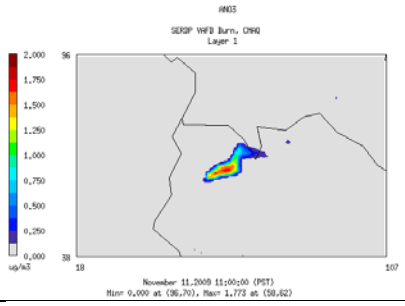	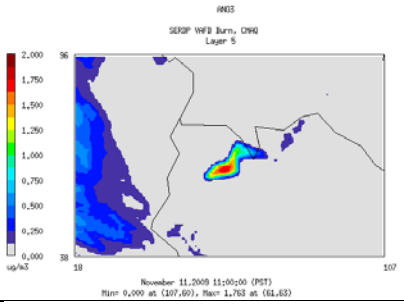	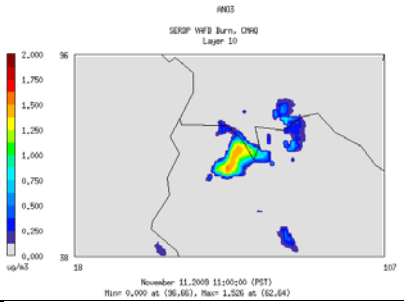
12 pm	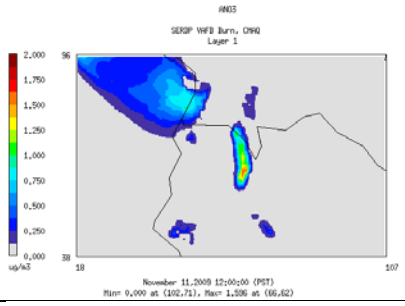	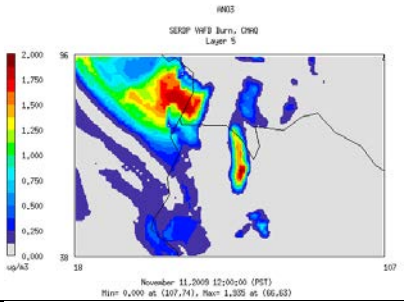	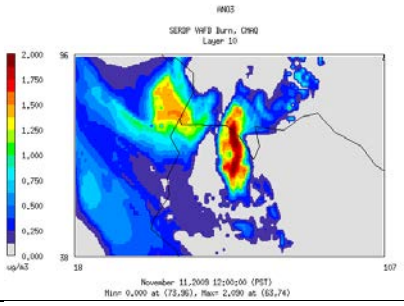
1 pm	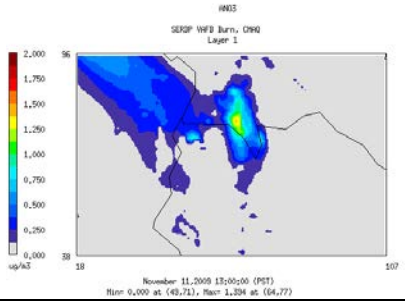	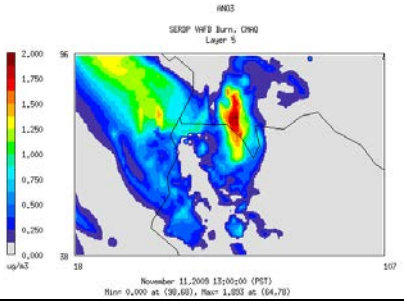	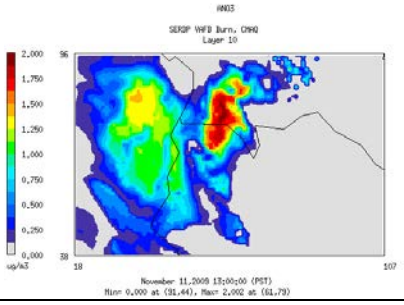
2 pm	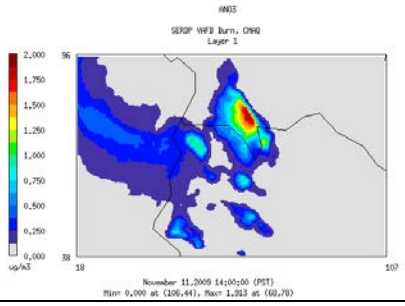	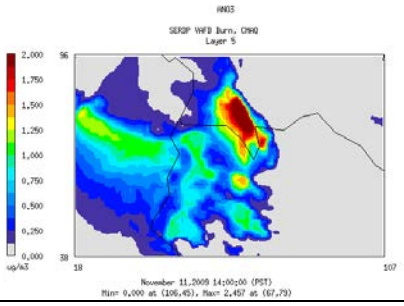	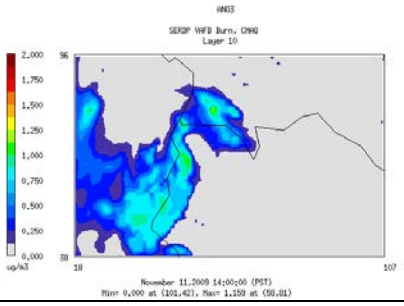

Figure 2i. Particulate Nitrate (NO3) hourly spatial concentrations at three different vertical layers between 10am to 2pm PST.

NH4	Layer 1 (~40m)	Layer 5 (~230m)	Layer 10 (~800m)
10 am	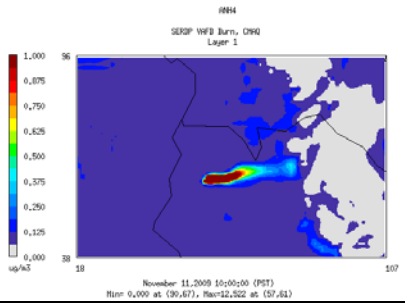	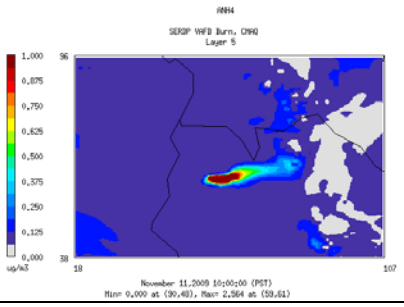	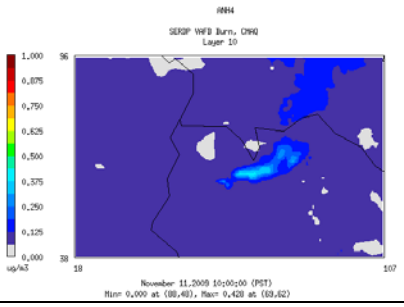
11 am	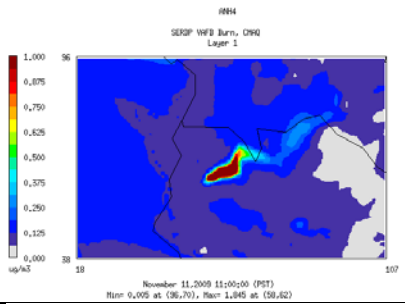	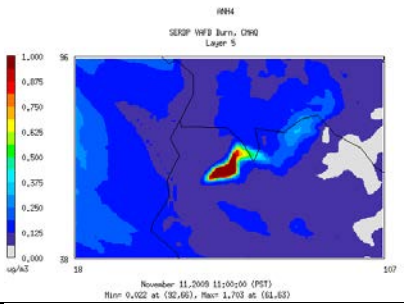	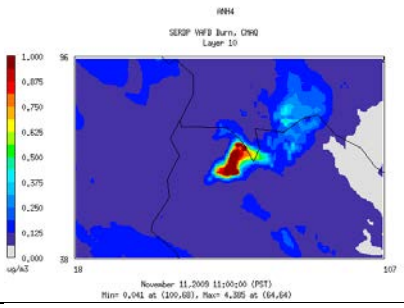
12 pm	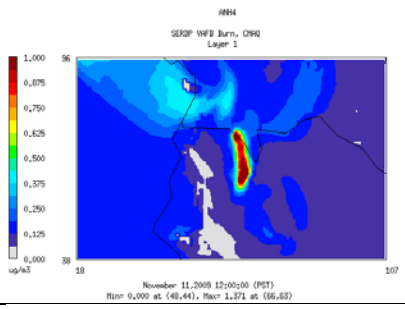	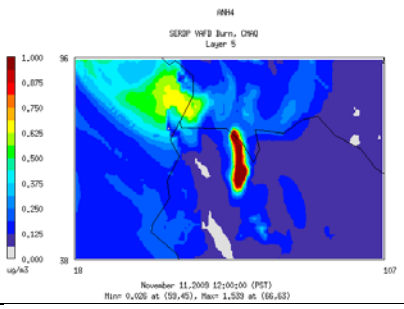	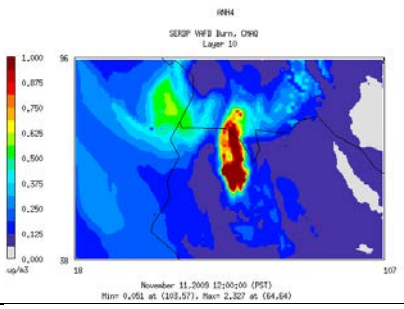
1 pm	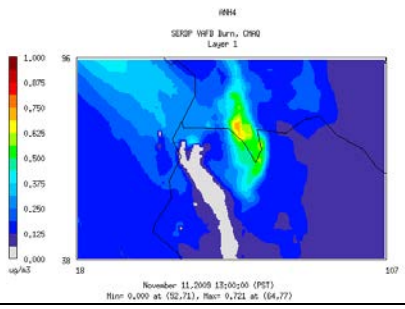	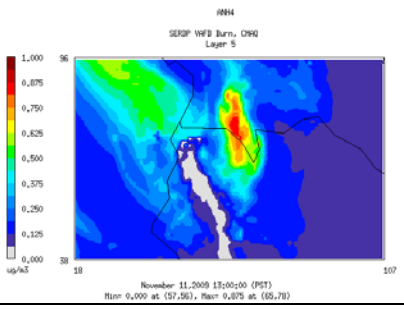	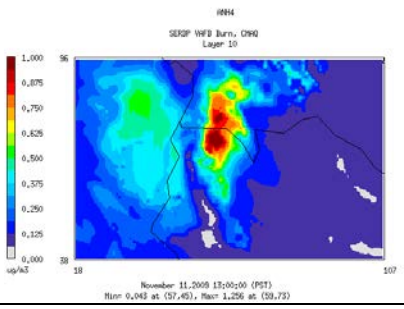
2 pm	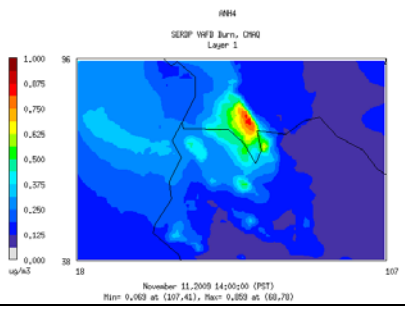	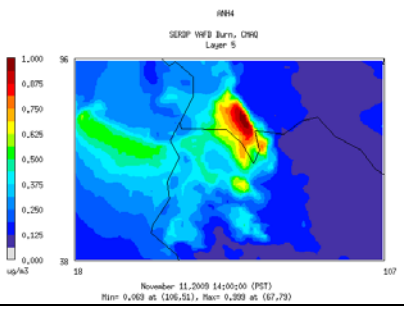	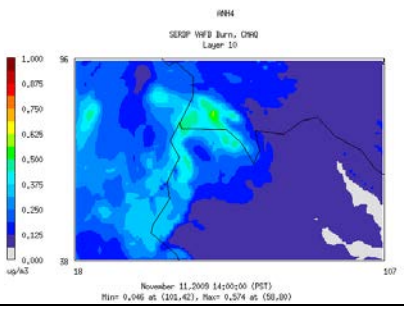

Figure 2j. Particulate Ammonium (NH4) hourly spatial concentrations at three different vertical layers between 10am to 2pm PST.

PM25	Layer 1 (~40m)	Layer 5 (~230m)	Layer 10 (~800m)
10 am	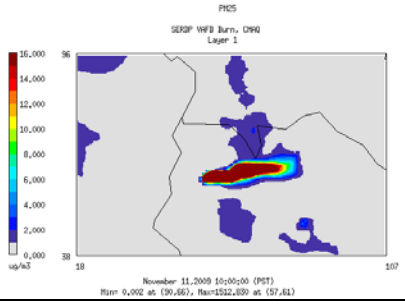	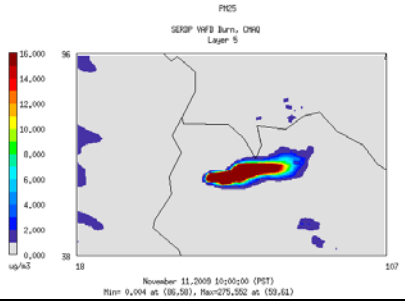	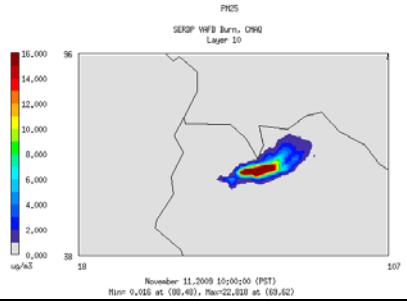
11 am	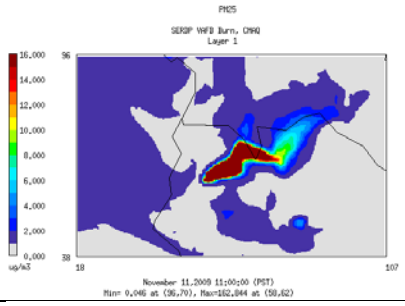	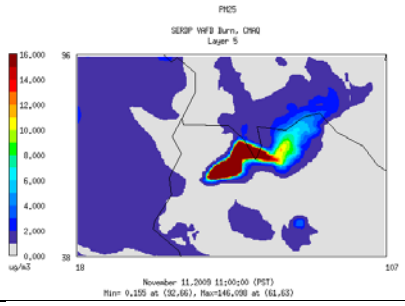	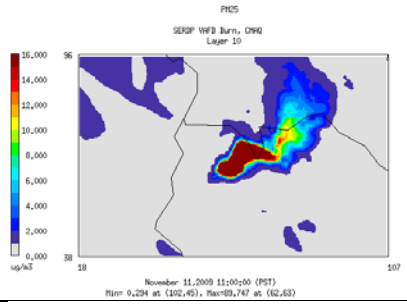
12 pm	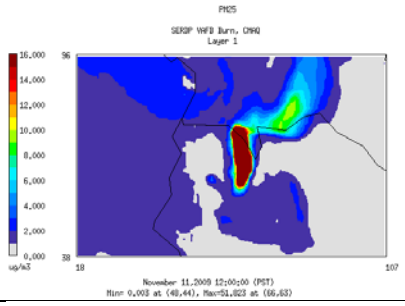	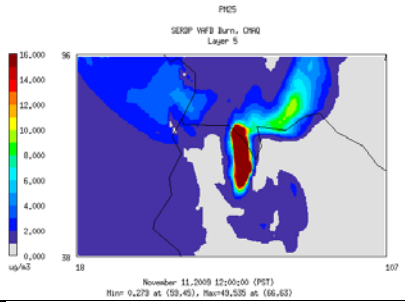	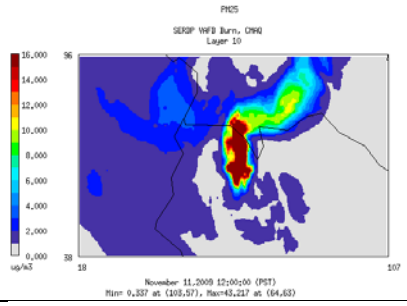
1 pm	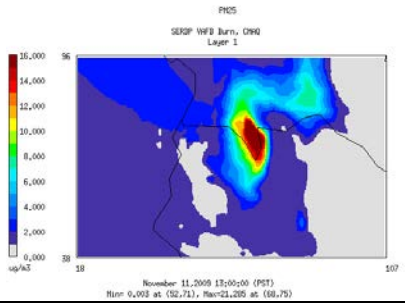	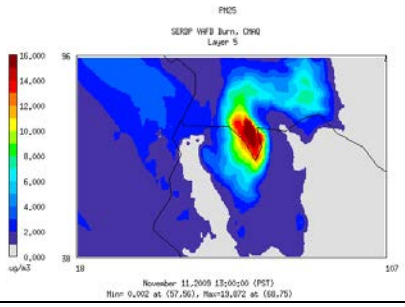	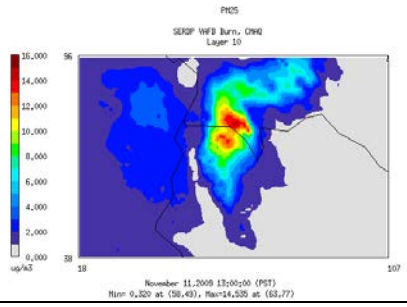
2 pm	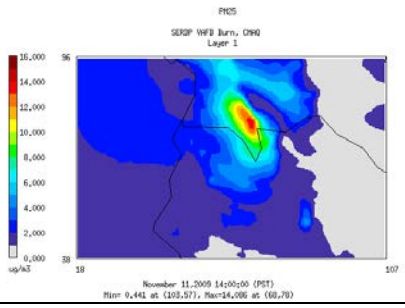	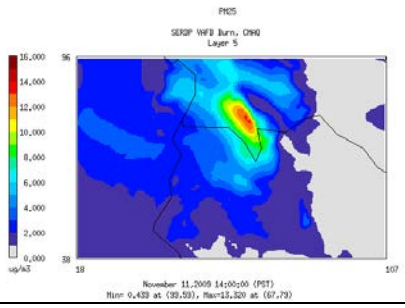	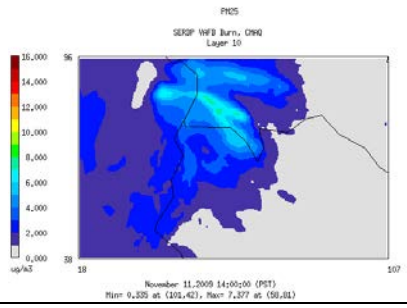

Figure 2k. PM25 hourly spatial concentrations at three different vertical layers between 10am to 2pm PST.

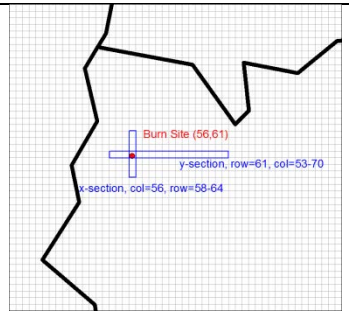

First 15 Levels at Column 56, Rows 58-64 (X cross-section)

	10 AM	11 AM	12 PM
CO	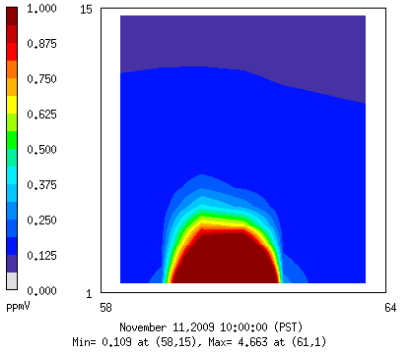	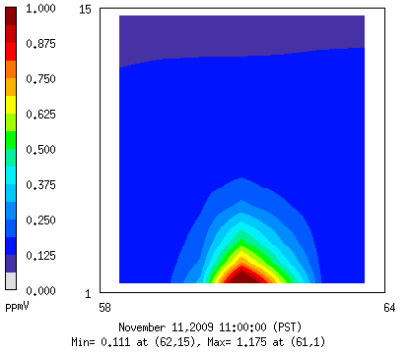	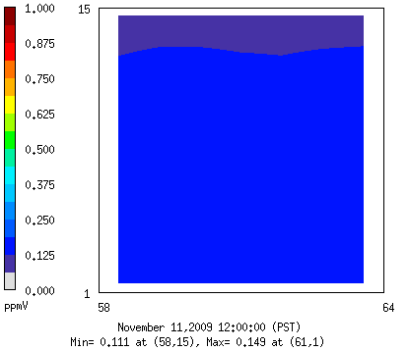
NOx	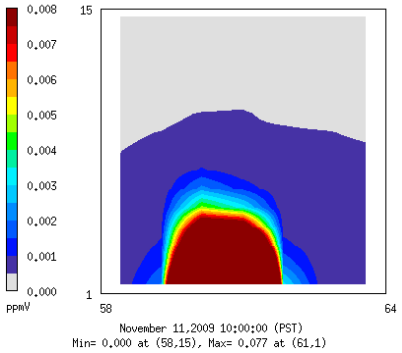	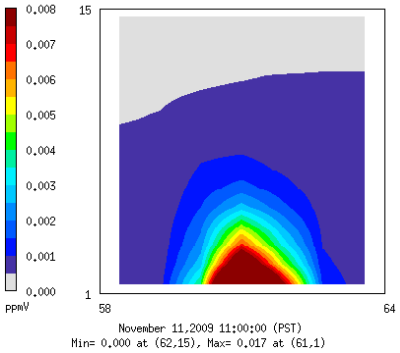	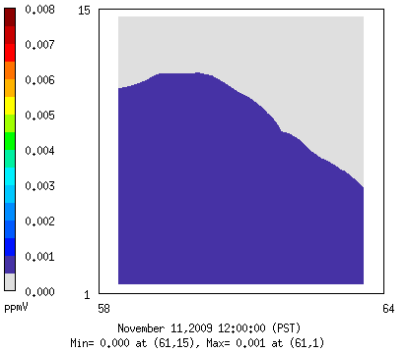

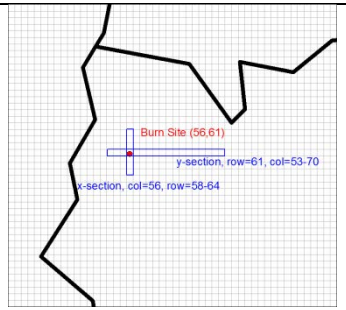

	First 15 Levels at Row 61, Columns 53-70 (Y cross-section)		
	10 AM	**11 AM**	**12 PM**
CO	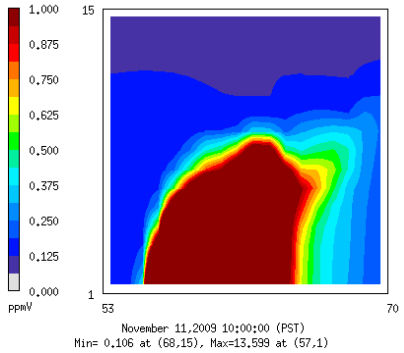	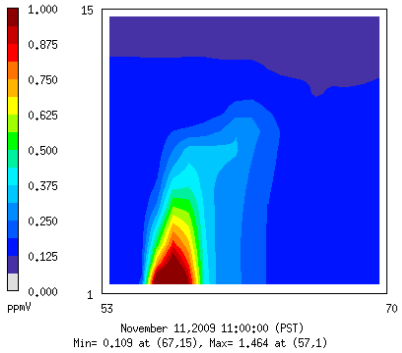	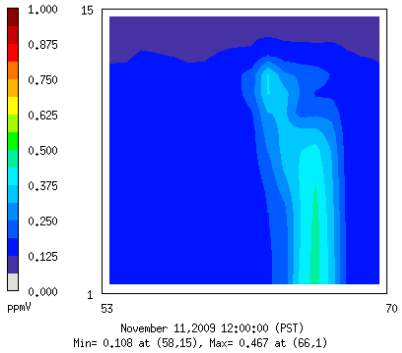
NOx	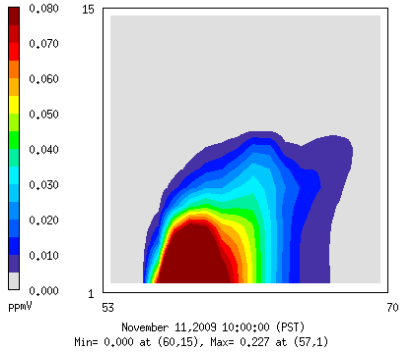	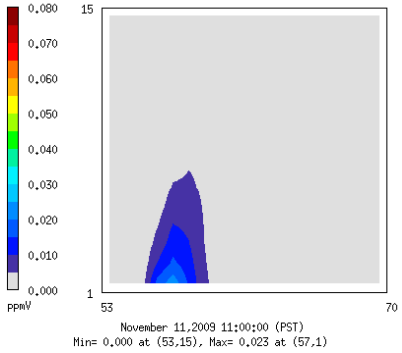	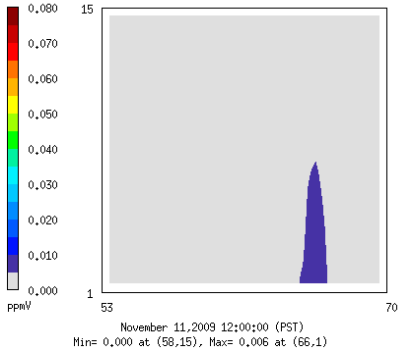

Figure 3a,b . Vertical concentration profiles of CO and NOx at locations 9(In both X-Y sections) near fire burn site.

Table 1: Corresponding sampling data to model grid cells

AFV Burn Location						AQ Model Grid Cells		
sample	**local time (hhmmss)**	**lon**	**lat**	**height (m)**	**Distance (km)**	**icol**	**jrow**	**layer**
Burn site		-120.517	34.8000	-	-	56	61	-
AMS Truck		-120.524	34.7928	Ground		56	60	1
FASS Tower		-120.315	34.4760	228		63	31	4
Aircraft Data								
s01	112124	-120.528	34.7928	559	0.94	55	60	8
s02	112823	-120.527	34.7901	214	1.23	55	60	4
s03	113430	-120.528	34.7888	196	1.37	55	60	4
s04	114053	-120.529	34.7899	197	1.29	55	60	4
s05	114752	-120.527	34.7946	236	0.72	56	60	5
s06	115233	-120.523	34.7951	241	0.66	56	60	6
s07	120002	-120.531	34.7916	233	1.17	55	60	6
s08	120348	-120.527	34.7916	260	1.05	56	60	6
s09	121124	-120.526	34.8032	544	0.30	56	61	9
s10	121700	-120.524	34.7947	695	0.69	56	60	10
s11	121927	-120.547	34.8675	682	7.69	56	66	10
s12	123036	-120.537	34.8368	649	4.16	56	64	10
s13	123658	-120.523	34.8037	1223	0.36	56	61	13
s14	124211	-120.522	34.8049	1232	0.51	56	61	13
s15	125337	-120.516	34.8383	1237	4.24	57	64	13
s16	125731	-120.519	34.8223	568	2.45	57	62	9
s17	130531	-120.513	34.8803	1452	8.91	58	67	13
s18	132215	-120.507	34.8981	1466	10.96	59	68	13
s19	145250	-120.502	34.8084	1405	2.26	58	61	13
s20	145836	-120.510	34.8157	784	2.12	57	62	9
s21	150248	-120.518	34.8001	538	0.62	56	61	9
s22	151202	-120.512	34.8016	552	1.17	57	61	9
s23	151544	-120.521	34.7976	296	0.48	56	60	6
s24	152246	-120.516	34.8031	508	0.85	56	61	9
s25	152744	-120.513	34.8019	546	1.04	57	61	9
s26	153217	-120.505	34.8009	457	1.82	57	60	8
s27	153631	-120.518	34.8024	474	0.63	56	61	9
s28	155219	-120.515	34.8044	346	0.94	57	61	7
s29	155803	-120.523	34.8022	376	0.20	56	61	7

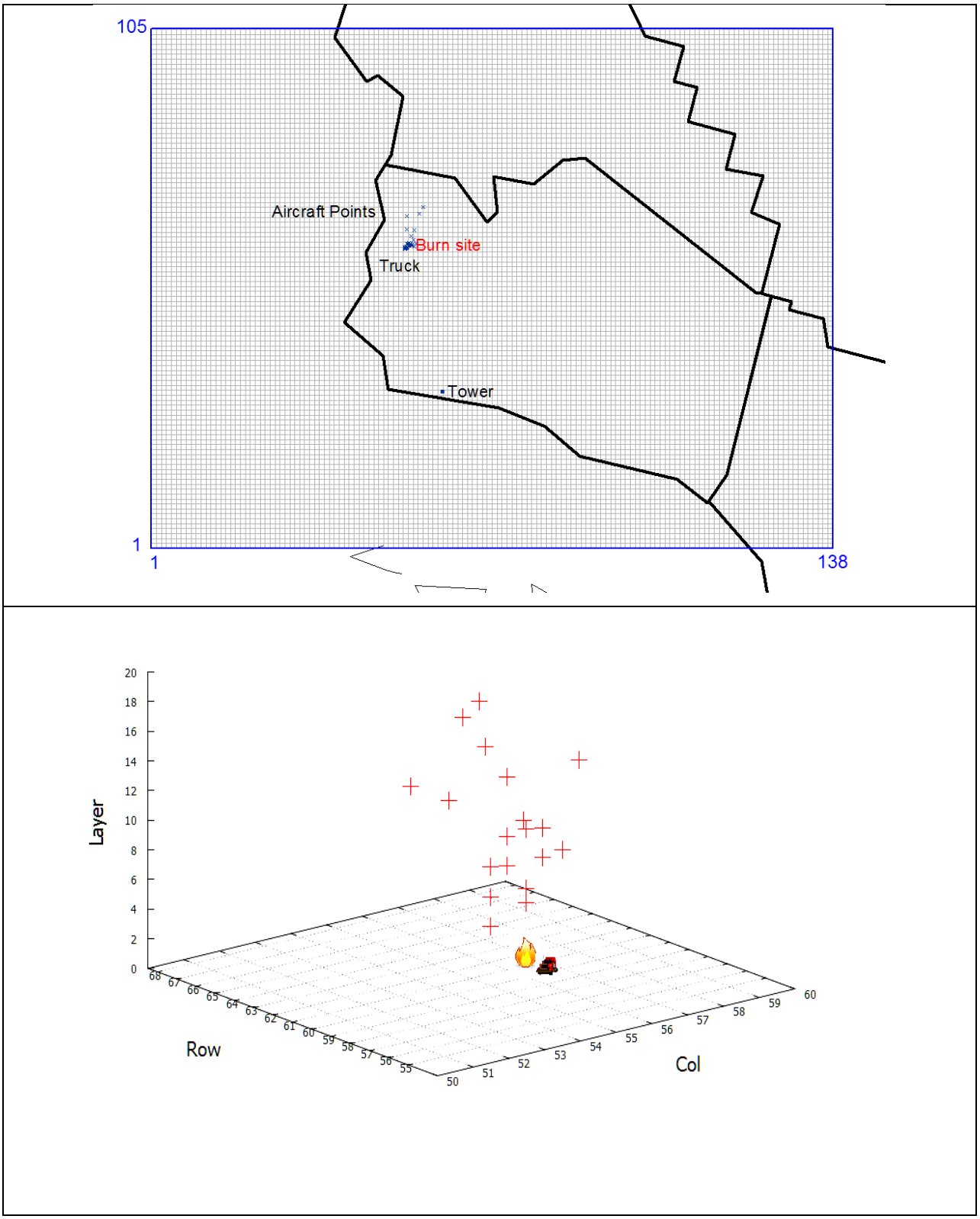

Figure 4. Aircraft sampling (+), AMS-Truck sampling, and fire burn locations relative to CMAQ modeling grid cells. Top: 2D locations, Bottom: 3D locations (note: FASS Tower sampling location not shown in 3D locations)

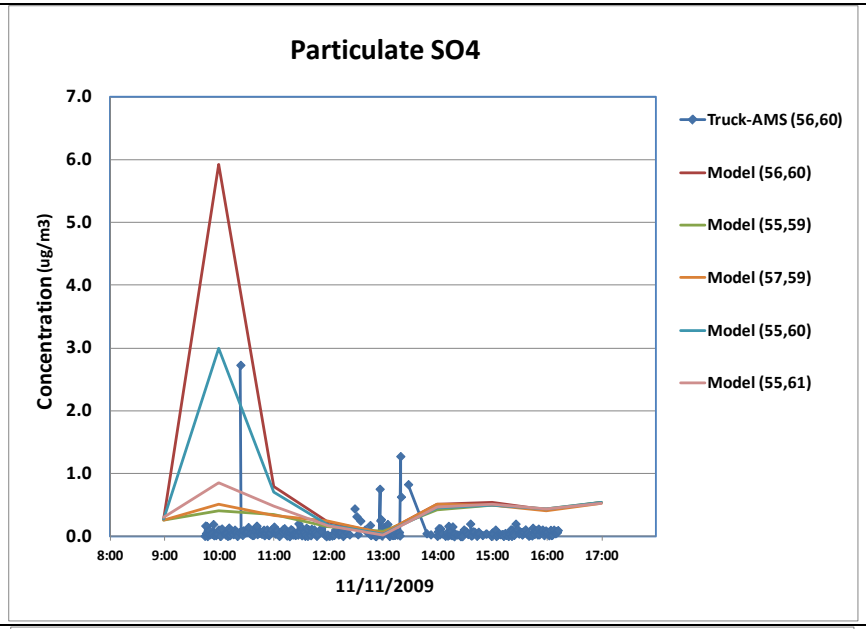

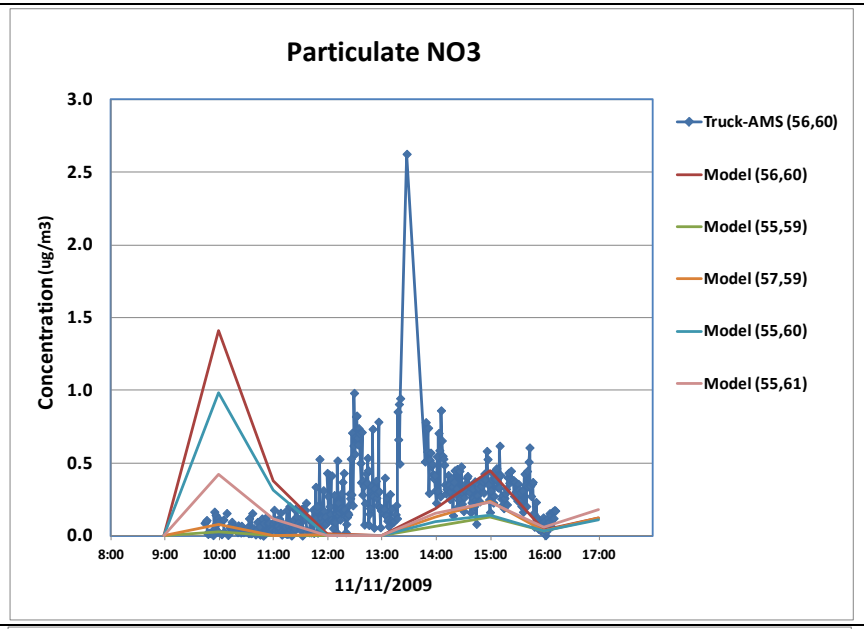

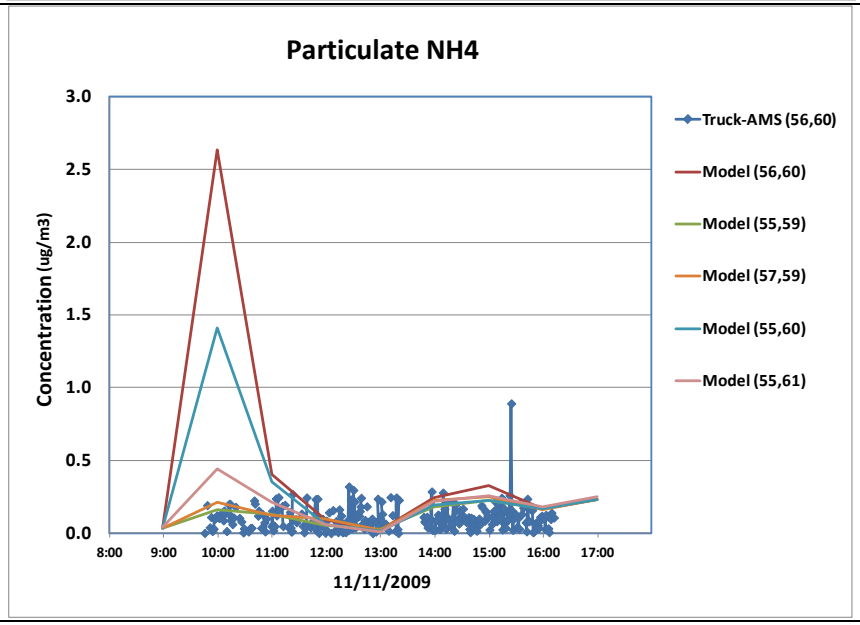

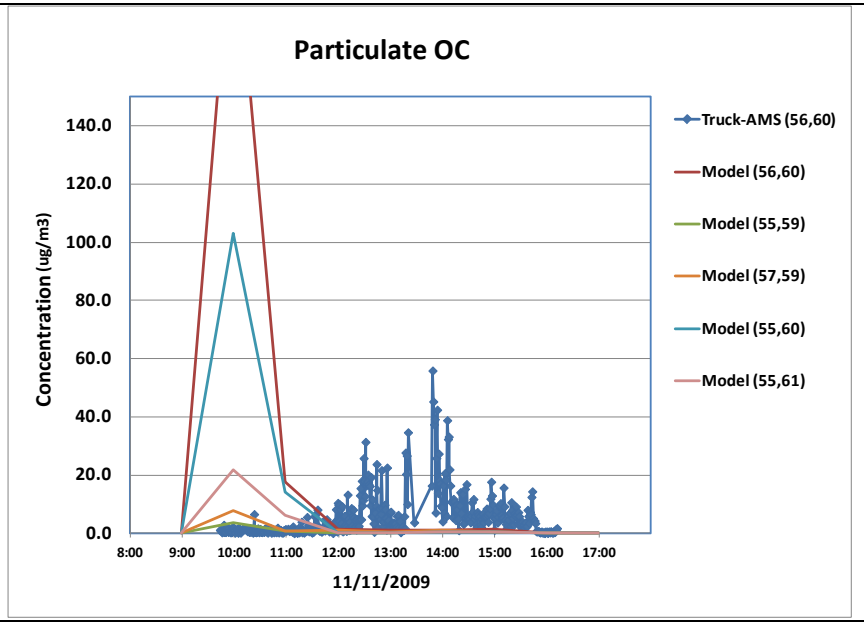

Figure 5. Truck AMS sampling data vs. various model results at nearby grid cells.

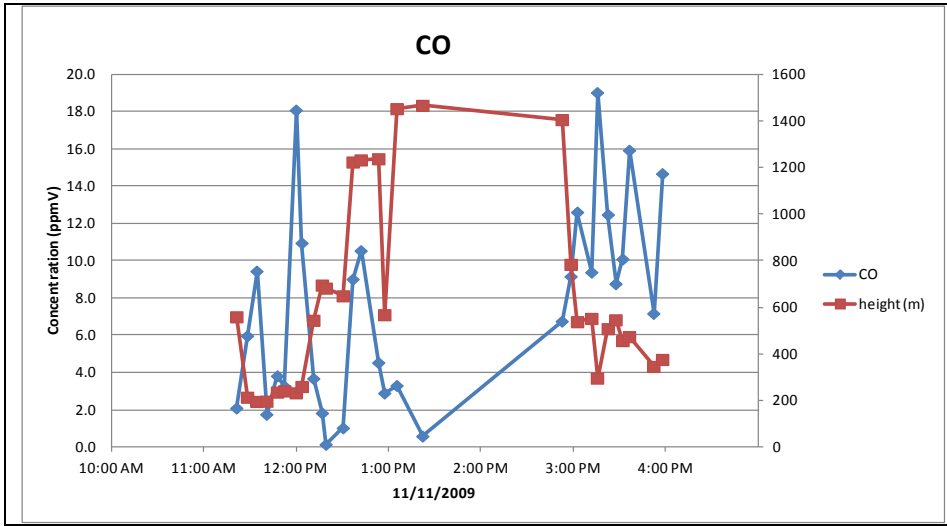
CO
Concentration (ppmV)
20.0
18.0
16.0
14.0
12.0
10.0
8.0
6.0
4.0
2.0
0.0
1600
1400
1200
1000
800
600
400
200
0
10:00 AM
11:00 AM
12:00 PM
1:00 PM
2:00 PM
3:00 PM
4:00 PM
11/11/2009
CO
height (m)

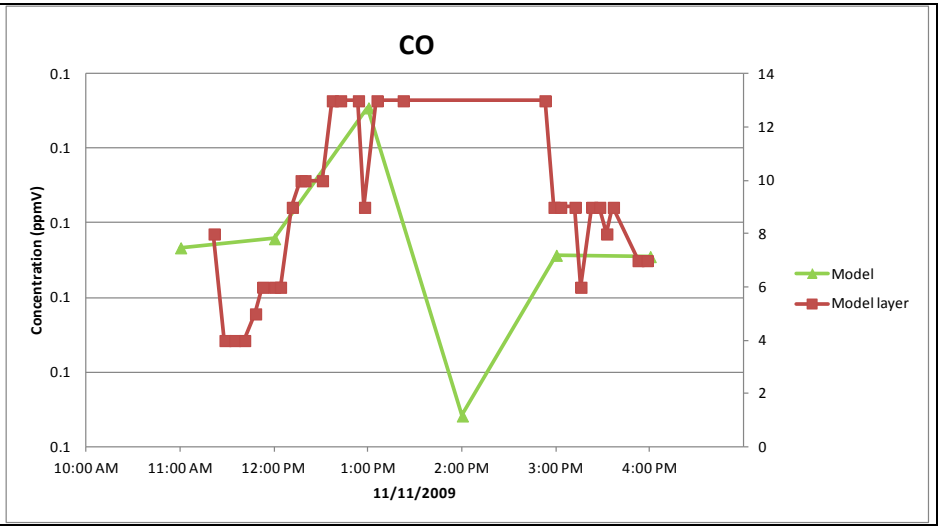
CO
Concentration (ppmV)
0.1
0.1
0.1
0.1
0.1
14
12
10
8
6
4
2
0
10:00 AM
11:00 AM
12:00 PM
1:00 PM
2:00 PM
3:00 PM
4:00 PM
11/11/2009
Model
Model layer

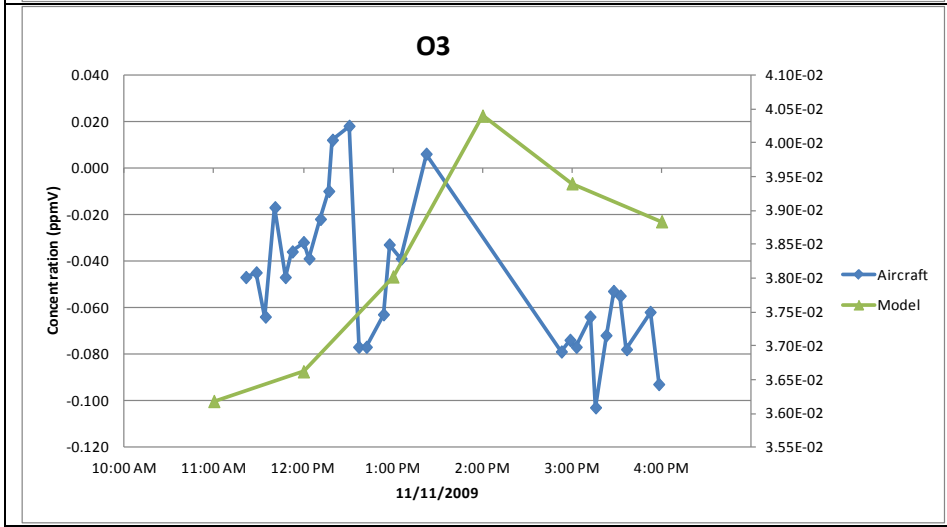
O3
Concentration (ppmV)
0.040
0.020
0.000
-0.020
-0.040
-0.060
-0.080
-0.100
-0.120
4.10E-02
4.05E-02
4.00E-02
3.95E-02
3.90E-02
3.85E-02
3.80E-02
3.75E-02
3.70E-02
3.65E-02
3.60E-02
3.55E-02
10:00 AM
11:00 AM
12:00 PM
1:00 PM
2:00 PM
3:00 PM
4:00 PM
11/11/2009
Aircraft
Model

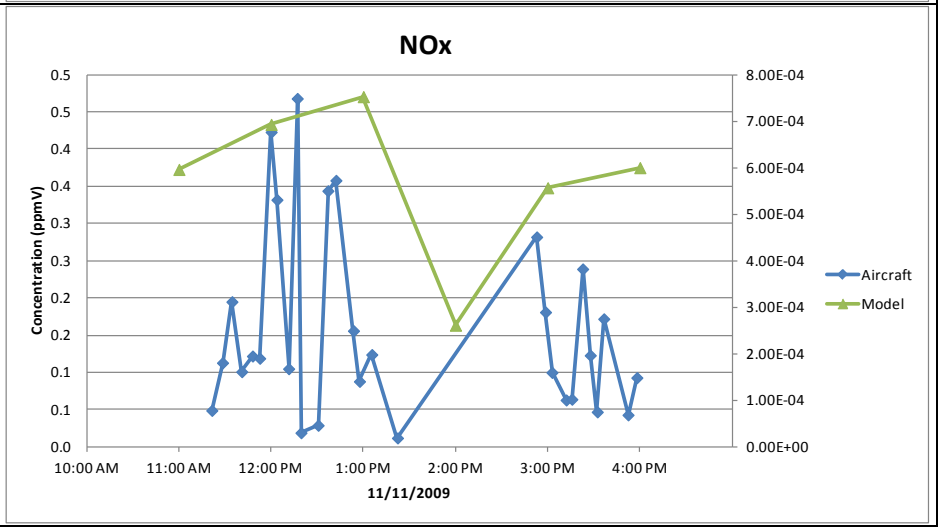
NOx
Concentration (ppmV)
0.5
0.5
0.4
0.4
0.3
0.3
0.2
0.2
0.1
0.1
0.0
8.00E-04
7.00E-04
6.00E-04
5.00E-04
4.00E-04
3.00E-04
2.00E-04
1.00E-04
0.00E+00
10:00 AM
11:00 AM
12:00 PM
1:00 PM
2:00 PM
3:00 PM
4:00 PM
11/11/2009
Aircraft
Model

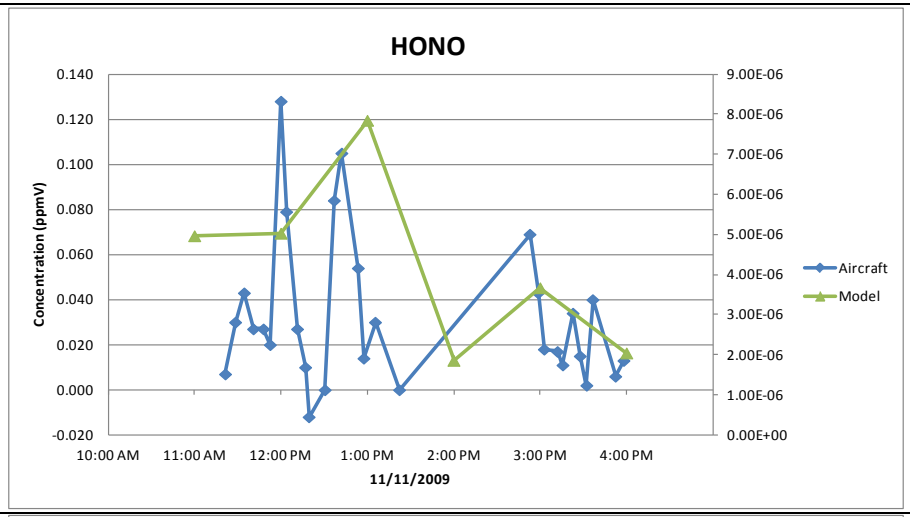
HONO
0.140
0.120
0.100
0.080
0.060
0.040
0.020
0.000
-0.020
9.00E-06
8.00E-06
7.00E-06
6.00E-06
5.00E-06
4.00E-06
3.00E-06
2.00E-06
1.00E-06
0.00E+00
Concentration (ppmV)
10:00 AM
11:00 AM
12:00 PM
1:00 PM
2:00 PM
3:00 PM
4:00 PM
11/11/2009
Aircraft
Model

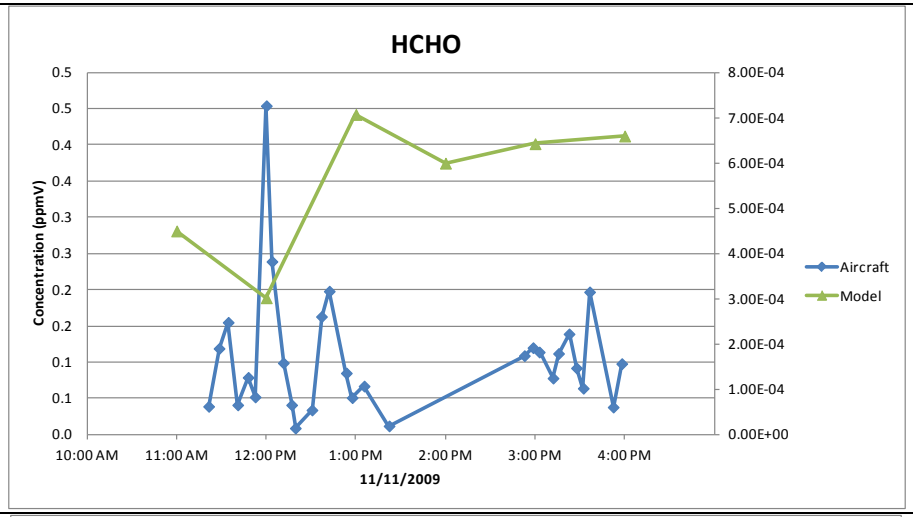
HCHO
0.5
0.5
0.4
0.4
0.3
0.3
0.2
0.2
0.1
0.1
0.0
8.00E-04
7.00E-04
6.00E-04
5.00E-04
4.00E-04
3.00E-04
2.00E-04
1.00E-04
0.00E+00
Concentration (ppmV)
10:00 AM
11:00 AM
12:00 PM
1:00 PM
2:00 PM
3:00 PM
4:00 PM
11/11/2009
Aircraft
Model

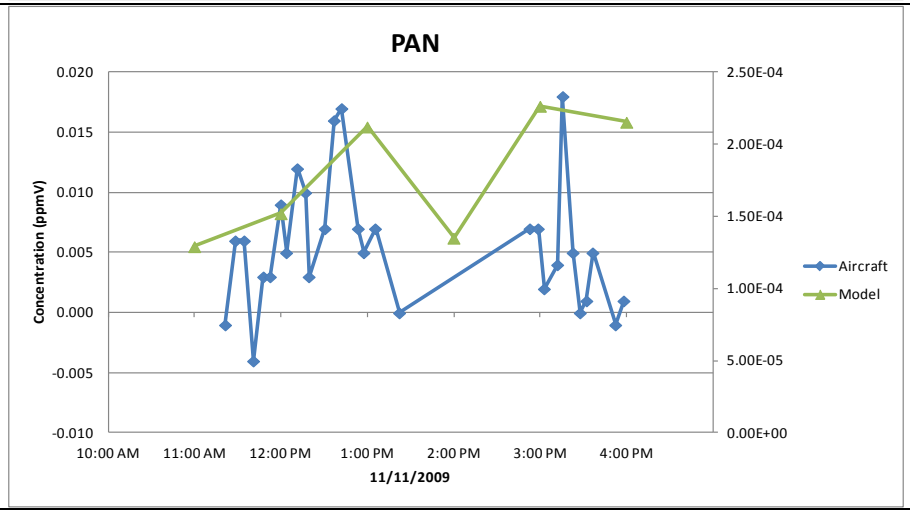
PAN
0.020
0.015
0.010
0.005
0.000
-0.005
-0.010
2.50E-04
2.00E-04
1.50E-04
1.00E-04
5.00E-05
0.00E+00
Concentration (ppmV)
10:00 AM
11:00 AM
12:00 PM
1:00 PM
2:00 PM
3:00 PM
4:00 PM
11/11/2009
Aircraft
Model

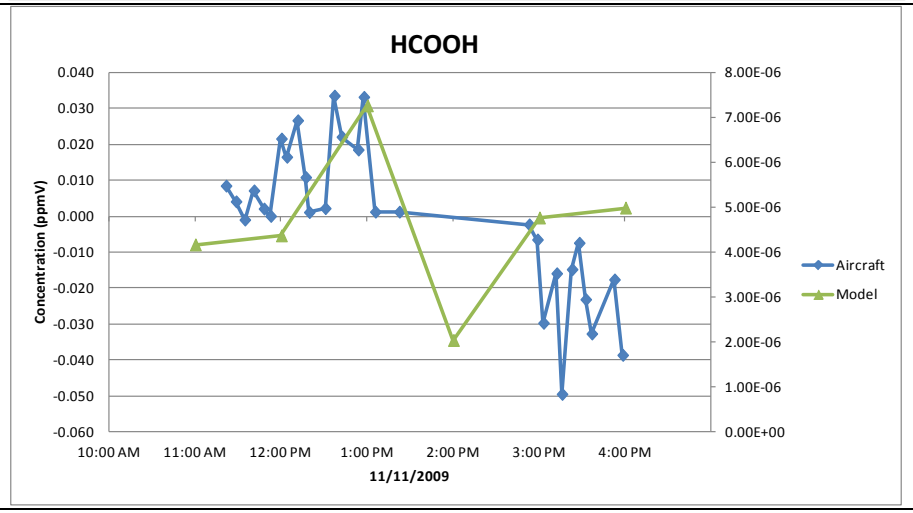
HCOOH
0.040
0.030
0.020
0.010
0.000
-0.010
-0.020
-0.030
-0.040
-0.050
-0.060
8.00E-06
7.00E-06
6.00E-06
5.00E-06
4.00E-06
3.00E-06
2.00E-06
1.00E-06
0.00E+00
Concentration (ppmV)
10:00 AM
11:00 AM
12:00 PM
1:00 PM
2:00 PM
3:00 PM
4:00 PM
11/11/2009
Aircraft
Model

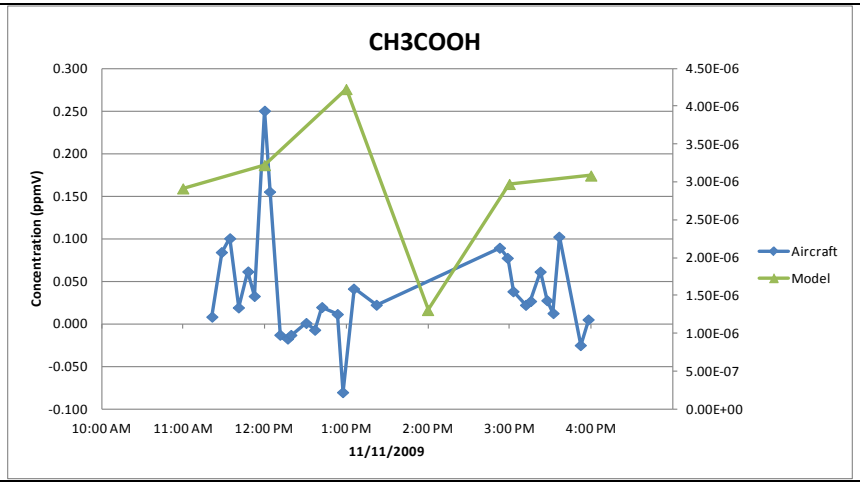

Figure 6a. Absolute values of aircraft data vs. model results (right axis)

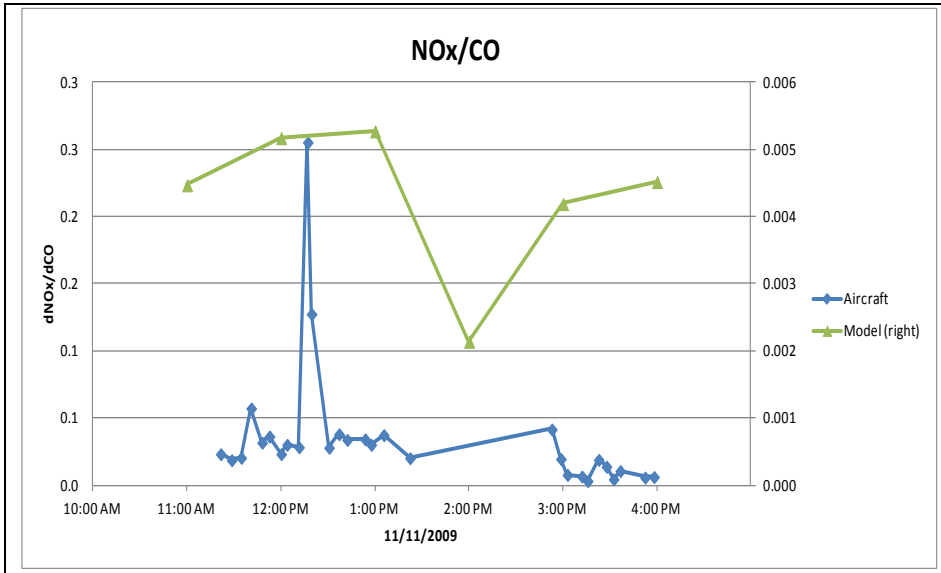
NOx/CO
dNOx/dCO
0.3
0.3
0.2
0.2
0.1
0.1
0.0
0.006
0.005
0.004
0.003
0.002
0.001
0.000
10:00 AM
11:00 AM
12:00 PM
1:00 PM
2:00 PM
3:00 PM
4:00 PM
11/11/2009
Aircraft
Model (right)

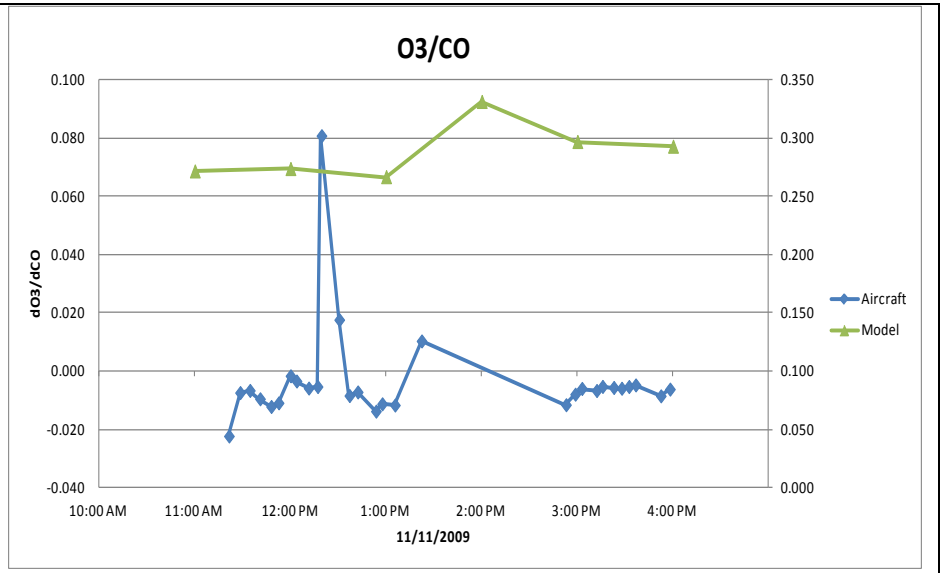
O3/CO
dO3/dCO
0.100
0.080
0.060
0.040
0.020
0.000
-0.020
-0.040
0.350
0.300
0.250
0.200
0.150
0.100
0.050
0.000
10:00 AM
11:00 AM
12:00 PM
1:00 PM
2:00 PM
3:00 PM
4:00 PM
11/11/2009
Aircraft
Model

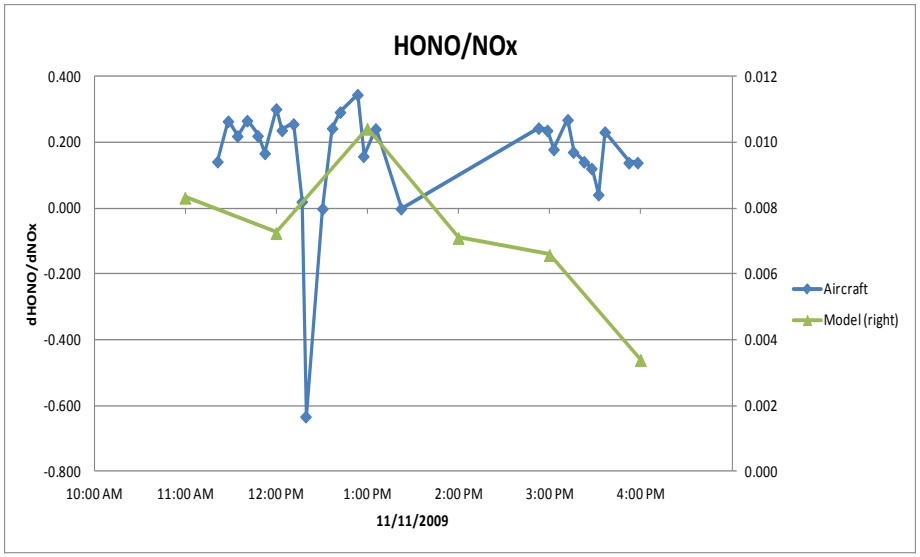
HONO/NOx
dHONO/dNOx
0.400
0.200
0.000
-0.200
-0.400
-0.600
-0.800
0.012
0.010
0.008
0.006
0.004
0.002
0.000
10:00 AM
11:00 AM
12:00 PM
1:00 PM
2:00 PM
3:00 PM
4:00 PM
11/11/2009
Aircraft
Model (right)

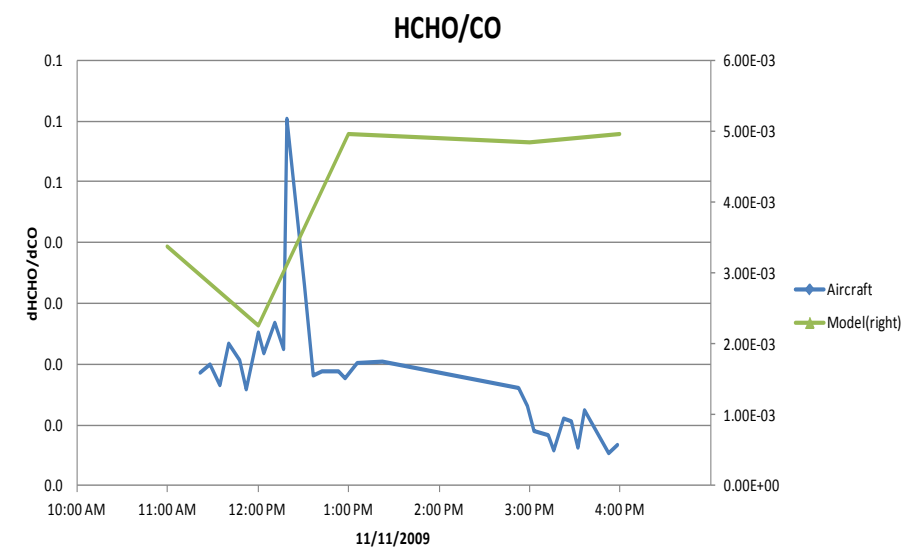
HCHO/CO
dHCHO/dCO
0.1
0.1
0.1
0.0
0.0
0.0
0.0
6.00E-03
5.00E-03
4.00E-03
3.00E-03
2.00E-03
1.00E-03
0.00E+00
10:00 AM
11:00 AM
12:00 PM
1:00 PM
2:00 PM
3:00 PM
4:00 PM
11/11/2009
Aircraft
Model(right)

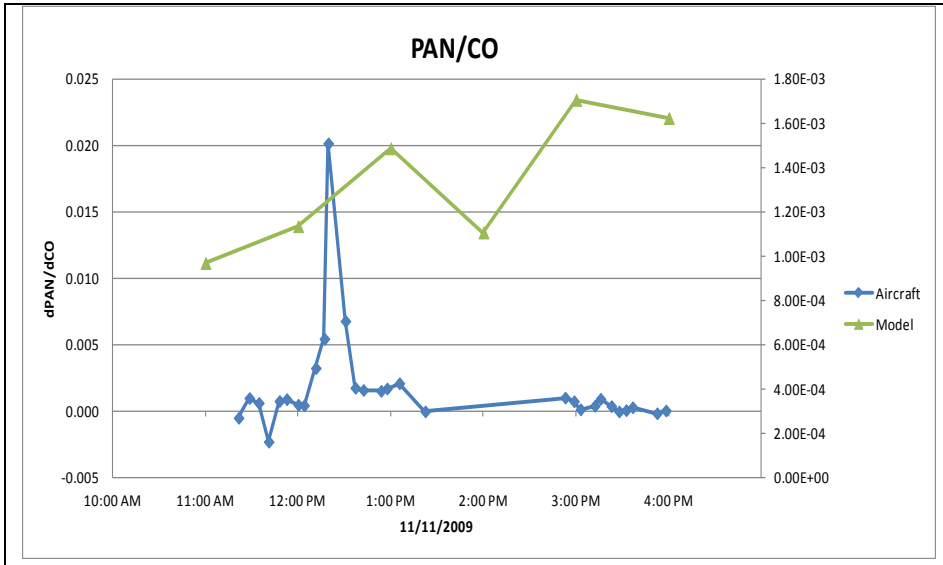

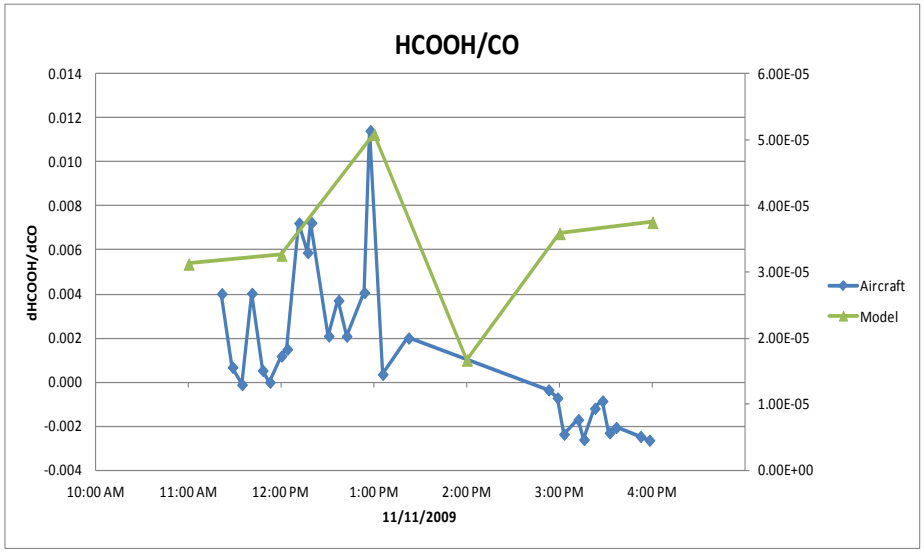

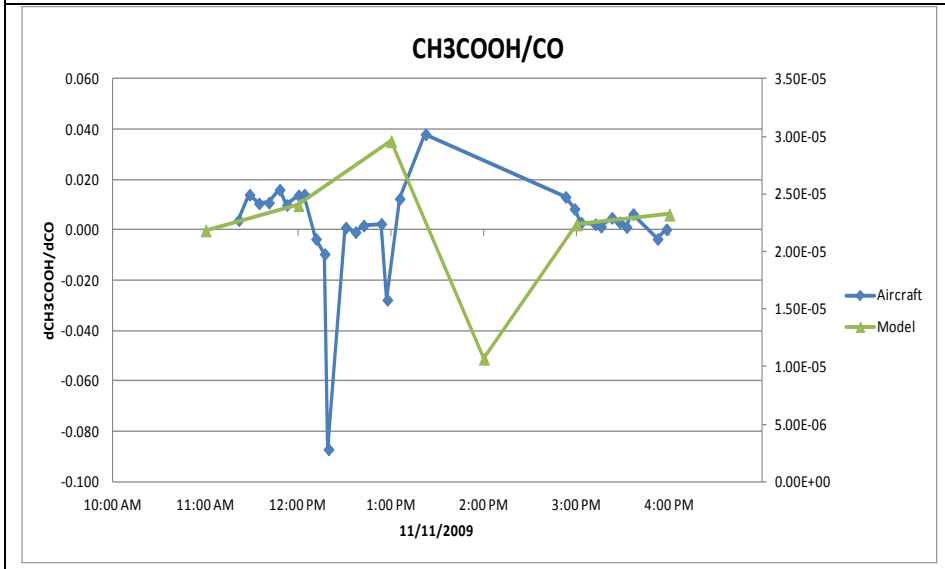

Figure 6b. Ratio of species from aircraft data vs. model results (right axis)

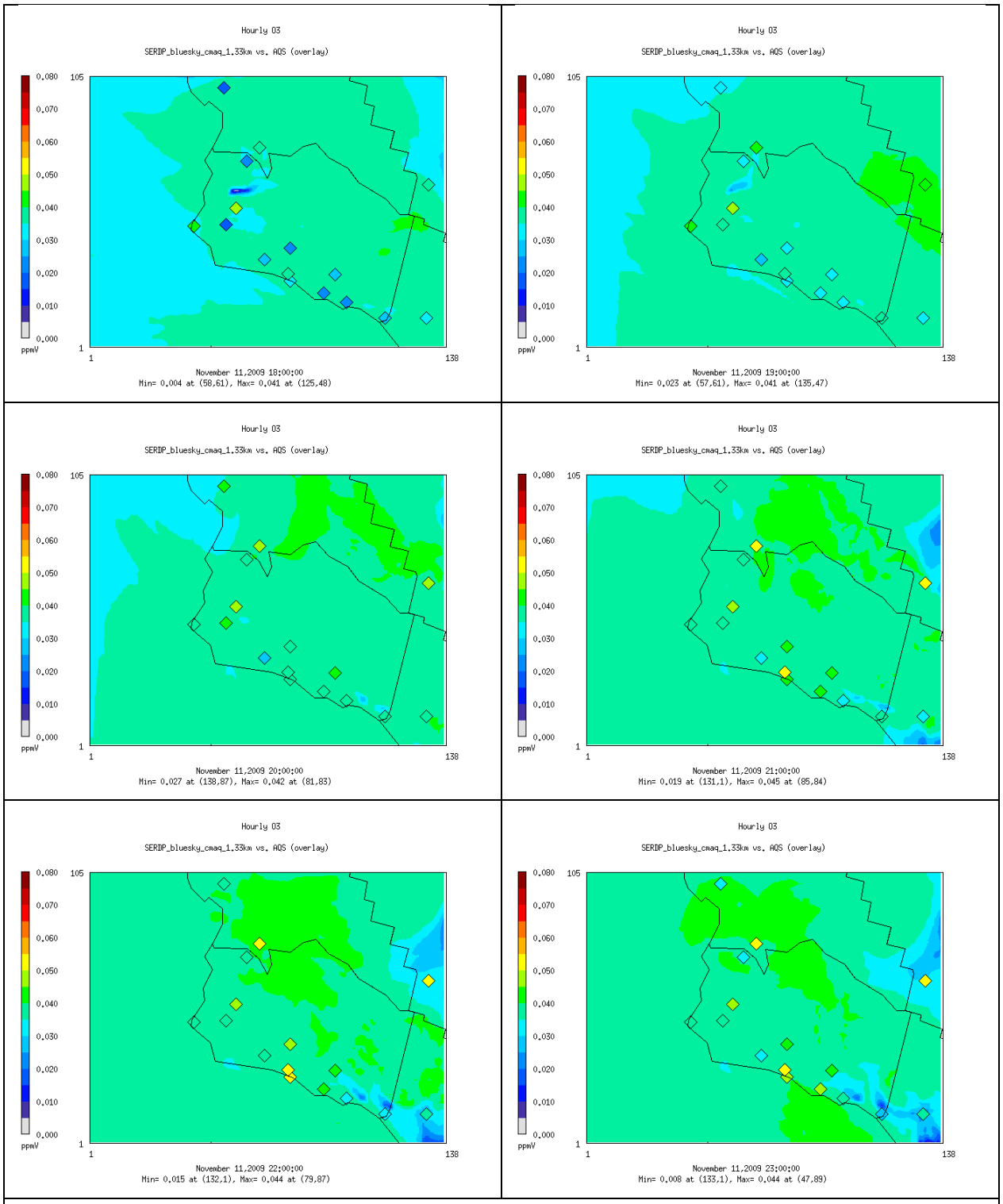

Figure 7. O3 AQS observation (in diamonds) vs. model overlay plots from 18:00 (GMT) to 23:00 (GMT) on 11/11/2009.

8 Appendix B

8.1 List of Scientific/Technical Publications

8.1.1 Peer-Reviewed Journal Publications

[1] Roberts, J. M., Veres, P., Warneke, C., Neuman, J. A., Washenfelder, R. A., Brown, S. S., ... De Gouw, J. (2010). Measurement of HONO, HNCO, and other inorganic acids by negative-ion proton-transfer chemical-ionization mass spectrometry (NI-PT-CIMS): application to biomass burning emissions, Atmos. Meas. Tech, 3(4), 981-990.

[2] Burling, I., Yokelson, R. J., Griffith, D. W., Johnson, T. J., Veres, P., Roberts, J., Gouw, J. D. (2010). Laboratory measurements of trace gas emissions from biomass burning of fuel types from the southeastern and southwestern United States. Atmospheric Chemistry and Physics, 10 (22): 11115-11130, 10(PNNL-SA-71185).

[3] Hosseini, S., Li, Q., Cocker, D., Weise, D., Miller, A., Shrivastava, M., Jung, H. (2010). Particle size distributions from laboratory-scale biomass fires using fast response instruments. Atmospheric Chemistry and Physics, 10(16), 8065-8076.

[4] Qi, L. (2010). Carbonaceous Aerosol Study Using Advanced Particle Instrumentation. PhD thesis, University of California, Riverside.

[5] Roberts, J. M., Veres, P., Warneke, C., Neuman, J. A., Washenfelder, R. A., Brown, S. S., ... De Gouw, J. (2010). Measurement of HONO, HNCO, and other inorganic acids by negative-ion proton-transfer chemical-ionization mass spectrometry (NI-PT-CIMS): application to biomass burning emissions, Atmos. Meas. Tech, 3(4), 981-990.

[6] Johnson, T. J., Profeta, L., Sams, R. L., Griffith, D. W., Yokelson, R. L. (2010). An infrared spectral database for detection of gases emitted by biomass burning. Vibrational Spectroscopy, 53(1), 97-102.

[7] Veres, P., Gilman, J. B., Roberts, J. M., Kuster, W. C., Warneke, C., Burling, I. R., de Gouw, J. (2010) Development and validation of a portable gas phase standard generation and calibration system for volatile organic compounds, Atmospheric Measurement Techniques 3 (2010), no. 3, 683–691.

[8] P. Veres, J.M. Roberts, I.R. Burling, C. Warneke, J. de Gouw, and R.J. Yokelson (2010), Measurements of gas-phase inorganic and organic acids from biomass fires by negative-ion proton-transfer chemical-ionization mass spectrometry, Journal of Geophysical Research 115, no. D23, D23302.

[9] Veres, P., Roberts, J. M., Burling, I. R., Warneke, C., de Gouw, J., Yokelson, R. J. (2010). Measurements of gas-phase inorganic and organic acids from biomass fires by negative-ion proton-transfer chemical-ionization mass spectrometry. Journal of Geophysical Research, 115(D23), D23302.

[10] Warneke, C., Roberts, J. M., Veres, P., Gilman, J., Kuster, W. C., Burling, I., ... de Gouw, J. A. (2011). VOC identification and inter-comparison from laboratory biomass burning using PTR-MS and PIT-MS. International Journal of Mass Spectrometry, 303(1), 6-14.

[11] Akagi, S. K., Yokelson, R. J., Wiedinmyer, C., Alvarado, M. J., Reid, J. S., Karl, T., ... Wennberg, P. O. (2011). Emission factors for open and domestic biomass burning for use in atmospheric models. Atmospheric Chemistry and Physics, 11(9), 4039-4072.

[12] Burling, I. R., Yokelson, R. J., Akagi, S. K., Urbanski, S. P., Wold, C. E., Griffith, D. W., ... Weise, D. R. (2011). Airborne and ground-based measurements of the trace gases and particles emitted by prescribed fires in the United States. Atmospheric Chemistry and Physics, 11(23), 12197-12216.

[13] Chang-Graham, A. L., Profeta, L. T., Johnson, T. J., Yokelson, R. J., Laskin, A., Laskin, J. (2011). Case study of water-soluble metal containing organic constituents of biomass burning aerosol. Environmental Science and Technology-Columbus, 45(4), 1257.

[14] Warneke, C., Roberts, J. M., Veres, P., Gilman, J., Kuster, W. C., Burling, I., ... de Gouw, J. A. (2011). VOC identification and inter-comparison from laboratory biomass burning using PTR-MS and PIT-MS. International Journal of Mass Spectrometry, 303(1), 6-14.

[15] Qi, L., Hosseini, S., Jung, H., Yokelson, B., Weise, D., Cocker III, D., Huang, Y. (2012). Chemical characterization of particle emissions from controlled burns of biomass fuels using a high resolution time-of-flight aerosol mass spectrometer. Atmos. Chem. Phys. Discuss, 12, 8397-8432.

[16] Roberts, J. M., Veres, P. R., Cochran, A. K., Warneke, C., Burling, I. R., Yokelson, R. J., ... de Gouw, J. (2011). Isocyanic acid in the atmosphere and its possible link to smoke-related health effects. Proceedings of the National Academy of Sciences, 108(22), 8966-8971. (correction DOI: 10.1073/pnas.1113250108)

[17] Akagi, S. K., J. S. Craven, J. W. Taylor, G. R. McMeeking, R. J. Yokelson, I. R. Burling, S. P. Urbanski et al. (2012). Evolution of trace gases and particles emitted by a chaparral fire in California. Atmospheric Chemistry and Physics 12, no. 3 (2012): 1397-1421.

[18] Yokelson, R. J., I. R. Burling, J. B. Gilman, C. Warneke, C. E. Stockwell, J. de Gouw, S. K. Akagi et al. (2012). Coupling field and laboratory measurements to estimate the emission factors of identified and unidentified trace gases for prescribed fires. Atmospheric Chemistry & Physics, 12: 21517-21578.

[19] Hosseini, S. (2012). Physical and Chemical Characterization of Particulate and Gas phase Emissions from Biomass Burning, PhD thesis, University of California, Riverside.

[20] Hosseini, S., Urbanski, S., Dixit, P., Li, Q., Burling, I., Yokelson, R., Johnson, T., Shrivastava, M., Jung, H., Weise, D.R., Miller, W., and Cocker, D. 2013. Laboratory characterization of PM emissions from combustion of wildland biomass fuels. Journal of Geophysical Research – Atmospheres, 118, 9914–9929, DOI: 10.1002/jgrd.50481.

[21] Hosseini, S., Miller, J. W., Cocker, D., Weise, D., Jung, H. (2013). A new biomass burning model for determining the fire intensity based on carbon ratios, In Prep., Journal of Atmospheric Chemistry and Physics.

[22] Hosseini, S., Li, Q., Yokelson, R., S., U., I., B., D., W., Miller, J. W., Jung, H., Cocker, D. (2013). Chemical characterization of gas phase emissions from combustion of various US vegetation types, In Prep, Atmospheric Chemistry and Physics.

[23] Hosseini, S.; Li, Q.; Shrivastava, M.; Weise, D.R.; Miller, W.; Cocker, D.; Jung, H. (Accepted 1/2/2014) Effect of low density polyethylene on smoke emissions from debris pile burning. Journal of Air and Waste Management Association

[24] Dixit, P., Hosseini, S., Tang, P., Li, Q., Jung, H., Miller, J. W., Cocker, D. (2013). Performance of High Resolution Time-of-Flight Aerosol Mass Spectrometer during Chemical Characterization of Particle Emissions from Controlled Biomass Burning, Submitted., Atmospheric Chemistry and Physics

8.1.2 Conference Papers

[1] Asa-Awuku, A., Bartolome, C., Cocker, D., Hosseini, S, Jung, H., Lozano, J., Mahalingam, S., Maynard, T., Miller, W., Princevac, M., Qi, L., Sharivastava, M., Switzer, D., Yokelson, R., Burling, I., Akagi, S., Roberts, J., Veres, P., Miller, A., Weise, D., Hao, W., Urbanski, S. (2009), New Tools for Estimating and Managing Local/Regional Air Quality Impacts of Prescribed Burns, Partners in Environmental Technology Technical Symposium and Workshop, Washington, D.C., December.

[2] Hosseini, S., Li, Q., Nakao, S., Shrivastava, M., Miller, W., Weise, D., Jung, H., and Cocker, D. (2009), Chemical and physical characterization of wood smoke under controlled conditions, Western States Section Combustion Institute.

[3] Hosseini, S., Miller, A., Li, Q., Cocker, D., Hao W., Yokelson, R., Weise, D., and Jung, H., (2009), Characterization of smoke particles by electron microscopy, energy dispersive spectroscopy and image analysis, 28th American Association for Aerosol Research.

[4] Kuster, W. C., J. B. Gilman, P. D. Goldan, C. Warneke, J. Degouw, P. R. Veres, I. R. Burling, and R. J. Yokelson. (2009), Measurements of Volatile Organic Compounds (VOCs) from Biomass Combustion-Emission Ratios, OH Reactivities and SOA Precursors, In AGU Fall Meeting Abstracts, vol. 1, p. 0172.

[5] Li, Q., Cocker, D., Hosseini, S., Shrivastava, M., Jung, H., Yokelson, R., and Weise, D. (2009), Chemical and physical characterization of PM2.5 from controlled burns of southwest biomass fuels, American Association for Aerosol Research, no. 28th Annual Conference.

[6] Maynard, T., Princevac, ., Mahalingam, S., Lozano, J. (2009), Laboratory study of particulate emissions factors of prescribed wildland fires, 3rd Southern California Symposium on Flow Physics, 1 page, San Diego, CA, April 2009.

[7] Akagi, S. K., raven, J. S., Taylor, J. W., McMeeking, G. R., Yokelson, R. J., Burling, I. R., Alvarado, M. J., Seinfeld, J., Coe, H. and Urbanski, S. P. (2010), Measurements of Trace Gases and Particles in Fresh and Aged Smoke from a Chaparral Fire in California, AGU Fall Meeting Abstracts, B41+.

[8] Akagi, S. K., J. S. Craven, J. W. Taylor, G. R. McMeeking, R. J. Yokelson, I. R. Burling, M. J. Alvarado, J. Seinfeld, H. Coe, and S. P. Urbanski. (2010), Measurements of trace gases and particles in fresh and aged smoke from a chaparral fire in California., In AGU Fall Meeting Abstracts, vol. 1, p. 0041.

[9] Burling, I. R., R. J. Yokelson, S. K. Akagi, T. J. Johnson, D. W. Griffith, S. P. Urbanski, J. W. Taylor et al. (2010), First results from a large, multi-platform study of trace gas and particle emissions from biomass burning." In AGU Fall Meeting Abstracts, vol. 1, p. 03.

[10] Burling, I. R., Yokelson, R. J., Akagi, S. K., Johnson, T. J., Griffith, D. W., Urbanski, S. P., Taylor, J. W., Craven, J. S., McMeeking, G. R., Roberts, J. M., Warneke, C., Veres, P. R., de

Gouw, J. A., Gilman, J. B., Kuster, W. C., Hao, W. M., Weise, D., Coe, H., and Seinfeld, J. (2010), First results from a large, multi-platform study of trace gas and particle emissions from biomass burning, AGU Fall Meeting Abstracts, C3+.

[11] Gilman, J. B., C. Warneke, W. C. Kuster, P. D. Goldan, P. R. Veres, J. M. Roberts, J. A. de Gouw, I. R. Burling, and R. J. Yokelson., (2010), OH reactivity and potential SOA yields from volatile organic compounds and other trace gases measured in controlled laboratory biomass burns, In AGU Fall Meeting Abstracts, vol. 1, p. 03.

[12] Hosseini, S., Li, Q., Cocker, D, Weise, D., Miller, A., Shrivastava, M., Jung, H. and Cocker D. (2010), Study of particle size distribution and morphology using fast response particle instruments and tem. paper presented at the, Western States Combustion Institute.

[13] Hosseini, S., Li, Q., Cocker, D., Miller, A., Shrivastava, M., Weise, D., Mahalingam, S., Princevac, M., Miller, W., and Jung, H. (2010), Particle size distributions during laboratory-scale biomass burns and prescribed burns using fast response instruments, 16th International Conference on Forest Fire Research.

[14] Lincoln, E., Hao, W., Baker, S., Yokelson, R. J., Burling, I. R., Urbanski, S. P., Miller, W., Weise, D. R., and Johnson, T. J. (2010), A prescribed fire emission factors database for land management and air quality applications., In AGU Fall Meeting Abstracts, vol. 1, p. 0037.

[15] Maynard, T., Hosseini, S., Jung, H., Princevac, M., Mahalingam, S., and Yokelson, R. (2010), Laboratory study of particulate emissions factors of prescribed wildland fires, 16th Joint Conference on the Applications of Air Pollution Meteorology with the A&WMA, 90th AMS Annual Meeting, Air Pollution Meteorology.

[16] McMeeking, G. R., aylor, J. W., ullivan, A. P., Flynn, M. J., Akagi, . K., Carrico, C. M., Collett, . L., Fortner, E., nasch, . B., Kreidenweis, S. M., okelson, R. J., Hennigan, C., Robinson, . L. and Coe, H. (2010), Black carbon aerosol properties measured by a single particle soot photometer in emissions from biomass burning in the laboratory and field, AGU Fall Meeting Abstracts, C2+.

[17] Weise, D., Miller, W., Cocker, D., Jung, H., Yokelson, R., Hao, W., Urbanski, S., Princevac, M., Mahalingam, S., Burling, I. (2010), Development of new fuels and emissions data for maritime chaparral and Madrean oak woodland fuel types, 3rd Fire Behavior and Fuels Conference, October 25-29, 2010, Spokane, Washington, USA.

[18] Weise, D., Jung, H., Cocker, D., Hosseini, S., Li, Q., Shrivastava, M, and McCorison, M. (2010), Do polyethylene plastic covers affect smoke emissions from debris piles?, Fire Behavior and Fuels Conference (Spokane, Washington, USA), International Association of Wildland Fire.

[19] Weise, D., Miller, W., Cocker, D., Jung, H., Yokelson, R., Hao, W., Urbanski, S., Princevac, M., Mahalingam, S., and Burling, I. (2010), Development of new fuels and emissions data for maritime chaparral and madrean oak woodland fuel types, Fire Behavior and Fuels Conference (Spokane, Washington, USA), International Association of Wildland Fire.

[20] Burling, I. R., R. J. Yokelson, S. K. Akagi, J. Taylor, J. S. Craven, T. J. Johnson, S. P. Urbanski et al. (2011), Biomass burning: space-based detection efficiency, differences between ground-based and airborne measurements, evolution of trace gases and particles." In AGU Fall Meeting Abstracts, vol. 1, p. 0285.

[21] Burling, I., Yokelson R., Akagi, S., Urbanski, S., Warneke, C., Veres, P., Gilman, J., Roberts, J., Kuster, W., Griffith, D., Johnson, T., and Weise, D. (2011), Results from a large, multiplatform study of trace gas and particle emissions from biomass burning, International Global Atmospheric Chemistry.

[22] Burling, I. R., Yokelson, R. J., Griffith, D. W., Roberts, J. M., Veres, P. R., Warneke, C., and Johnson, T. J. (2009). Laboratory Investigation of Trace Gas Emissions from Biomass Burning on DoD Bases, AGU Fall Meeting Abstracts, D125+.

[23] Cocker, D., Li, Q., Jung, H., Miller, J. W., Shrivastava, M., Mahalingam, S., ... Weise, D., American Association for Aerosol Research (2011). Chemical and physical characterization of emissions from laboratory combustion of southwestern and southeastern US biomass fuels.

[24] Giordano, M., Asa-Awuku, A., Hosseini, S., Cocker III, D., American Association for Aerosol Research (2011). Significant Changes in Optical and CCN Properties of Photochemically Aged Wood Smoke.

[25] Hosseini, S., Li, Q., Miller, A., Sharivastava, M., Cocker, D., Miller, W., Mahalingam, S., Princevac, M., Weise, D., Odman, M.T., Reardon, J., Johnson, T., Jung, H. (2010), Particle size distribution from a controlled biomass burning in the laboratory using fast response particle instruments" WSSCI Spring 2010 Meeting, Boulder, March 21-23.

[26] Hosseini, S., Jung, H., Qi, L., Weise, D., Miller, W., and Cocker, D. (2010), PM emissions from laboratory combustion of biomass fuels, Conference of American Association for Aerosol Research.

[27] Wang, Z., Chien, C., Tonnesen, G., Miller, W., Princevac, M., Gonzalez, H., Moore, R. (2011), Meteorological and Air Quality Modeling of a 2009 Prescribe Burn Event, AMS Ninth Symposium on Fire and Forest Meteorology, 1, Palm Springs, CA, October 2011.

[28] Lu, V., Tsui, K., Bartolome, C., Princevac, M., Venkatram, A., Mahalingam, S., Achtemeier, G., Weise, D. (2012), Laboratory Measurements and Characterization of Smoldering Smoke From Pine Needle Fuel Beds, AMS 92nd Annual Meeting, 1, New Orleans, LA, January.

[29] Alvarado, M. J., T. Soni, R. J. Yokelson, S. K. Akagi, J. S. Craven, J. W. Taylor, G.R. McMeeking, I. R. Burling, S. P. Urbanksi, C. E. Wold, J. H. Seinfeld, H. Coe, D. R. Weise, J. D. Crounse, P. F. DeCarlo, T. Karl, T. Campos, A. Weinheimer, F. Flocke, P. O. Wennberg, L. Mauldin, J. L. Jimenez, and S. Hall. 2012. Recent Observations of High OH Concentrations and Rapid Ozone Formation in Biomass Burning Plumes Simulated with the ASP Model, Abstract P-2-021, presented at the International Global Atmospheric Chemistry Program Meeting "Atmospheric Chemistry in the Anthropocene", Beijing, China, 17-21 September.

[30] David R. Weise, Wayne Miller, Robert Yokelson, Shawn Urbanski, David R. Cocker, III, Heejung Jung, Marko Princevac, Ian Burling, Sheryl Akagi, Seyedehsan Hosseini. 2013. Recent Emissions Research in Southwestern Shrub and Grassland Fuels. International Smoke Symposium, 22 Oct 2013, Adelphi, MD; also 18th Air Pollution Joint Conference with A&WMA, 7 Feb 2014, Atlanta, GA entitled "*Measuring Smoke Emissions on DOD Installations: 1. Southwestern Shrub and Grassland Fuels*".

[31] David R. Weise, Heejung Jung, David R. Cocker, III, Seyedehsan Hosseini, Qi Li, Manishkumar Shrivastava, Michael McCorison. 2013. Impact of Polyethylene Plastic on Smoke

Emissions from Debris Piles. International Smoke Symposium, 22 Oct 2013, Adelphi, MD; also 18th Air Pollution Joint Conference with A&WMA, 7 Feb 2014, Atlanta, GA. Oral presentation